APPLICATION OF GEOSTATISTICAL METHODS AND WAVELETS TO THE ANALYSIS OF HYPERSPECTRAL IMAGERY AND THE TESTING OF A MOVING VARIOGRAM

Final Report (RSSUSA - 5/4)

Dr Margaret A. Oliver

April 2000 to March 2001

United States Army

ENVIRONMENTAL RESEARCH OFFICE OF THE U.S. ARMY

London, England

CONTRACT NUMBER - N68171-00-M-5508

REPORT DOCUMENTATION PAGE

Form Approved
OMB No. 0704-0188

1. AGENCY USE ONLY (Leave blank)	2. REPORT DATE	3. REPORT TYPE AND DATES COVERED
	21.3.01	Final April 2000 – March 2001

4. TITLE AND SUBTITLE
Application of geostatistical methods and wavelets to the analysis of hyperspectral imagery and the testing of a moving variogram

5. FUNDING NUMBERS
N68171
00-M-5508

6. AUTHOR(S)
Dr Margaret A Oliver

7. PERFORMING ORGANIZATION NAME(S) AND ADDRESS(ES)
University of Reading, Whiteknights,
Reading, RG6 2AH, UK

8. PERFORMING ORGANIZATION REPORT NUMBER
RSS USA-5/4

9. SPONSORING/MONITORING AGENCY NAME(S) AND ADDRESS(ES)
USARDSG-UK, Environmental Sciences Branch
Edison House, 233 Old Marylebone Road,
London, NW1 5TH, UK

10. SPONSORING/MONITORING AGENCY REPORT NUMBER

11. SUPPLEMENTARY NOTES
Final Report:
Summary of work to date

12a. DISTRIBUTION/AVAILABILITY STATEMENT
No limitation on distribution/availability

12b. DISTRIBUTION CODE

13. ABSTRACT (Maximum 200 words)

Part I of this report describes the analysis on moving averages, variances and variograms for NIR from a SPOT image of part of Fort A. P. Hill. The relation between elevation from a digital elevation model, the raw elevation data and NIR and NDVI were explored in detail. The correlations are weak in spite of an apparent visual relation. Part II describes the analyses of the hyperspectral 'hymap' data. The results illustrate the difficulty of deciding how many and which wavebands to retain. Certain groups of bands reappear in different analyses, but equally there are less stable groupings. The PCA results do not discriminate as well as the raw variograms and certain classifications. Eight groups of bands seem to appear regularly. The pixel maps show that even within these groups different information emerges. Part IV of the report describes the analysis of the National Soil Inventory of England and Wales. Geostatistical methods and wavelet analysis are compared. Part IV of the report of the project is an aide memoire for sampling. It embraces both design-based sampling, which is based on classical statistics, and model-based sampling which is underpinned by geostatistics. This work is a guide to sampling field-based information or pixels from images.

14. SUBJECT TERMS	15. NUMBER OF PAGES
Keywords: moving variograms, factorial kriging, wavelet analysis, sampling	16. PRICE CODE

17. SECURITY CLASSIFICATION OF REPORT	18. SECURITY CLASSIFICATION OF THIS PAGE	19. SECURITY CLASSIFICATION OF ABSTRACT	20. LIMITATION OF ABSTRACT

NSN 7540-01-280-5500

Standard Form 298 (Rev. 2-89)
Prescribed by ANSI Std. Z39-18
298-102

TABLE OF CONTENTS

LIST OF TABLES

LIST OF FIGURES

LIST OF FIGURES (continued)

LIST OF FIGURES (continued)

LIST OF FIGURES (continued)

PREFACE

This report was sponsored by the United States Army Research, Development and standardization Group-UK (USARDGSG-UK), London, NW1 5TH, United Kingdom, under contract PR-N68171-00-M-5508, entitled, "Application of geostatistical methods and wavelets to the analysis of hyperspectral imagery and the testing of a moving variogram". It is monitored by the U. S. Army Topographic Engineering Center (TEC), Alexandria, Virginia 22315-3863. The work was done by the University of Reading, Whiteknights, Reading, RG6 6DW, United Kingdom. The USARDGSG-UK Program Manager is Mr. Jerry Comati, and the TEC Contracting Officer's Representative is Mr. James Shine

EXECUTIVE SUMMARY

This report contains the three interim reports, together with the most recent results. In addition, there is an Appendix. Part I describes the analysis on moving averages, variances and variograms for NIR from a SPOT image of part of Fort A. P. Hill. The computer programs for these have already been provided to the Topographic Engineering Center. The maps of the variances and the diagram of the variograms show areas of the image that are not stationary and where kriging is likely to perform less well in prediction than wavelet analysis. This proves the findings of Project PR-N 68171-98-M-5311. This section also includes the analysis of a part of the image called 'aphillcut' to distinguish it from the larger section of image used that ahs been used. This explored in detail any relation between elevation from a digital elevation model, the raw elevation data and NIR and NDVI. The correlations are weak in spite of an apparent visual relation. The strongest relation was between the moving averages for NDVI and elevation for a window of 10×10 pixels.

Part II describes the analyses of the hyperspectral 'hymap' data. This includes a correlation analysis, principal component analysis (PCA), variography, mapping, multivariate non-hierarchical classification and factorial kriging. The results illustrate the difficulty of deciding how many and which wavebands to retain. Certain groups reappear in different analyses, but equally there are less stable groupings. The PCA results are not particularly discriminatory, whereas those for the raw variograms and certain classifications appear to identify about eight groups of bands. The pixel maps show that even within these groups different information emerges. Further interpretation of some of these results requires input from personnel at TEC.

Part IV of the report describes the analysis of the National Soil Inventory of England and Wales. The aim was to compare geostatistical methods, mainly ordinary kriging and factorial kriging, with wavelet analysis on a different kind of data from imagery. The data were from sampling locations on a 5-km grid and pH and zinc were selected for analysis. The variogram of pH showed that there was long-range trend in the data, which had to be removed for the geostatistical analysis whereas the wavelet analysis is not affected by it. Zinc was markedly skewed and the data were transformed to common logarithms for the geostatistical analysis, which again was not necessary for the wavelet analysis. The results have shown some interesting features. There appears to be no local non-stationarity in these data, which meant that kriging performed better than the wavelet analysis in terms of the distribution of the errors for the 10-km subsample. However, for the 40-km subsample the wavelet analysis performed better. The variograms for both properties were nested and the short-range variation was evident in the high frequency wavelet transform for the 20-km grid. The variogram can provide a guide as to what sampling interval should be focused on in a multiresolution analysis using wavelets.

Part IV of the report of the project is a stand-alone piece of work, mainly prepared by Professor Richard Webster. This is an aide memoire for sampling. It embraces both design-based sampling, which is based on classical statistics, and model-based sampling which is underpinned by geostatistics. This work is a guide to sampling field-based information or
pixels from images. It starts with what the user should consider before sampling, i.e. the target population, the sample support (volume of sample), the individuals, what the data are to be used for, what kind of predictions are required. Based on the kind of predictions required the user will decide either to have a sample design for design-based estimation or one for model-based prediction.

PART I: MOVING AVERAGES, VARIANCES AND TILED VARIOGRAMS FOR FORT A. P. HILL

This first section of the report contains several sections of work. The analysis and computer programs for the first part of the report on the moving averages, variances and variograms were completed in the previous project. There was insufficient time, however, to complete the written part of this work. The complete section is now included although files of the results and computer programs had been sent to TEC in digital form. Four days of the present contract were spent working at the Topographic Engineering Center and one day at the Virginia Institute of Marine Science. In addition time has been spent on the wavelets and kriging paper for submission to the Proceedings of the Sixth International Geostatistics Congress. This paper can only be accessed on CD-Rom at present, the published proceedings will come out in 2001. The rest of this report will comprise work done on the image and digital elevation model for Fort A. P. Hill, and on the latest hyperspectral imagery.

Moving averages, variances and tiled variograms

The computation of a variogram for a region carries with it the implication that the underlying variation is stationary in the intrinsic sense. The analyst assumes that the expected differences between places, at least for small lag distances, are zero and that the expected squared differences are constant for any given lag:

$$\mathrm{E}[Z(\mathbf{x}) - Z(\mathbf{x}+\mathbf{h})] = 0 \qquad (1)$$

and

$$\mathrm{E}[\{Z(\mathbf{x}) - Z(\mathbf{x}+\mathbf{h})\}^2] = 2\gamma(\mathbf{h}). \qquad (2)$$

Here, in the usual geostatistical convention, $Z(\mathbf{x})$ and $Z(\mathbf{x}+\mathbf{h})$ are the values of the random variable Z at positions $\mathbf{x}$ and $\mathbf{x}+\mathbf{h}$, where $\mathbf{h}$ is the lag, and $\gamma(\mathbf{h})$ is the semivariance at that lag.

The equations above refer to the random process $Z(\mathbf{x})$, and in any one realization the actual values depart from its expectation. Geostatisticians are used to this and accept Equation (1) without demur in many instances. Equation (2) is assumed to hold everywhere; i.e. the semivariance depends on the lag only and not on the position. Geostatisticians are used to this too; usually they have too few data to explore its validity. Remote images from satellites, each comprising several hundred thousand pixels, however, may cause us to question the assumption when some parts of an image are plainly more variable than others. The SPOT image of AP Hill is one such; Figure 1, a pixel map of NIR, is an example. This is the part of A. P. Hill that we examined originally. With so many data we can examine the changes in the variogram over the region, and the result can help us to decide whether our assumption of stationarity is reasonable.

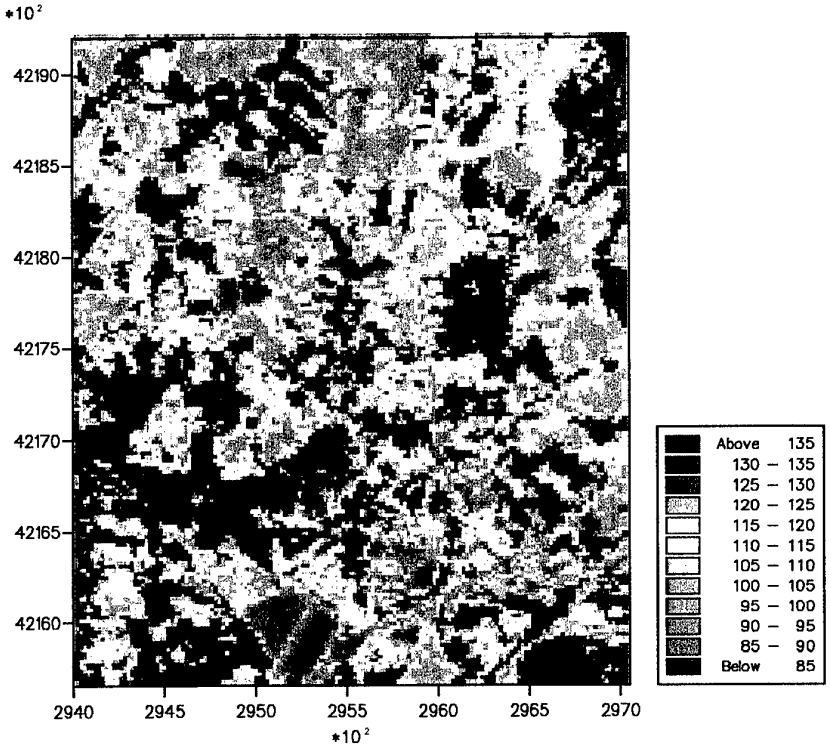

Figure 1. Pixel map of NIR for the original part of the SPOT image for Fort A. P. Hill. The coordinates are given as UTMs.

Analysis

We computed three sets of criteria to evaluate the likely stationarity; the moving average, the moving variance, and the local variogram. The first two are defined as follows.

Moving average. This is computed by placing over the image a window containing n pixels and summing the values of NIR within the window:

$$\bar{z}(\mathbf{x}_c) = \frac{1}{n}\sum_{i=1}^{n} z(\mathbf{x}_i). \qquad (3)$$

where $z(\mathbf{x}_i)$ is the value of the ith pixel in the window, and $\mathbf{x}_c$ denotes the centre of the pixel. The window is moved one pixel at a time, and at each new position $\bar{z}(\mathbf{x}_c)$ is computed. In this way a map of moving averages is built.

Moving variance. The moving variance, ($\sigma^2(\mathbf{x}_c)$, is computed in an analogous way from

$$\sigma^2(\mathbf{x}_c) = \frac{1}{n-1}\sum_{i=1}^{n} \{z(\mathbf{x}_i) - \bar{z}(\mathbf{x}_c)\}^2. \qquad (4)$$

Again, a map of the local variances can be made.

Local variogram. Semivariances can be calculated for a window from

$$\gamma(\mathbf{h}_c) = \frac{1}{2m(\mathbf{h})} \sum_{j=1}^{m(\mathbf{h})} \{z(\mathbf{x}_j) - z(\mathbf{x}_j + \mathbf{h})\}^2, \qquad (5)$$

where the index j refers to those pixels for which a paired comparison is possible at the particular lag $\mathbf{h}$, and $m(\mathbf{h})$ is the number of such comparisons.

Computing local variograms for the same windows as for the average and variance runs into some difficulties.

1. Experimental variograms are unreliable with fewer than about 100 data. So it has seemed unreasonable to attempt to compute them for small windows, i.e. less than 10 × 10.

2. They are time-consuming, though not so time-consuming as to make the task impossible on a modern workstation.

3. Displaying the hundreds of thousands of variograms is fraught.

So, instead of moving the window one pixel at a time we divided the image into square tiles without any overlap. Also, to provide an intelligible display we chose tiles of 15 × 15 = 225 pixels. From experience we know that this size of sample estimates the local variogram well. We then computed the variogram to a maximum lag of 12.5 pixels.

Results

We computed the moving averages and moving variances for square windows of sides 3, 5, 7, 9, 11, and 15 pixels. The results are displayed in Figures 2a to 7a. In Figure 2a (3 × 3 window) the features in the original image, Figure1 are still visible. For example the lakes in the north and centre (blue areas) and the line of the road running N-S (green). The latter is not as evident as in Figure 1. In Figure 3a (5 × 5 window) the lakes are still evident, but the outline is no longer distinct and the line of the road is barely visible. As the window widens further, Figures 4a to 7a, the coarse features of the image become increasingly apparent. The map for the window of 9 × 9 pixels is very similar to that for the long-range structure from factorial kriging (see previous final report). There is little evidence of non-stationarity.

The margins of the maps, which broaden as the window increases in size, are the global average. This value is given when the window dimensions cannot be fitted due to edge effects.

Analogous maps of the moving variances are shown in Figures 2b to 7b. These tell a different story.

The smallest window, $3 \times 3 = 9$ pixels, shows local, mostly sinuous, patches of image where the variance is much larger than the general background, Figure 2b. In particular the variances are large at the margins of the lakes, and their shape is evident. Increasing the window to 25 pixels leaves a basically sinuous pattern, but with the patches of large variance beginning to broaden, Figure 3b. This broadening continues as the window is enlarged, and the sinuosity has almost disappeared and is confined to patches of medium variation with the window of 81 pixels, Figure 5b. The patches of large variance appear as blobs, as they do with the wider windows. As for the maps of the moving averages, the uniform bands at the margins are of the global variance.

Figure 8 shows the variograms in their corresponding tiles, and so is effectively a map. In each tile the experimental variogram appears as the set of points, the left-most of which is at the origin and the right-most at a lag of 12.5 pixels is scaled so that it lies near the right hand margin of the tile. The ordinates are scaled in the range 0 to 20 000 NIR^2. The horizontal line through the points is the local variance of the data. The full image is 151 pixels (columns) 178 (rows). The width of the tiles, 15 pixels, will not divide exactly into either, and so there are gaps at the right and top of the image.

Over most of the image the local variance is small, and it is difficult to see what autocorrelation there is. In a relatively few squares, however, the variance is evidently strongly structured. These squares also happen to be the ones with the largest variances, and perhaps it is because they have the large variances that it is possible to display the results in an informative way.

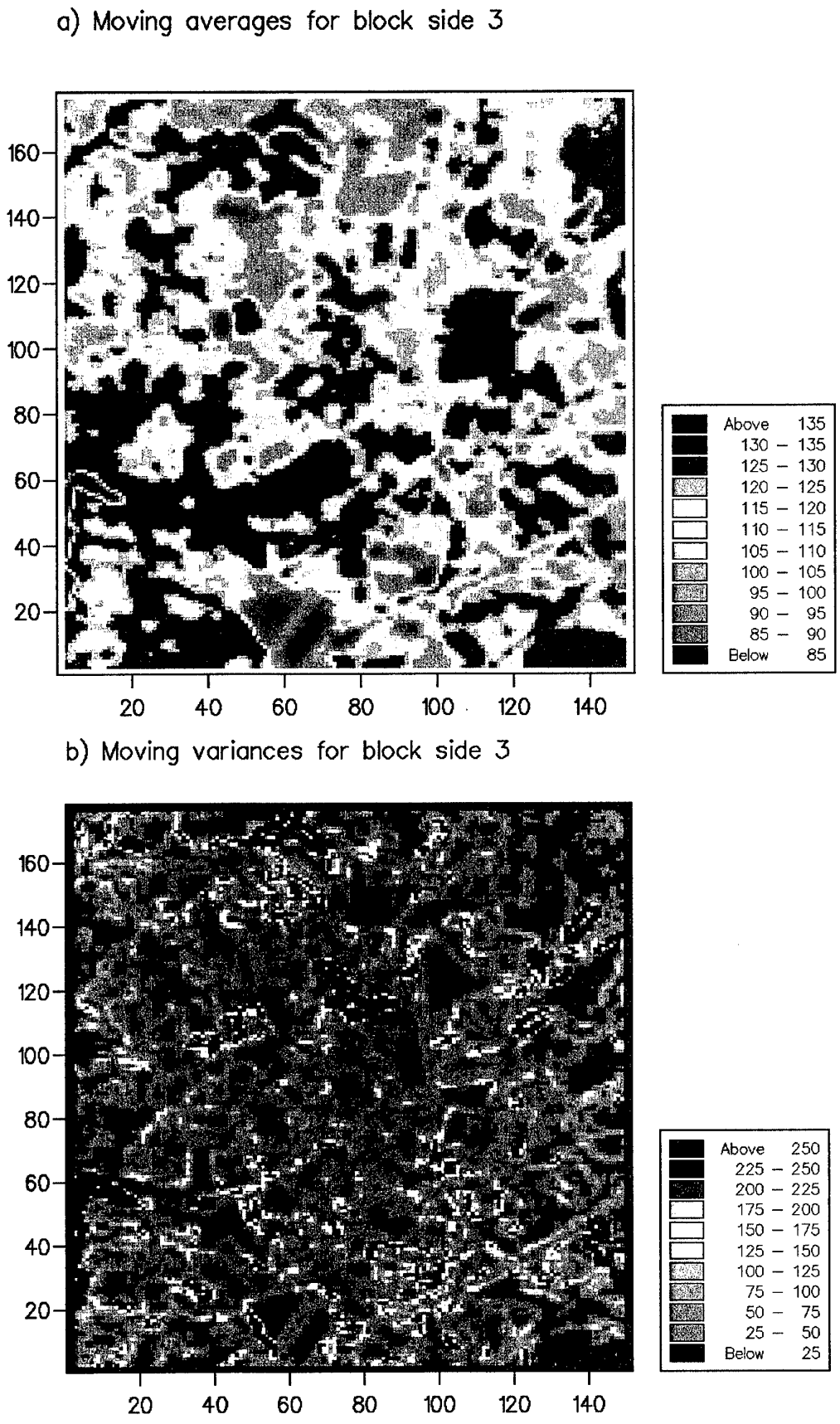

Figure 2. Pixel maps of NIR (Fort A. P. Hill): a) moving averages and b) moving variances, for blocks of side 3.

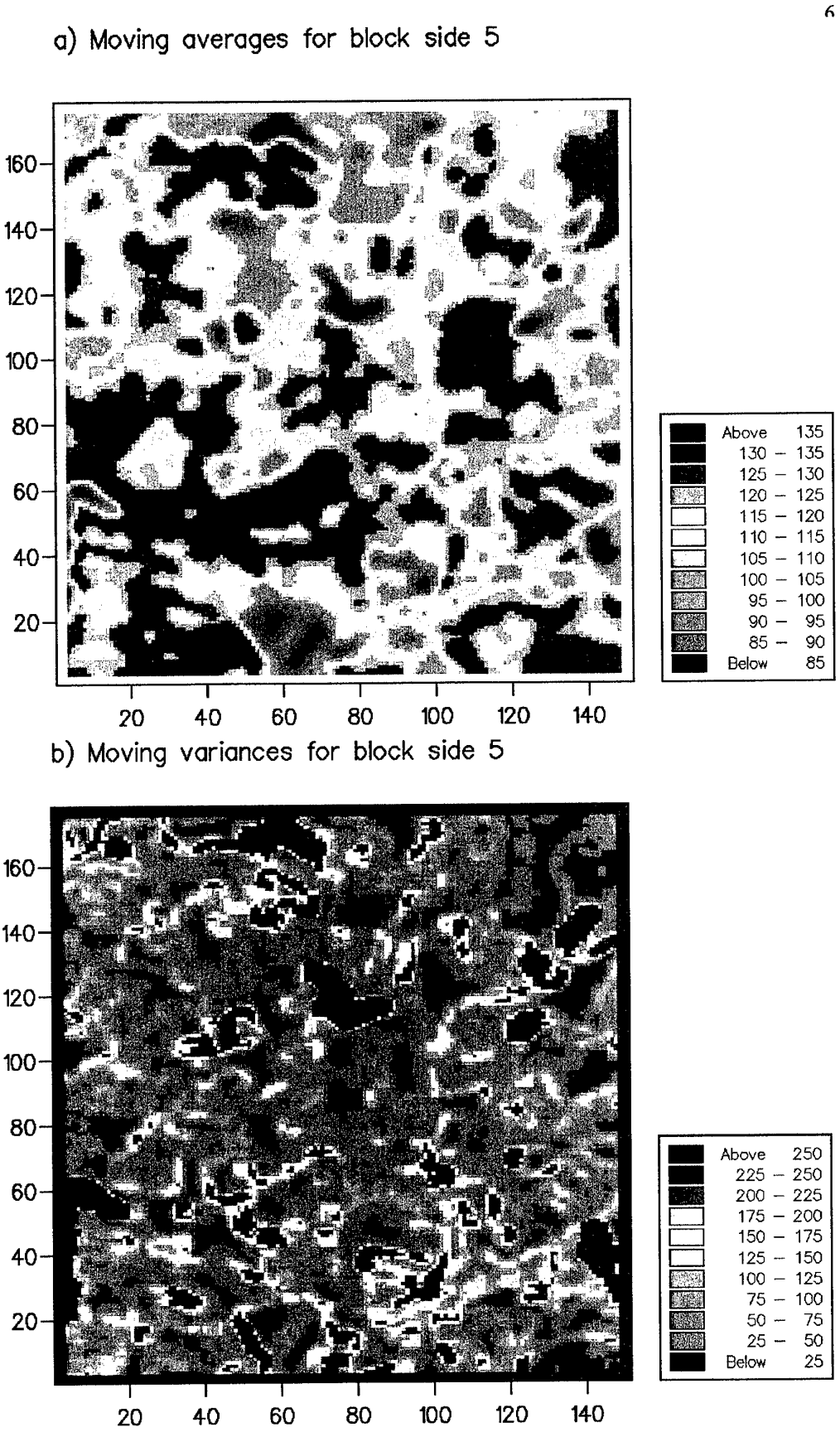

Figure 3. Pixel maps of NIR (Fort A. P. Hill): a) moving averages and b) moving variances, for blocks of side 5.

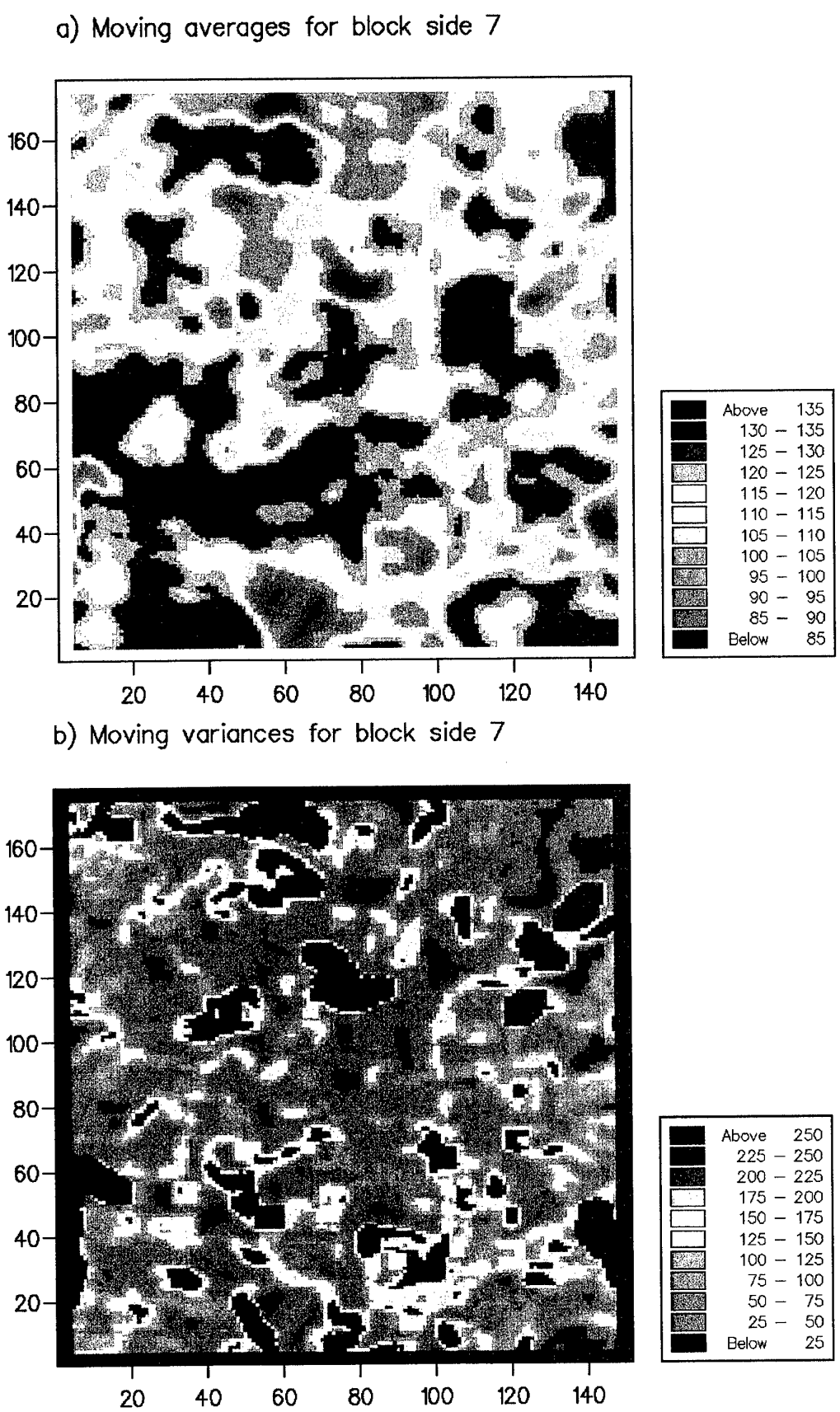

Figure 4. Pixel maps of NIR (Fort A. P. Hill): a) moving averages and b) moving variances, for blocks of side 7.

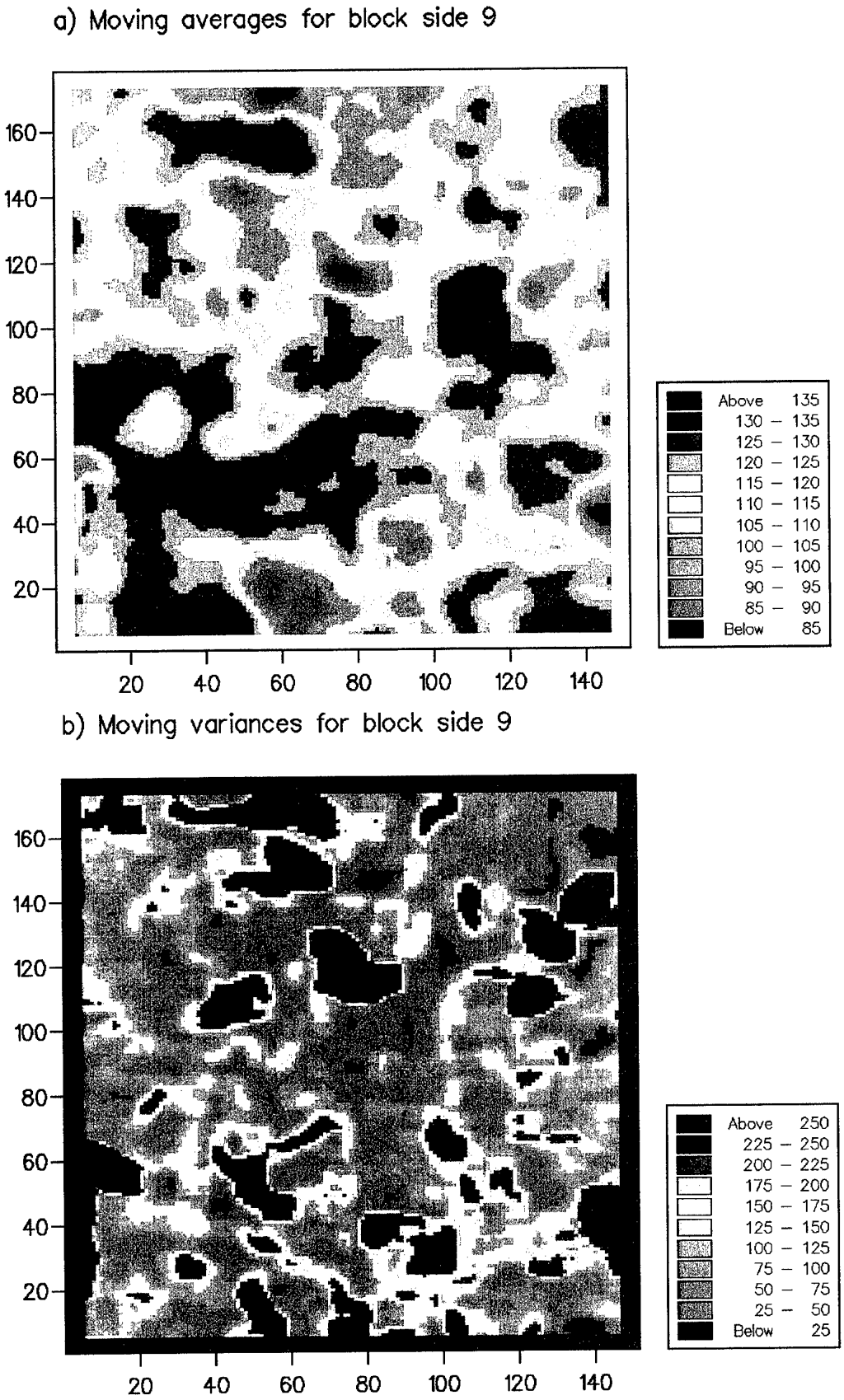

Figure 5. Pixel maps of NIR (Fort A. P. Hill): a) moving averages and b) moving variances, for blocks of side 9.

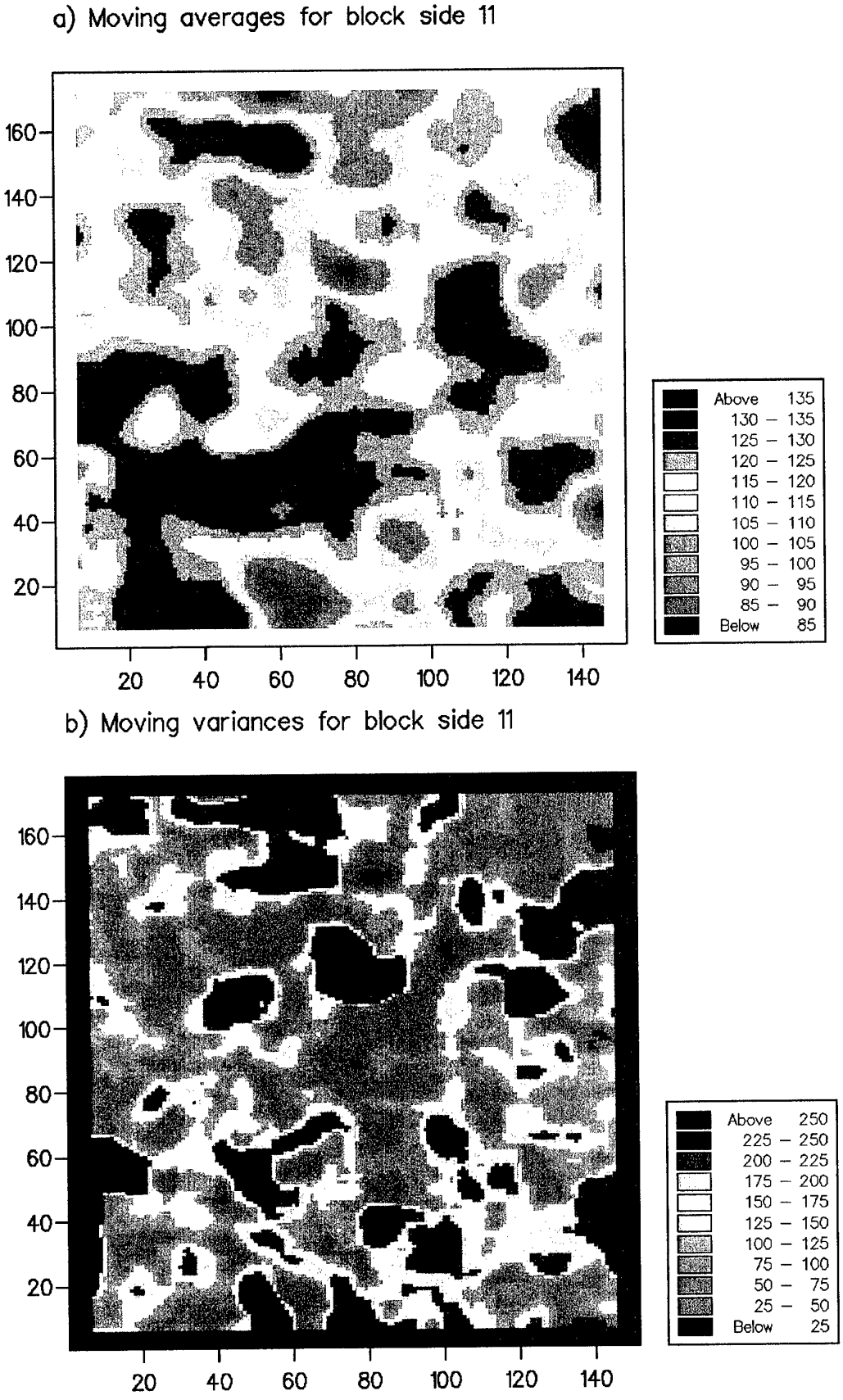

Figure 6. Pixel maps of NIR (Fort A. P. Hill): a) moving averages and b) moving variances, for blocks of side 11.

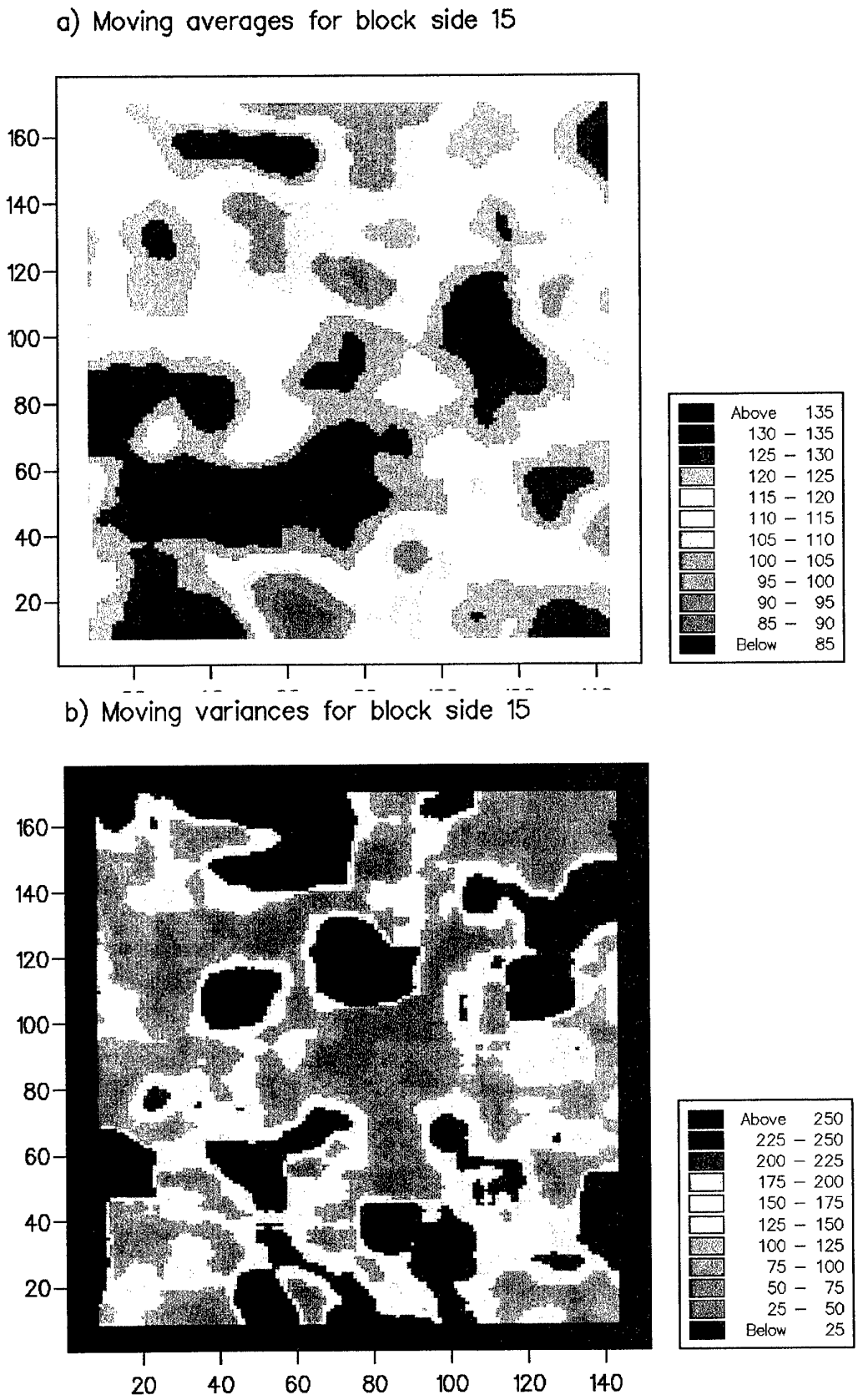

Figure 7. Pixel maps of NIR (Fort A. P. Hill): a) moving averages and b) moving variances, for blocks of side 15

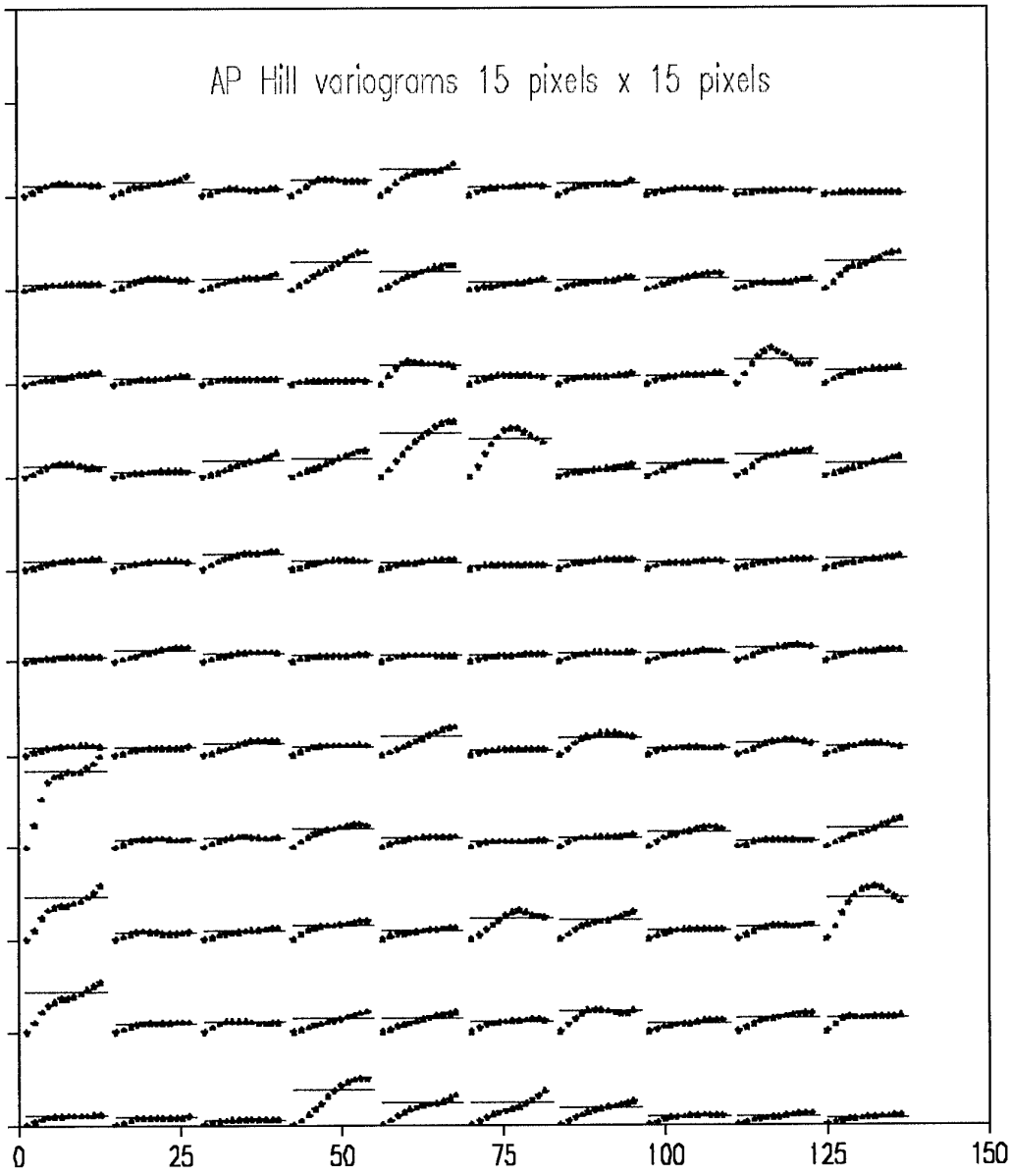

Figure 8. Mosaic of variograms that correspond to the square windows of 15 × 15 pixels.

Conclusions

The maps of moving average show increasingly clearly the coarse features of the image as the moving window is widened. There is little evidence of trend and none sufficient to suggest that the generating process is non-stationary. The maps of moving variance, however, reveal small patches where the variation is much larger than over most of the image. They suggest that the process is not stationary locally in the variance and that the intrinsic hypothesis should not be assumed.

The steeply sloping local variograms confirm this view. It was precisely in these areas of local non-stationarity that the wavelet analysis performed better than kriging in the data reconstruction (Oliver *et al.* 2000). One thing that we shall try later in this project is to use a moving variogram for kriging to compare with the wavelet results.

REPORT ON VISIT BY DR OLIVER TO TEC JUNE 14-21 2000

Part of the first morning was spent with Mr J. Shine and Mr E. Bosch discussing how the time should be spent during the visit. Several things were achieved at TEC during the four and a half days that I was there.

1) Mr Shine and I started work again on a short paper for the International Journal of Remote Sensing. This is now almost complete and needs the final conclusions to be added. The figures are now complete; the final variogram was fitted by a triple spherical function. This paper will be ready to be sent to the Journal in the near future.

2) In addition I went through various Genstat routines with Mr Shine. In trying to krige part of an image the program gave us an error message about the grid size. Since my return to England I have contacted Rothamsted Experimrntal Station where Genstat is developed and I was told that this has been resolved in the new version of the product which TEC is shortly to receive when the license is renewed.
3) In discussing the results of comparing the digital elevation model with the image data I discovered that the original data for elevation were available without having been smoothed by some form of interpolation. We extracted those using Imagine with some help for the area where we have been working. These data have now been re-analysed, but there is little improvement in the correlations.

4) Jim Shine and I were fortunate enough to have a meeting with Colonel Jack Marin from West Point. He showed us some ways of dealing with hyperspectral imagery using neural networks. We have started to analyse the 'hymap' data and we hope that the variogram will identify bands that describe different ground textures.

5) Mr E. Bosch and I worked on the soil data from England and Wales. He has done a wavelet analysis of a selected part of the data in the central part of the country. I did the factorial kriging of the same area to compare the wavelet analysis for the multispectral analysis. We shall continue with this work when Mr Bosch visits England in August.

6) I spent one day at the Virginia Institute of Marine Science. Kevin Slocum is registered as a PhD student there and I am one of his PhD committee members. His oral examination took place on June 16th. It was successful and from my perspective interesting. In the afternoon I gave a

lecture which included some general geostatistics, but mainly focused on the work that I have been involved in at TEC. I presented the factorial kriging analysis of Fort A.P.Hill and also the latest work on wavelets. The ensuing discussion was lively.

One outcome of this visit was a request to teach a short geostatistics course there.

FORT A. P. HILL: APHILLCUT

In the previous final report we examined the digital elevation model for 5-m and 20-m resolutions. Although there appears to be a relation between NIR and elevation visually this was not proved by the correlation coefficients that we computed, which were small. Mr Shine and Dr Oliver selected a section of the image that we had been working on that minimized the areas of hard-standing because we felt that these could be reducing the overall correlation.

Figure 9a shows pixel map of NIR for the part of the image called aphillcut: it is in the north western part of the original image, Figure1. It is an area of 76 × 83 pixels compared with the 151× 178 pixels of the original image: it is half the area. Figure 9b shows the pixel map of NDVI (Normalized Vegetation Index). The maps show similar patterns of variation. Variograms were recomputed and modelled for NIR and NDVI, Figure 10a and b, respectively. They show the experimental semivariances as symbols and the solid lines are the fitted models. Table 1 gives the model parameters. They were both fitted best by nested spherical functions, and their distance parameters are very similar: the short-range component is near to 140 m and the long-range one is about 230 m. The latter is shorter than that for the larger image possibly because we have fitted the model to a shorter overall lag distance because the experimental variograms became slightly irregular.

Table 1. Model parameters for selected properties

Variable	Model	Model parameters					
		c_0	c_1	c_2	a_1	a_2	α
Sub-sampled DEM	Stable exponential	0.00	105.7		5.653		1.633
NIR	Double spherical	0.00	115.4	109.1	6.577	10.49	
NDVI	Double spherical	0.00	0.002707	0.002187	6.940	11.72	

Note: c_0 is the nugget variance, c_1 and c_2 the sills of the autocorrelated variance, a_1 and a_2 the range of spatial dependence and α is the exponent parameters for the stable exponential model.

a)

b)

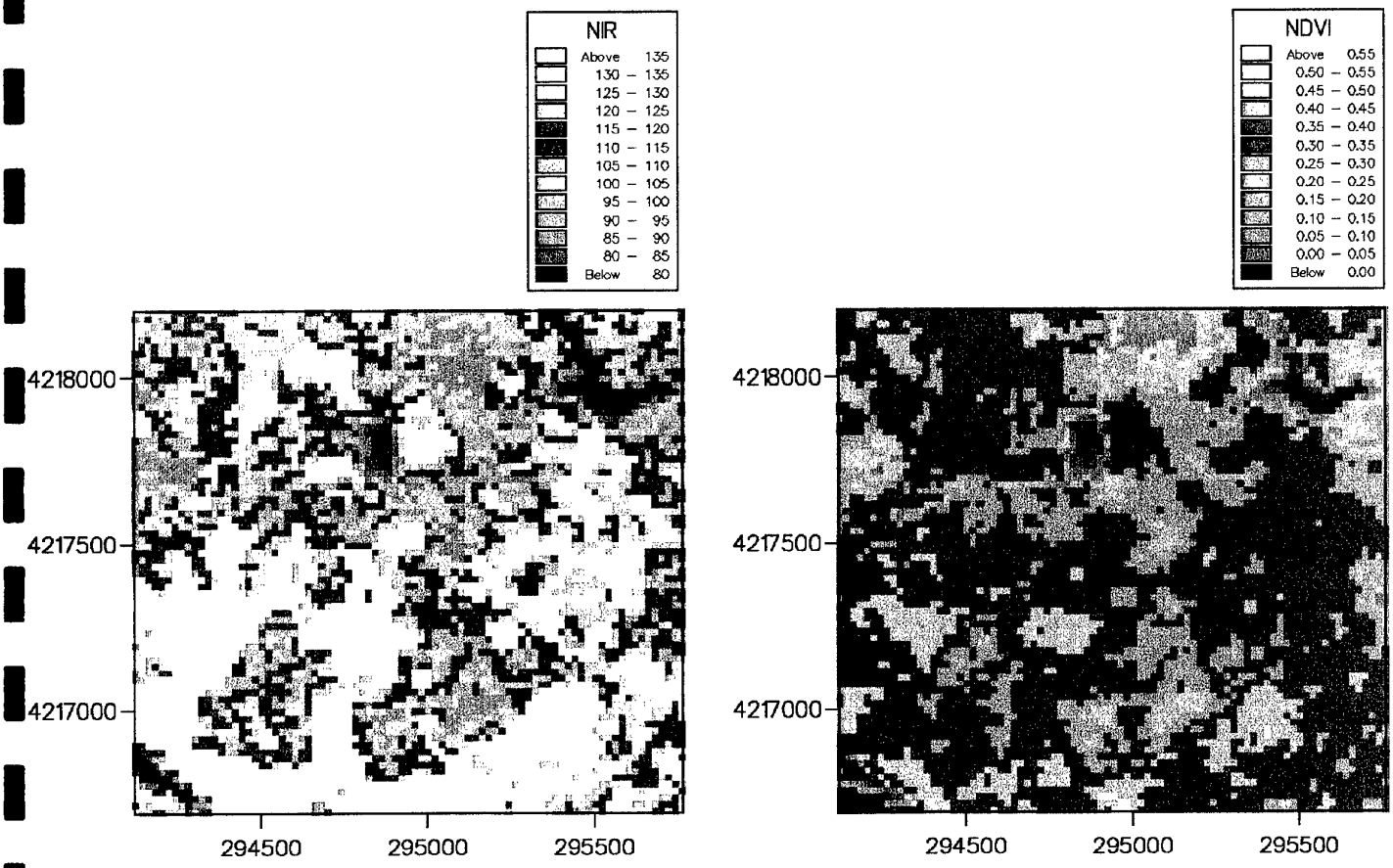

Figure 9. Pixel maps of part of the SPOT image 'aphillcut' for a) NIR and b) NDVI.

a)

b)

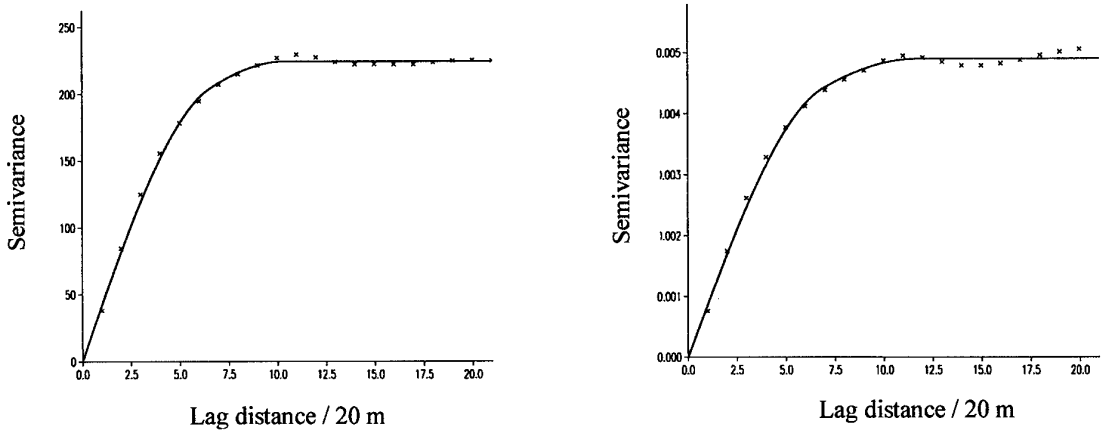

Figure 10. Experimental variograms and fitted model for a) NIR and b) NDVI, using the data from 'aphillcut'.

The original digital elevation model for this area was at a 5-m resolution. We sub-sampled this to obtain information at the same resolution as the SPOT image (20-m). At the time that these data were analysed we did not know that the DEM comprised interpolated data from 30-m resolution measurements of elevation. Both the 5-m and 20-m data elevation data showed strong trend as for the larger area. The trend was modelled by linear, quadratic and cubic functions fitted to the coordinates. Table 2 shows the proportion of the variance accounted for by the three functions for both data sets. Five transects along rows and columns of the data were selected from the image for a wavelet analysis by E. Bosch. These were also examined for trend. Table 3 gives the percentage variance accounted for by trend. It is clear that the trend is quite variable from place to place.

Table 2. Trend analysis for the original and sub-sampled DEM data.

	% variance accounted for		
	Linear	Quadratic	Cubic
Full DEM data	15.7 %	31.7 %	41.7 %
Sub-sampled DEM*	14.5 %	30.2 %	40.4 %

* DEM data was sub-sampled to match the co-ordinates of the spectral values from the SPOT data.

Table 3. Trend analysis for transects taken from the full DEM data.

Transect	% of variance accounted for by trend
Transect 1: along y axis	5.8
Transect 2: along y axis	41.5
Transect 3: along x axis	16.5
Transect 4: along x axis	21.3
Transect 5: along y axis	30.1

The variogram was computed for the 20-m elevation data using the residuals from the cubic trend function. Figure 11 a shows the experimental variogram. It is upwardly concave near to the origin and the usual models that we fit were not appropriate. Since we consider the Gaussian model to be unreliable we have fitted a stable exponential function whose equation is given by

$$\gamma(h) = c\left\{1 - \exp\left(-\frac{h^{\alpha}}{r^{\alpha}}\right)\right\}$$

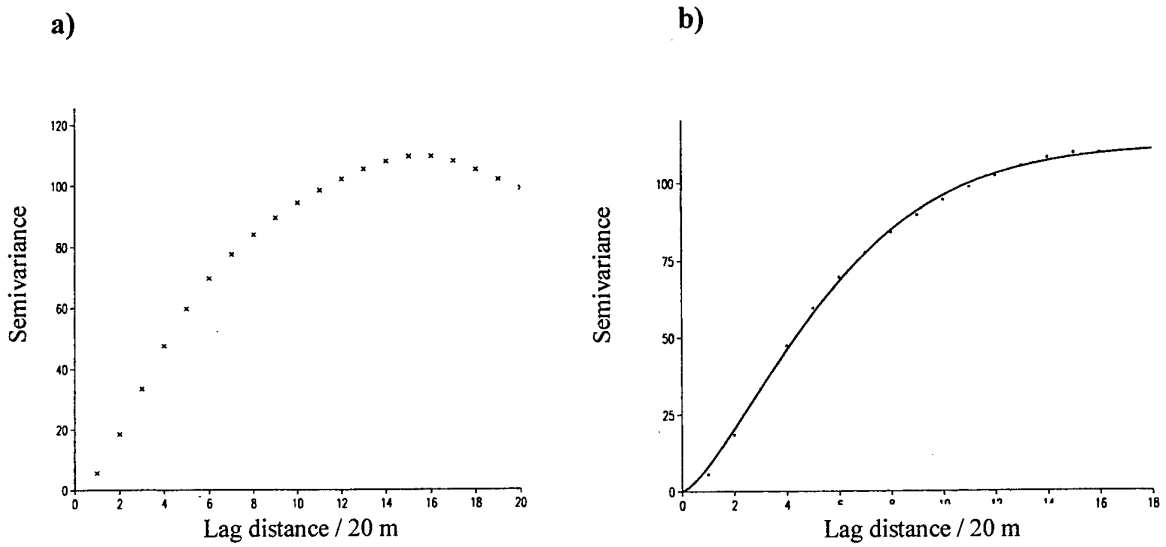

Figure 11. a) Experimental variogram for the elevation data for 'aphillcut', b) the fitted stable exponential model where the exponent was 1.6.

where c is the sill variance, h is the lag and α is an exponent that must be less than 2. Figure 11b shows the experimental semivariances and the fitted stable exponential model for elevation. Table 1 gives the model parameters. The approximate working range for the exponential function is 340 m.

To use this variogram the kriging program had to be amended, as we have not used it before for kriging. Kriging was done on the residuals (for the 20-m data) because the presence of trend violates the assumptions of geostatistics. After kriging the trend was added back to the estimates using the residuals. Figure 12 shows the kriged estimates of elevation for the 'aphillcut' area. A visual inspection of the maps for NIR (Figure 9a) and Figure 12 shows that the valley systems in the DEM correspond with the large NIR values, while the interfluves have intermediate NIR values.

For the correlation analysis the raw elevation data on a 30 m grid were used, Figure 13. They were compared with coincident pixel information for NIR and NDVI, Figure 14a and b. Figure 15a and b shows the maps of the differences between the elevation data and the pixel information from the SPOT image. Table 4 shows that these correlations between the raw data are small. Since we know from experience that local noise in data can sometimes obscure relations between variables we computed the correlation coefficients between the punctually and block kriged estimates and moving averages for the DEM, NIR and NDVI. Figures 16 and 17 show the moving averages for these variables for the 10 by 10 window. The strongest relation, albeit still weak, is between the DEM and NDVI for the moving average computed with a window of 10 × 10 pixels. It is evident that the visual relation between the observed pattern in the image data and the DEM does not appear to be as strong statistically as visually.

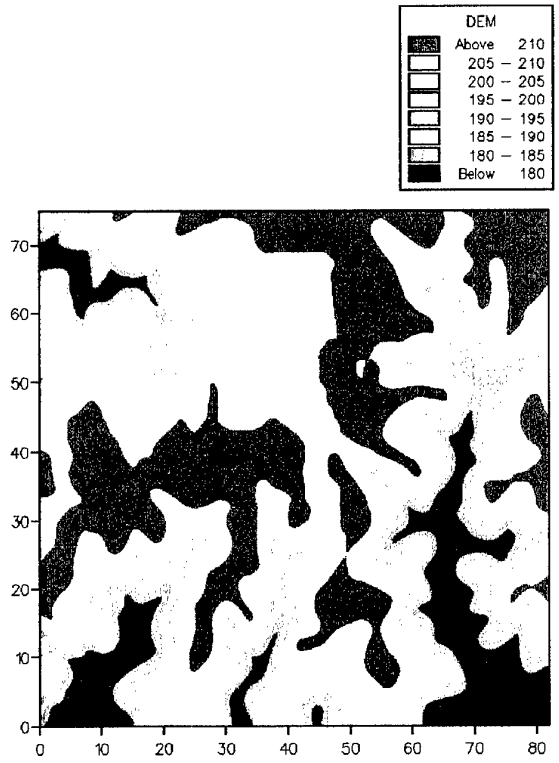

Figure 12. Map of punctually kriged estimates of elevation using the stable exponential model for 'aphillcut'.

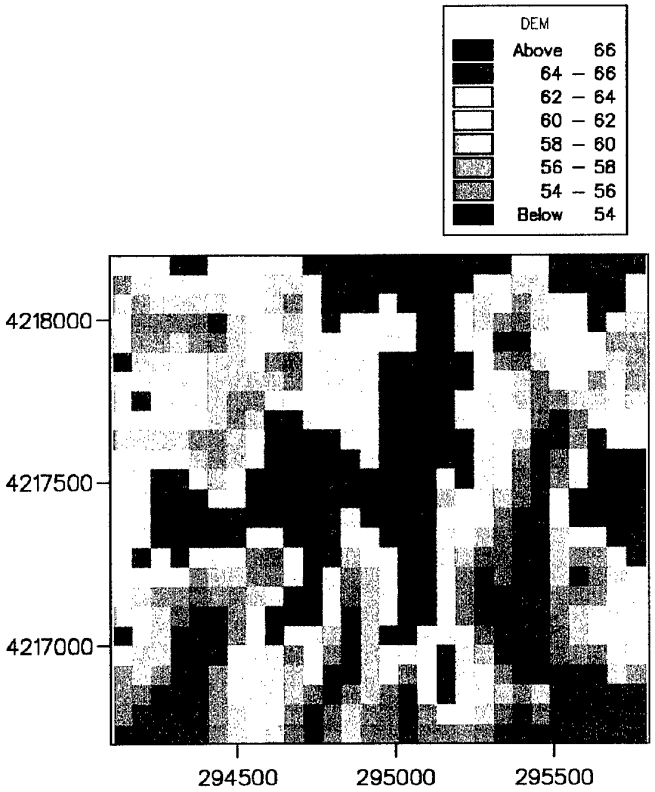

Figure 13. Pixel map of original (raw) elevation values on the 30 m grid for 'aphillcut'.

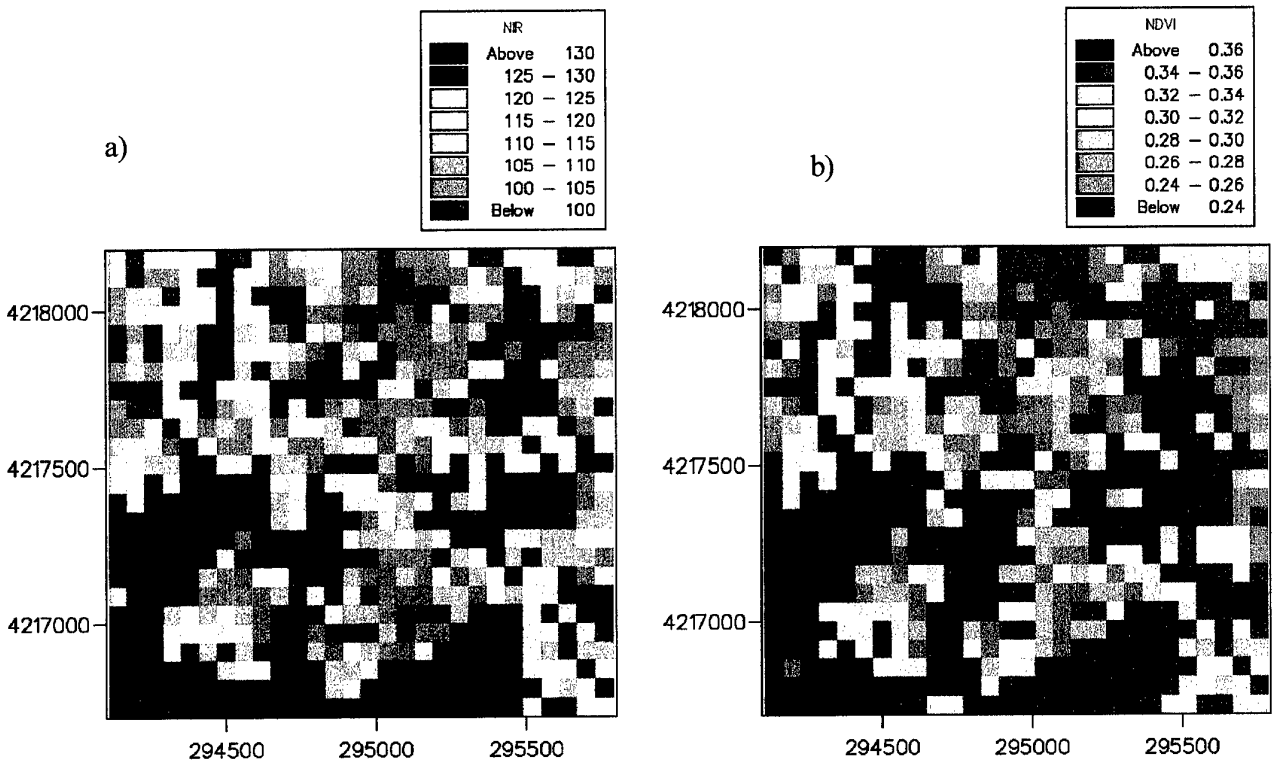

Figure 14. Pixels values of a) NIR and b) NDVI, for SPOT pixels that coincided with the raw elevation values for 'aphillcut'.

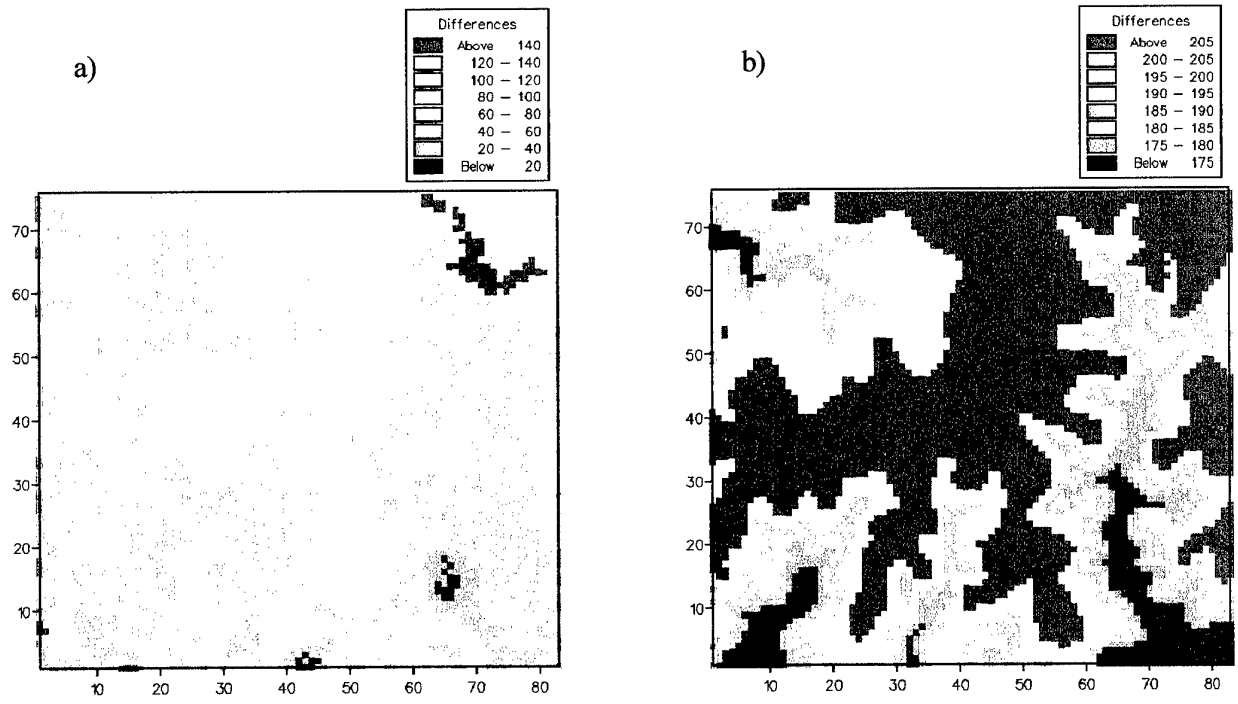

Figure 15. Differences between pixel values and elevation values for a) NIR, and. b) NDVI.

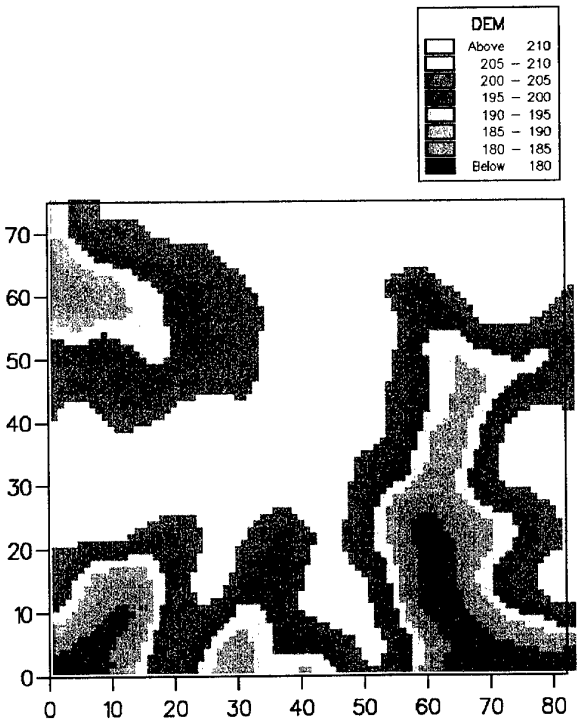

Figure 16. Pixel map of the moving average for a block of 10 × 10 pixels for elevation for 'aphillcut'.

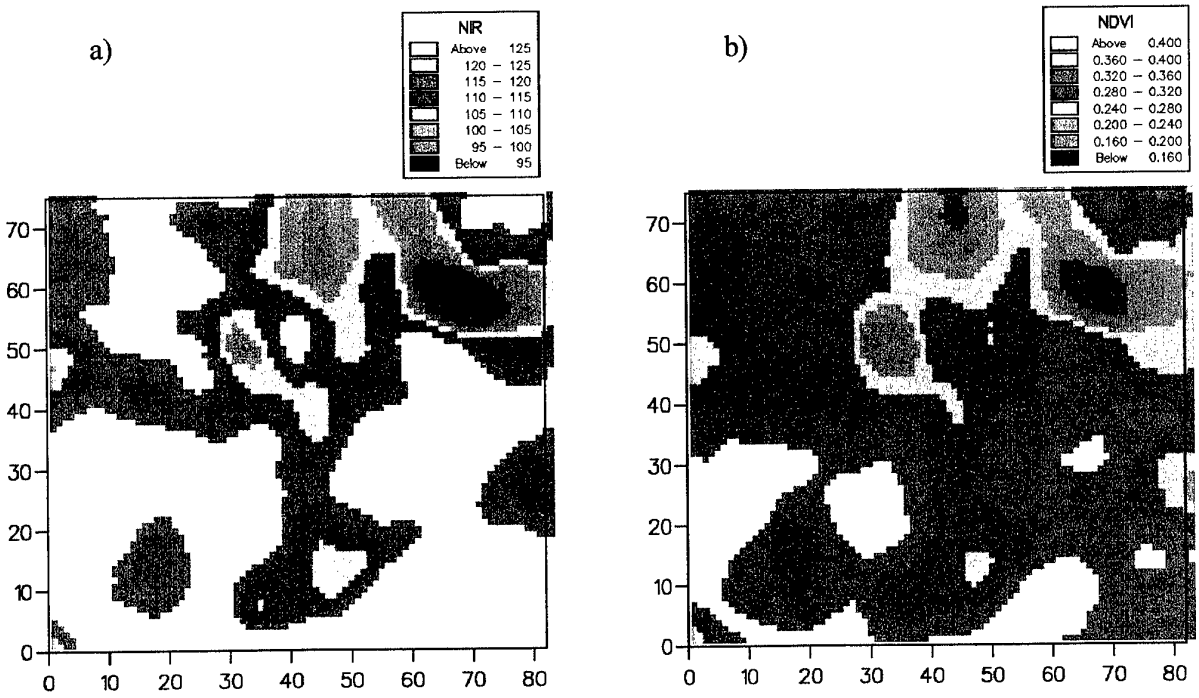

Figure 17. Pixel map of the moving average for a block of 10 × 10 pixels for a) NIR and b) NDVI, for 'aphillcut'.

Table 4. Correlation coefficients for DEM, NIR and NDVI.

Property 1	Property 2	Correlation coefficient
DEM	NIR	-0.172
DEM	NDVI	-0.175
DEM residuals	NIR	-0.034
DEM residuals	NDVI	-0.042
Block kriged DEM	Block kriged NIR	0.235
Block kriged DEM	Block kriged NDVI	0.219
DEM moving average: block side of 3	NIR moving average: block side of 3	-0.197
DEM moving average: block side of 3	NDVI moving average: block side of 3	-0.203
DEM moving average: block side of 10	NIR moving average: block side of 10	-0.315
DEM moving average: block side of 10	NDVI moving average: block side of 10	-0.330

Summary

The purpose of this detailed investigation between the DEM information and the image data was to assess the strength of their coregeonalization. If it had been stronger it could have been used to restore compressed image information using cokriging. The coregionalization is too weak to exploit in this area, but it might be worth considering elsewhere.

PART II HYPERSPECTRAL IMAGERY

The hyperspectral imagery of part of Fort A. P. Hill, Virginia, was sent as 'hymap' data in May. However, some errors were found in the original data after the analysis presented in the first interim report. Therefore, that analysis has been completely redone as part of the new analysis. The spectral information had been subdivided into 126 bands, and the pixel size is 7 m × 7m. The area examined in the report is a subset of the SPOT image examined previously. It corresponds with 'aphillcut', which is a subset of the SPOT image used for making comparisons with the digital elevation model (DEM) in more detail (see pages 15 to 22). Our aim in this investigation is to determine whether some of the bands duplicate information using principal components analysis, a non-hierarchical classification, the variogram, pixel maps and factorial kriging.

Correlation matrix

The correlation matrix was computed as part of the principal component analysis on a reduced data set of one pixel in a block of 9. Appendix 1 gives the correlation matrix. There are groups of bands with correlations greater that 0.8 showing strong relations among the bands. The most obvious groups that emerge are: bands 1 to 18, 20 to 61, 96 to 125, which is also correlated with bands 1 to 18, and 66 to 94. It is difficult to identify more subtle groupings, but those identified emerge in other analyses described later. Is it also likely that these will contain similar spatial information?.

Principal Components Analysis

Prinicpal components analysis (PCA) is a multivariate analysis that aims to reduce the dimensionality of the data to explore the relations among variables. For this reason it has been widely used for exploring hyperspectral imagery as a means of limiting the number of bands used for further analysis. However, this approach might not be entirely satisfactory because some potentially valuable information might be excluded from further analysis (Green *et al.*, 1988; Chang and Du, 1999).

The PCA was done on the correlation matrix between all of the bands (see Appendix 1). The questions posed are:
Can the number of bands containing relevant information be reduced by examining the correlation matrix or by a PCA?
Do the strongly correlated bands imply that from a spatial context these are mainly redundant and that we can look at one to obtain the information of value?
We shall examine some of the strongly correlated bands to assess whether this is so.

Tables 5 and 6 give the results of the principal component analysis (PCA). Table 5 gives the latent roots or eigenvalues of the first ten principal axes. The first two account for just over 90% of the variation, Table 5. This is an expression of the extent of correlation between the wavebands. Table 6 gives the latent vectors for the first five principal axes

only since those for roots 6 to 10 account for so little of the variation. For PC1 bands 18 to 19, 61 to 62, 66 to 94 and 99 to 122 have large latent vectors. For PC2 bands 20 to 59 have large values, and for PC3 it is bands 1 to 13. For PC4 bands 63 to 66, and band 95 have large latent vectors and for PC5 it is band 126. For PCs 6 to 10 the wavebands that have large values for PCs 4 and 5 dominate; little new information appears to emerge. The limiting values of the latent vectors have been chosen by eye, based on the level at which there is an abrupt change to a smaller value.

Figure 17 shows the spectrum of a range of ground cover types. In general they have a similar form with distinct changes occurring at certain points in the spectrum for most ground cover types. It is interesting to observe that boundaries or changes occur at waveband positions: 13, 18, 35 to 37, 47, 58, 60, 63, 70 and 94. These have some association with the groupings of the wavebands that have large latent vectors for PCs 1 and 2, and is what we might expect.

Table 5 Selected latent roots or eigenvalues of the correlation matrix for the hyperspectral image data

Latent Roots	Latent roots	% variance
1	83.65	66.39
2	33.40	26.51
3	3.90	3.09
4	1.93	1.53
5	0.71	0.56
6	0.41	0.33
7	0.37	0.30
8	0.29	0.23
9	0.26	0.20
10	0.20	0.16

Table 6. Latent vectors or eigenvectors of the correlation matrix for the hyperspectral image datafor the first five principal components.

	PC1	PC2	PC3	PC4	PC5
	1.0000	2.0000	3.0000	4.0000	5.0000
1	-0.0782	-0.0654	0.2224	0.0912	-0.0746
2	-0.0764	-0.0900	0.2281	0.0312	-0.0266
3	-0.0773	-0.0928	0.2191	0.0249	-0.0165
4	-0.0779	-0.0945	0.2117	0.0196	-0.0115
5	-0.0791	-0.0944	0.2071	0.0142	-0.0184
6	-0.0830	-0.0857	0.2101	0.0111	-0.0358
7	-0.0894	-0.0636	0.2157	0.0071	-0.0694
8	-0.0924	-0.0507	0.2129	0.0044	-0.0818
9	-0.0928	-0.0526	0.2039	0.0057	-0.0744
10	-0.0905	-0.0682	0.1914	-0.0003	-0.0731
11	-0.0889	-0.0780	0.1774	-0.0053	-0.0646
12	-0.0888	-0.0823	0.1626	-0.0054	-0.0525
13	-0.0883	-0.0869	0.1474	-0.0040	-0.0395
14	-0.0873	-0.0910	0.1360	-0.0159	-0.0577
15	-0.0863	-0.0959	0.1224	-0.0122	-0.0309
16	-0.0855	-0.0993	0.1101	-0.0124	-0.0156
17	-0.0875	-0.0956	0.1022	-0.0115	-0.0139
18	-0.1008	-0.0423	0.1097	-0.0188	-0.0791
19	-0.0994	0.0472	0.1084	-0.0032	-0.0731
20	-0.0802	0.1091	0.1058	0.0129	-0.0250
21	-0.0681	0.1298	0.1019	0.0254	0.0113
22	-0.0641	0.1352	0.0955	0.0309	0.0278
23	-0.0628	0.1369	0.0949	0.0265	0.0308
24	-0.0630	0.1373	0.0898	0.0281	0.0330
25	-0.0633	0.1374	0.0852	0.0273	0.0337
26	-0.0637	0.1373	0.0806	0.0250	0.0345
27	-0.0636	0.1377	0.0766	0.0252	0.0363
28	-0.0634	0.1382	0.0737	0.0254	0.0385
29	-0.0635	0.1382	0.0708	0.0233	0.0376
30	-0.0641	0.1379	0.0668	0.0242	0.0386
31	-0.0641	0.1378	0.0666	0.0243	0.0388
32	-0.0650	0.1368	0.0589	0.0274	0.0430
33	-0.0661	0.1358	0.0591	0.0140	0.0332
34	-0.0674	0.1344	0.0482	0.0224	0.0413
35	-0.0700	0.1317	0.0441	0.0123	0.0299
36	-0.0709	0.1303	0.0406	0.0053	0.0242
37	-0.0712	0.1302	0.0373	0.0036	0.0250
38	-0.0710	0.1309	0.0340	0.0079	0.0316
39	-0.0703	0.1317	0.0322	0.0112	0.0366
40	-0.0692	0.1331	0.0343	0.0097	0.0378
41	-0.0686	0.1339	0.0348	0.0077	0.0362
42	-0.0682	0.1344	0.0333	0.0081	0.0389
43	-0.0681	0.1345	0.0327	0.0060	0.0382
44	-0.0686	0.1338	0.0286	0.0077	0.0399
45	-0.0699	0.1322	0.0235	0.0090	0.0413
46	-0.0718	0.1294	0.0180	0.0112	0.0406
47	-0.0762	0.1237	0.0085	-0.0039	0.0181
48	-0.0810	0.1155	-0.0057	-0.0128	0.0058
49	-0.0837	0.1102	-0.0139	-0.0172	-0.0052
50	-0.0849	0.1082	-0.0189	-0.0154	-0.0041

51	-0.0861	0.1060	-0.0256	-0.0111	-0.0004
52	-0.0863	0.1054	-0.0262	-0.0135	-0.0037
53	-0.0857	0.1067	-0.0266	-0.0149	-0.0008
54	-0.0848	0.1084	-0.0275	-0.0124	0.0044
55	-0.0844	0.1091	-0.0298	-0.0093	0.0095
56	-0.0842	0.1093	-0.0306	-0.0116	0.0093
57	-0.0846	0.1084	-0.0320	-0.0147	0.0053
58	-0.0856	0.1062	-0.0371	-0.0142	0.0073
59	-0.0873	0.1022	-0.0433	-0.0156	0.0069
60	-0.0898	0.0961	-0.0516	-0.0176	0.0056
61	-0.0923	0.0883	-0.0606	-0.0131	0.0126
62	-0.0920	0.0845	-0.0660	0.0005	0.0333
63	-0.0222	-0.0092	-0.0652	0.5980	-0.1605
64	-0.0386	-0.0201	-0.0758	0.5664	-0.1191
65	-0.0735	-0.0417	-0.0876	0.3890	-0.0471
66	-0.0947	-0.0524	-0.0924	0.1789	0.0144
67	-0.1007	-0.0548	-0.0816	0.0605	0.0059
68	-0.1020	-0.0508	-0.0810	0.0524	0.0018
69	-0.1035	-0.0446	-0.0844	0.0201	0.0216
70	-0.1046	-0.0385	-0.0856	-0.0049	0.0086
71	-0.1056	-0.0313	-0.0868	-0.0192	-0.0124
72	-0.1063	-0.0242	-0.0887	-0.0234	-0.0246
73	-0.1067	-0.0176	-0.0902	-0.0234	-0.0337
74	-0.1070	-0.0118	-0.0904	-0.0260	-0.0426
75	-0.1072	-0.0068	-0.0899	-0.0299	-0.0534
76	-0.1072	-0.0025	-0.0912	-0.0266	-0.0524
77	-0.1072	0.0010	-0.0914	-0.0273	-0.0569
78	-0.1070	0.0038	-0.0937	-0.0240	-0.0548
79	-0.1069	0.0063	-0.0936	-0.0274	-0.0619
80	-0.1068	0.0082	-0.0937	-0.0288	-0.0651
81	-0.1068	0.0091	-0.0933	-0.0277	-0.0679
82	-0.1068	0.0091	-0.0916	-0.0286	-0.0718
83	-0.1068	0.0087	-0.0894	-0.0311	-0.0739
84	-0.1069	0.0080	-0.0889	-0.0283	-0.0703
85	-0.1070	0.0061	-0.0855	-0.0361	-0.0739
86	-0.1070	0.0028	-0.0851	-0.0329	-0.0703
87	-0.1071	0.0005	-0.0827	-0.0345	-0.0732
88	-0.1072	-0.0019	-0.0817	-0.0355	-0.0683
89	-0.1072	-0.0040	-0.0830	-0.0356	-0.0659
90	-0.1072	-0.0068	-0.0828	-0.0377	-0.0655
91	-0.1071	-0.0093	-0.0819	-0.0433	-0.0674
92	-0.1070	-0.0115	-0.0833	-0.0434	-0.0609
93	-0.1067	-0.0122	-0.0827	-0.0445	-0.0702
94	-0.1041	-0.0133	-0.0810	-0.0462	-0.0727
95	-0.0651	-0.0817	-0.0375	0.2465	0.3031
96	-0.0849	-0.1015	-0.0266	0.0329	0.1521
97	-0.0873	-0.0999	-0.0254	-0.0140	0.0720
98	-0.0889	-0.0960	-0.0299	-0.0146	0.0365
99	-0.0916	-0.0903	-0.0374	0.0041	0.0997
100	-0.0933	-0.0873	-0.0251	-0.0247	0.0376
101	-0.0951	-0.0836	-0.0203	-0.0177	0.0403
102	-0.0967	-0.0794	-0.0168	-0.0162	0.0427
103	-0.0978	-0.0759	-0.0138	-0.0232	0.0228
104	-0.0988	-0.0729	-0.0153	-0.0229	0.0185
105	-0.0995	-0.0705	-0.0166	-0.0262	0.0037
106	-0.1001	-0.0681	-0.0204	-0.0276	-0.0037

107	-0.1007	-0.0656	-0.0263	-0.0289	-0.0091
108	-0.1013	-0.0627	-0.0335	-0.0304	-0.0151
109	-0.1020	-0.0597	-0.0425	-0.0268	-0.0097
110	-0.1022	-0.0584	-0.0443	-0.0284	-0.0106
111	-0.1022	-0.0584	-0.0420	-0.0292	-0.0099
112	-0.1019	-0.0602	-0.0369	-0.0263	-0.0002
113	-0.1011	-0.0639	-0.0267	-0.0218	0.0085
114	-0.1002	-0.0670	-0.0222	-0.0235	0.0064
115	-0.0994	-0.0699	-0.0234	-0.0188	0.0246
116	-0.0989	-0.0714	-0.0262	-0.0191	0.0277
117	-0.0982	-0.0730	-0.0285	-0.0283	0.0275
118	-0.0970	-0.0770	-0.0264	-0.0206	0.0536
119	-0.0958	-0.0805	-0.0188	-0.0256	0.0438
120	-0.0942	-0.0849	-0.0153	-0.0199	0.0702
121	-0.0929	-0.0877	-0.0084	-0.0288	0.0500
122	-0.0906	-0.0918	-0.0071	-0.0083	0.1073
123	-0.0896	-0.0941	0.0006	-0.0183	0.0850
124	-0.0865	-0.0960	0.0044	-0.0050	0.1211
125	-0.0837	-0.0957	0.0119	0.0043	0.1422
126	-0.0558	-0.0700	0.0010	0.0736	0.7547

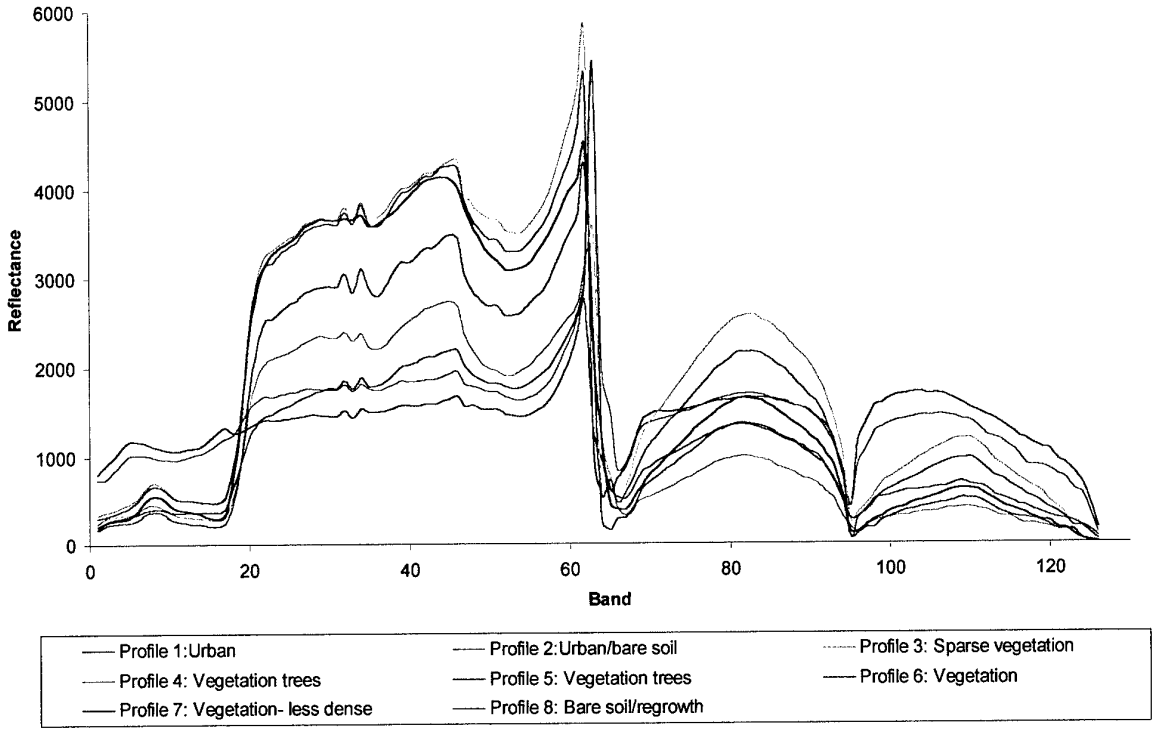

Figure 18 Spectral information from the hymap image of part of A. P. Hill for six ground cover types.

Non-hierarchical classification

For this multivariate classification (see Webster and Oliver, 1990) there is no assumption that there is any hierarchy in the multivariate structure of the data. The majority of multivariate methods of classification are based on a hierarchy of classes, such as nearest neighbour, median clustering etc. Since there is no natural hierarchical structure in the spectral data the non-hierarchical method was used. The subdivision occurs at one level only, and the method is often known as dynamic clustering. Essentially the aim is to minimize the variation within groups and maximize that between them based on a selected mathematical criterion. These include the sum of squares (SSP) within classes, Wilks' criterion or the trace $\mathbf{W}^{-1}\mathbf{B}$, where $\mathbf{W}$ is the SSP matrix within groups and $\mathbf{B}$ is the between-groups SSP matrix. The chosen test criterion is calculated after an arbitrary partition of the data (or a pre-existing classification can be used if available), and individuals are moved from group to group and the criterion calculated afresh each time. The procedure continues iteratively until no improvement seems possible. In Genstat (Genstat 5 Committee, 1993) local optimal solutions in the classification are avoided by

changing to moving pairs of individuals and then returning to single ones again (see Webster and Oliver, 1990 for more detail).

For this analysis I wanted to classify the wavebands and not the pixels, therefore I selected the bands for just 52 pixels scattered over the image. These data were then reorganised so that the bands appeared as the individuals and the pixels as the variables. I used the three criteria given above, but the results for the sum of squares within criterion was the only one to give a satisfactory result. This was because of the degree of correlation in the data. To avoid possible problems from local optima I started with 15 classes and went in steps of one to six classes. The criterion value was plotted against the number of classes, Figure19. The class at which the greatest change in the criterion value occurred was selected. This was for 8 classes in this analysis. The wavebands belonging to each class are given in Table 9. They show some relation with the bands associated with the first 5 PCs, and also with the major changes in the spectrum, Figure18. It is evident at this early stage of the analysis that some patterns are emerging.

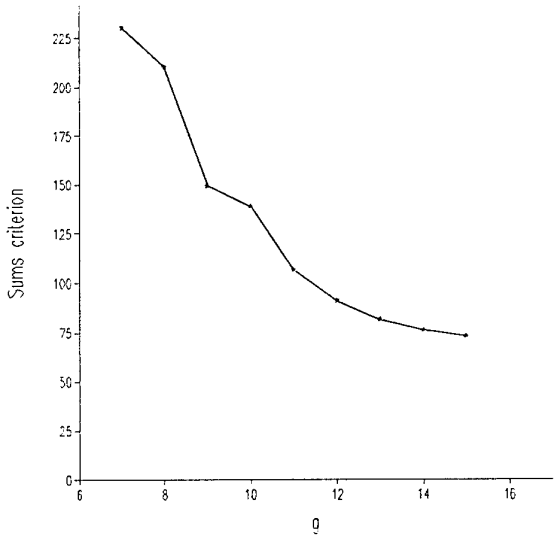

Figure 19. Sum of squares within criterion plotted against group size, g.

Variography

Experimental variograms were computed from the full pixel information for all wavebands, Figures 20 to 30. Several bands have variograms with similar forms. Overall there appear to be six main shapes of variogram evident, disregarding the size of the nugget and sill variances. The variograms within the following groups of bands appear to be similar: bands (a) 1 to 17; (b) 20 to 62; (c) 63 to 64; (d) 19, 65, 71 to 94, 126; (e) 66 to 70, 95; (f) 96 to 125, 18 (see also Table 9). These show some relation with the groups identified by the non-hierarchical classification and the PCA. Bands 63 and 64 have pure nugget variograms, which are different from all of the others, and bands 95 and 126 also have variograms that are different which also emerges in the results of the PCA.

The experimental variograms of bands 1 to 18 and 65 to 126 have a wavelike form which suggests that there is some repetition in the variation at a distance of about 1000 m. We can be fairly certain that this is not a sampling effect because of the large size of the data set. This repetition is likely to relate to the nature of the physiography in the region, for example the two large valley systems (see Figure12).

Experimental variograms were also computed from the scores of the first five principal components (Figure 31). The variograms for PC1 to PC3 resemble some of the main structural features seen in the individual variograms, but not precisely so. The experimental variograms for PC4 is pure nugget, which resembles the variograms for bands 63 and 64, which also load heavily on this component. Therefore, we can interpret this component as containing no spatial information. The variogram for PC5 shows some structure, albeit little. It has a form similar to the variogram for band 126, which also loads heavily on PC5.

Overall the variograms suggest that there is little noise in the wavebands, apart from bands 63, 64 and 126. This is of interest since most variograms show strong spatial structure. The PCA also identified these wavebands that exhibit little structure.

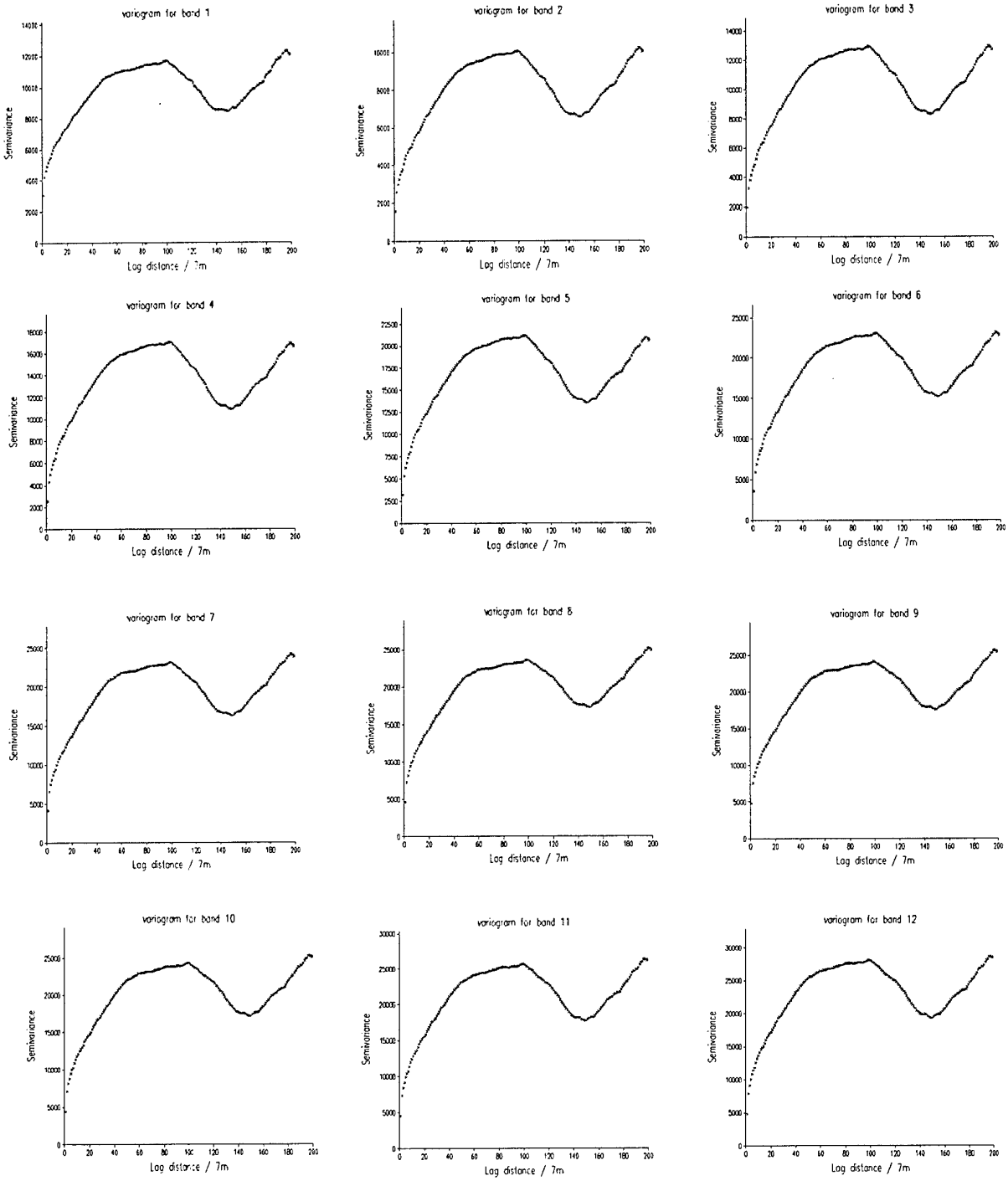

Figure 20. Experimental variograms for bands 1 to 12.

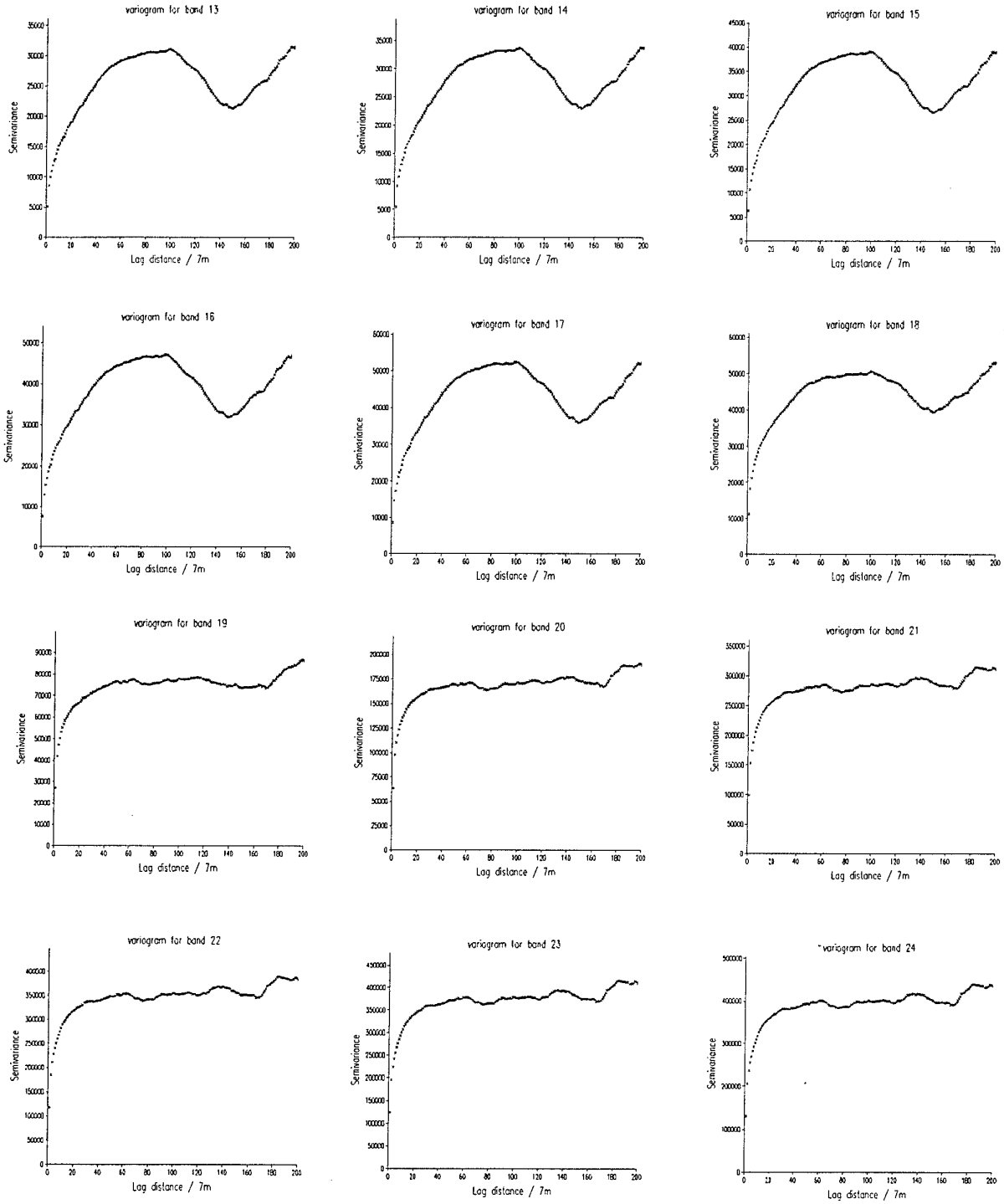

Figure 21. Experimental variograms for bands 13 to 24.

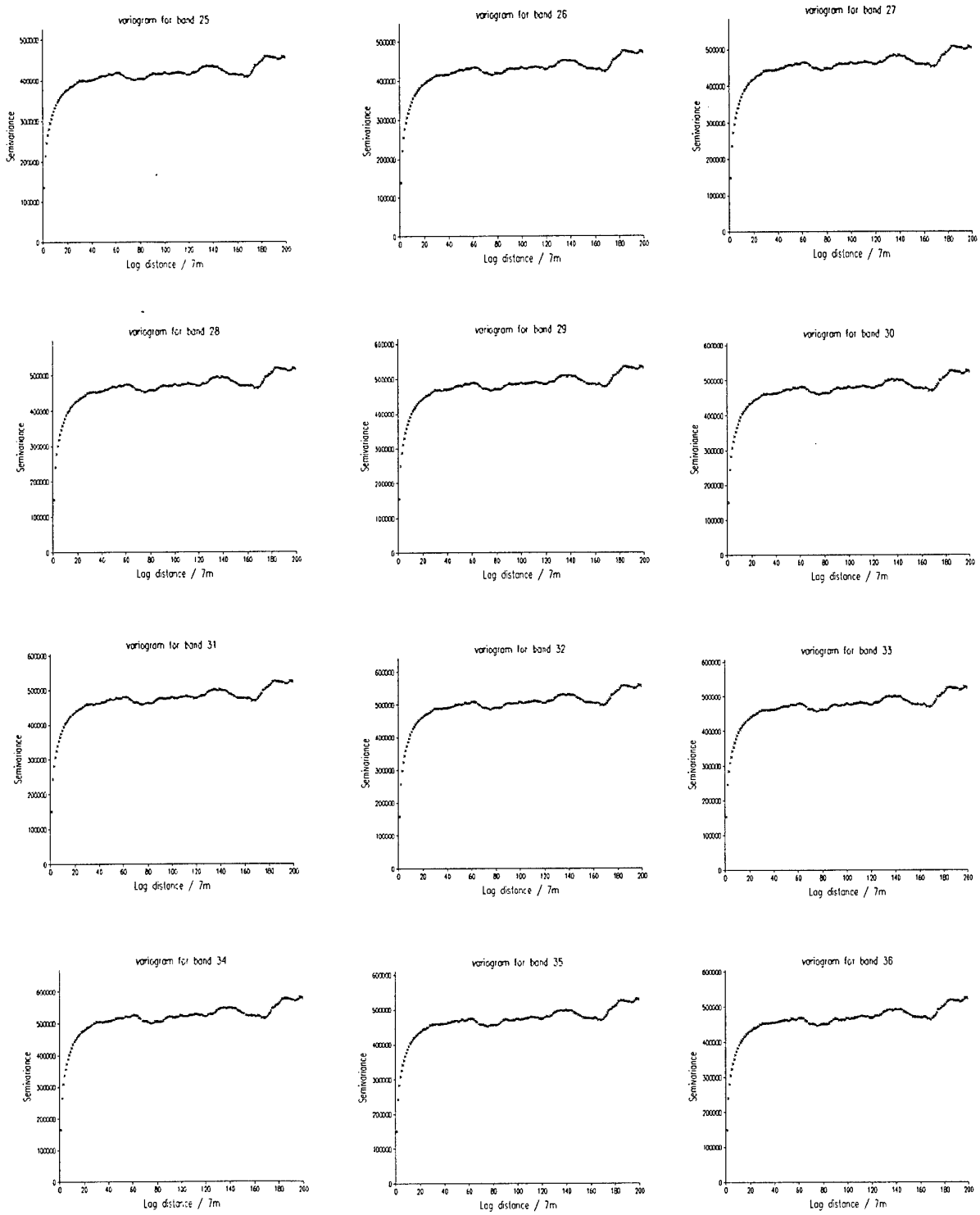

Figure 22. Experimental variograms for bands 25 to 36.

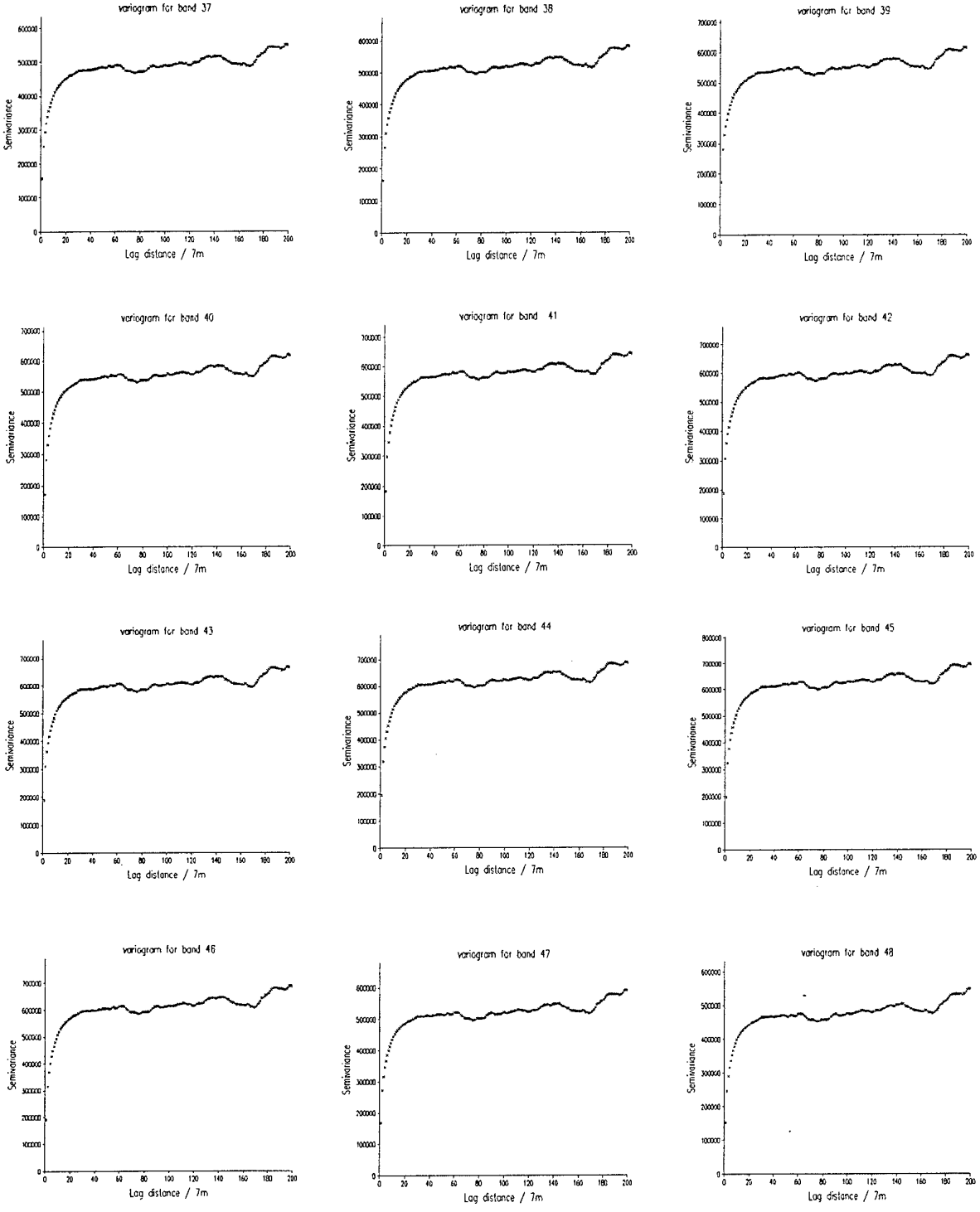

Figure 23. Experimental variograms for bands 37 to 48.

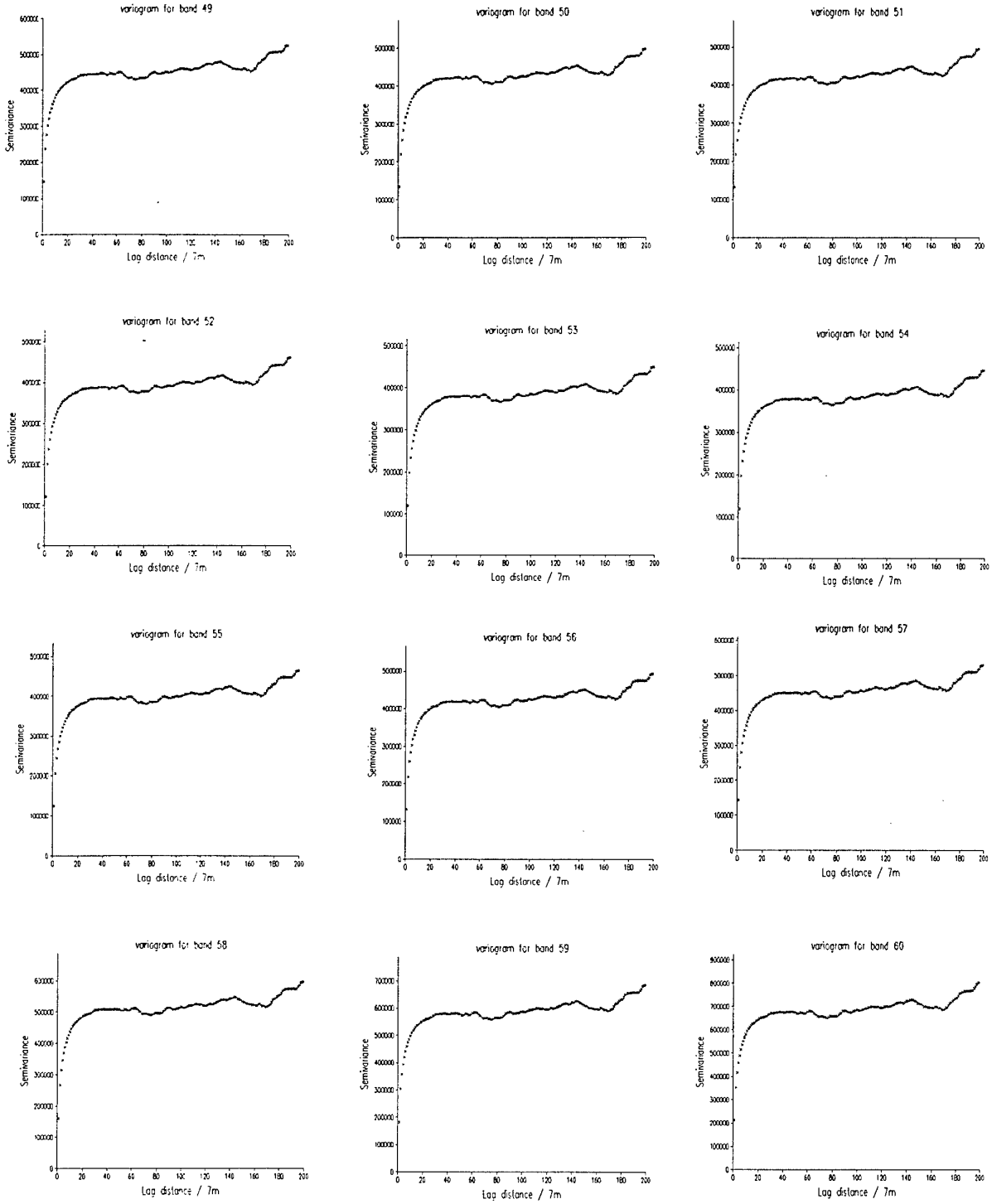

Figure 24. Experimental variograms for bands 49 to 60.

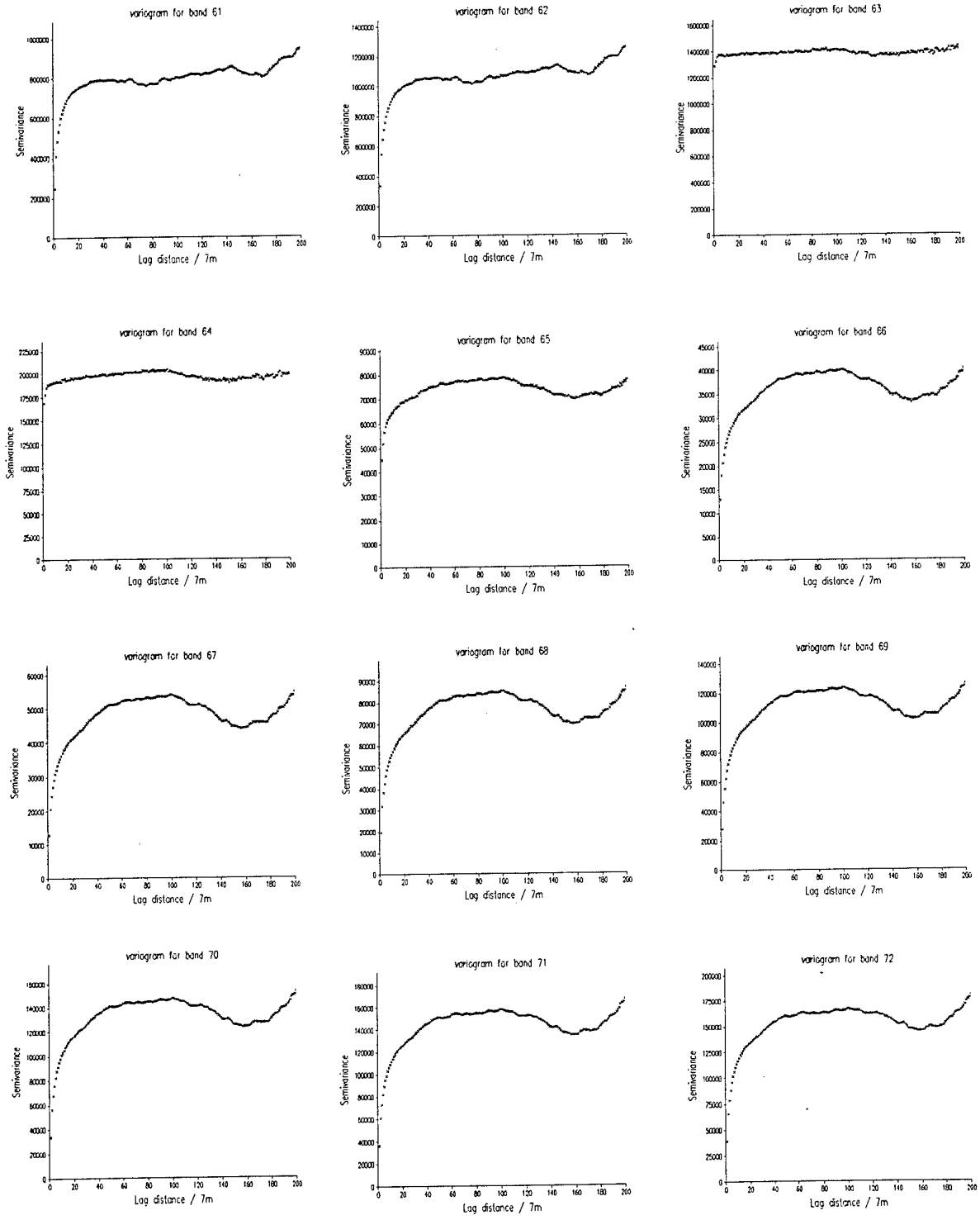

Figure 25. Experimental variograms for bands 61 to 72.

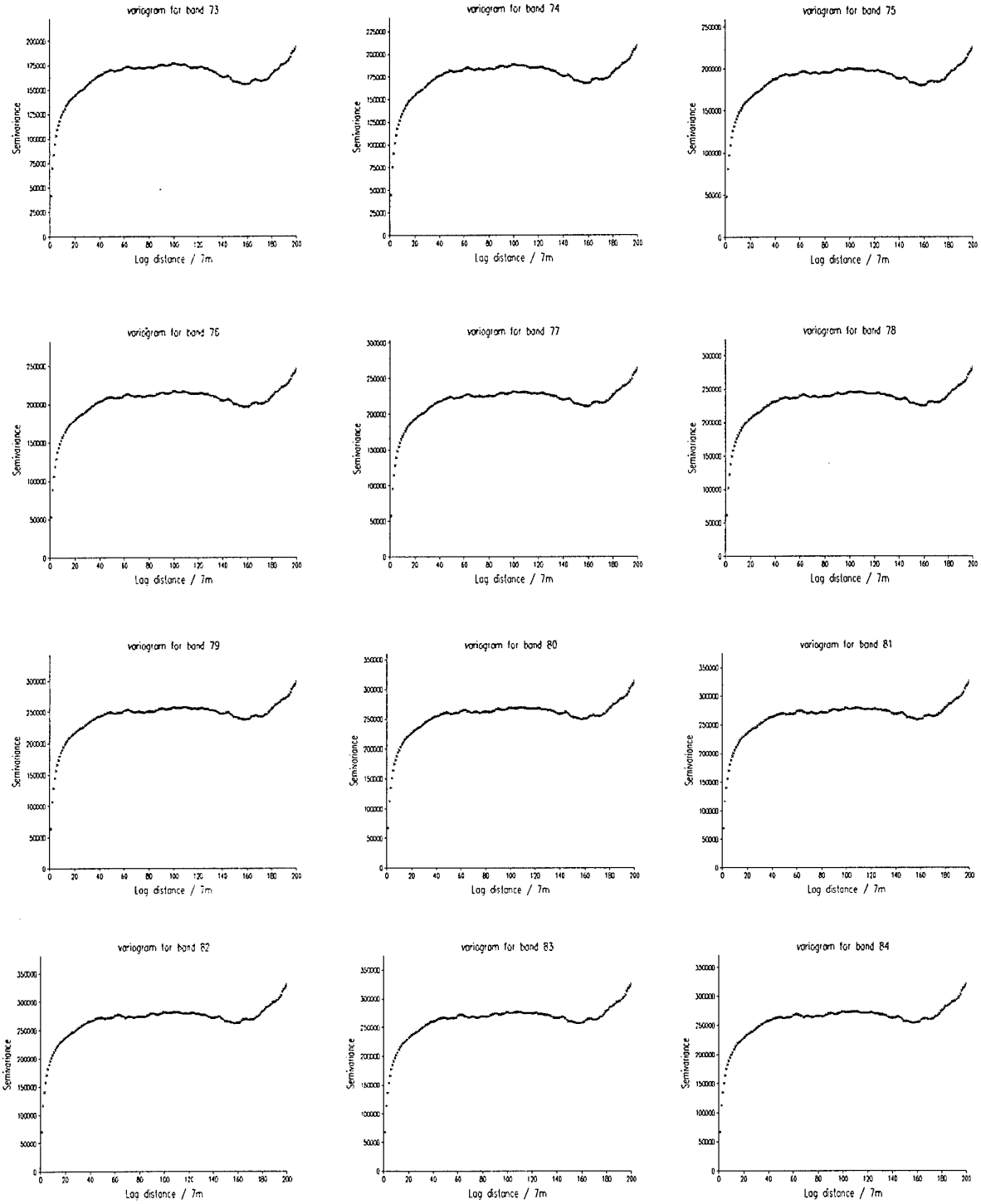

Figure 26. Experimental variograms for bands 73 to 84.

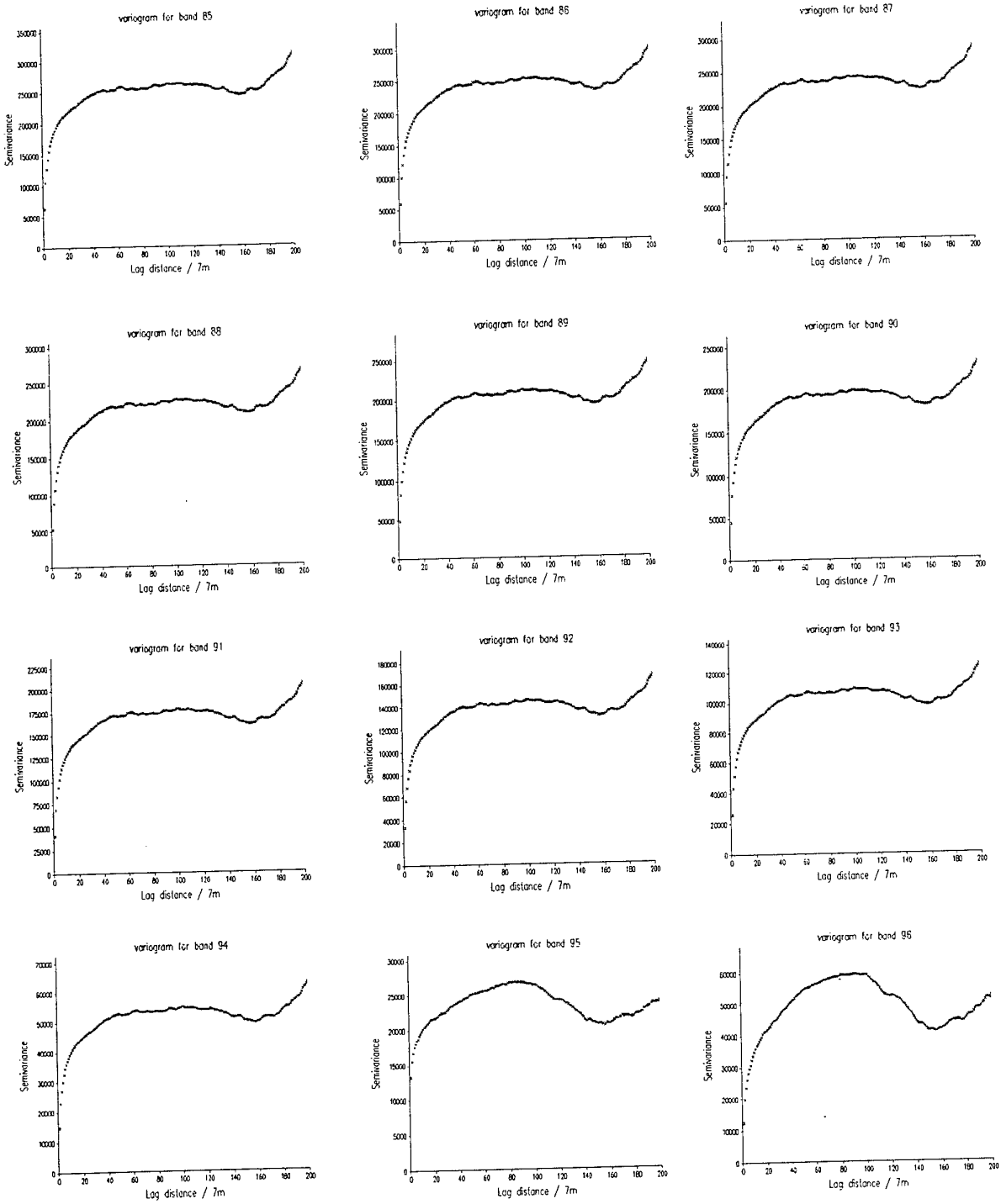

Figure 27. Experimental variograms for bands 85 to 96

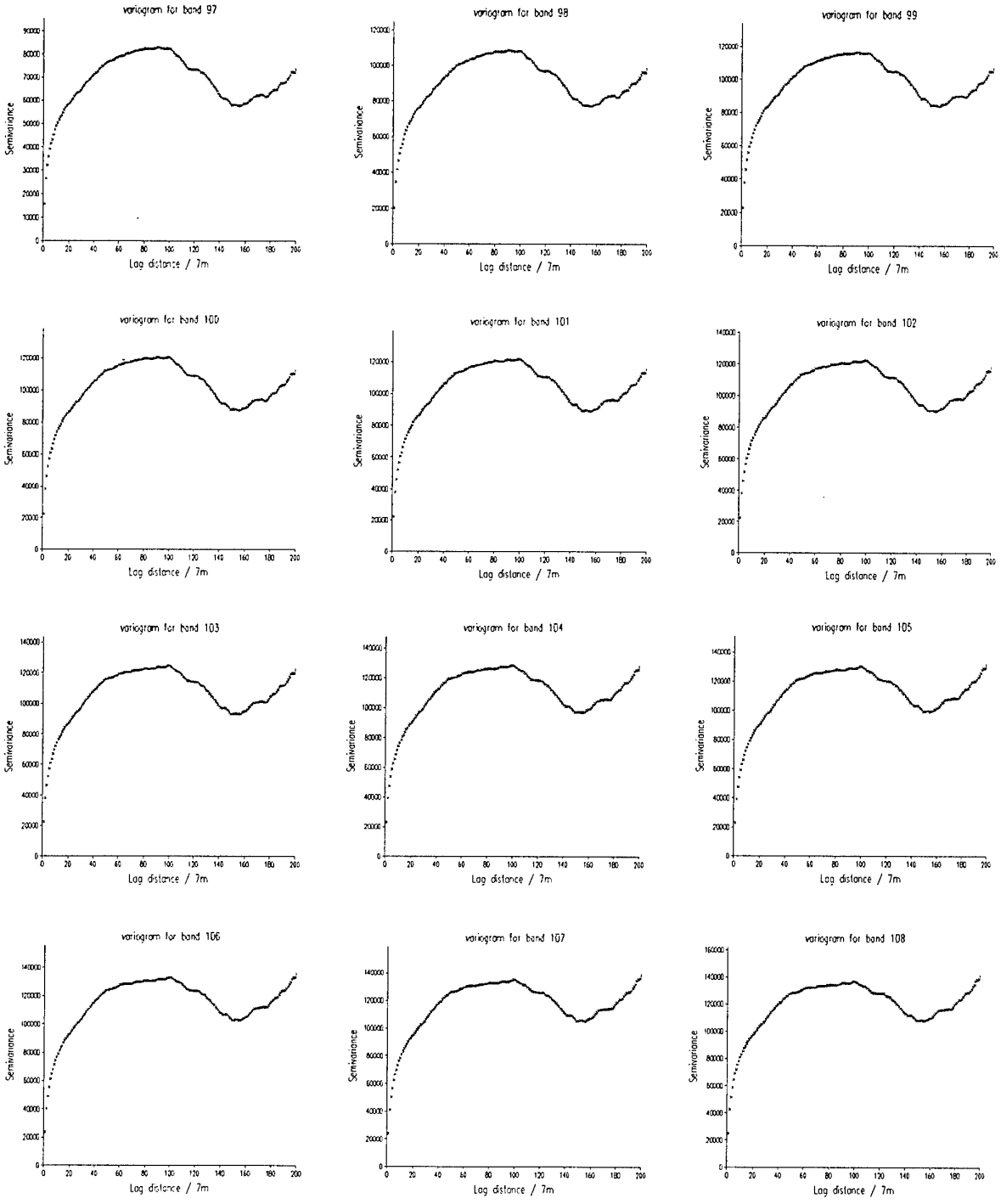

Figure 28. Experimental variograms for bands 97 to 108

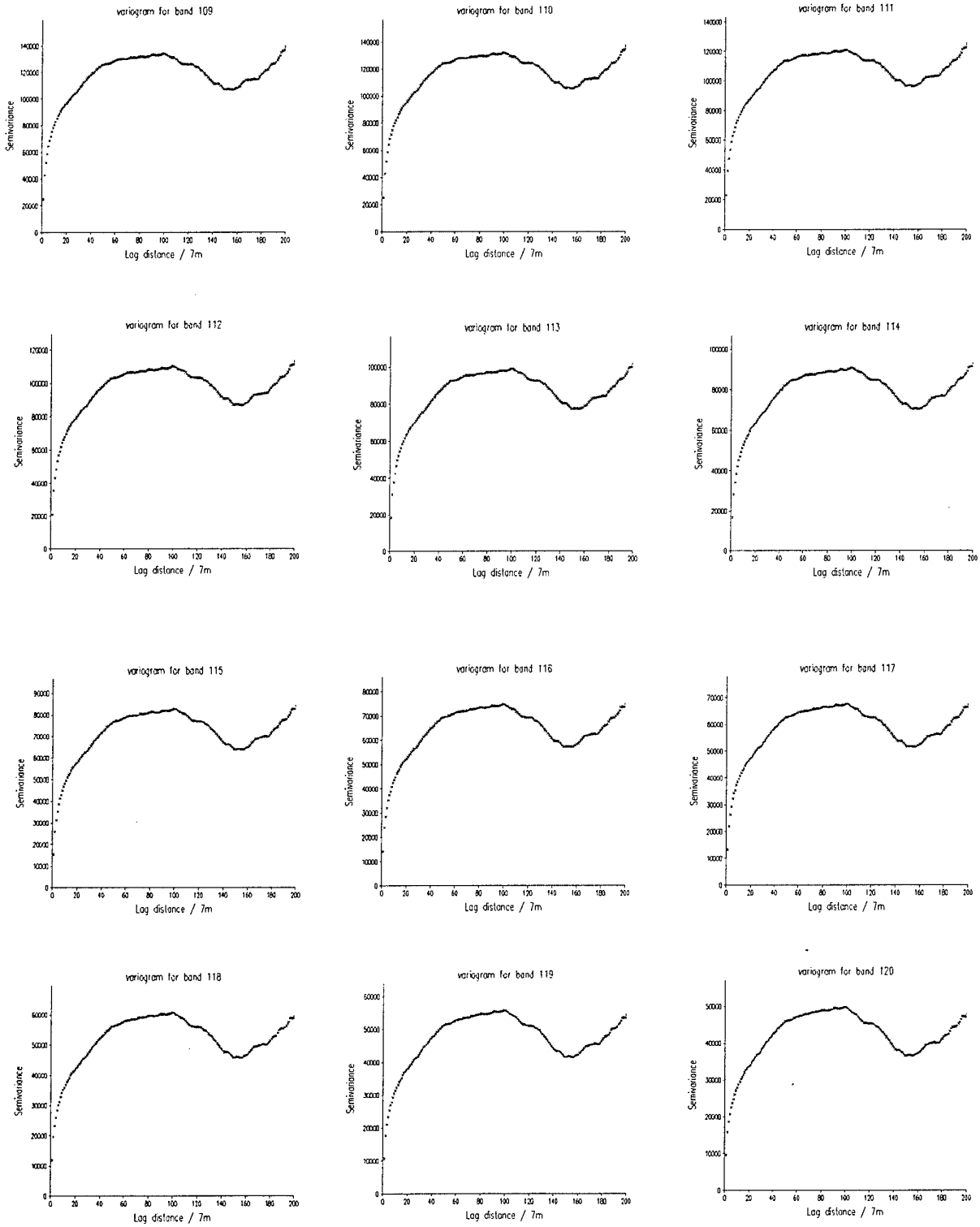

Figure 29. Experimental variograms for bands 109 to 120

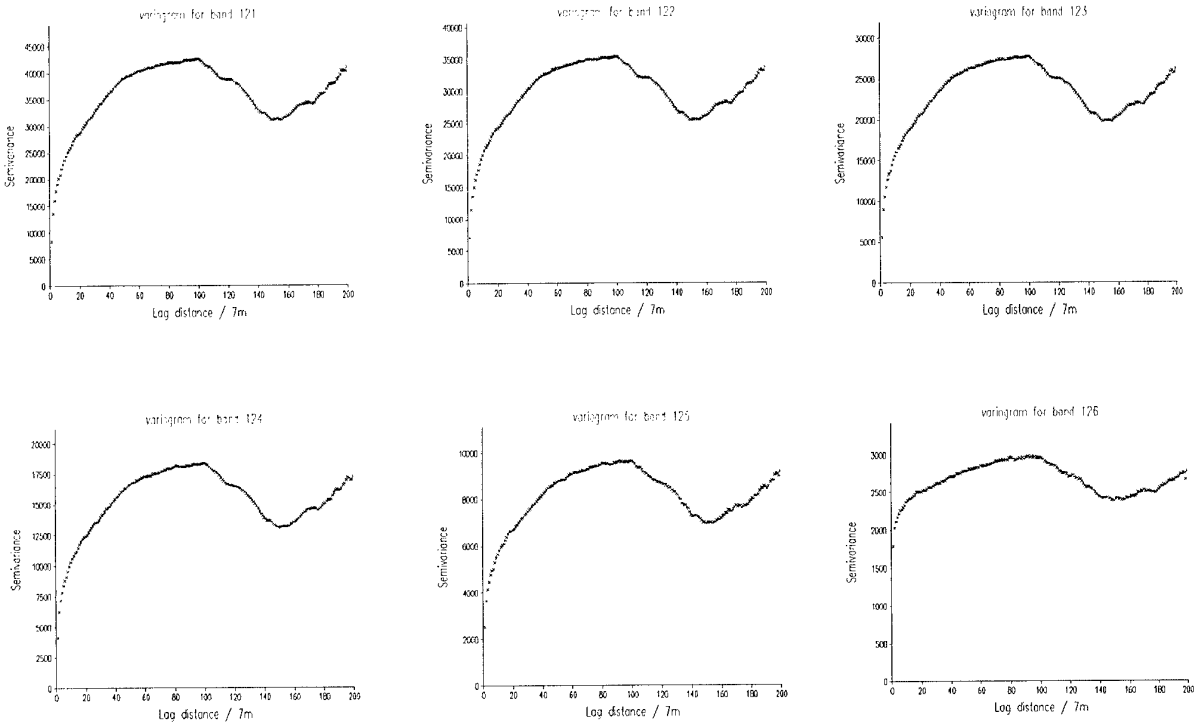

Figure 30. Experimental variograms for bands 121 to 126

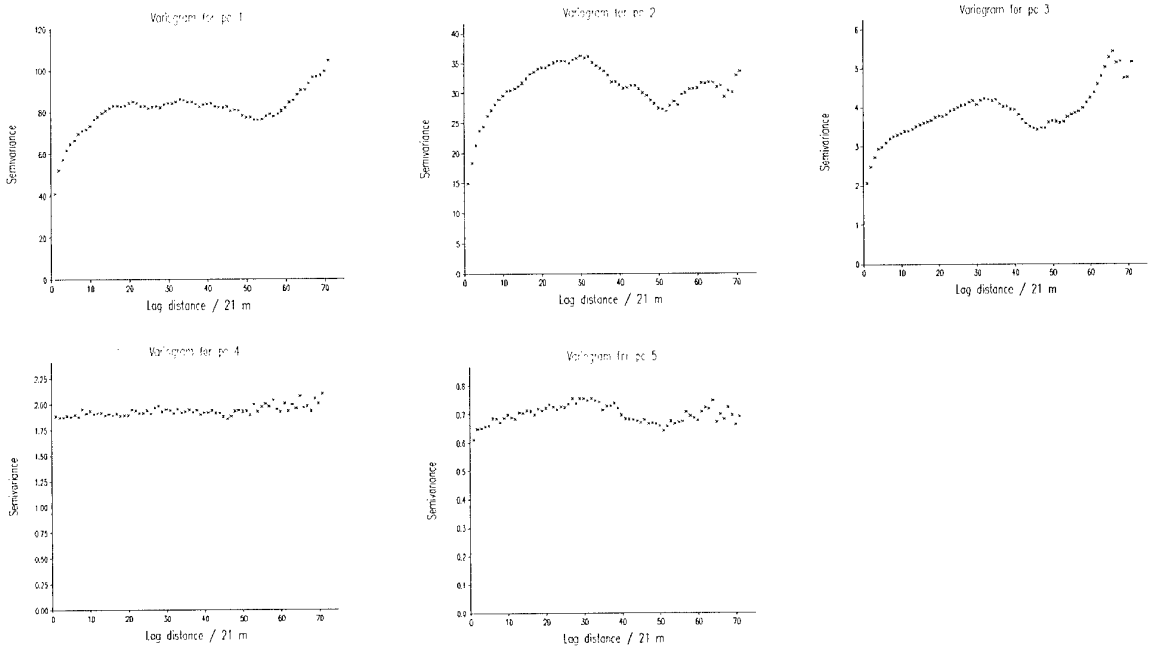

Figure 31. Experimental variograms for principal components 1 to 5.

Variogram modelling

Mathematical models were fitted to the experimental variograms of each band and the principal components. Nested models, either spherical or exponential provided the best fit to most of the variograms in the least squares sense. No attempt was made to model the periodicity as the wavelength was fairly constant for those variograms showing signs of repetition. The variograms of the bands and the first five principal components were modelled to a lag distance that enabled a stable fit, lags of 60, 90, 95 and 100 were used. Figures 32 to 43 show the experimental variograms as symbols and the fitted models as lines. It is difficult to distinguish between the experimental values and the models in many instances because of the density of the experimental values and the good fit of the models.

Table 7 gives the parameters of the fitted models, and Table 8 the summary statistics of the models fitted to the wavebands (not for the models fitted to the PCs). Apart from bands 63 and 64 which are pure nugget the models are nested exponential or spherical functions. Many models have no nugget variance, but for others it is large. To summarise the features of the models the pure nugget variograms have been removed, but they were included for later analyses. There are also considerable differences in the sill variances of the models even within groups of variograms that have similar structures. For the exponential models the distance parameter has been multiplied by 3 in Table 7 to give the approximate range of spatial dependence. The first distance parameter of the nested functions is remarkably similar throughout. It has a small range of between 25.2 m (7 × 3.6) for band 20 and 43 m (7 × 6.14 for band 95). The average is 34.3 m for the wavebands and for PC1 it is 35.5 m (1.69 × 21). This corresponds closely with the short-range structure identified from the 1 m imagery analysed and described in project report N68171-97-C-9092. There is much more variation in the size of the long-range structure. The smallest value for the long-range component is 185.5 m (7 × 26.5) and this extends to a maximum of 994 m (7 × 142), which corresponds to the size of one of the structures identified in the SPOT image for this area. The average long-range component is 422.6 m (7 × 60.37).

The average nugget variance (excluding the values for bands 63 and 64) is 911, with a minimum of zero and a maximum of 33249. The average sill variance of the first structure is 128862.5, with a range of 682 to 589718, which is considerable. For the second structure the average sill variance is 113863.8, with a minimum of 911 and a maximum of 464529, which is slightly less than for the first structure. It is evident from Figures 32 to 43 that the overall sill variance varies considerably, whereas the long-range component is more consistent within the groups that can be identified visually from the experimental variograms, Figures 20 to 30.

Bands 1 to 17 and 70 to 73 have a consistent long-range component of about 475 m, which is close to that for PC1, 435.5 m. For bands 19, 74 to 94 the long-range component is about 390 m, for bands 20 to 62 it is about 225 m, and for bands 65 to 69 it is just over 500 m. For bands 96 to 101 and 115 to 125, and PC5 it is about 700 m. For

bands 102 to 115 it is about 600 m, and for bands 95 and 126, and PCc 2 and 3 it is about 900 m. It is evident that from this crude grouping based on the long-range component that eight groups emerge, if the pure nugget variograms are considered as a group on their own, Table 9. This is the same number of groups as for the classification of the raw data, Table 9. It is interesting to note that there is an order in the values of the long-range component with the order of the wavebands – sometimes decreasing and at others increasing.

The forms of the variograms of the PCs appear to be similar to groups of variograms, Figure 43. This relates more to the long-range component than to the short-range component, , except for PC1. The relations between the PC models and groups of wavebands is described above. Since the PCA was done a sample of the data (1 in 9 pixels) the values for the range have been multiplied by 21 to obtain the values in metres.

To classify the model parameters in the same way as that for the raw digital data the parameters were standardized to zero mean and unit variance. This is because the different scales on which the parameters have been measured would give too much weight to the sill and nugget variances. The standardized model parameters were classified in the way described above and the number of classes selected was based on the group with largest change in the criterion. As far as I know the classification of the model parameters of the wavebands is novel. Table 9 gives the results of the classification for an optimal classification with eight classes.

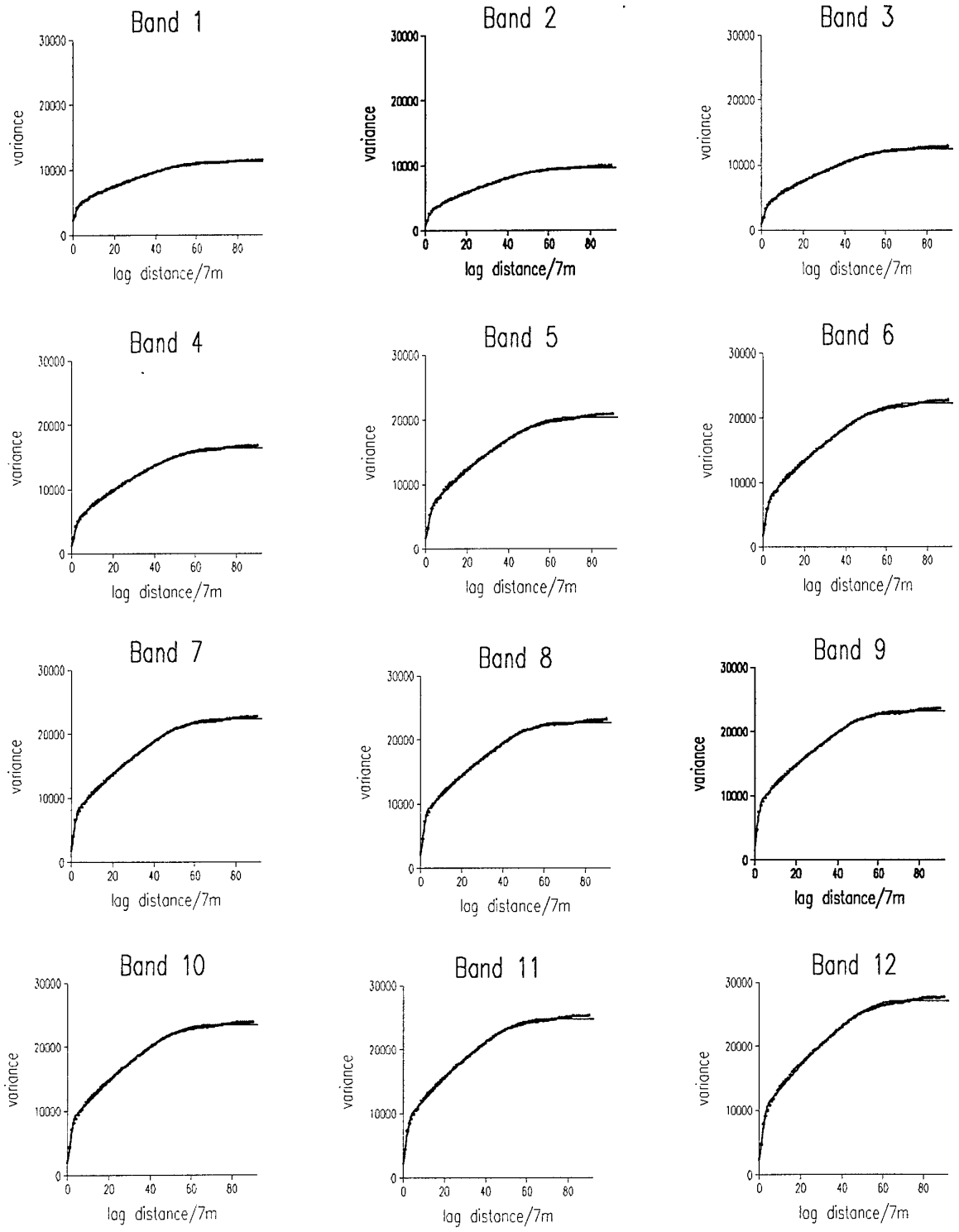

Figure 32: Experimental; variograms (symbols) and fitted models (lines) for bands 1 to 12.

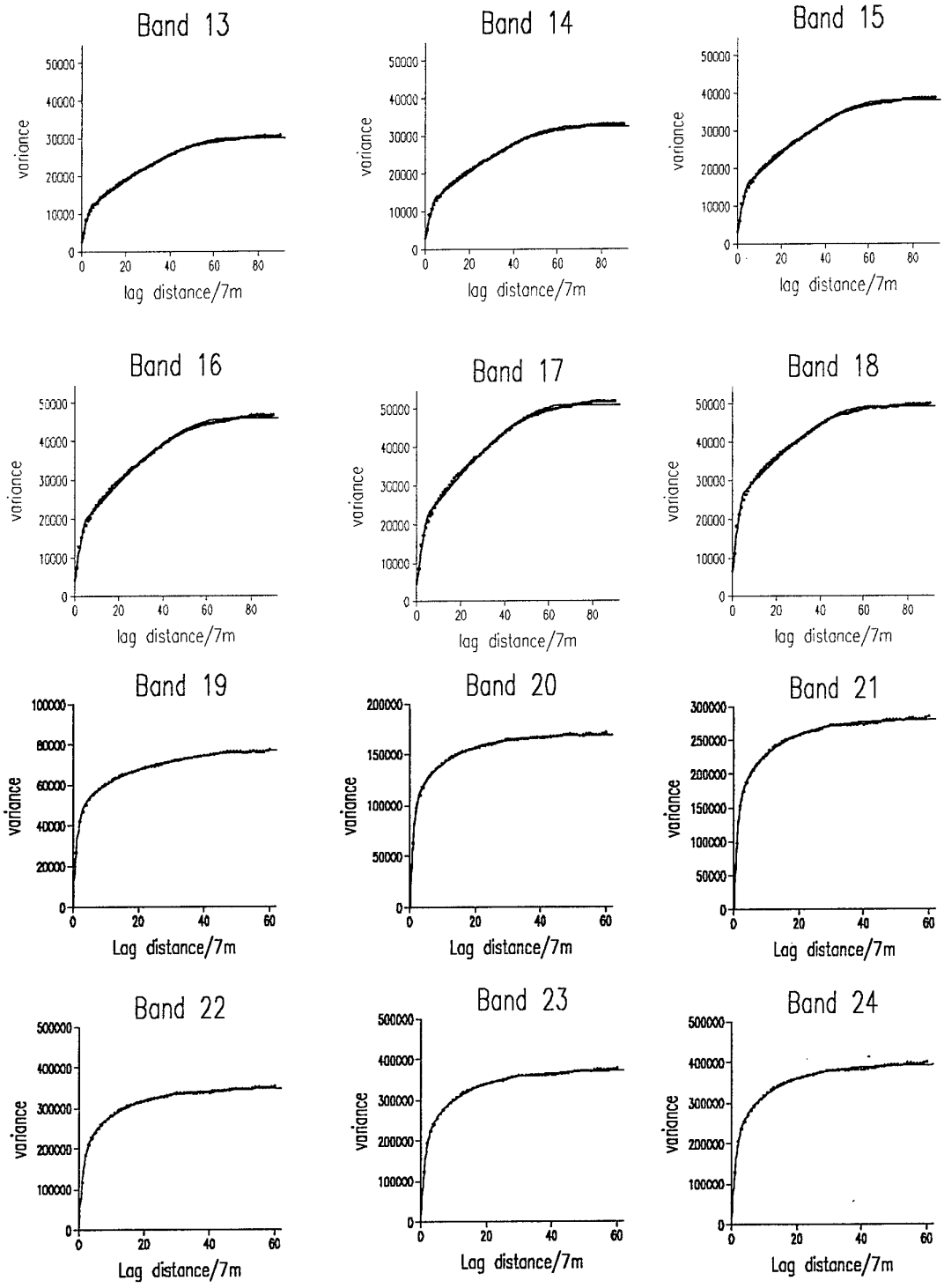

Figure 33: Experimental; variograms (symbols) and fitted models (lines) for bands 13 to 24

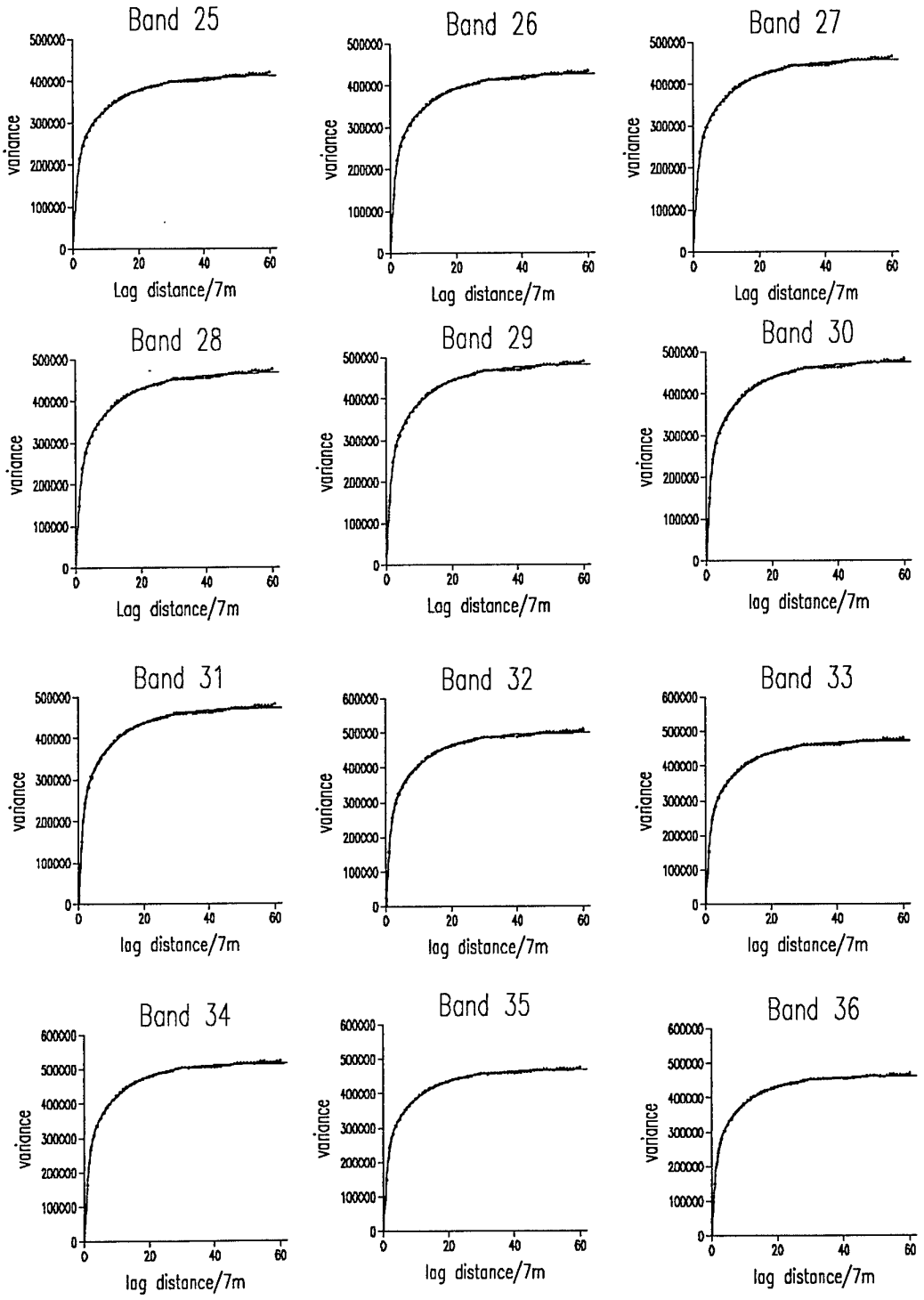

Figure 34: Experimental; variograms (symbols) and fitted models (lines) for bands 25 to 36

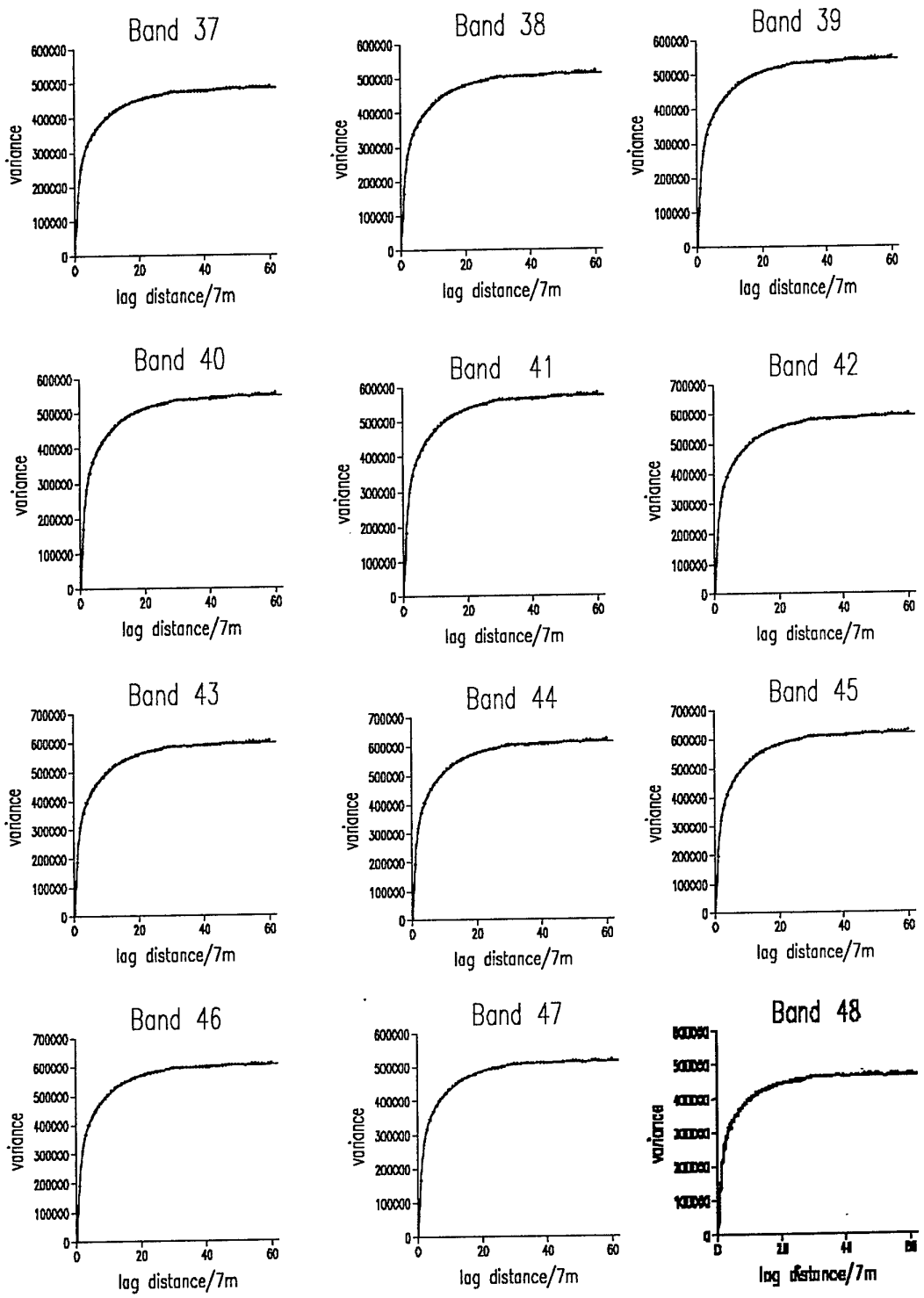

Figure 35: Experimental; variograms (symbols) and fitted models (lines) for bands 37 to 48

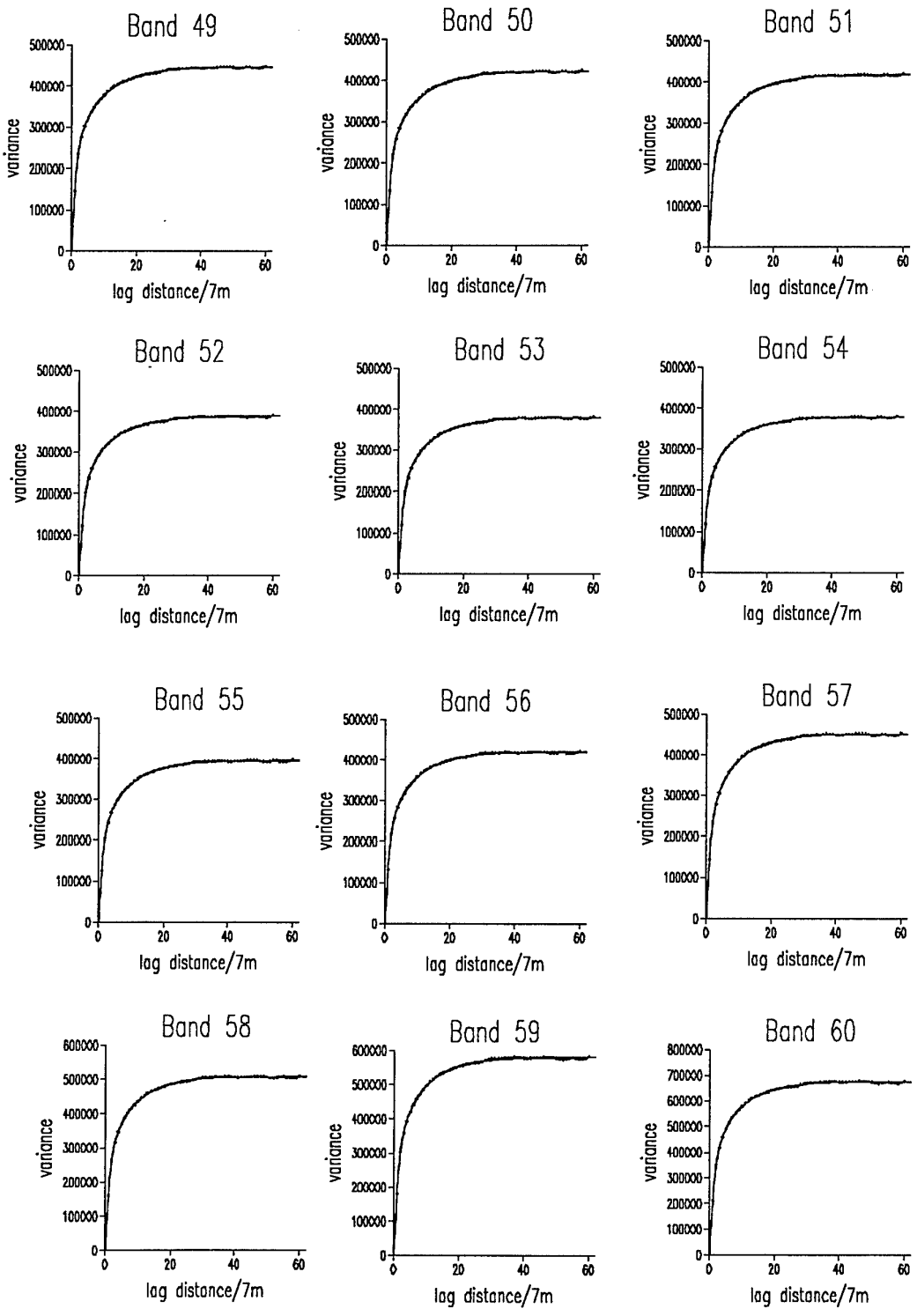

Figure 36: Experimental; variograms (symbols) and fitted models (lines) for bands 49 to 60-

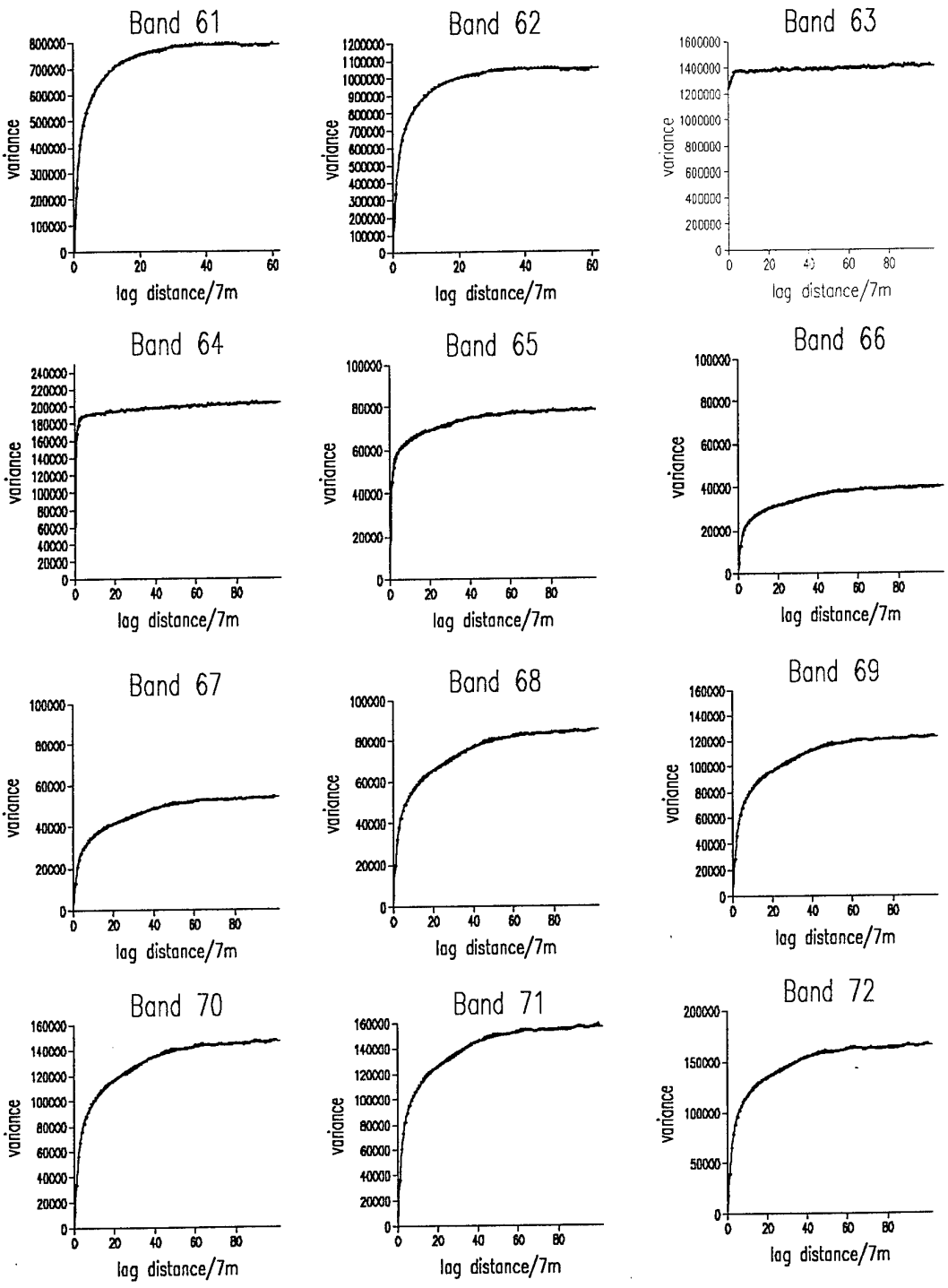

Figure 37: Experimental; variograms (symbols) and fitted models (lines) for bands 61 to 72

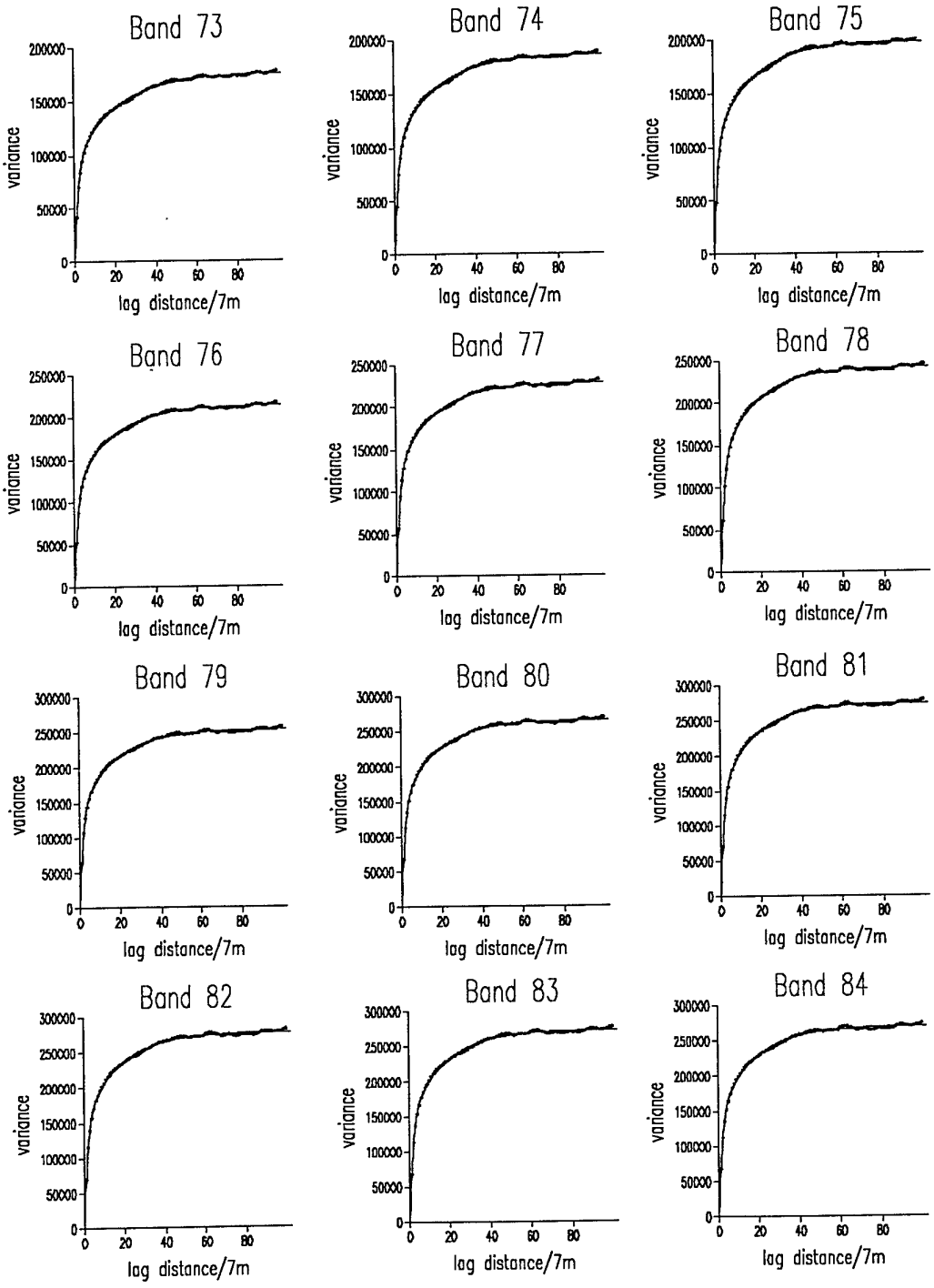

Figure 38: Experimental; variograms (symbols) and fitted models (lines) for bands 73 to 84

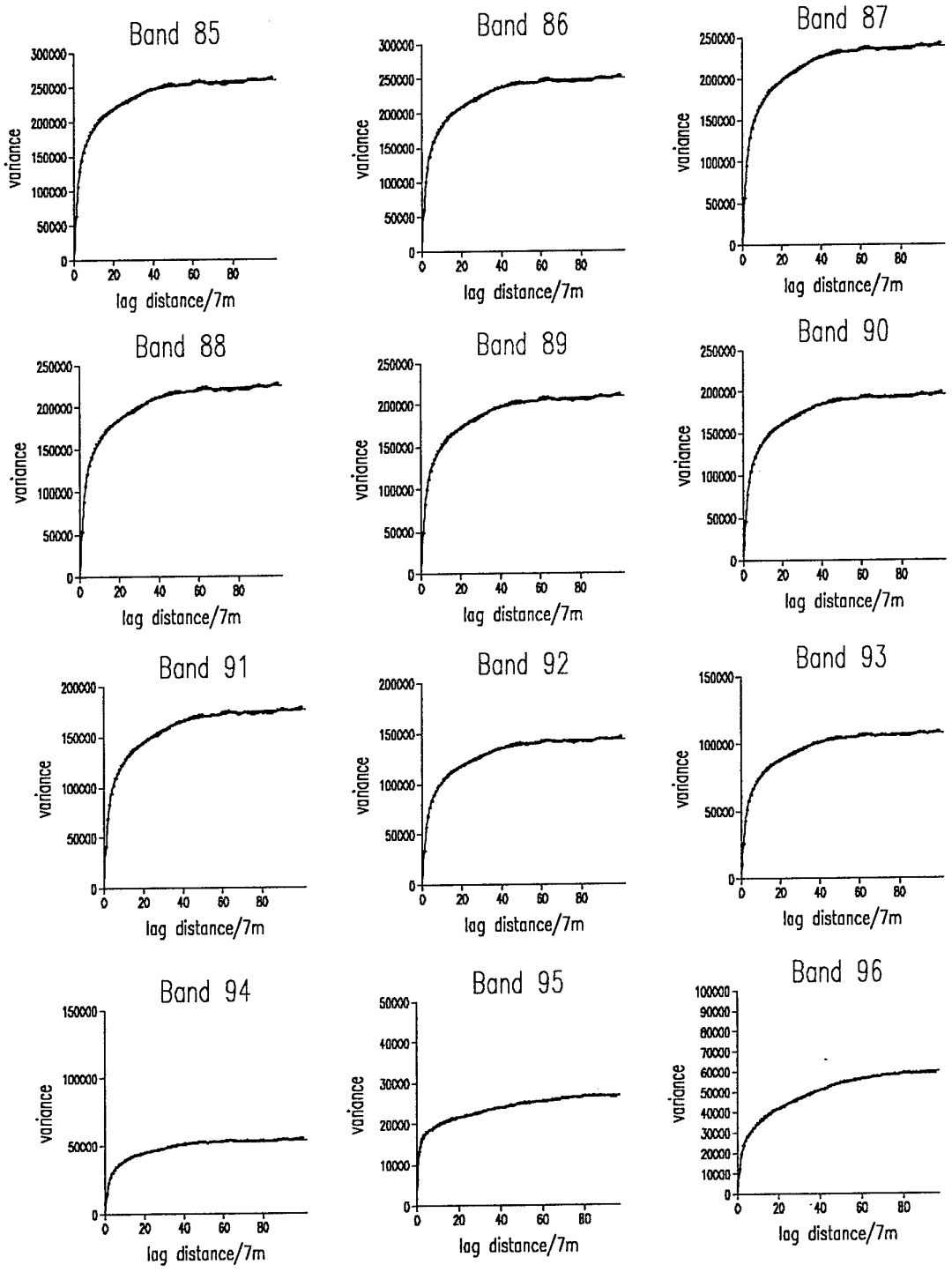

Figure 39: Experimental; variograms (symbols) and fitted models (lines) for bands 85 to 96

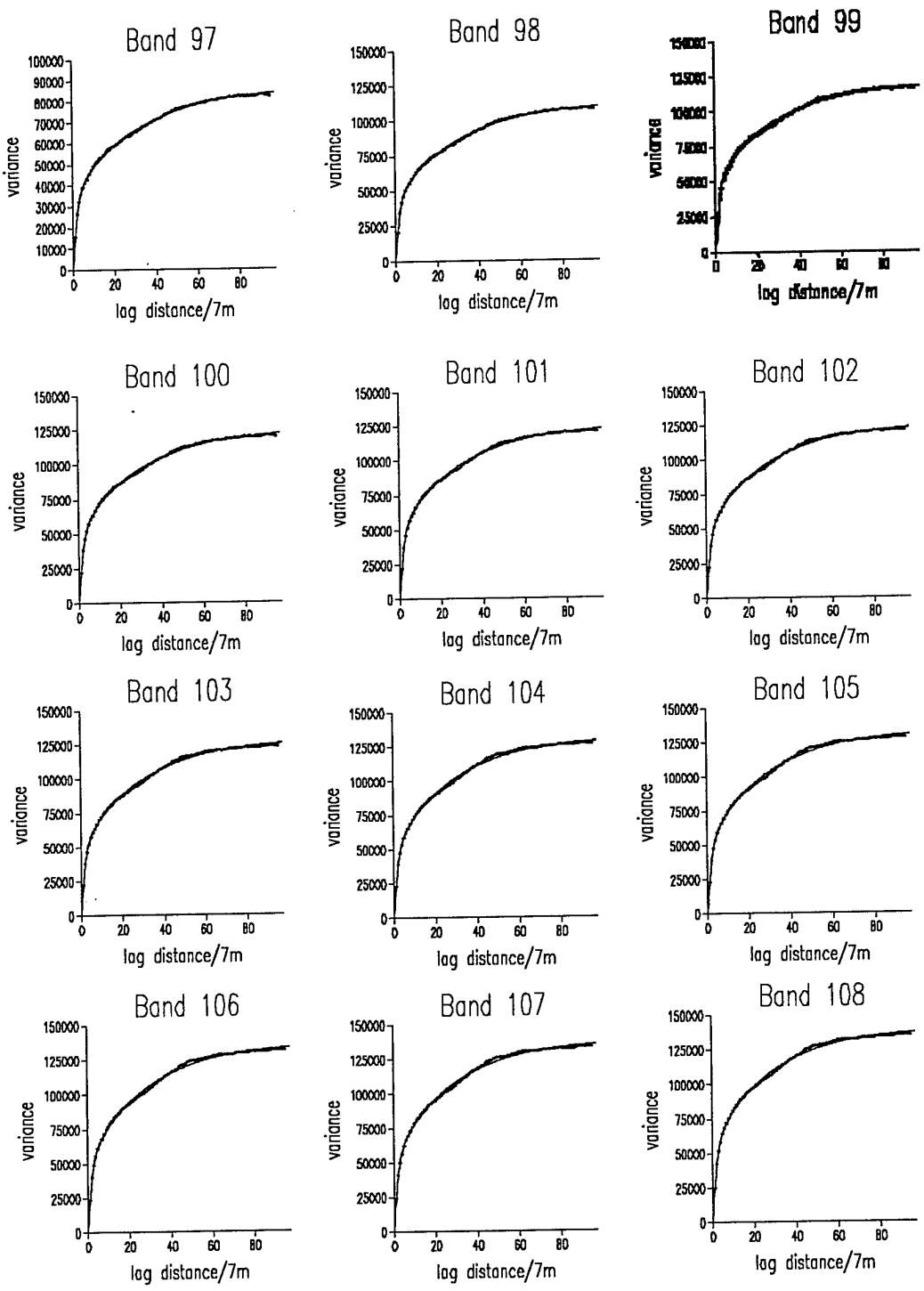

Figure 40: Experimental; variograms (symbols) and fitted models (lines) for bands 97 to 108

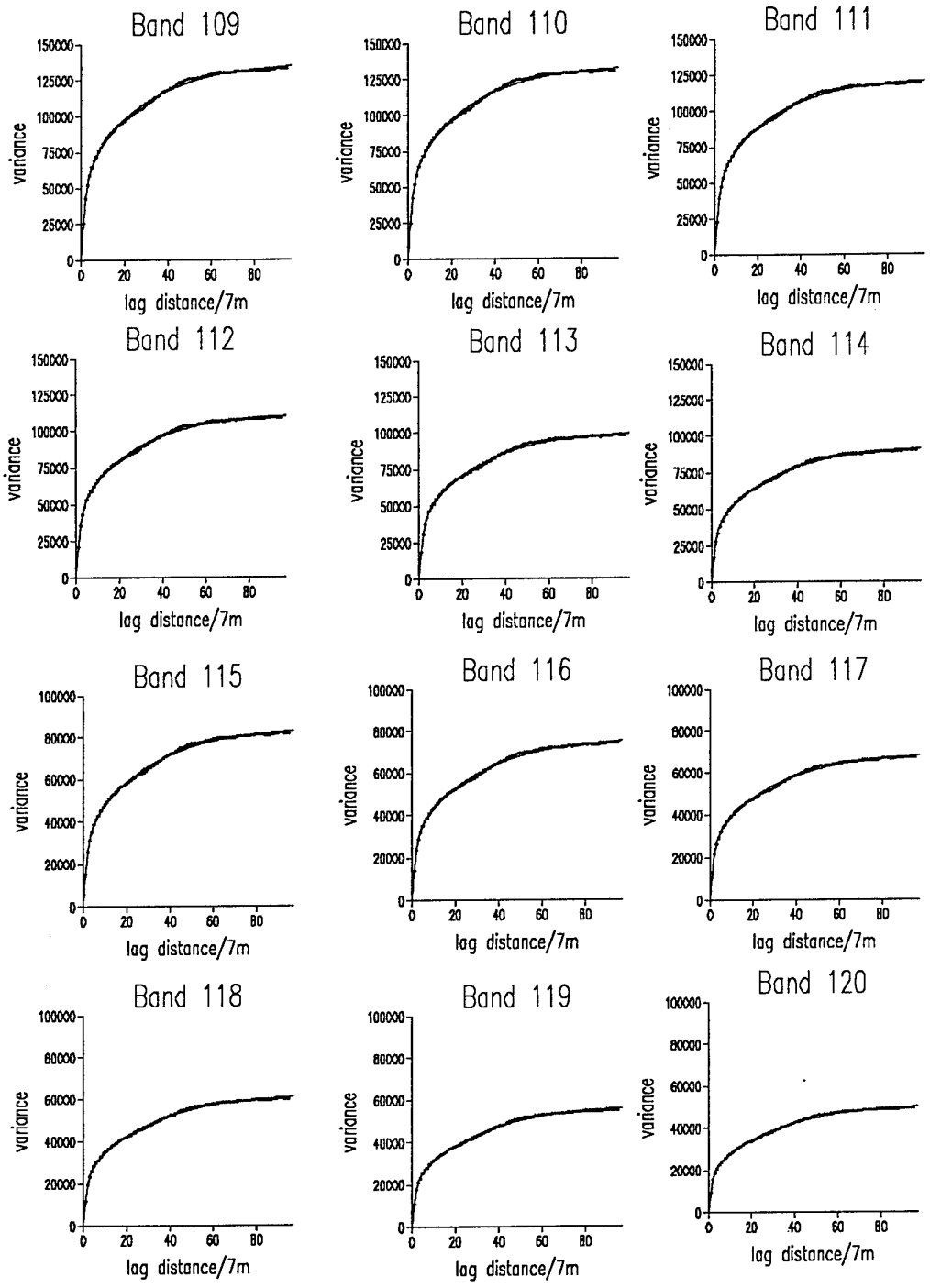

Figure 41: Experimental; variograms (symbols) and fitted models (lines) for bands 109 to 120

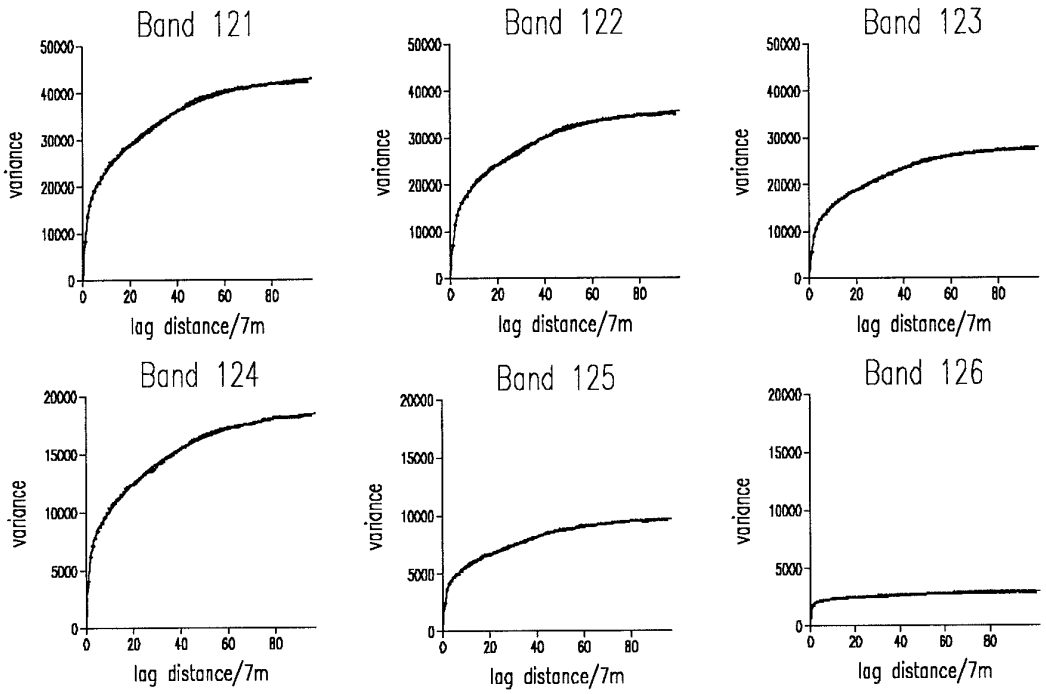

Figure 42: Experimental variograms (symbols) and fitted models (lines) for bands 109 to 126

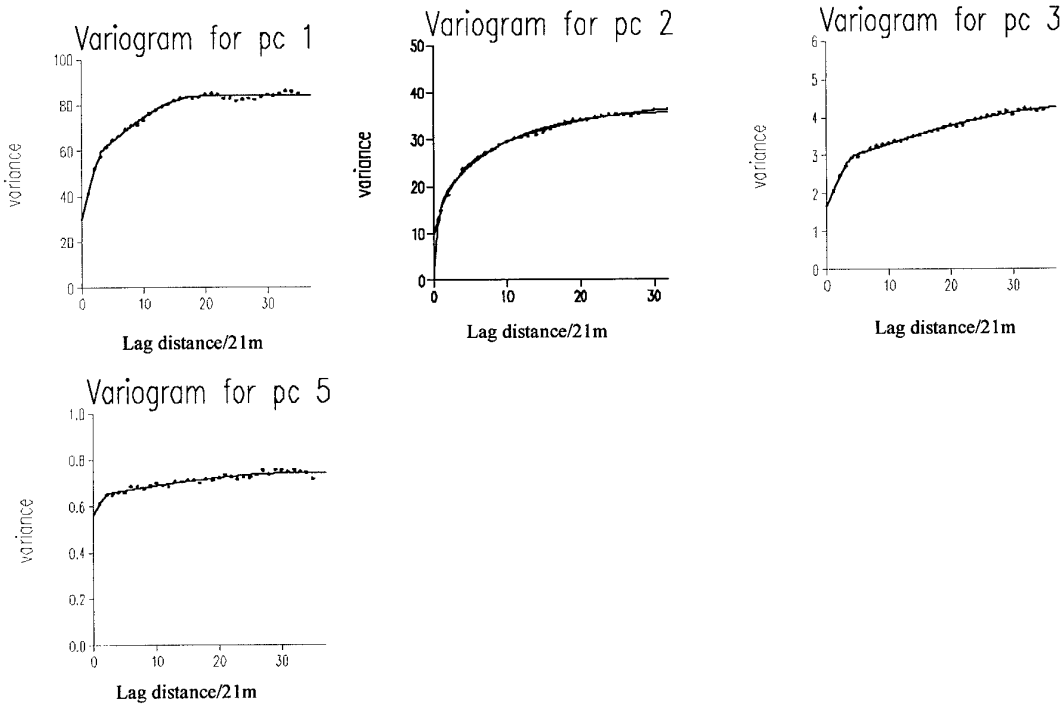

Figure 43: Experimental variograms (symbols) and fitted models (line) for PCs 1, 2, 3 and 5

Table 7. Model parameters fitted to the individual wavebands

Band	Lag Distance	Model type	Nugget variance	Sill 1 variance	Sill 2 variance	Range 1 /7m	Range 2 /7m
1	630 m	Double (D) S	2,194	2,454	6,697	4.54	70.9
2	"	D Spherical(S)	763	2,168	6,726	4.51	69.8
3	"	DS	931	2,829	8,707	4.58	69.4
4	"	DS	1,235	3,756	11,422	4.64	69.3
5	"	DS	1,526	4,688	14,183	4.63	69.4
6	"	DS	1,672	5,109	15,407	4.43	69.7
7	"	DS	1,776	5,513	15,023	3.91	69.0
8	"	DS	2,059	5,973	14,718	3.81	68.1
9	"	DS	2,133	6,197	14,881	3.83	67.7
10	"	DS	1,943	6,123	15,361	4.03	67.9
11	"	DS	2,218	6,325	16,241	4.54	68.2
12	"	DS	2,369	7,058	17,716	4.76	68.0
13	630 m	DS	2,530	7,910	19,589	4.94	67.8
14	"	DS	2,837	8,751	20,991	5.31	68.0
15	"	DS	3,274	10,420	24,326	5.48	68.1
16	"	D Exponential	3,968	12,853	28,978	5.59	68.2
17	"	DE	4,617	14,654	31,740	5.69	68.0
18	"	DE	6,550	17,357	25,291	5.47	62.8
19	420 m	DE	1,877	46,309	30,147	4.05	58.8
20	420 m	DE	0	105,304	64,437	3.60	37.5
21		DE	0	163,557	117,817	3.69	37.1
22		DE	0	196,399	153,169	3.80	37.4
23	420 m	DE	0	207,745	165,444	3.82	37.2
24		DE	0	219,071	175,665	3.85	36.9
25		DE	0	228,765	183,876	3.87	36.5
26		DE	0	237,056	192,098	3.92	36.2
27		DE	0	252,297	206,424	3.92	35.6
28		DE	0	256,250	211,930	4.01	35.5
29		DE	0	264,459	218,230	3.97	35.0
30		DE	0	260,462	215,512	4.00	34.7
31		DE	0	259,435	214,695	4.01	34.7
32	420 m	DE	0	274,028	228,245	4.06	34.4
33		DE	0	259,864	213,750	3.96	33.4
34		DE	0	283,580	234,582	4.07	33.5
35		DE	0	258,307	211,490	4.04	32.7
36		DE	0	255,783	208,660	4.04	32.3
37		DE	0	267,707	218,144	4.04	32.0
38		DE	0	283,374	231,956	4.10	31.9
39		DE	0	299,100	246,504	4.14	31.8
40		DE	0	301,733	248,919	4.21	31.7
41		DE	0	316,027	259,568	4.08	31.4
42	420 m	DE	0	325,911	268,242	4.12	31.3
43		DE	0	328,631	270,379	4.14	31.1
44		DE	0	338,345	278,064	4.13	30.8
45		DE	0	341,894	280,043	4.13	30.4
46		DE	0	334,013	273,185	4.21	30.1
47	420 m	DE	0	286,330	230,068	4.11	29.1

Band	Lag	Model	Nugget	Sill 1	Sill 2	Range 1	Range 2
	Distance	Type	variance	variance	variance	/7m	/7m
48		DE	0	262,810	208,206	4.19	28.7
49	420 m	DE	0	250,368	196,616	4.10	28.3
50		DE	0	236,895	185,881	4.29	28.6
51		DE	0	234,075	184,197	4.32	28.5
52		DE	0	217,567	171,108	4.38	28.4
53		DE	0	213,340	167,915	4.36	28.0
54		DE	0	212,154	167,472	4.36	27.5
55		DE	0	220,978	175,298	4.38	27.2
56		DE	0	234,720	186,016	4.42	27.0
57		DE	0	252,250	199,785	4.37	26.6
58	420 m	DE	0	284,362	224,839	4.39	26.5
59		DE	0	325,181	255,795	4.45	26.5
60	420 m	DE	0	380,422	296,471	4.47	26.7
61		DE	0	446,103	345,732	4.52	27.4
62		DE	0	589,718	464,529	4.32	27.4
63	700 m	Nugget	1,426,939	0	0	0	0
64	700 m	Nugget	206,244	0	0	0	0
65	700 m	DE	33,249	25,198	20,448	5.17	77.9
66		DE	5,375	16,649	18,479	5.51	78.8
67		DE	1,607	24,643	28,465	5.46	78.6
68		DE	1,211	40,009	44,987	5.46	76.6
69	700 m	DE	1,345	60,240	62,838	5.80	72.2
70		DE	1,158	73,645	73,244	5.81	69.9
71		DE	627	80,459	76,677	5.79	67.1
72	700 m	DE	606	86,480	79,523	5.76	64.4
73		DE	383	92,558	82,770	5.71	62.0
74		DE	199	99,442	87,174	5.66	59.8
75	700 m	DE	0	106,567	91,838	5.61	58.1
76		DE	61	115,822	98,271	5.57	56.6
77		DE	0	124,535	104,273	5.54	55.2
78		DE	230	132,558	109,660	5.50	53.9
79		DE	0	139,608	114,274	5.54	53.0
80	700 m	DE	0	146,342	119,305	5.51	52.3
81		DE	0	151,397	123,717	5.54	52.2
82		DE	0	151,644	126,115	5.55	52.6
83		DE	0	147,987	124,776	5.57	53.2
84		DE	0	145,674	124,339	5.52	53.3
85		DE	0	138,991	120,982	5.62	54.8
86		DE	0	131,893	118,719	5.63	56.5
87	700 m	DE	0	124,839	115,278	5.66	57.6
88		DE	0	116,355	108,500	5.63	58.3
89		DE	0	108,452	101,444	5.69	58.7
90		DE	0	101,576	95,289	5.67	59.6
91	665 m	DE	0	91,225	85,598	5.72	60.3
92		DE	0	74,737	69,993	5.67	60.7
93	665 m	DE	1,515	55,033	51,927	5.73	61.9
94		DE	3,028	26,624	24,952	5.81	62.3
95	665 m	DE	10,283	7,345	10,353	6.14	*123.0*
96	665 m	DE	1,805	23,104	37,521	5.51	*100.0*
97		DE	345	34,529	51,617	5.79	*97.2*

Band	Lag Distance	Model Type	Nugget variance	Sill 1 variance	Sill 2 variance	Range 1 /7m	Range 2 /7m
98	665 m	DE	0	44,366	69,023	5.60	*96.6*
99		DE	1,058	48,591	71,392	5.83	93.0
100		DE	0	50,496	74,630	5.84	91.5
101		DE	0	49,527	76,319	5.81	90.6
102		DE	0	48,798	77,307	5.67	89.2
103		DE	0	48,948	79,529	5.69	88.6
104		DE	0	49,921	82,203	5.66	88.1
105		DE	0	50,054	83,666	5.72	87.6
106		DE	0	51,445	85,290	5.72	86.8
107		DE	0	53,025	85,464	5.79	85.9
108		DE	0	55,139	84,812	5.81	84.7
109		DE	0	55,707	81,411	5.80	83.3
110		DE	0	55,545	79,107	5.78	82.2
111		DE	0	51,118	72,298	5.77	82.7
112		DE	0	45,907	66,565	5.63	84.0
113		DE	0	39,890	61,411	5.58	85.9
114		DE	0	35,916	57,262	5.54	87.2
115	665 m	DE	0	33,002	52,092	5.50	89.0
116		DE	0	30,091	46,979	5.37	90.8
117		DE	0	27,672	42,148	5.31	91.5
118		DE	0	24,094	38,685	5.11	93.1
119		DE	0	21,269	36,464	4.91	94.9
120		DE	0	18,749	33,032	4.82	95.5
121	665 m	DE	0	15,730	28,708	4.59	*96.8*
122		DE	0	13,563	23,278	4.68	*96.3*
123		DE	0	10,568	18,439	4.55	*98.9*
124	665 m	DE	429	6,564	12,208	4.23	101.4
125		DE	486	3,590	6,027	4.06	104.6
126	700 m	DE	1,507	682	911	5.62	142.0
PC1	245 m	DS	29.69	22.40	31.67	3.617	19.29
PC2	210 m	DE	9.670	11.44	17.42	6.729	44.79
PC3	245 m	DS	1.694	1.085	1.521	4.739	41.67
PC5	245 m	DS	0.559	0.086	0.099	2.543	33.92

Table 8. Summary statistics of model parameters of hymap wavebands.

Parameter	Mean	Minimum	Maximum
Nugget variance	911	0	33249
Sill of first structure	128862	682	589718
Sill of second structure	113864	911	464529
Range of first structure	4.9 (34.3 m)	3.6 (25.2 m)	6.1 (42.7 m)
Range of second structure	60.4 (422.8 m)	26.5 (185.5 m)	142.0 (994.0 m)

Mapping of hyperspectral wavebands

Pixel maps of the digital information for each band have been plotted in Figures 44-64. The choice of map colour scale was based on the minimum, maximum and mean values for each band. To enable as much comparison as possible the same scale was used for groups of bands. The maps show clearly the range of spatial textures that become evident for different bands, however without some additional expertise from TEC it is not clear how to interpret the variety present. It is evident that some spectra pick out the detail in the built up area in the north central part of the map whereas others, such as band 57 seem to pick out the physiography more. Many maps have similar features, but the texture varies even for those with similar variograms. The maps of bands 63 to 65 and band 126 are mainly noise. For bands 63 and 64 this was expected because of the pure nugget variograms. Bands 65 and 126 have large nugget to sill variances of 42% and 49%, respectively which is expressed by the speckled appearance of their maps.

Factorial kriging of selected wavebands

Wavebands were selected on the basis of the long-range parameters of their variogram models. Figures 65 to 73 show the maps of the long- and short-range components of the variation. The short-range component was fairly consistent for the different wavebands and this is evident in the maps based on this scale of variation. They resemble the texture that was evident in the 1-m imagery for the site. Roads, tracks, buildings and the woodland texture are evident. The maps of the long-range component differ because they are based on different spatial scales. Bands 95 and 126 (Figures 72 and 73) have the largest long-range component. However, the variation of these components appears to be more 'noisy' than for the others and this was evident in the raw pixel maps. Bands 22, 47 and 58 (Figures 66, 67 and 68) have the shortest long-range components. The texture in the valley (red) and spurs (green or yellow) can be seen. This probably reflects the intricate physiography of the area. Bands 10, 66 and 83 (Figures 65, 69 and 70) have intermediate long-range components. The texture associated with the small tributary valleys is most clear in these maps.

Further discussion with personnel at TEC is needed to improve the interpretation of this analysis as with the raw pixel maps.

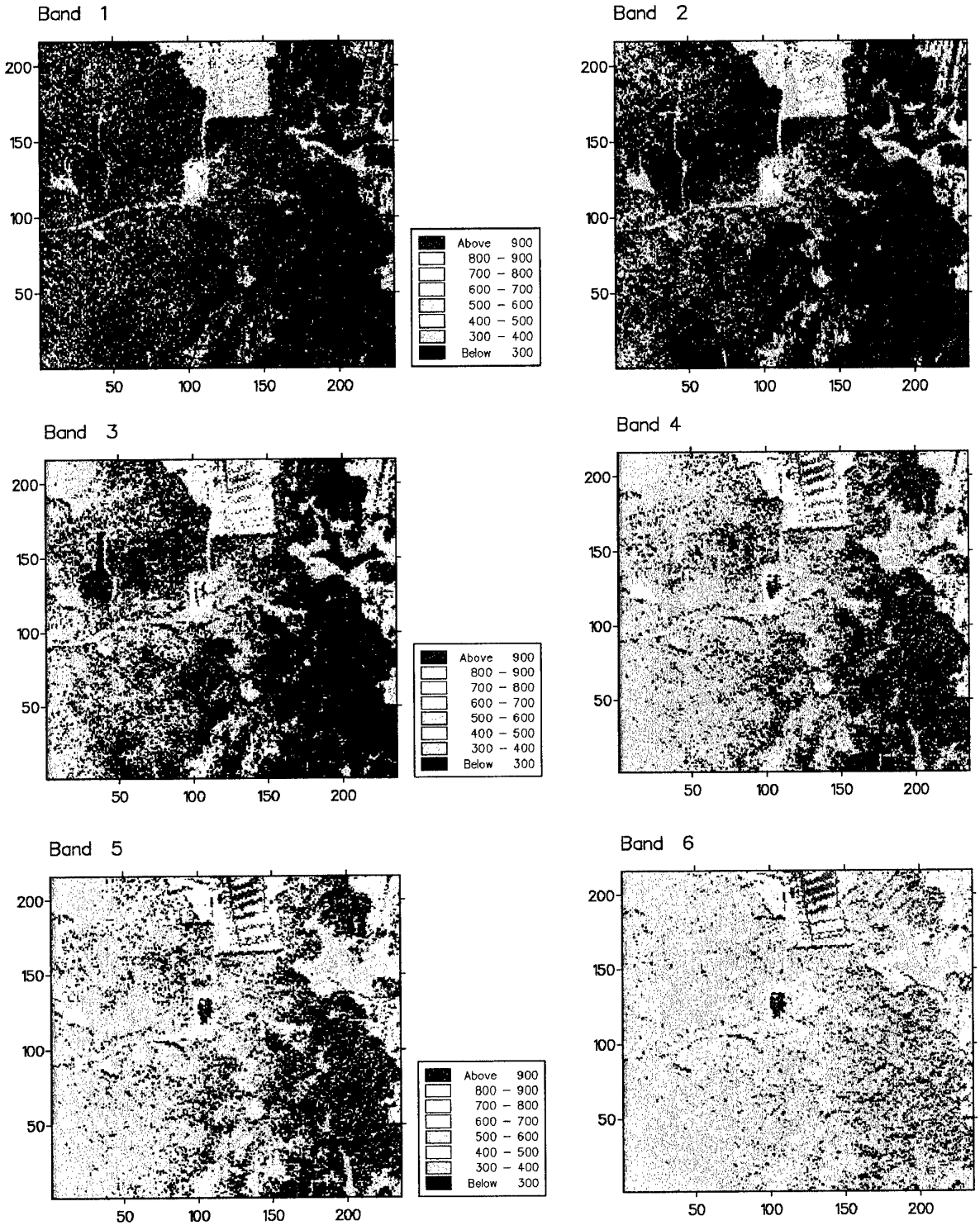

Figure 44. Pixel maps of wavebands 1 to 6 for the hymap image data.

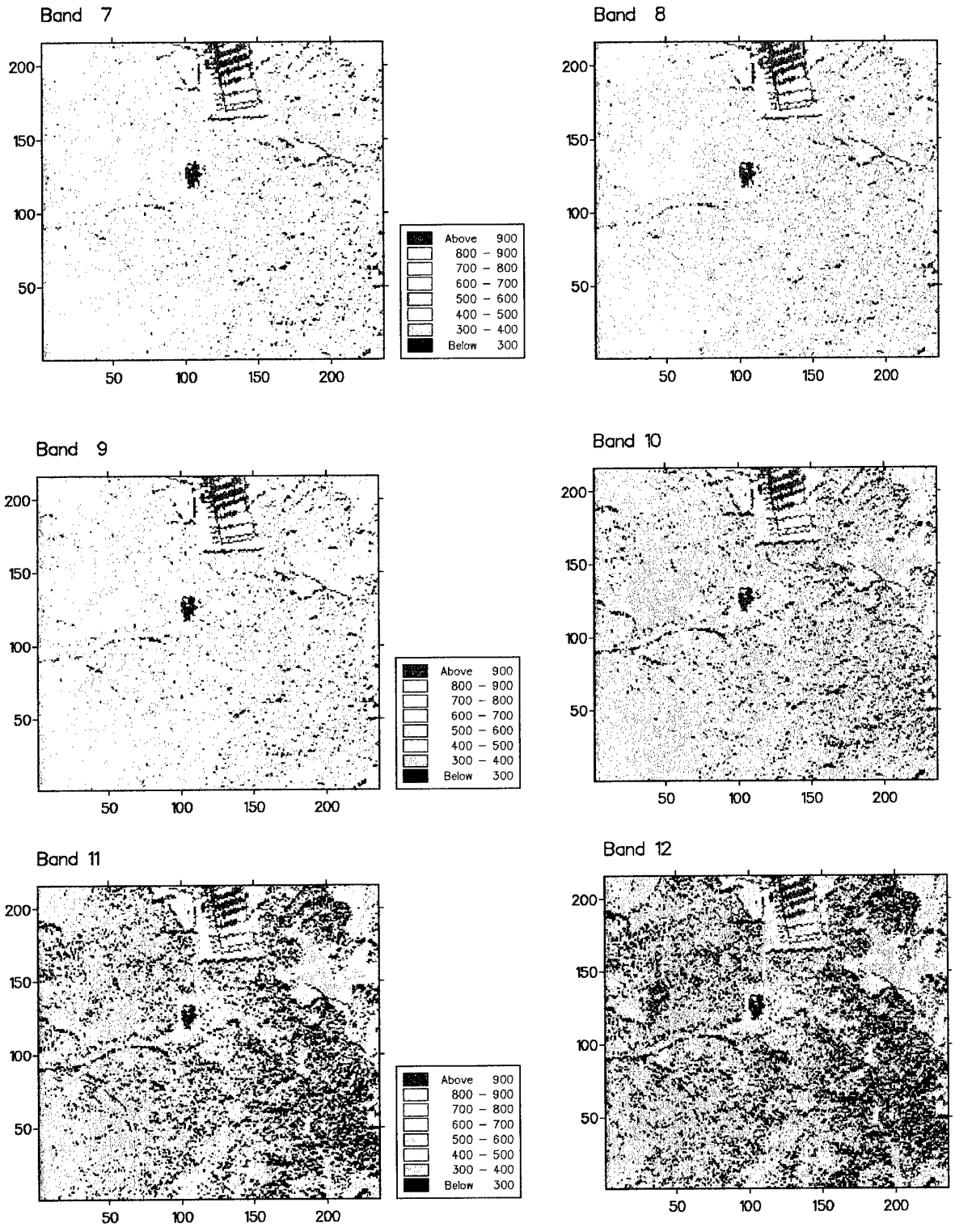

Figure 45. Pixel maps of wavebands 7 to 12 for the hymap image data

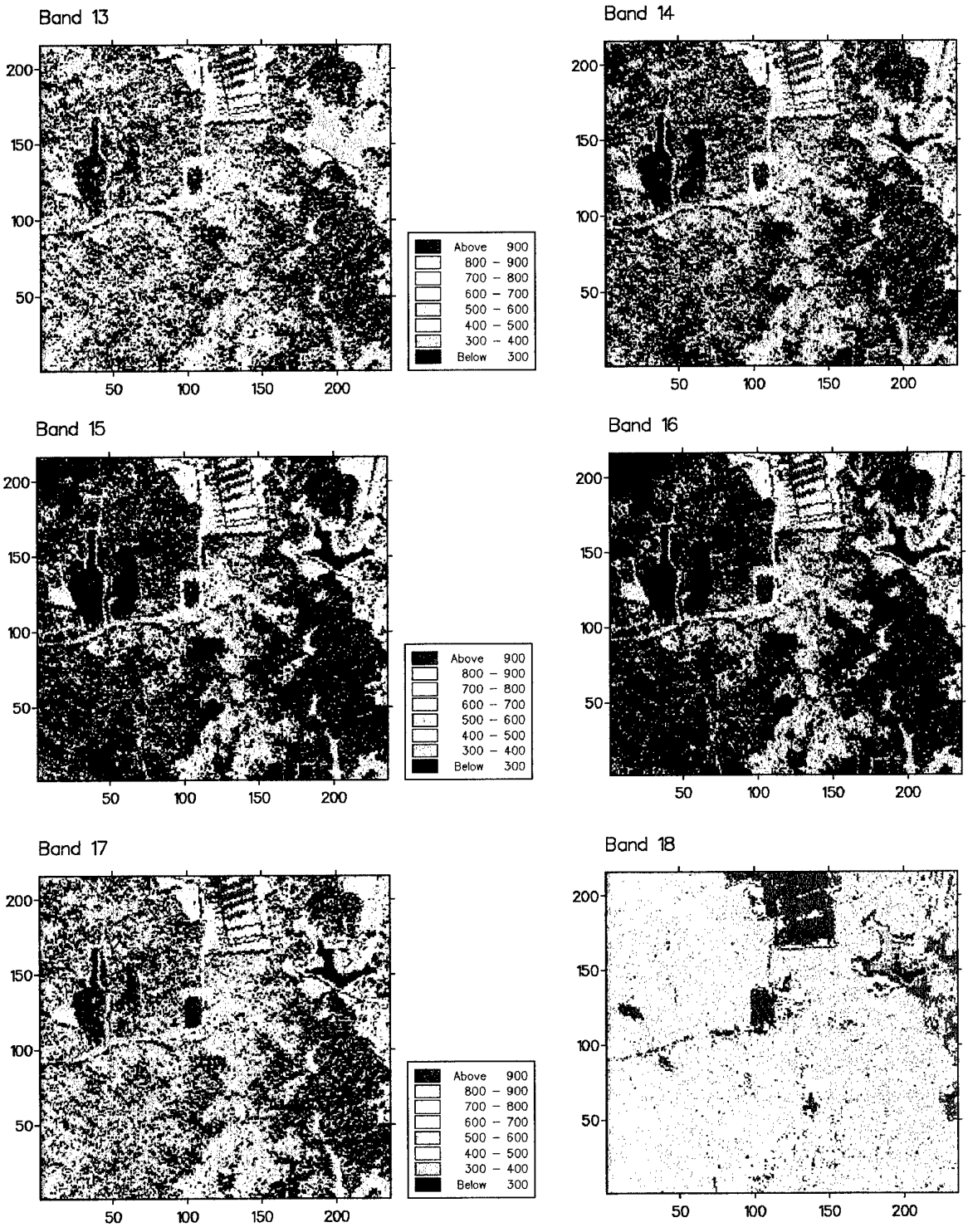

Figure 46. Pixel maps of wavebands 13 to 18 for the hymap image data

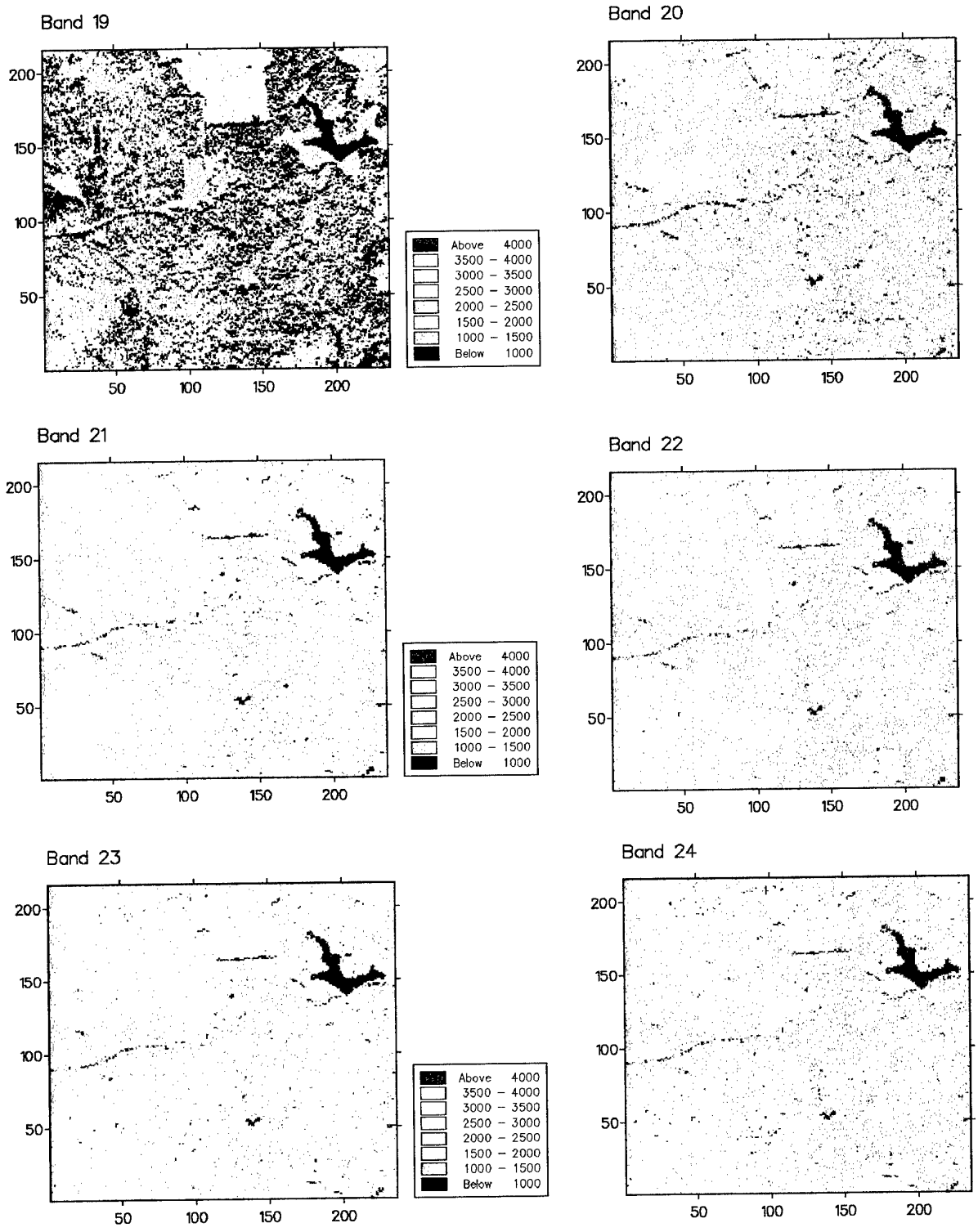

Figure 47. Pixel maps of wavebands 19 to 24 for the hymap image data

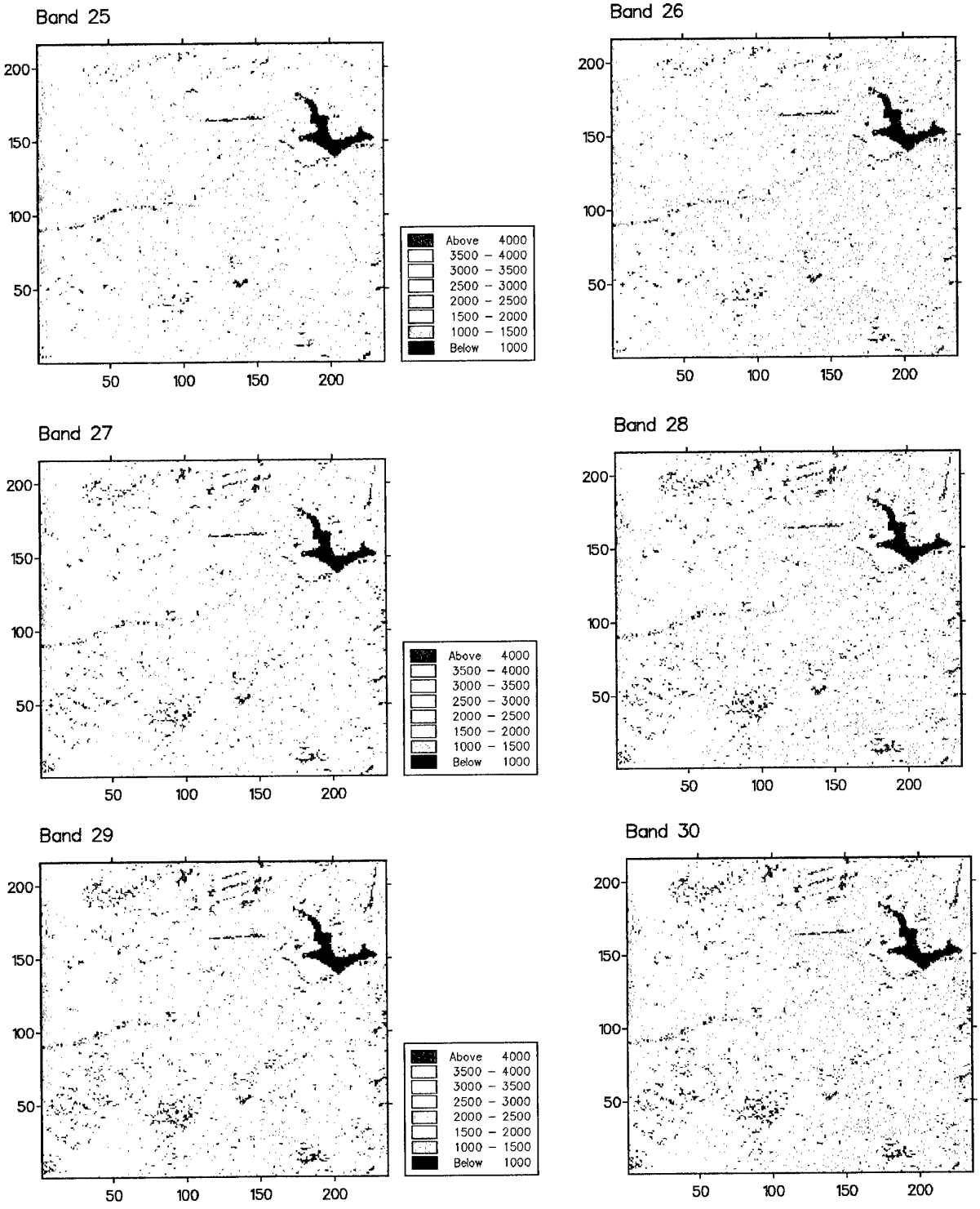

Figure 48. Pixel maps of wavebands 25 to 30 for the hymap image data

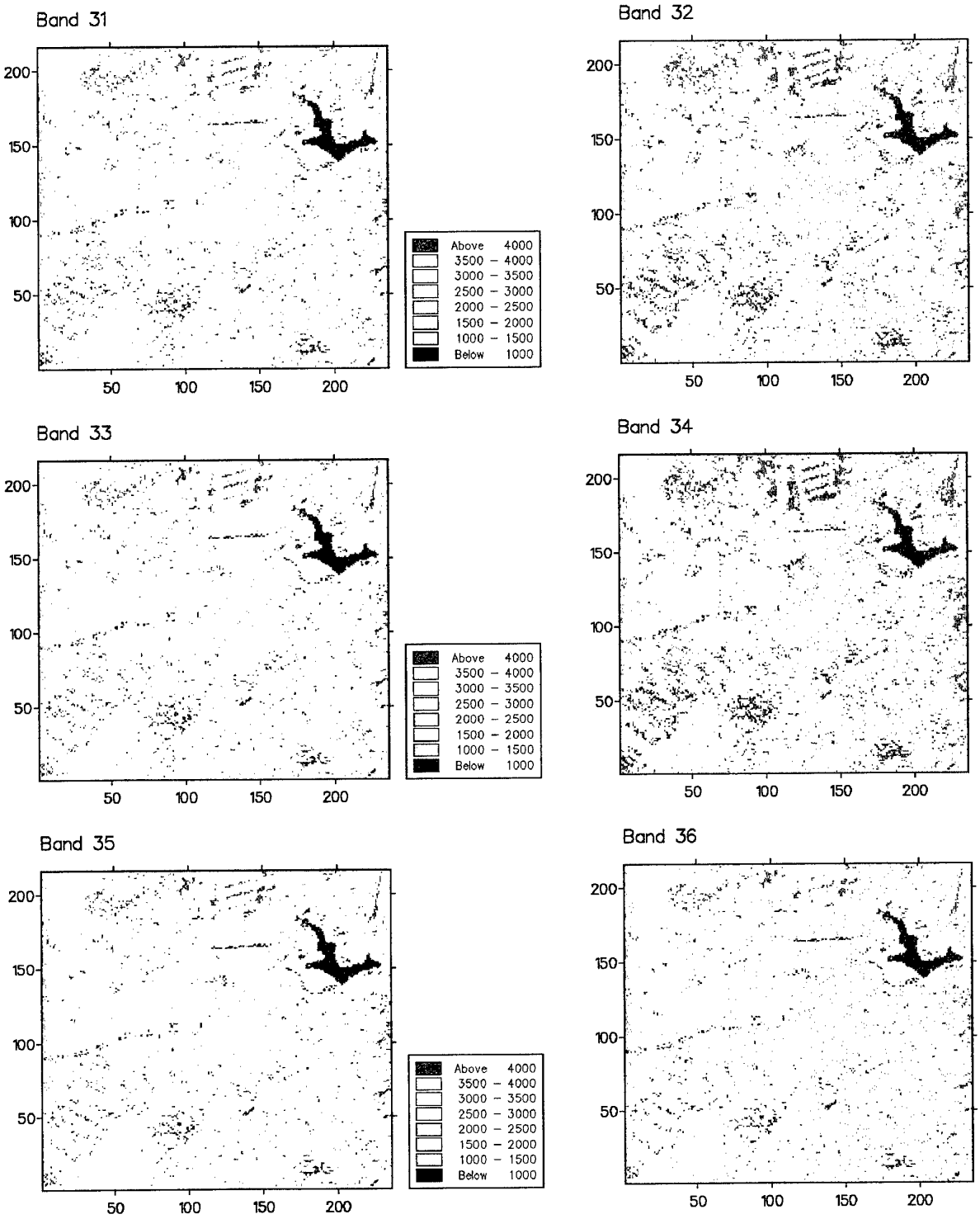

Figure 49. Pixel maps of wavebands 25 to 36 for the hymap image data

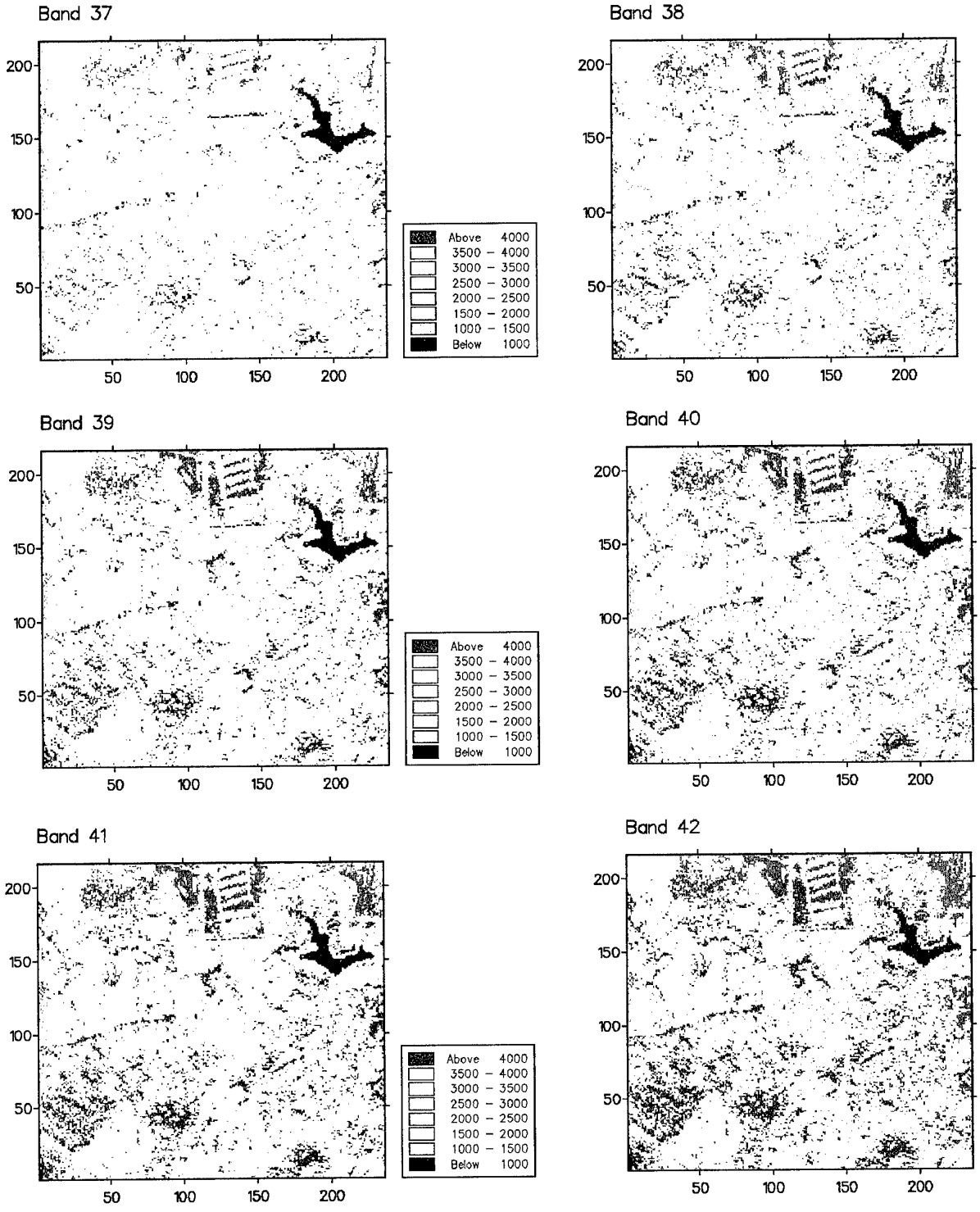

Figure 50. Pixel maps of wavebands 37 to 42 for the hymap image data

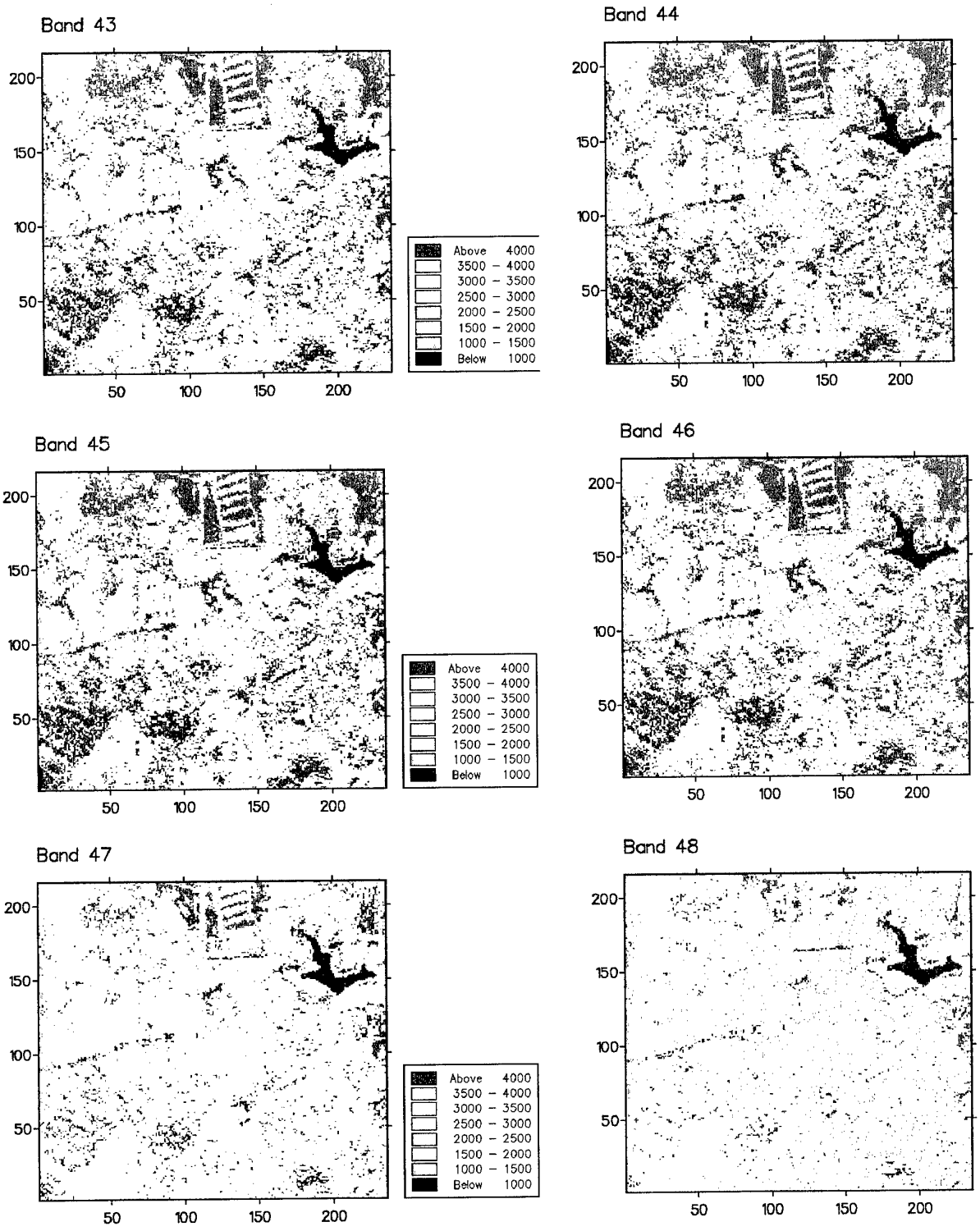

Figure 51. Pixel maps of wavebands 43 to 48 for the hymap image data

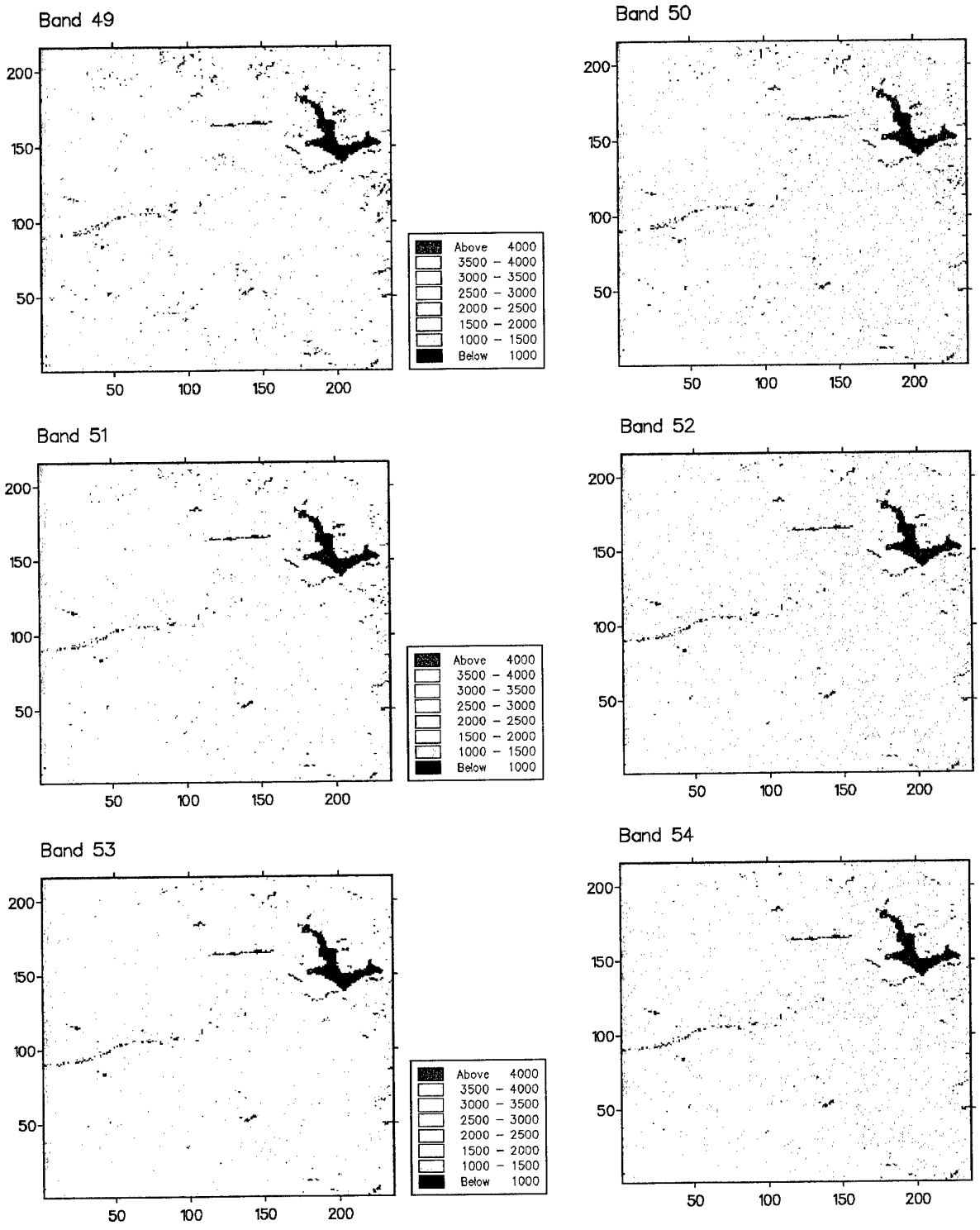

Figure 52. Pixel maps of wavebands 49 to 54 for the hymap image data

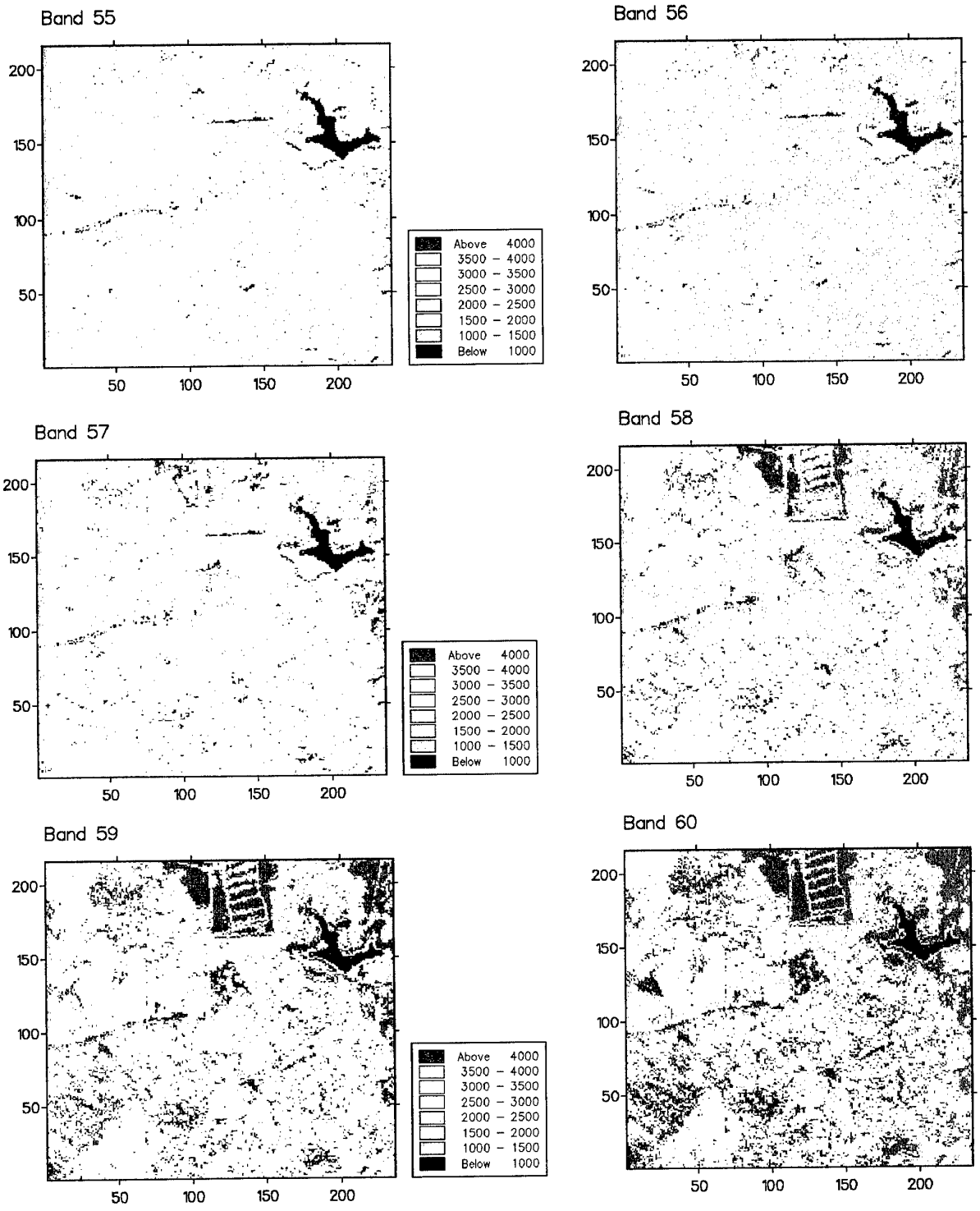

Figure 53. Pixel maps of wavebands 55 to 60 for the hymap image data

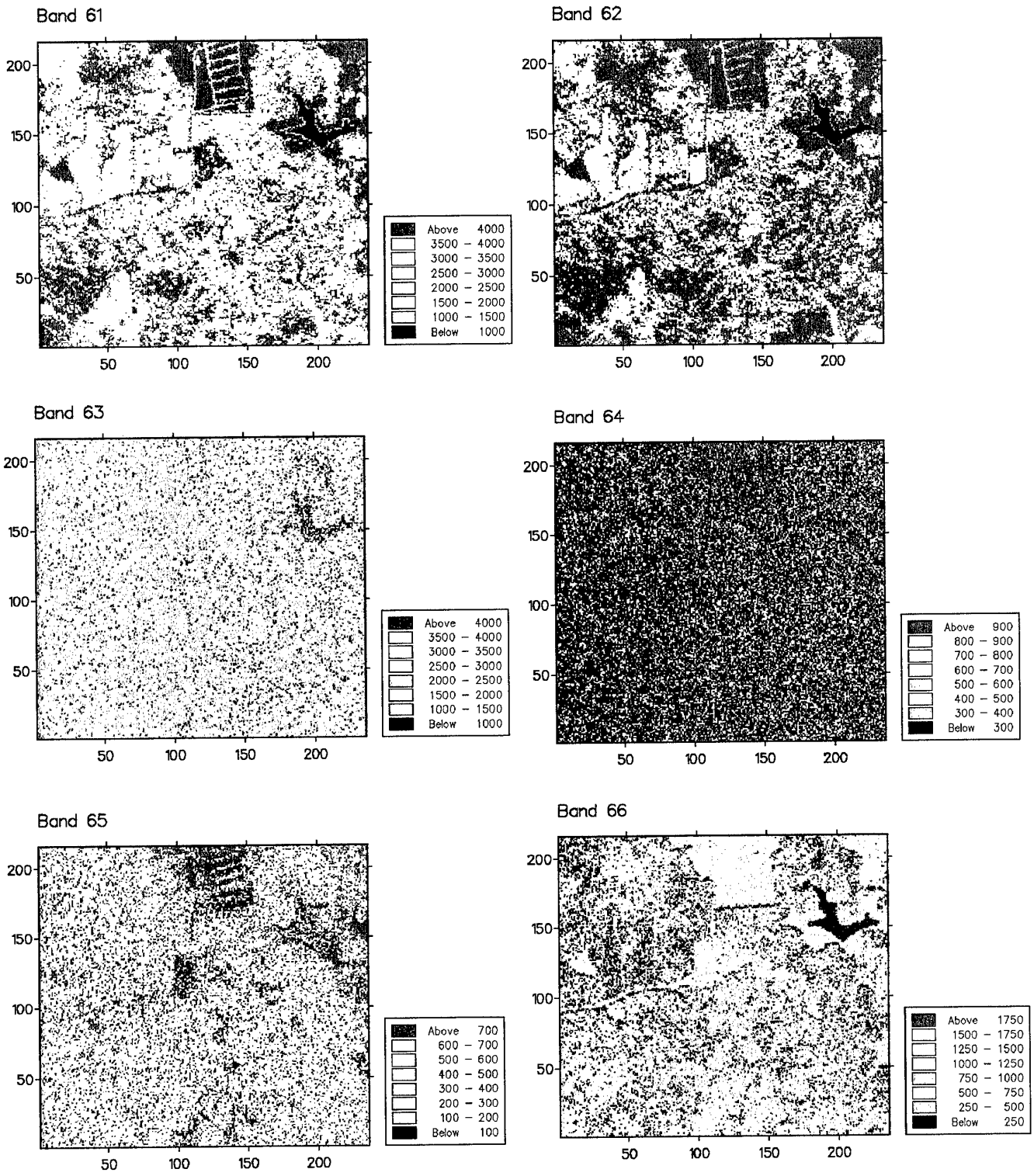

Figure 54. Pixel maps of wavebands 61 to 66 for the hymap image data

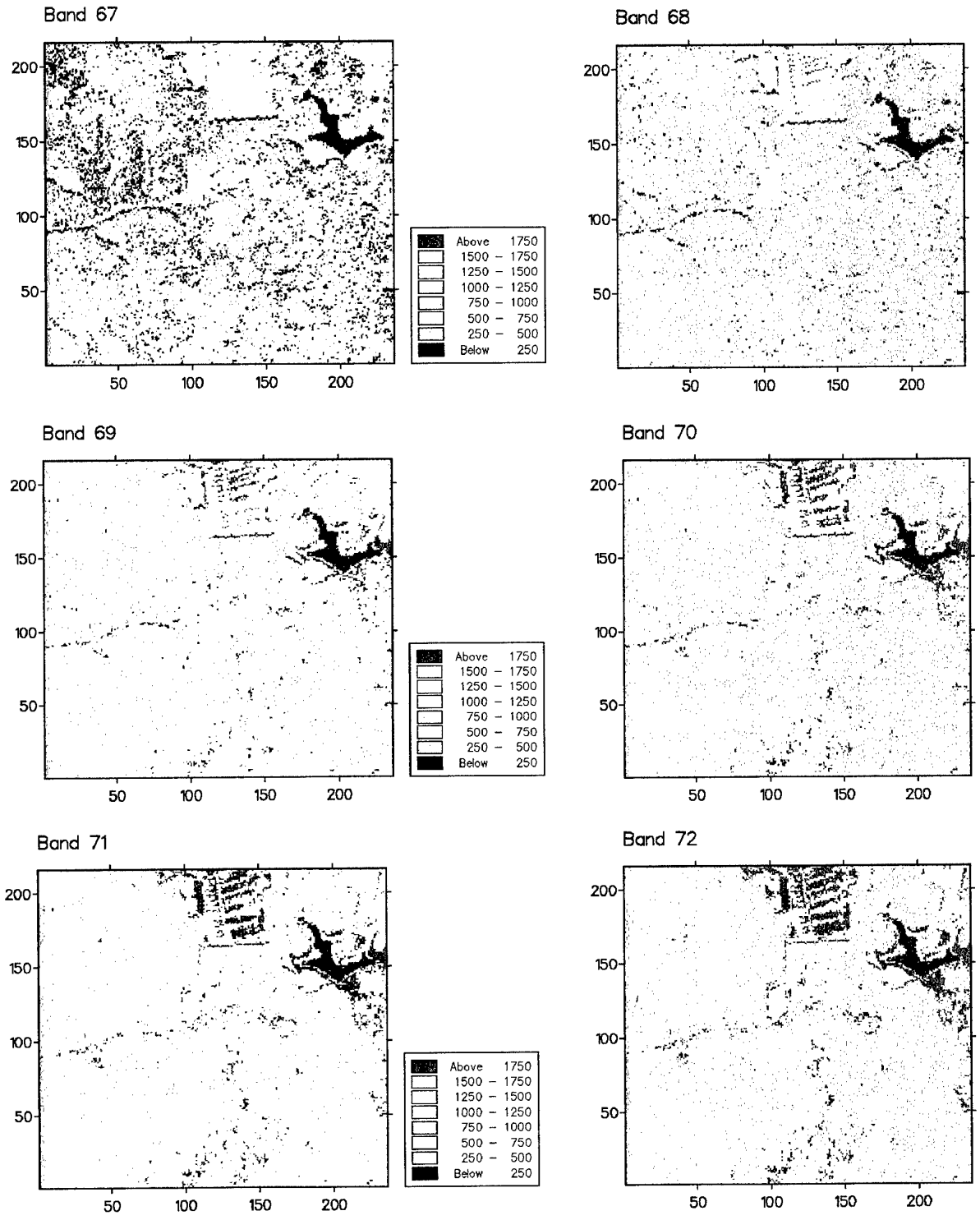

Figure 55. Pixel maps of wavebands 67 to 72 for the hymap image data

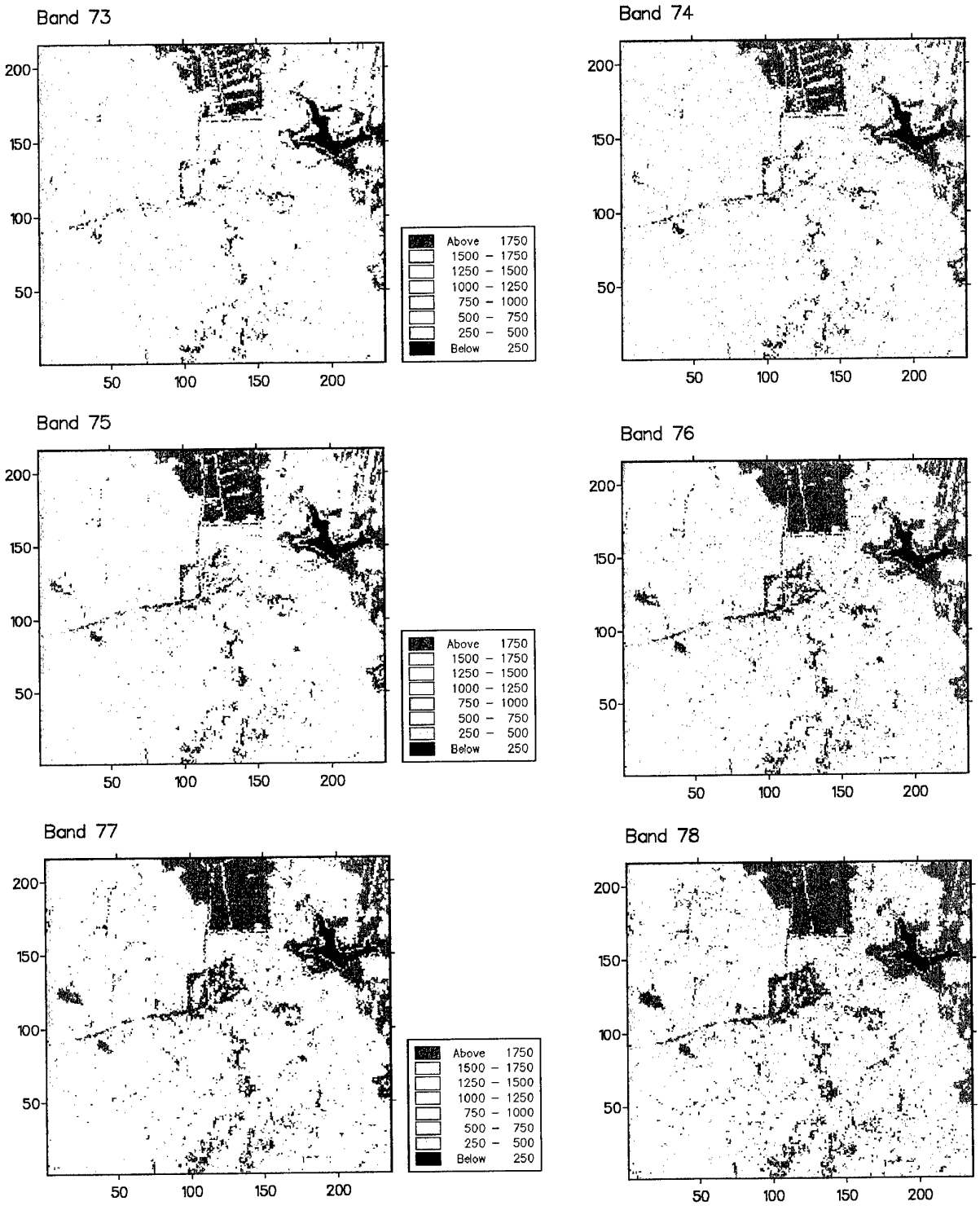

Figure 56. Pixel maps of wavebands 73 to 78 for the hymap image data

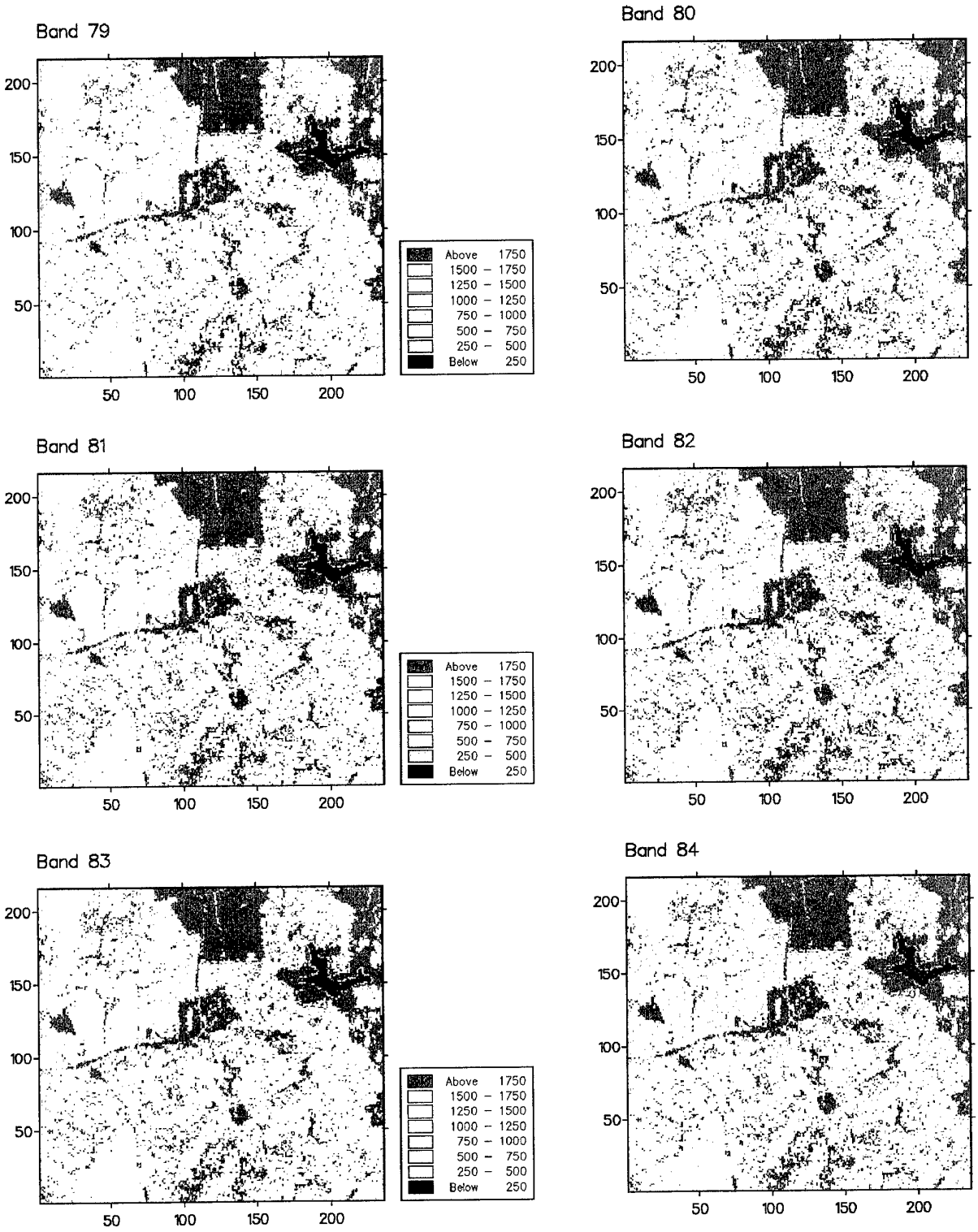

Figure 57. Pixel maps of wavebands 79 to 84 for the hymap image data

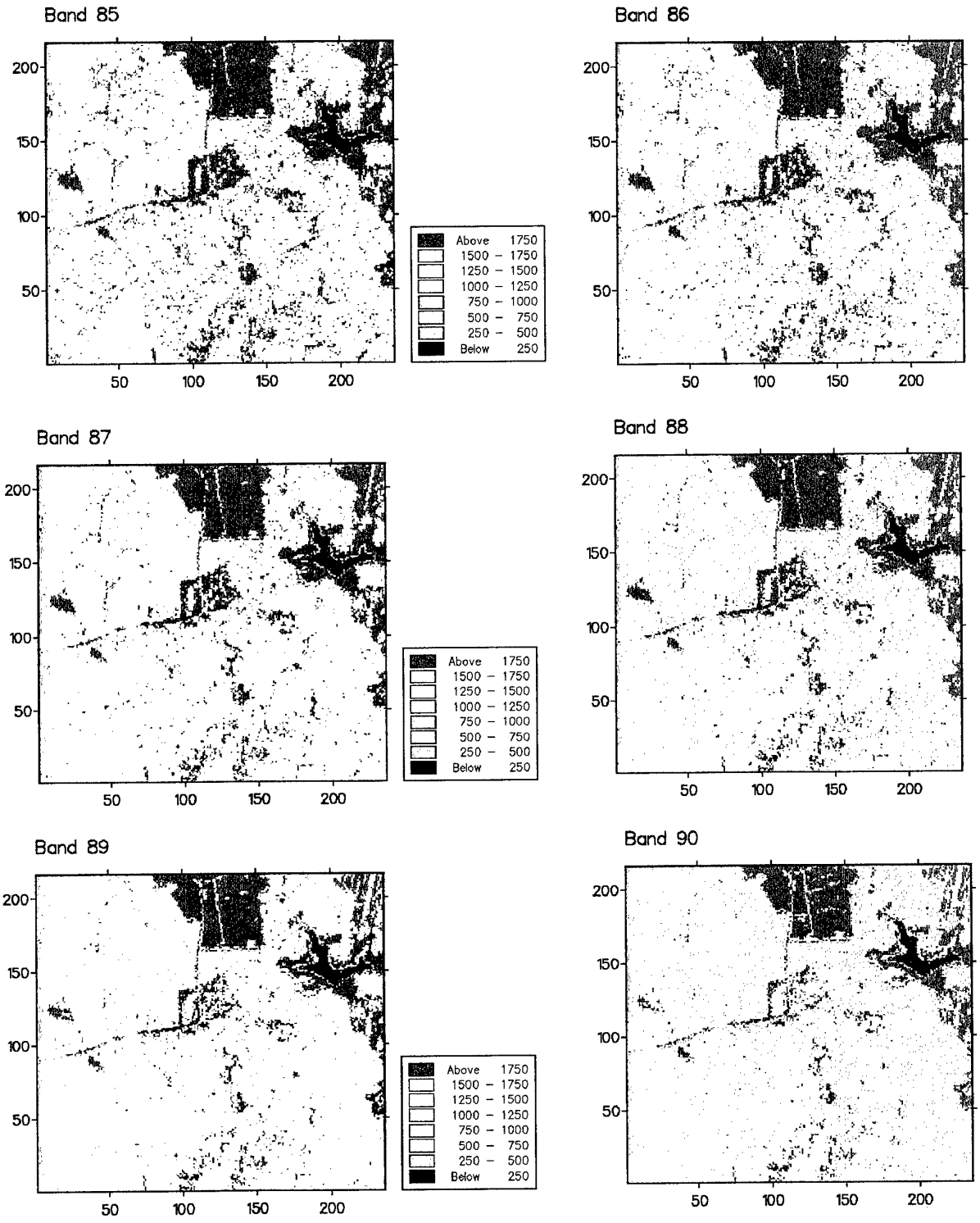

Figure 58. Pixel maps of wavebands 86 to 90 for the hymap image data

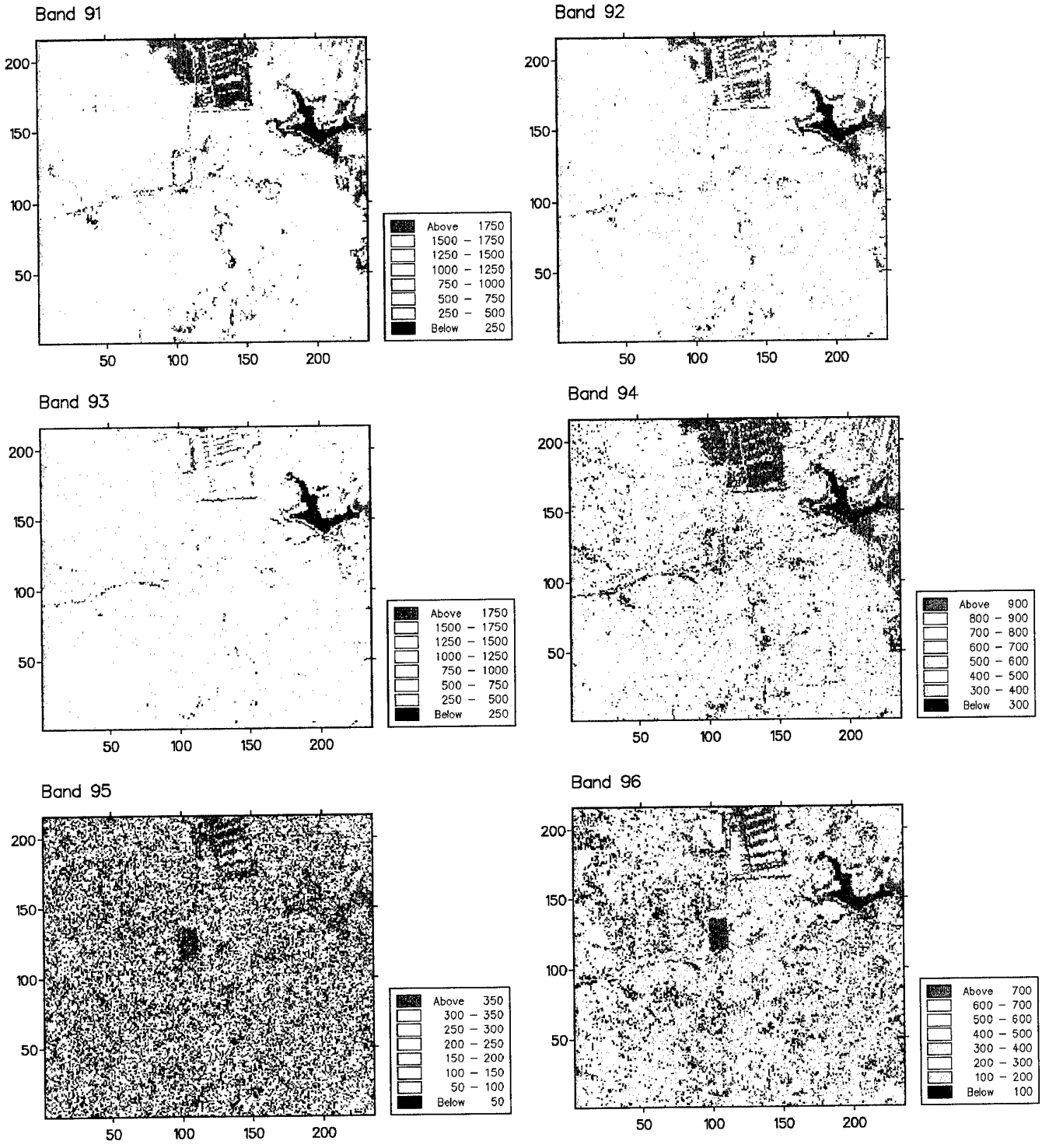

Figure 59. Pixel maps of wavebands 91 to 96 for the hymap image data

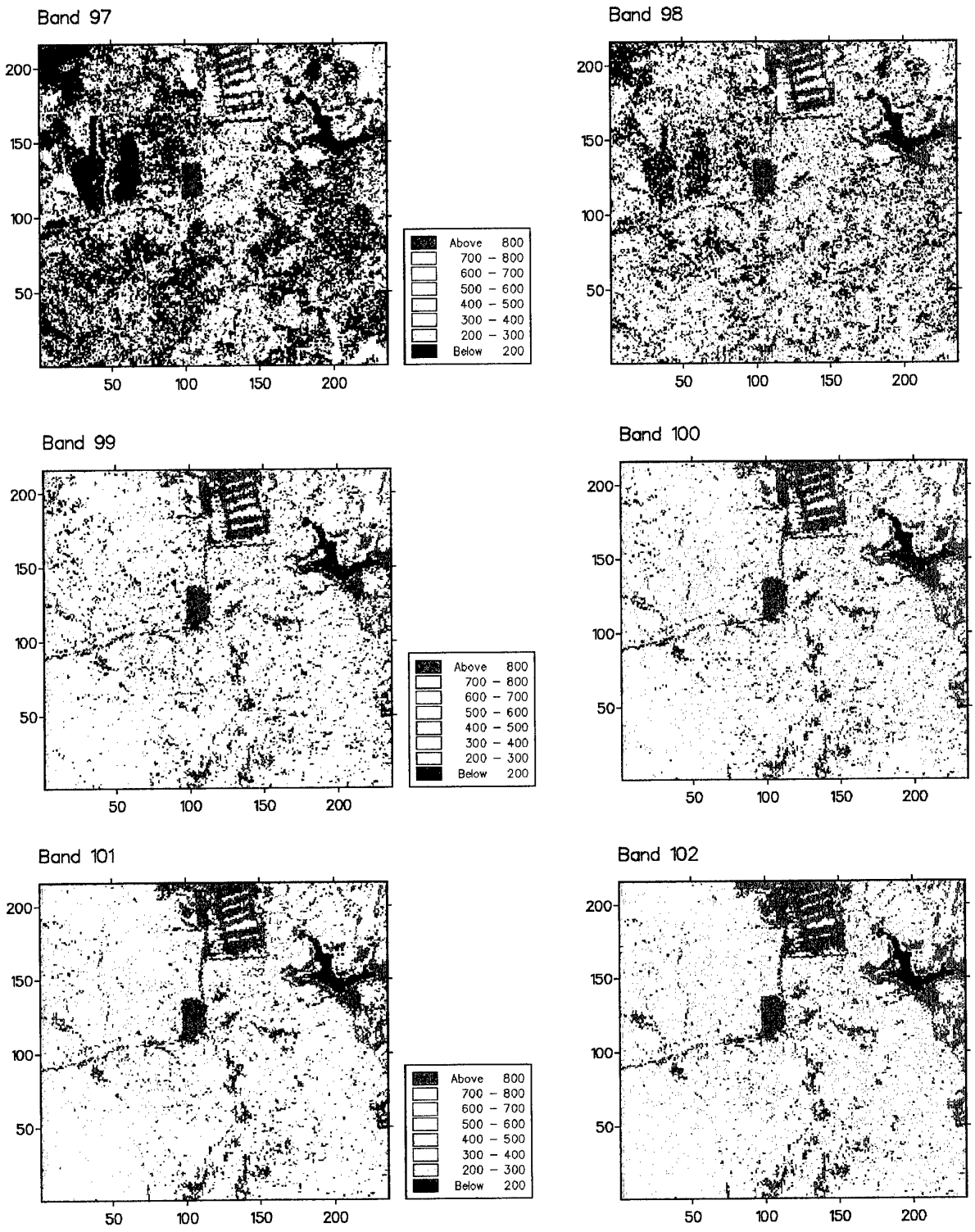

Figure 60. Pixel maps of wavebands 97 to 102 for the hymap image data

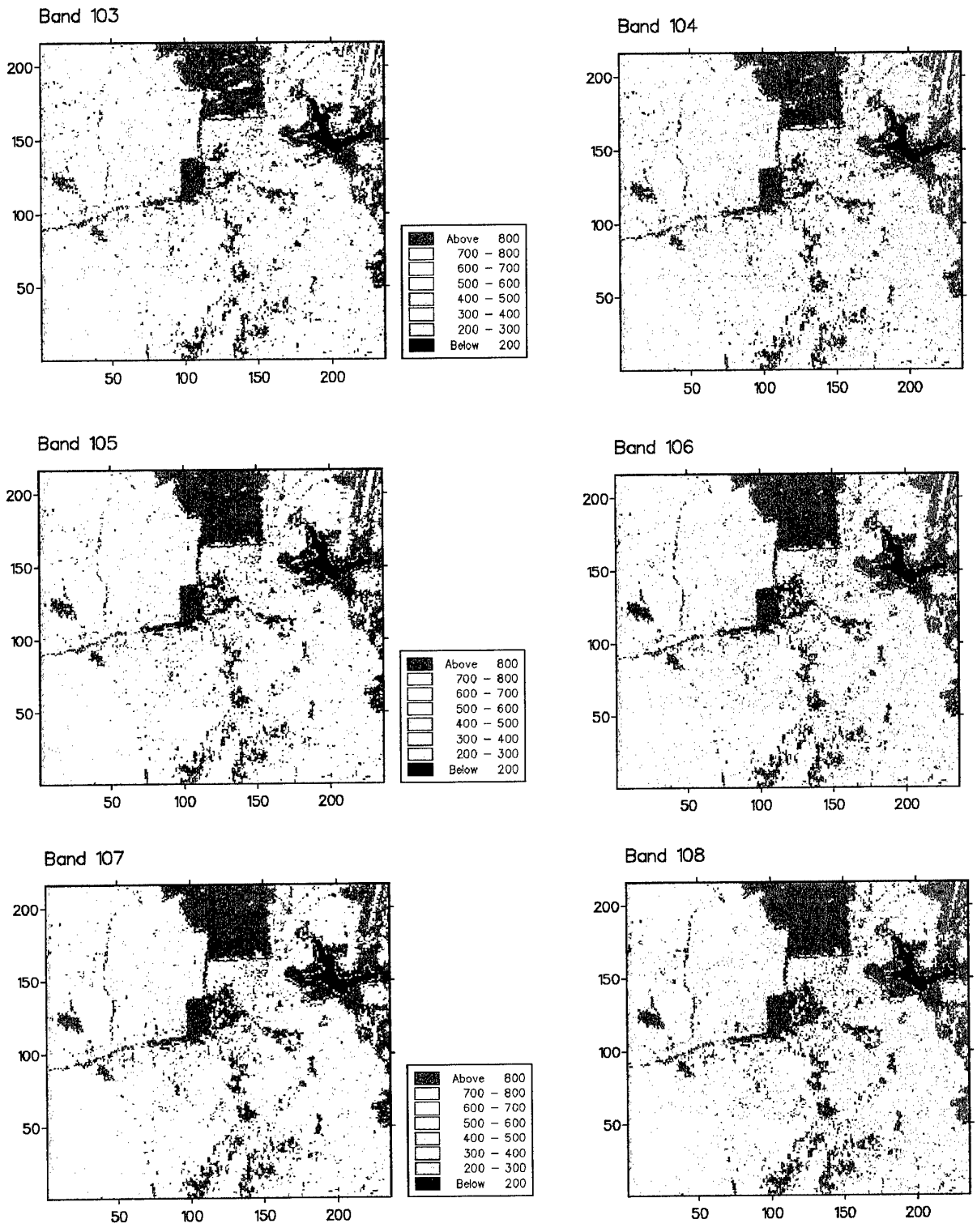

Figure 61. Pixel maps of wavebands 103 to 108 for the hymap image data

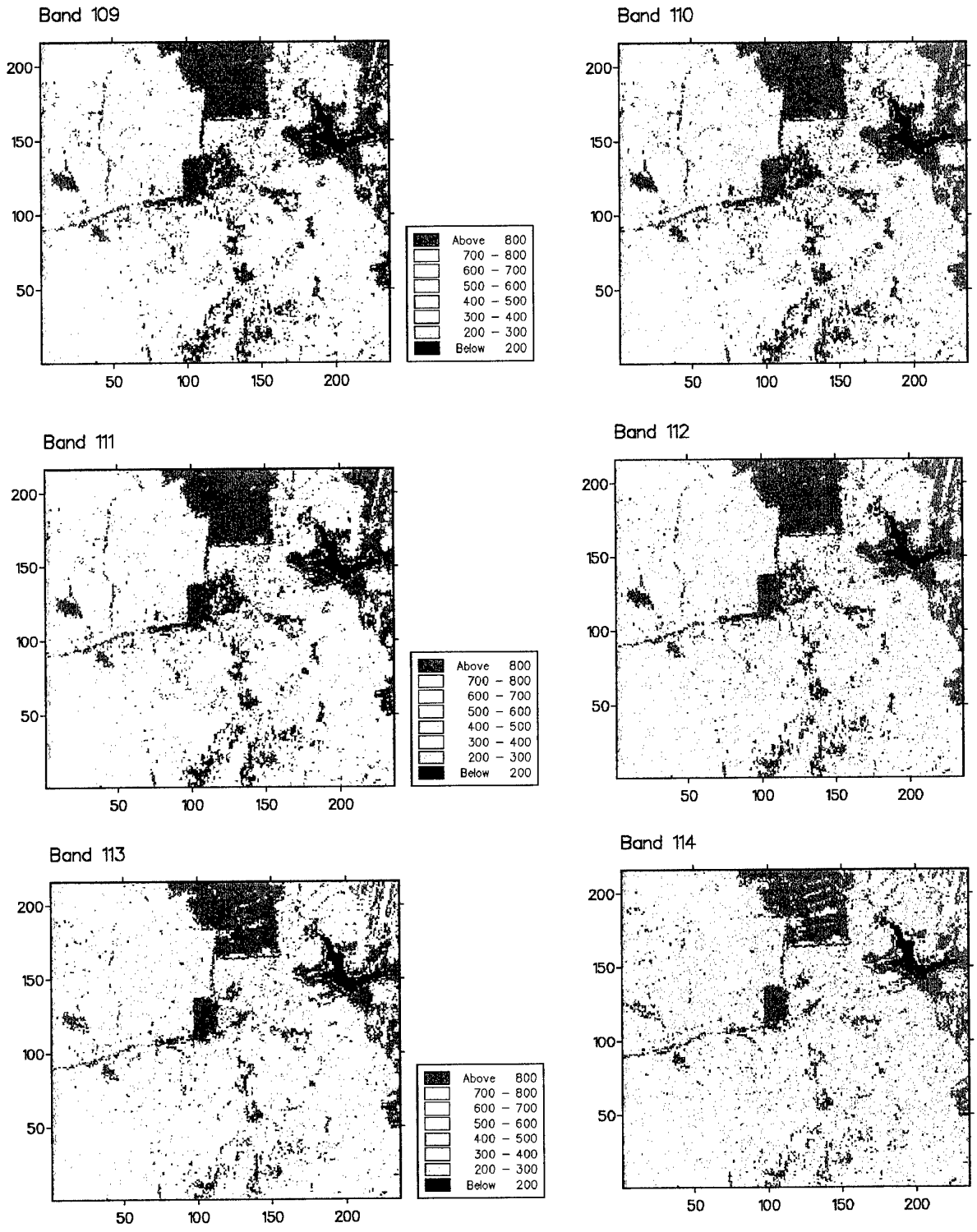

Figure 62. Pixel maps of wavebands 109 to 114 for the hymap image data

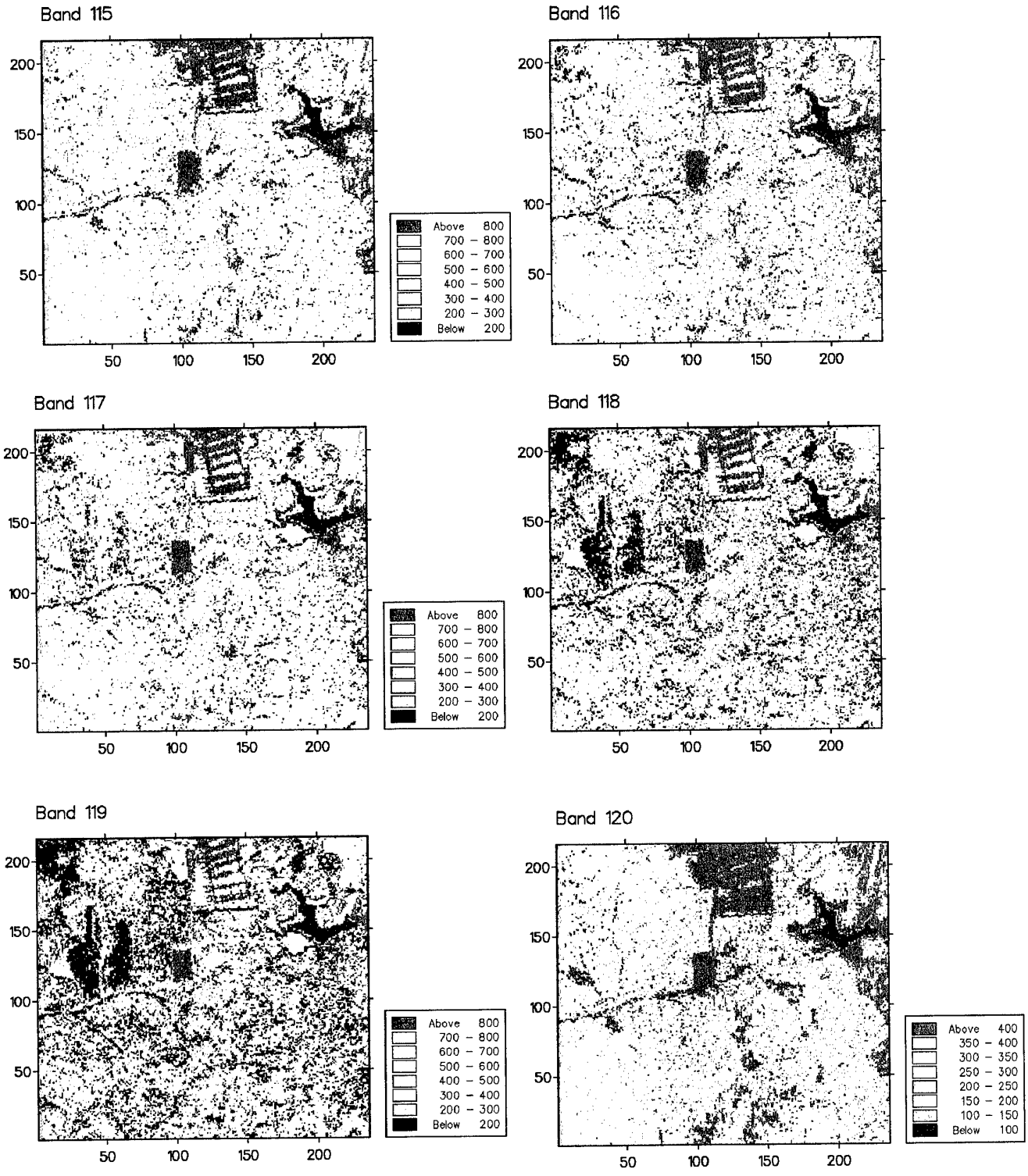

Figure 64. Pixel maps of wavebands 115 to120 for the hymap image data

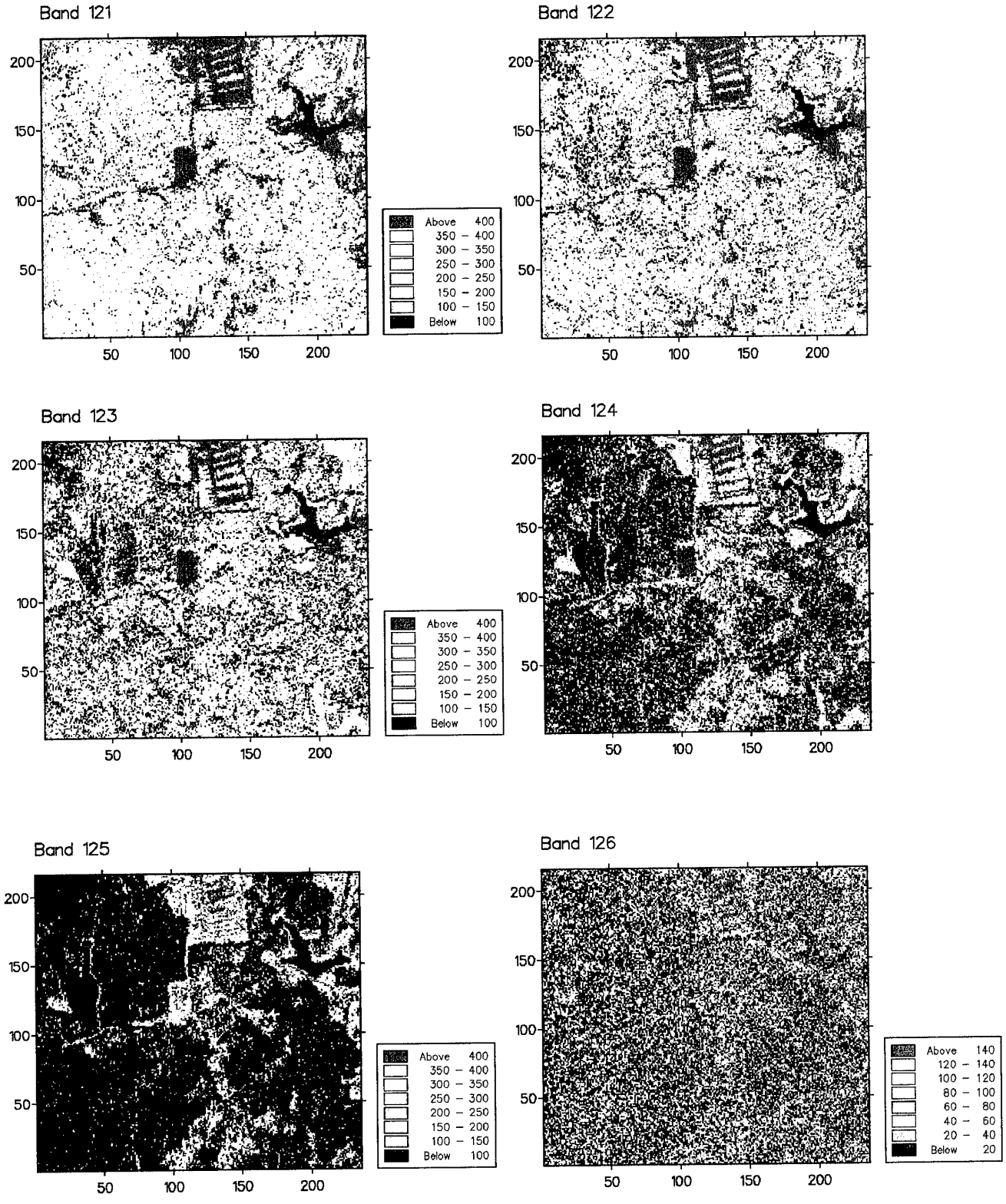

Figure 64. Pixel maps of wavebands 121 to 126 for the hymap image data

Summary of classification results

Table 9 shows the groupings of the bands that emerge from both visual (V) and statistical (S) appraisals. For the spectra shown in Figure18 it is the major changes that are noted in the classification in Table 9. For the maps a grouping has not been attempted at present – it is merely the changes in the texture that are noted in Table 9. The groupings identified from the correlation matrix are also reflected in those for the first 5 Pcs and in the experimental variograms.

Table 9. Suggested groupings of bands based on visual and analytical results.

Method	*Major changes in the spectra*							
Spectra (V)	13	18	35 – 37	50	60	63	70	93
	PC 1	*PC 2*	*PC 3*	*PC 4*	*PC 5*			
PCA eigenvectors (S)	18 – 19 61 – 62 66 – 94 99 –122	20 – 59	1 – 13	63 – 66 95	126			
	Class 1	*Class 2*	*Class 3*	*Class 4*	*Class 5*	*Class 6*	*Class 7*	*Class 8*
Classification of raw data (S)	1 – 18 64 – 69 94 –126	70 – 93 19	20 – 21	27 – 39 57 – 58 47 –48	40 – 46 59 – 60	22 – 26 49 – 56	61 – 62	63
Experimental variogram form (V)	1 – 17	20 – 62	63 – 64	19, 65 71 – 94 126	66 – 70 95	96 –125 18		
Variogram:long-range (S/V)	1 – 17	19 74 – 94	20 – 62	63 – 64	65 – 69	96 –101	102–115	95 126
Classification of model parameters (S)	1 – 13 19 120–125	14 – 18 69 – 94	63 – 64	27 –28 58 – 60	61 – 62	20 – 27 49 – 57	65 – 68 95 – 119 126	
	Sequence of changes noted in maps							
Maps (V)	1 – 17	18, 19, 20	21 – 38	39 – 46	47 – 57	58 – 62	63 – 65	66 - 69
	70 – 74 126	75 – 89	90 – 92	93 – 94	95	96 – 103	104 – 112	113 – 125

a)

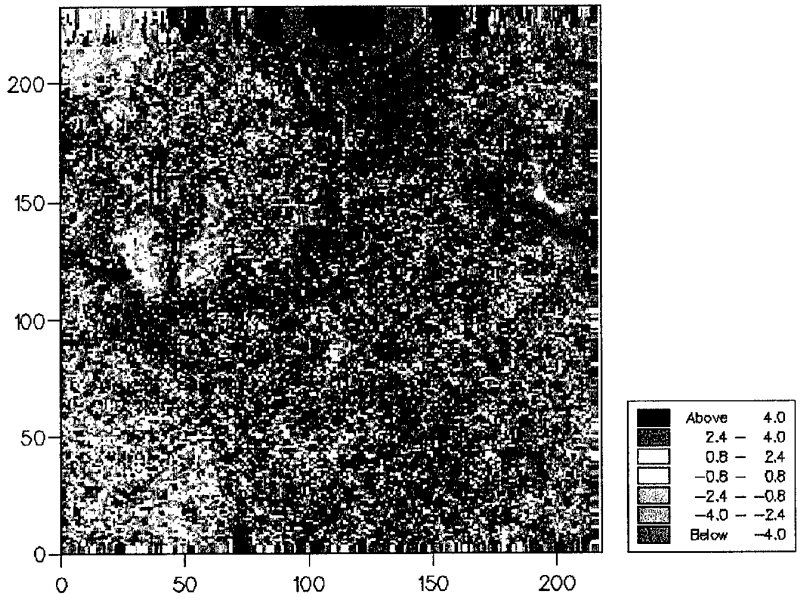

b)

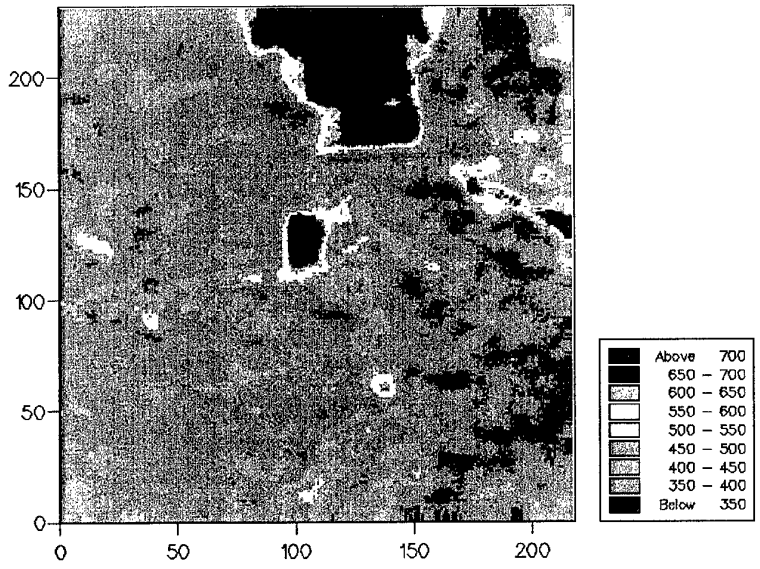

Figure 65. Factorially kriged estimates for waveband 10:
a) short-range component and b) long-range component.

a)

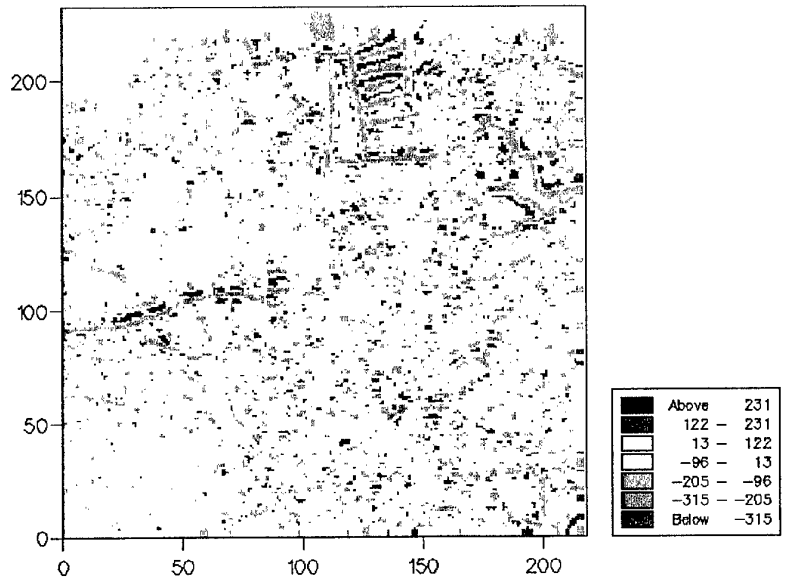

b)

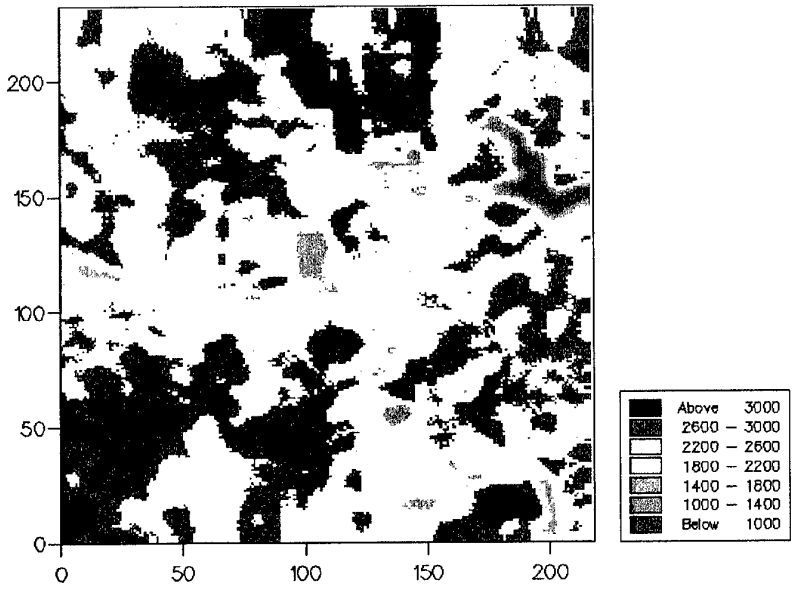

Figure 66. Factorially kriged estimates for waveband 22:
a) short-range component and b) long-range component.

a)

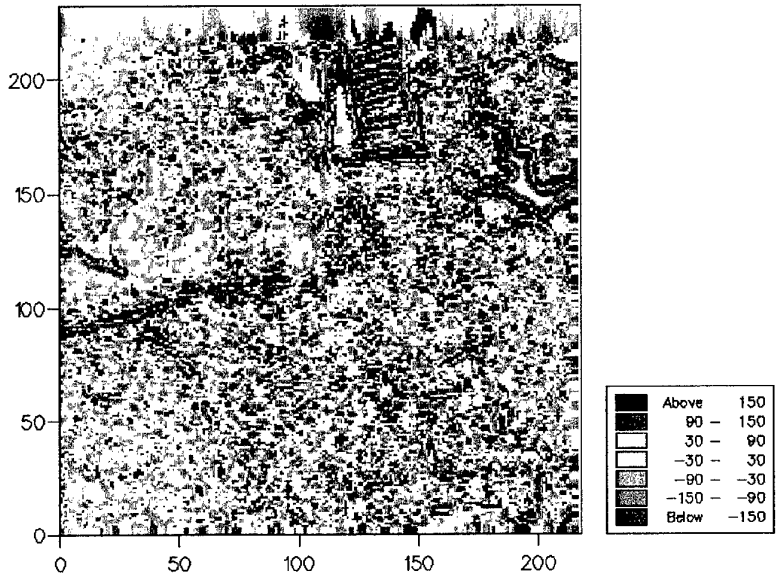

b)

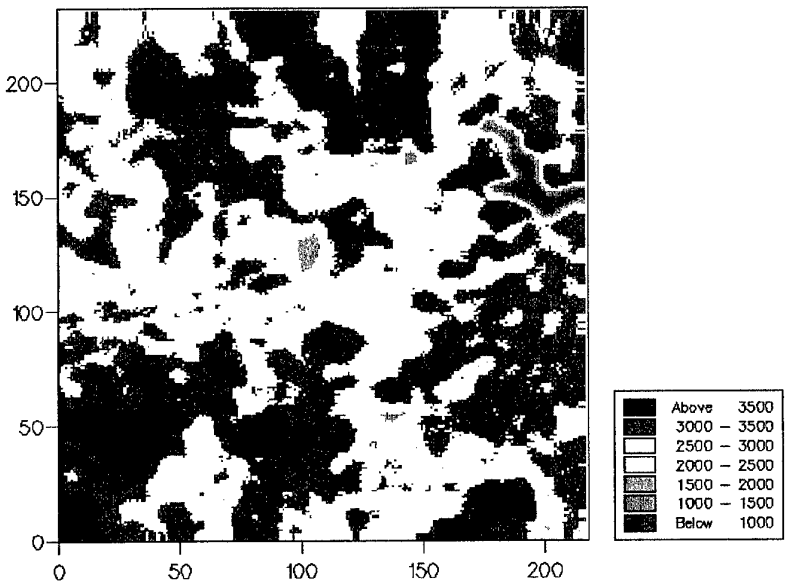

Figure 67. Factorially kriged estimates for waveband 47:
a) short-range component and b) long-range component.

81

a)

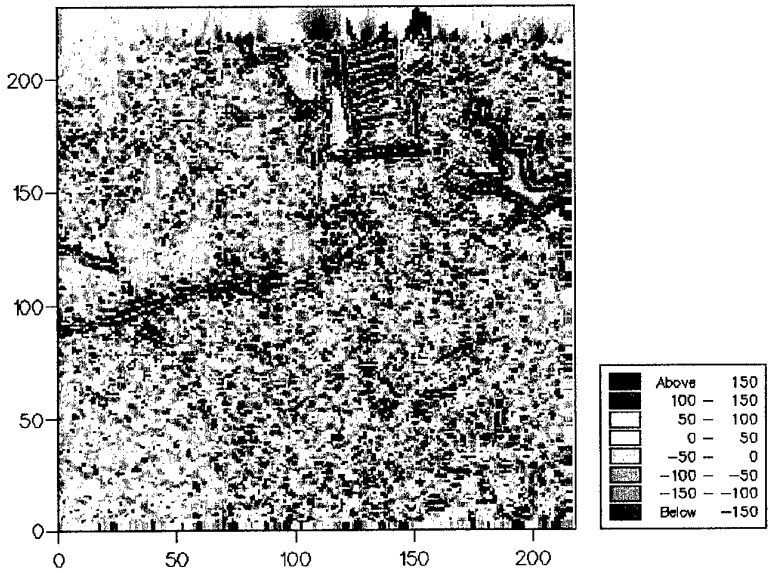

b)

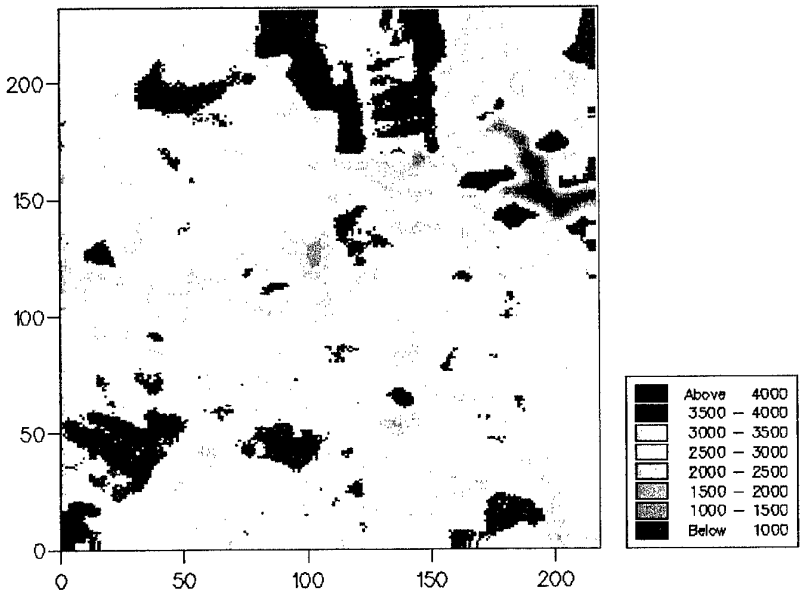

Figure 68. Factorially kriged estimates for waveband 58:
a) short-range component and b) long-range component.

a)

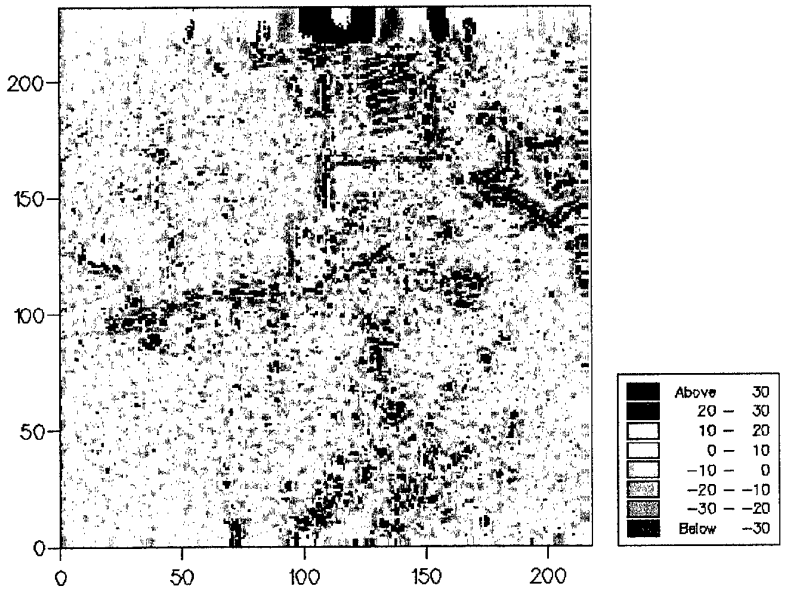

b)

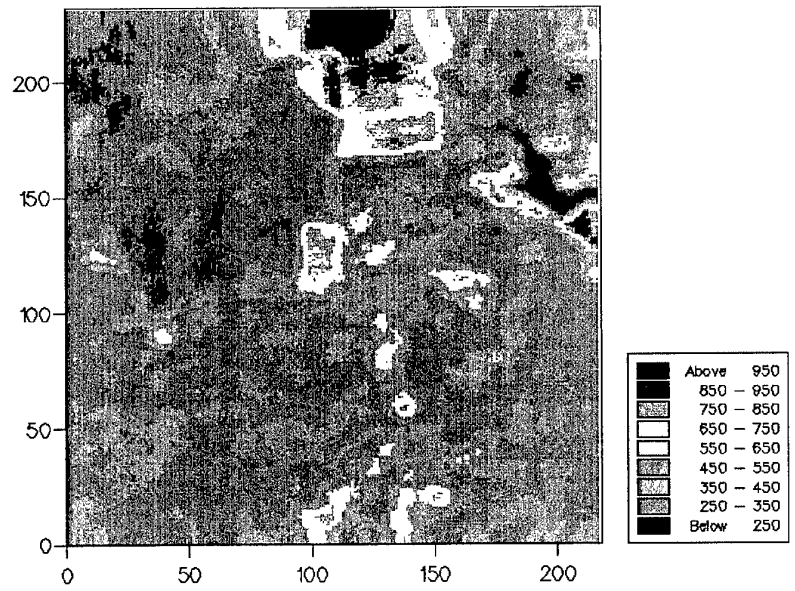

Figure 69. Factorially kriged estimates for waveband 66.
a) short-range component and b) long-range component.

a)

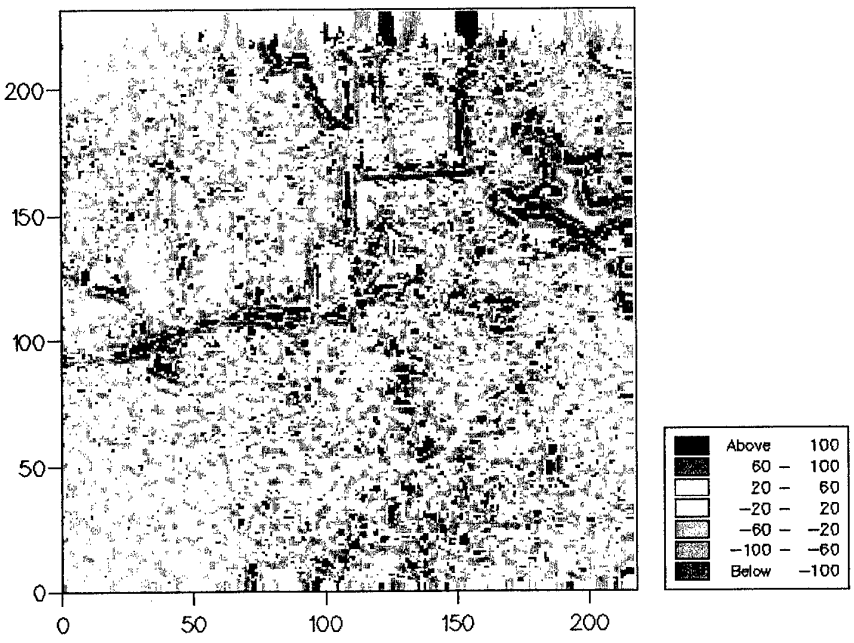

b)

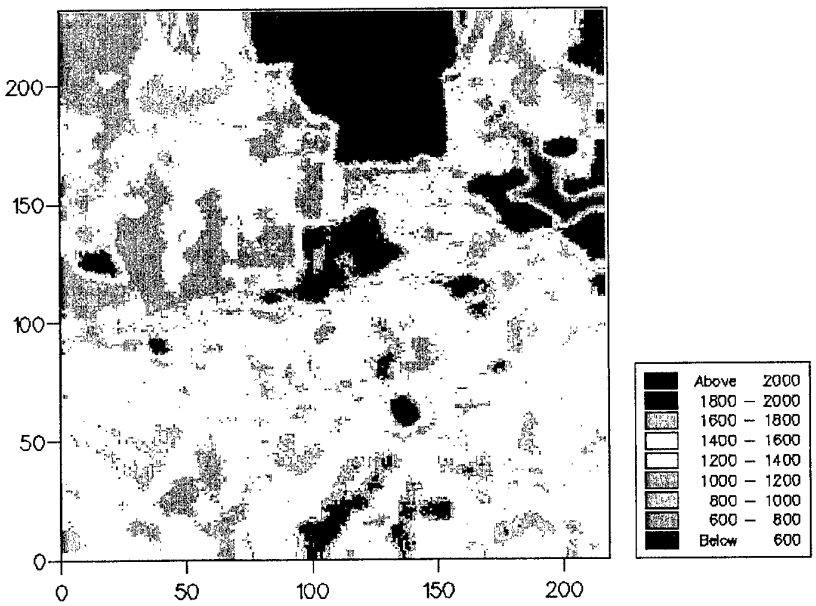

Figure 70. Factorially kriged estimates for waveband 83:
a) short-range component and b) long-range component.

a)

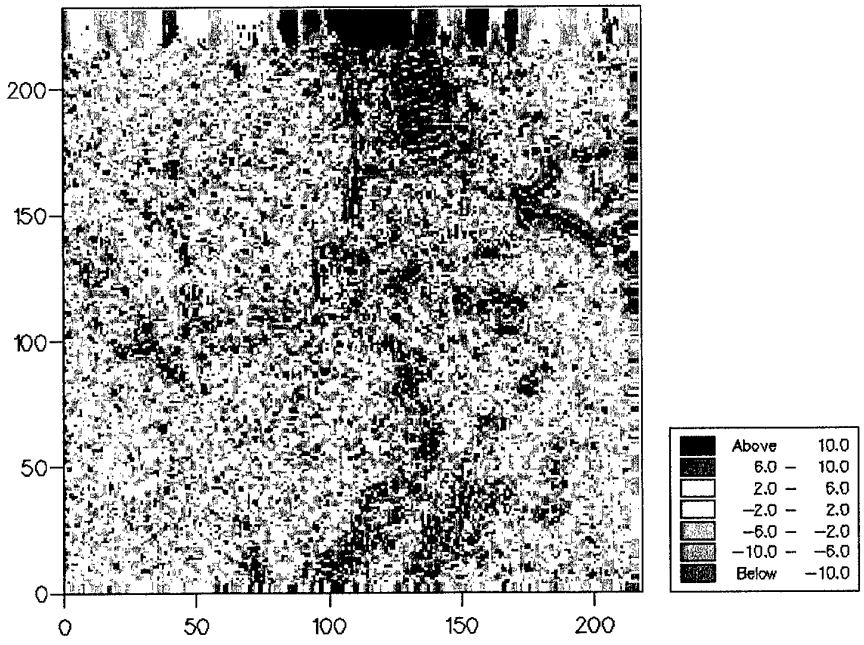

b)

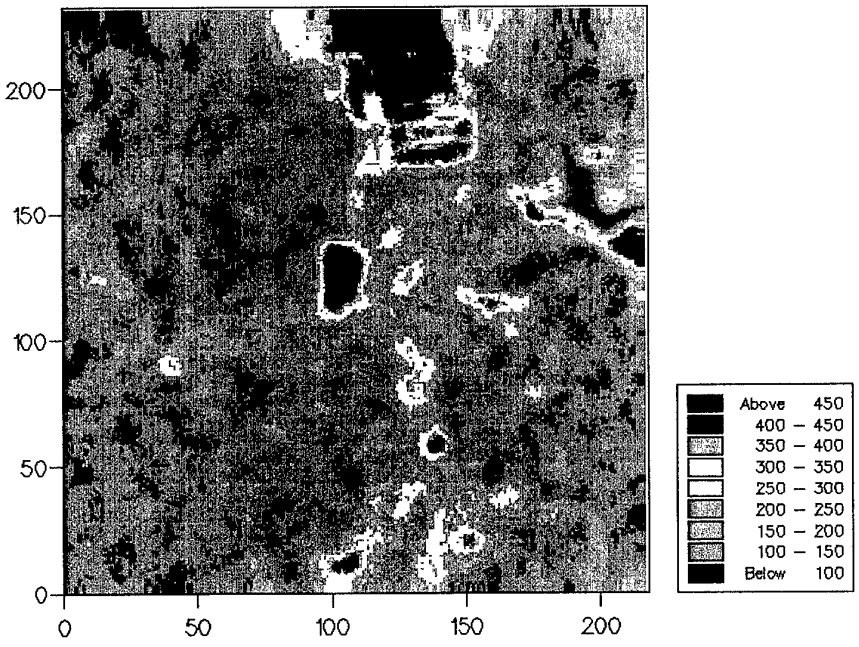

Figure 71. Factorially kriged estimates for waveband 95:
a) short-range component and b) long-range component.

a)

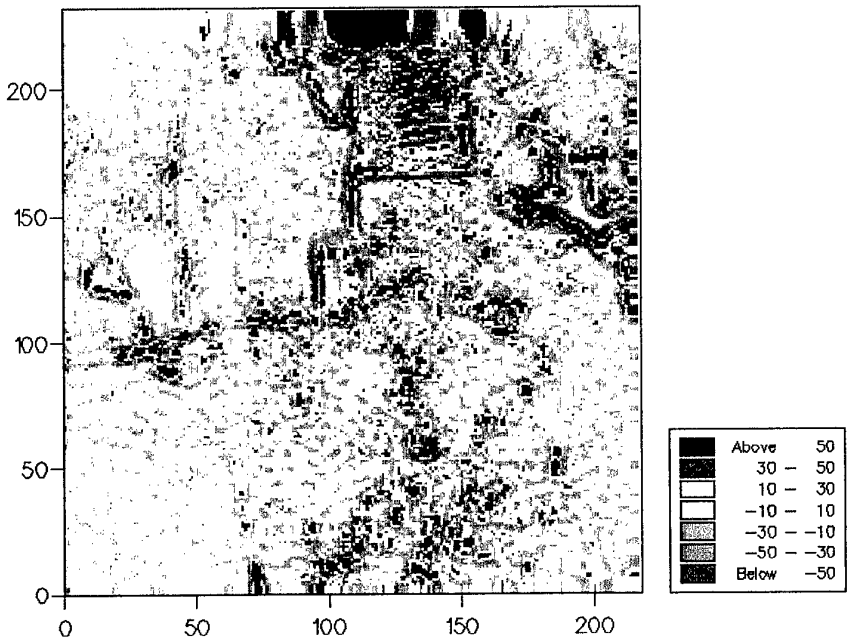

b)

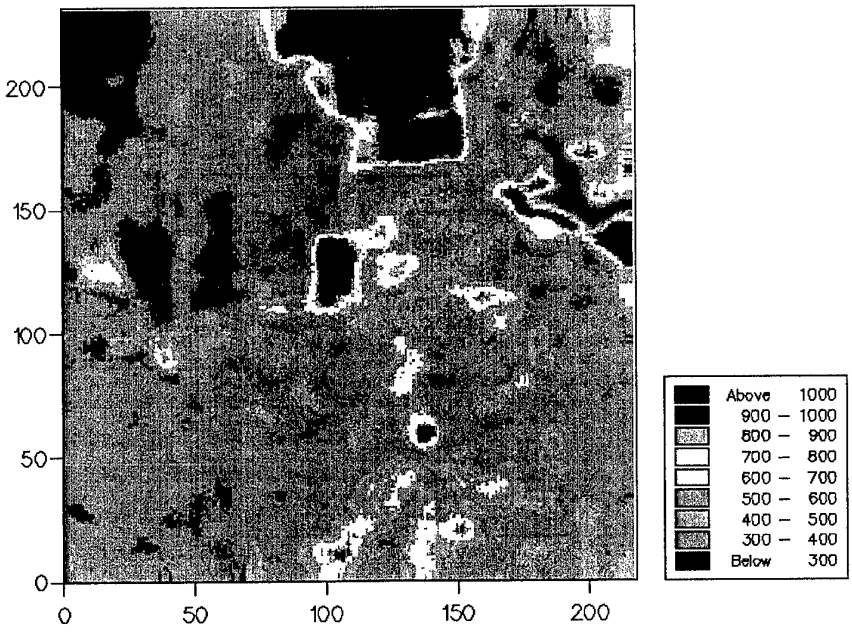

Figure 72. Factorially kriged estimates for waveband 115:
a) short-range component and b) long-range component.

a)

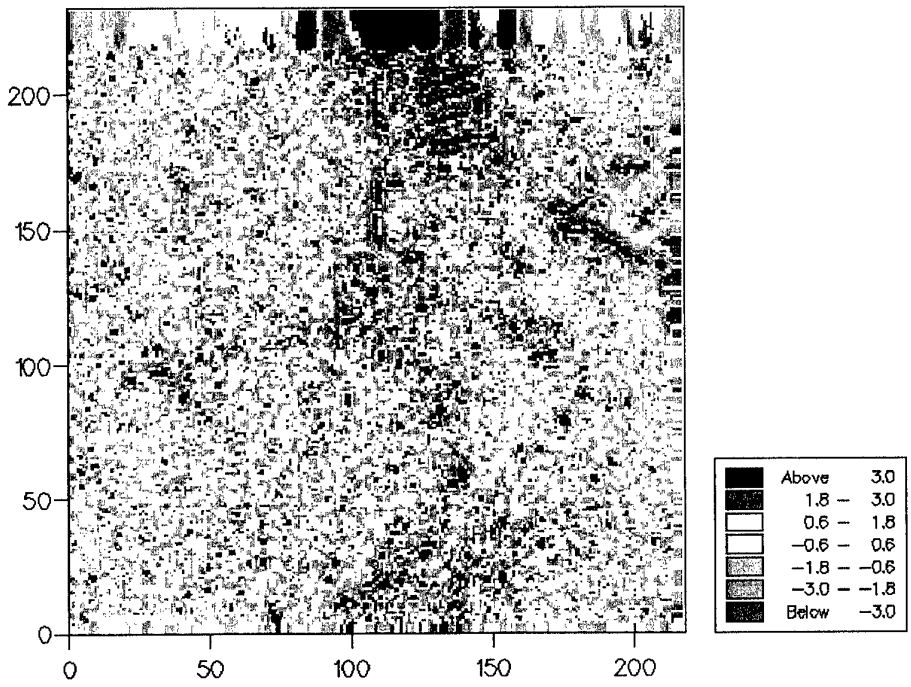

b)

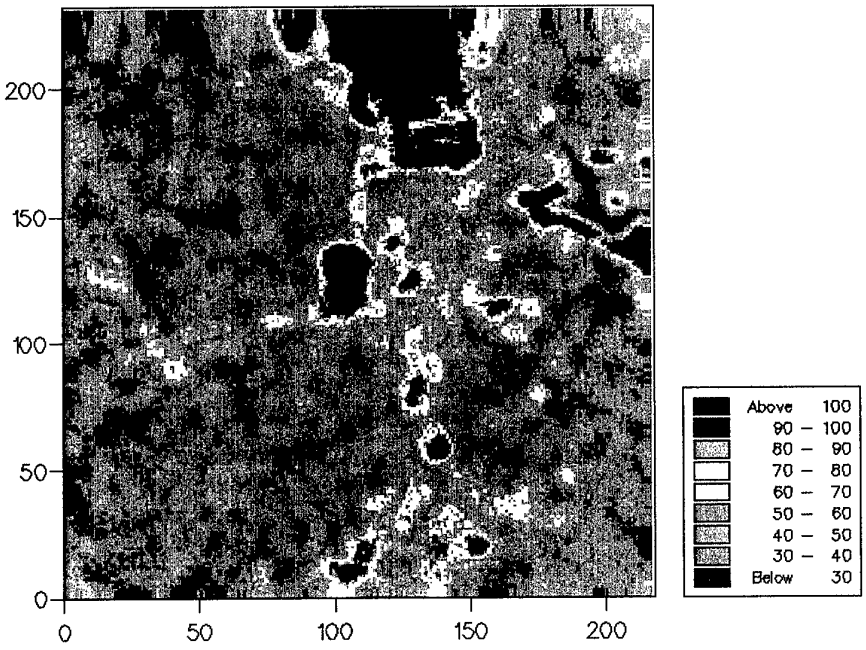

Figure 73. Factorially kriged estimates for waveband 126:
a) short-range component and b) long-range component.

PART III: A GEOSTATISTICAL AND WAVELET ANALYSIS OF THE NATIONAL SOIL INVENTORY OF ENGLAND AND WALES

Introduction

It was decided while on a visit to TEC by Mr W. Clark that Mr E. Bosch and Dr M. A. Oliver should extend the comparison of the geostatistical and wavelet analysis that they had done on the Fort A. P. Hill SPOT image to a large data set of soil information. The reason for this was to see how the techniques performed when the initial data are a sample rather than complete cover as in the image. For the SPOT image we had full cover of pixel information which we then sampled. Kriging and the low frequency wavelet coefficients were used to restore the data that had been removed (see report ?? and Oliver *et al.*, 2000). For the soil data we started with sample information and resampled this for the analyses. The wavelet analysis of the soil data was done by Mr E. Bosch during Dr Oliver's visit to TEC in June 2000.

The National Soil Inventory of England and Wales

The soil data that we have analysed are part of the National Soil Inventory (NSI) of England Wales, which was carried out by the Soil Survey of England and Wales between 1978 and 1983 (McGrath & Loveland, 1992). The aim of the survey was to provide a record of the soil information in these countries and both toxicity and deficiency of some elements of the soil that affect both grazing animals and arable crops at the national level. For the NSI to be an unbiased estimate of the distribution of types of land and their properties, strict protocols were applied to site location and description, soil sampling strategy, and soil profile description. This was very unlike the practice of 'free' soil survey which is commonly used to produce conventional soil maps (Avery, 1987). Considerable effort also went into quality control of pre-treatment and analysis of the samples, data recording, error trapping and construction of the database, because of the number of samples and the magnitude of the subsequent analytical programme (Loveland, 1990; McGrath & Loveland, 1992).

The number of samples was restricted to those falling at the intersections of a 5-km orthogonal grid. The sampling grid was offset 1 km north and east of the origin of the Ordnance Survey National Grid. If the sampling point fell on anything other than land, e.g. on a road, building, water-body etc., then the sampling point was moved 100 m north of the grid node. If that failed to locate suitable soil, then the point was moved 100 m west *from the originally intended point.* This process was repeated in steps of 100 m and 200 m from the grid node, in the order north, east, south and west. If no suitable soil was found after this procedure, then the site was abandoned for sampling purposes, although the land-use at the original sampling point was recorded so that the inventory was complete and to make clear the reason for the deviation. If a new sampling point was found, then the standard procedure for description and sampling was followed at that

point (see below). In this way, an unbiased record of the occurrence of various forms of land-use was maintained.

The principal interest was in agricultural land. No attempt was made to devise a sampling strategy to cover urban areas adequately. In total 5691 sites were sampled. The grid-reference located the site to within 10m on the ground, i.e. to an accuracy which would place any return visit within the original soil sampling sub-grid (see below).

Sampling

The soil profile was described in a pit dug to 80 cm (or less if rock was encountered) at each sampling point, using standard terminology (Hodgson, 1974). However, sampling was restricted to the uppermost 15 cm of *mineral* soil (or less if rock intervened), or of peat, as appropriate, i.e. litter layers were not sampled, as they were regarded as ephemeral. The actual sampling depth was recorded. Twenty-five cores of soil were taken at the nodes of a 4m grid within a 20 m x 20 m square centred on the Ordnance Survey (OS) 5-km grid-point. The cores were taken with a screw-type, mild-steel auger, to avoid contamination from traces of elements such as chromium and manganese present in stainless, plated or similar special steels. The cores of soil were bulked and mixed well in the field and double-bagged. in food-grade polythene bags, and a waterproof and rot-proof label ('Synteape') placed between the bags.
Samples were air-dried and milled in a mild-steel roller-mill (Waters & Sweetman, 1955) to pass a 2-mm aperture sieve. Preliminary work had shown that no detectable contamination of the samples arose from this procedure. The resulting data set comprises up to 127 analytical and descriptive parameters for each of 5691 points across England and Wales (Loveland, 1990; McGrath & Loveland, 1992). This collection of data is a unique and invaluable resource,

In this analysis we have examined only pH and total Zinc because they represent other variables well. From a principal components analysis (PCA) Zn was seen to load heavily on the first component and pH on the third axis, which reflected the effects of pareent material (PM) and leaching. The pH was measured by a combination electrode and pH meter in a 1:2.5 soil-water suspension (MAFF, 1986) on soil <2-mm. Zinc was determined using the <150 micrometre soil. It was extracted by *aqua regia*, and determined by ICP-AES (RES) (McGrath & Cunliffe, 1985).

Analysis

Figures 74a and 75a show the full set of pixel information on the 5-km grid for pH and Zn. (They have a different colour scale from the remaining maps because they were prepared on a different computer for the Ministry of Agriculture analysis. Nevertheless the variation can be compared and the relative area that we have worked on). The analysis for this project was carried out on a subset of the full NSI data. This was because the wavelet analysis requires a set of data that is square and can be sampled in octaves. The outline of the data for England and Wales is irregular and we selected data from the

central part of the country to obtain as large a square as possible that would suit the needs of the analysis. This resulted in a data set with 3500 sites. For the wavelet analysis the data were 'padded' with zeros so that there were no gaps. The latter arose because of the shape of the coastline and the urban areas within the country that were not sampled (see Figures 74a and 75a); they appear as white patches. Figures 74b and 75b show the data that were extracted for the analysis in this report.

a)

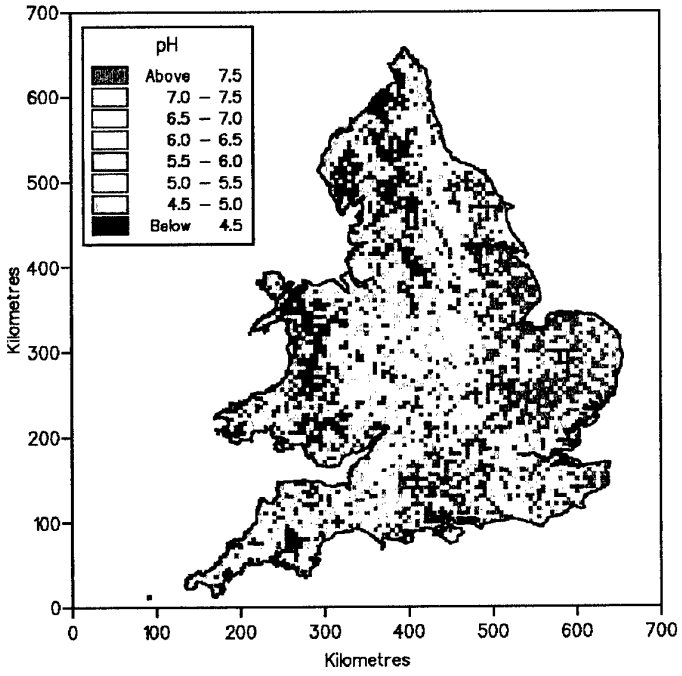

b)

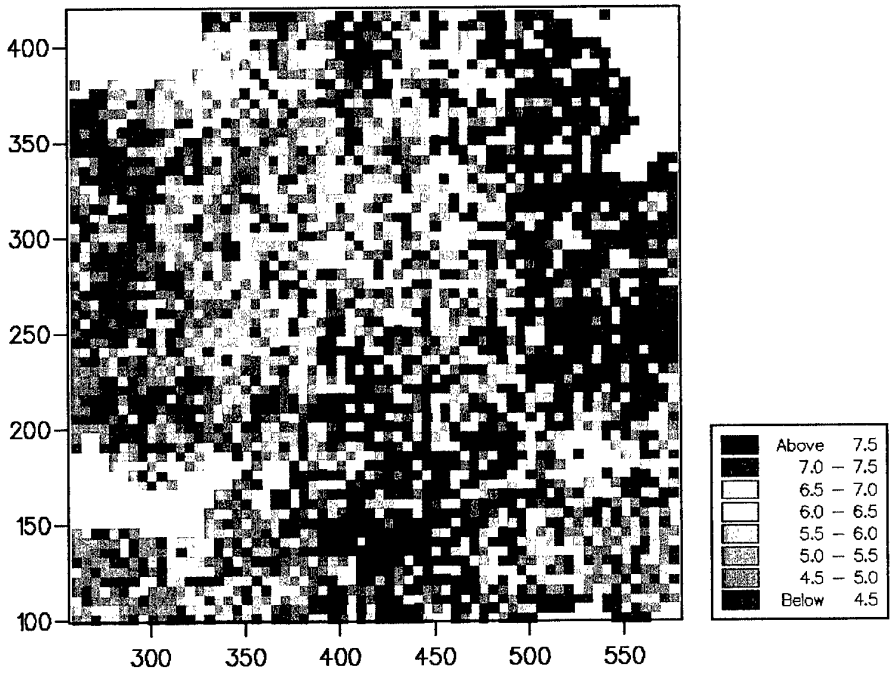

Figure 74. Pixel maps for pH: a) Original data for England and Wales, and b) Original data selected from the full data for analysis

a)

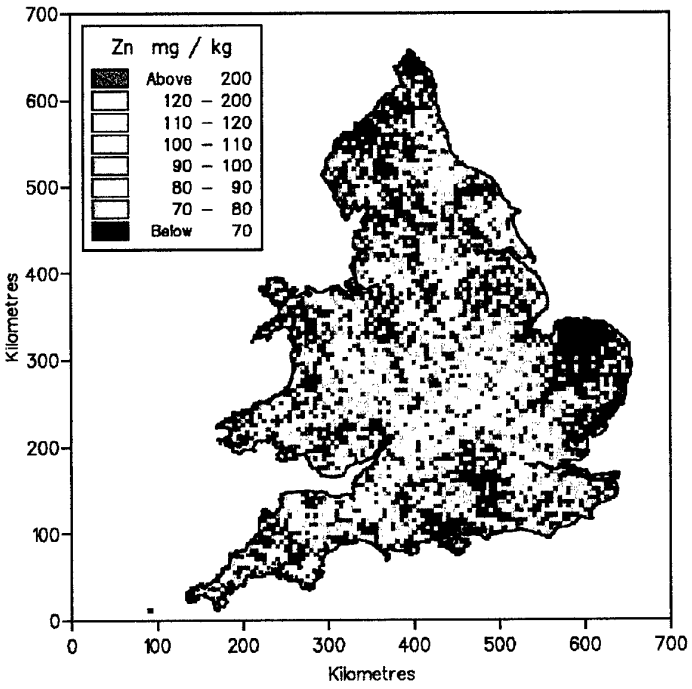

b)

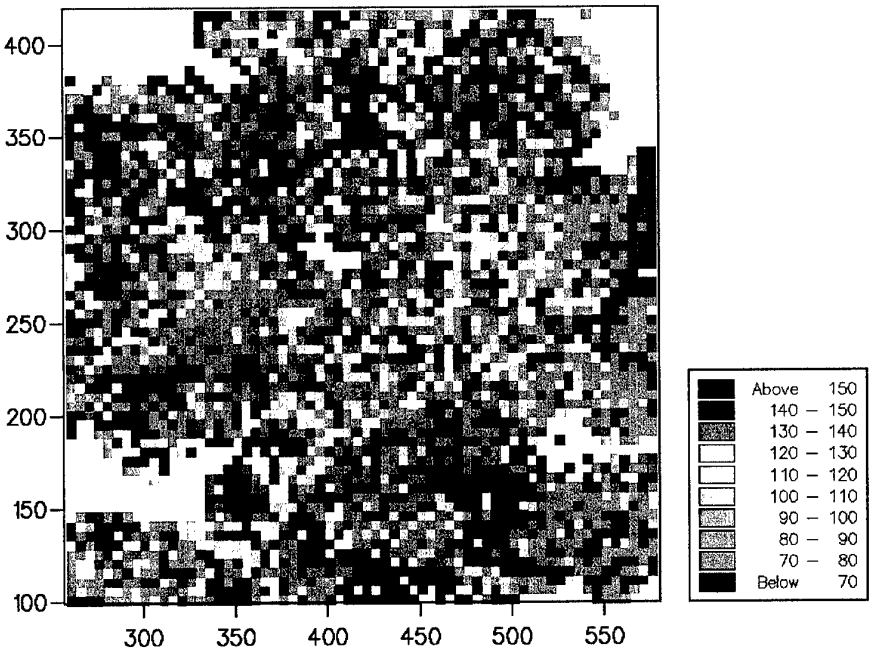

Figure 75. Pixel maps for Zinc: a) Original data for England and Wales, and b) Original data selected from the full data for analysis

Table 10 gives the summary statistics of the subset of the data. Zinc was strongly positively skewed which can be seen from Table 10 and Figure 76a, therefore it was transformed to common logarithms (log_{10}), Figure 76b. This transformation has produced a log-normal distribution which is common for many elements, Figure 76b and Table 10. The histogram for pH shows that this has a close to normal distribution, Table 10. A near-normal distribution is necessary for the variogram analysis because it is based in variances, which are unstable if the data do not have a near normal distribution.

a) Zinc b) $Log_{10}Zn$ c) pH

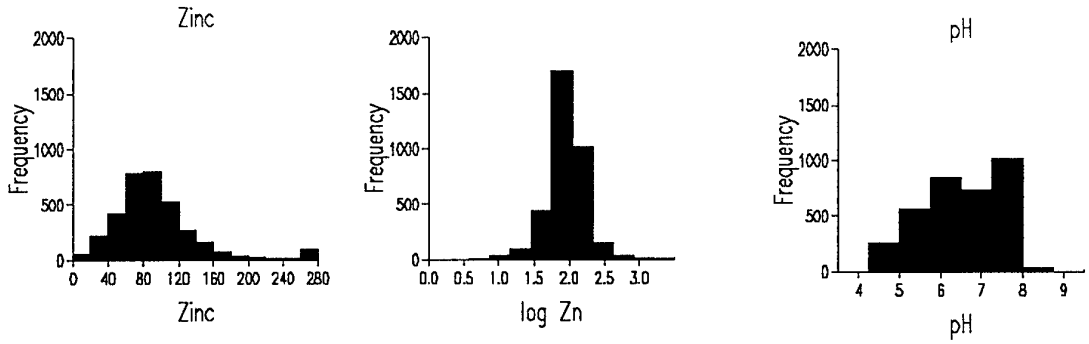

Figure 76. Histograms from the subset of the NSI data for Zinc and pH.

The data on the 5-km grid were further subsampled to compare the results of data reconstruction by both kriging and wavelet analysis. The subsampling produced grids of 10-km (1 site in every block of 4 sites resulting in 869 sites), 20-km (1site in every block of 16 sites resulting in 219 sites), and 40-km (1 site in every block of 64 sites resulting in 57 sites).

Table 10. Summary statistics for pH and Zinc for the subset of data used in the analysis.

Statistic	pH	Zinc	$Log_{10}Zn$
Minimum	3.200	6.00	0.7782
Maximum	9.100	3648.0	3.562
Mean	6.094	103.95	1.934
Variance	1.627	14273.2	0.0595
Standard deviation	1.275	119.47	0.2440
Skewness	-0.2377	14.03	-0.0002

GEOSTATISTICAL ANALYSIS

Variogram analysis

The spatial structure in the data was determined by computing the experimental variograms of pH and $\log_{10}$Zn. For the full set of data Zn and pH showed no marked evidence of anisotropy, therefore omnidirectional variograms only were computed. For both the full data and the subset the experimental variogram of pH showed evidence of trend. The semivariances continued to increase after an initial sill had been reached (Figure 77a). This suggests the presence of smooth continuous variation that violates the assumptions of geostatistics, which assumes that the variable is random. Therefore, we modelled the trend by linear and quadratic functions of the co-ordinates so that the analysis could be done on the residuals from the trend. The linear function was less effective in accounting for the trend than the quadratic one: the latter removed over 30% of the trend in both cases. The variogram was then computed afresh on the residuals, and this now shows a more simple bounded form, Figure 77b.

Most of the variograms were fitted by nested functions. The models fitted to the data included single exponential, spherical, and power functions including linear, double exponential and spherical, and exponential with linear functions. For $\log_{10}$Zn (Figure 77c) and pH of the residuals double spherical models provided the best fit. The equations for the models are given below.

Double exponential

$$\gamma(h) = c_0 + c_1\{1 - \exp(-h/r_1)\} + c_2\{1 - \exp(-h/r_2)\}$$

where c_1 and r_1 are the sill and distance parameter of the first structure, and c_2 and r_2 are the sill and distance parameter of the second structure.

Double spherical

$$\gamma(h) = c_0 + c_1\left\{\frac{3h}{2a_1} - \frac{1}{2}\left(\frac{h}{a_1}\right)^3\right\} + c_2\left\{\frac{3h}{2a_2} - \frac{1}{2}\left(\frac{h}{a_2}\right)^3\right\} \qquad \text{for } h \le a_1$$

$$\gamma(h) = c_0 + c_2\left\{\frac{3h}{2a_2} - \frac{1}{2}\left(\frac{h}{a_2}\right)^3\right\} \qquad \text{for } a_1 \le h \le a_2$$

$$\gamma(h) = c_1 + c_2 \qquad \text{for } h \ge a_2$$

where c_1 and a_1 are the sill and distance parameter of the first structure, and c_2 and a_2 are the sill and distance parameter of the second structure.

a) pH – raw data

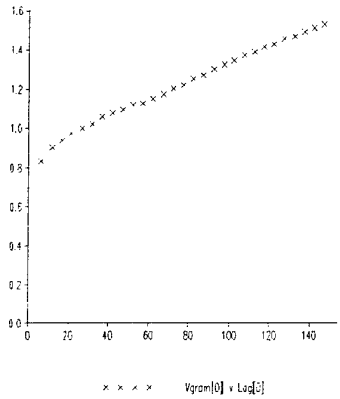

b) pH residuals

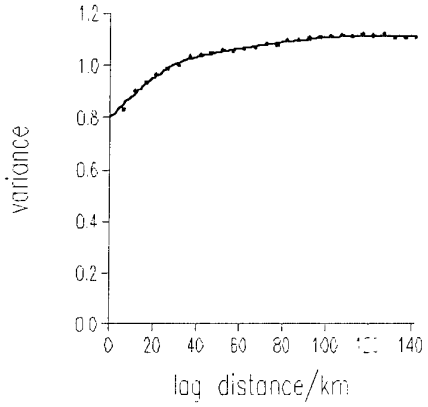

c) $Log_{10}Zn$

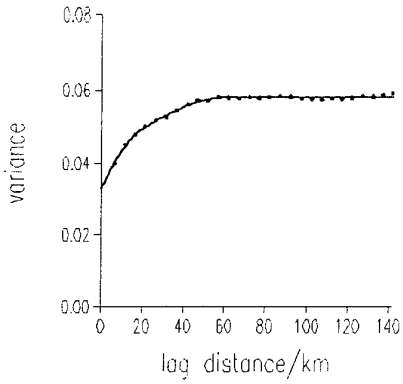

Figure 77. Experimental variograms (symbols) and fitted models (lines): a) raw values of pH, b) pH residuals, and c) $log_{10}Zn$.

These results show that there are two main scales of spatial variation: a short-range component of about 18 km for $log_{10}Zn$ and 37 km for pH (residuals), and a long-range component of 61 km for $log_{10}Zn$ and 118 km for pH (residuals). The average short-range component for the full data for the range of properties examined was 24 km, and the average of the long-range component was 89 km. There are slight differences in the ranges for these subsets, but they are within similar orders of magnitude. A characteristic of the variograms of the subset and of the full data is their large nugget variance (c_0): it is more than 60% of the sill variance for most variables. Most of the nugget variance can be accounted for by variation over distances less than the sampling interval of the grid. This shows that the 5-km grid interval misses a considerable proportion of the variation in the soil.

Figure 74 shows the pixel map of pH. There are two spatial scales of variation evident in the map. Areas with a pH of less than 6 are in the western part of the country in the main, which is also where the main uplands are, and where agriculture is dominated by grassland systems - optimum pH between 5 and 6.. These are also the wettest parts of England and Wales. Much of central and eastern England has pH values of 7 and above, partly reflecting geology and the distribution of calcareous soils, but also the widespread use of lime on arable soils (optimum pH *c.* 6.5 - 7.5). There are areas of lower pH in the S associated with the Tertiary sands and gravels. The E-W differences in pH values reflect the pattern of rainfall as well as elevation and land-use. Figure 75 shows the original values as a pixel map for total Zn. There are many areas with large concentrations, and the most extensive of these follows the Jurassic clay band from SW to NE across the country. There are other areas trending N to S from the Midlands of England to Tynemouth (not on the subset map). These seem to be associated with the Carboniferous shales and sandstones, as do the areas of large concentrations in central Wales.

Kriging

Ordinary kriging and factorial kriging (kriging analysis) have been described in earlier reports (Contract Nos. N68171-97-C-9029; N68171-98-M-5311). Ordinary kriging was used to reconstruct the data after subsampling them to produce smaller data sets. Punctual kriging was used so that the estimates and maps could be compared with predictions from subsets of the data. The estimation grid was chosen to coincide with the 5-km sampling grid. Estimates were made at the nodes of this grid so that we could compare the kriged estimates at the sampling points with the original values where these had been removed. At the places where there were data punctual kriging returns the sample value there. The original variograms were used for the analysis because it is unlikely that their structure would change over time. In addition those from the subsets have large nugget variances and they are less reliable because there are few comparisons for each semivariance, especially for the 40-km grid.

For pH ordinary kriging was done on the residuals and the quadratic trend added back to the estimated residuals afterwards.

The ordinary kriged logarithmically transformed predictions for Zinc were back-transformed for mapping so that the variation could be seen on the original scale in which the variable had been measured. This is not straightforward because the kriging variance must be taken into account. The equation for back-transformation is:

$$\hat{Z} = \exp\{\hat{Y}(\mathbf{x}_0) \times \ln 10 + 0.5\sigma_Y^2(\mathbf{x}_0) \times (\ln 10)^2\}$$

where $\hat{Y}(\mathbf{x}_0)$ is the estimated value of $\log_{10}$Zn at $\mathbf{x}_0$ and σ^2_Y is the estimation variance.

Factorial kriging was done on the full set of data to examine the different scales of variation in the data and to compare the results with those of the multi-resolution wavelet analysis. The aim is to filter out the different scales of variation, so that the independent

components of the spatial structure can be examined as an aid to further interpretation. Factorial kriging estimates the long- and short-range components separately. The variation is nested for both pH and Zn; the variograms have two spatial structures. The pixel maps of the raw data, Figures 74 and 75 suggest that there are two scales of variation, and this is confirmed by the variogram results. The variation at the longer scale appears to be related to the geology for Zn and pH and also rainfall and elevation for the latter. Zinc is a good example of many of the other variables for this analysis. For the long-range

WAVELET ANALYSIS

The method for this analysis was described in a previous report (N68171-98-M-5311) and also in Oliver *et al.* (2000) for SPOT image data. This is the first analysis that we are aware of using soil data in two dimensions. There are few data sets in the world for soil that are on a grid and would provide adequate data for this analysis. Wavelets enable data reconstruction and multi-resolution analysis by deriving the low frequency and high frequency coefficients from the data. The low frequency wavelet transform has been used to restore the data from the subsamples on the original 5-km grid and to identify the long-range spatial component at the coarser resolutions. The average of the high frequency wavelet transforms has been used to identify the short-range component. The advantage of wavelet analysis at the outset for the pH data is that there is no need to take account of trend. An important advantage of this analysis is that it is unaffected by non-stationarity.

RESULTS FOR pH

The following series of maps (Figures 78 to 80) shows the reconstructed values of pH from ordinary kriging and the low frequency wavelet coefficients for the three sampling grids. One noticeable difference between the maps is that the kriged maps appear more 'spotty'. This is because kriging returns the sample value at the data point, whereas the wavelet analysis is a predicted value at the data points as well as at other points. Another difference arises from the fact that the data were padded for the wavelet analysis with zeros – these are the larger blue areas beyond the coastline and also the urban areas where there were no sampling locations. Figure 78b for the data on a 10-km grid there is slightly more of the original detail in the variation evident, whereas the kriged map (Figure 78a) shows the effect of smoothing from kriging.

For Figure 79a and b the effects of the greatly reduced number of sampling sites is evident in the loss of detail. For Figure 79a the margin around the map is because there were no data there to krige from. Kriging, Figure 79a, has smoothed the variation more than wavelet analysis, Figure 79b, and the spotty appearance of the former map is the effect of punctual kriging. Figure 80a and b shows the kriged and low frequency wavelet coefficients for the 40-km grid. It is clear that much detail has been lost and that there is more difference between these two maps than between those in Figures 78 and 79. Visually the wavelet analysis appears to have performed better at this level of sampling

which is what we found for the image data (Oliver *et al.*, 2000). The more sparse the sampling the better the wavelet analysis appears to perform in comparison with kriging. Figures 81 to 83 show the maps of the comparisons between the predictions from ordinary punctual kriging and the low frequency wavelet transform, and the original values at the sampling sites of the 5-km grid. Figure 81a and b show the comparisons, i.e. the absolute differences, for predictions based on the 10-km sampling grid. Figure 81a for the kriged comparisons is a more spotty map than the one from the wavelet analysis: the sampling points are evident as the blue pixels where there is no error. For the wavelet analysis for this sampling grid there are fewer zero or small errors than for kriging, This is confirmed by the histograms of the differences, Figure 84a and b. Kriging also appears to perform better for predicting the values from the 20-km grid than the wavelet analysis in terms of the small errors, Figure 82a and b. The histogram of the kriged differences, Figure 84c, is somewhat misleading because there are fewer comparisons for kriging than for the wavelet analysis, and it is likely that there would be more of the larger errors than is evident in the histogram. The slight negative skewness in this histogram suggests that there is some bias in the predictions. The histograms, Figure 84c and d, for this sampling grid (20-km) are more similar than for the 10-km one. The comparisons for the predictions from the 40-km grid suggest that the wavelet analysis has performed slightly better at this level of sampling, which was the case for the SPOT image data (Oliver *et al.*, 2000). These histograms, Figure 84d and e show that the wavelet analysis has more smaller errors. There are fewer comparisons for kriging because the method requires a minimum of 4 points within the search radius and this fails at the margins of the error when the sampling points become sparse.

Summary

These results are interesting when compared with the analysis of the SPOT data. The NSI data appear not contain locally non-stationary data for pH. These would occur where there are marked boundaries in the soil, for example. At the sampling interval used here of 5-km local non-stationarity is less likely than for more intensively sampled data and remotely sensed data. Therefore, the errors for kriging are less than they were for the analysis of the SPOT data where there were marked changes at lakes and other boundaries causing local non-stationarity. Since kriging is an exact interpolator and wavelet analysis is not, there remains the need to combine the methods. It seems that some progress on this has been made at the Centre de Géostatististique, Fontainebleau. However, at the moment it is difficult to ascertain the extent of this and we shall endeavour to take this forward.

Another point of interest from this analysis is that the pH data form the NSI survey contain long distance trend. This means that part of the variation depends on the spatial coordinates. This violates the assumptions of geostatistics in the same way as local trend or drift, i.e. local non-stationarity. This affected the variogram, as was evident above, Figure 77a and b, and meant that we had to remove the trend and do the analysis on the residuals, and add back the trend after kriging. This is clearly a considerable amount of additional effort over and above the straightforward analysis. It is evident from the results

of the wavelet analysis that the prediction are unaffected by the trend. Therefore, if there is a choice of method available – situations with known trend present would benefit from the wavelet analysis.

a)

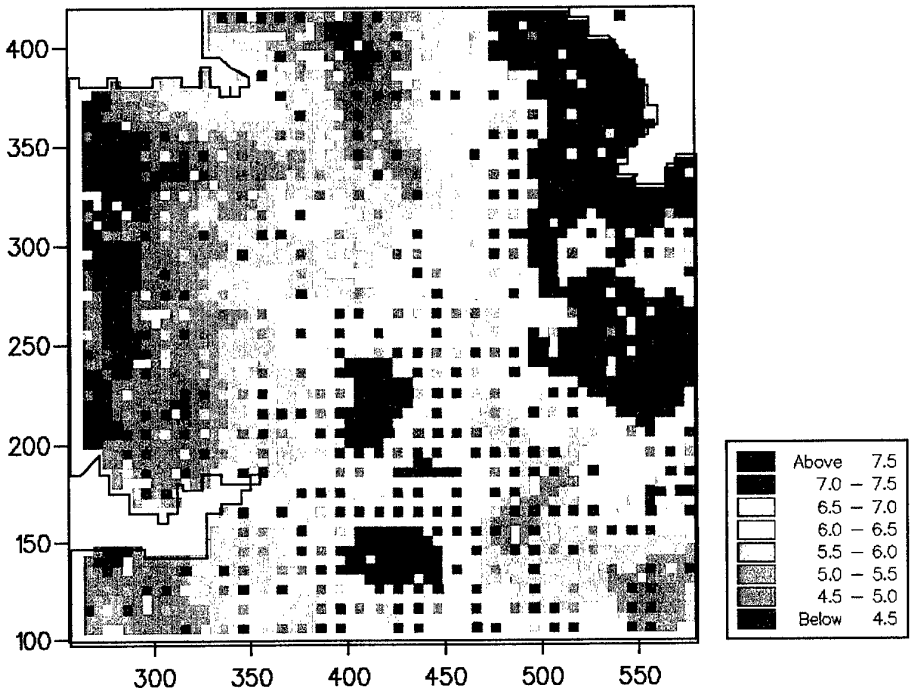

b)

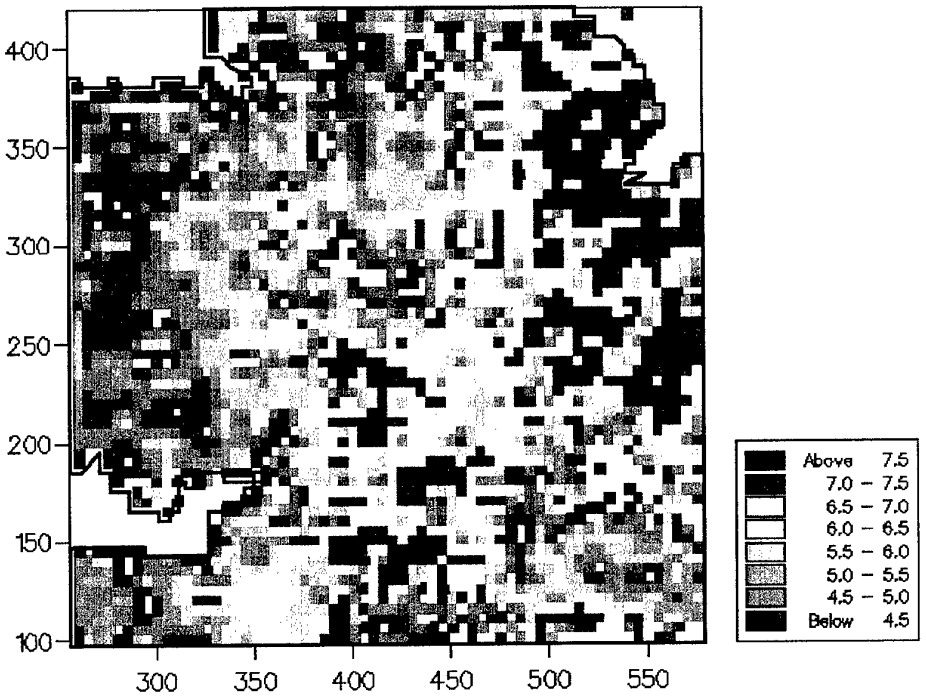

Figure 78. Predictions of pH at a 5-km interval from data on a 10-km grid: a) kriged estimates and b) low frequency wavelet transform

a)

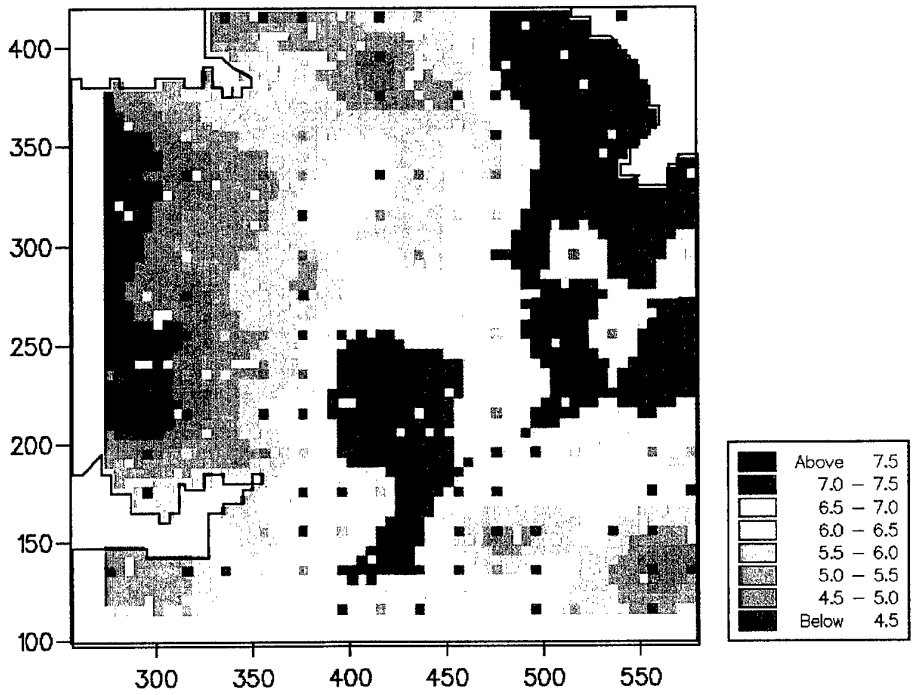

b)

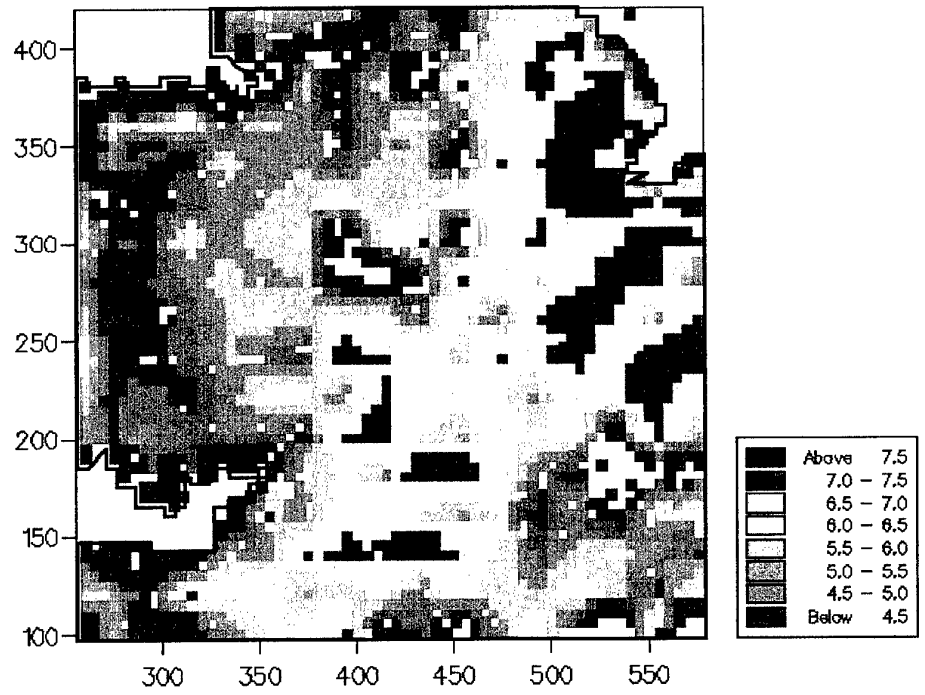

Figure 79. Predictions of pH at a 5-km interval from data on a 20-km grid; a) kriged estimates and b) low frequency wavelet transform

a)

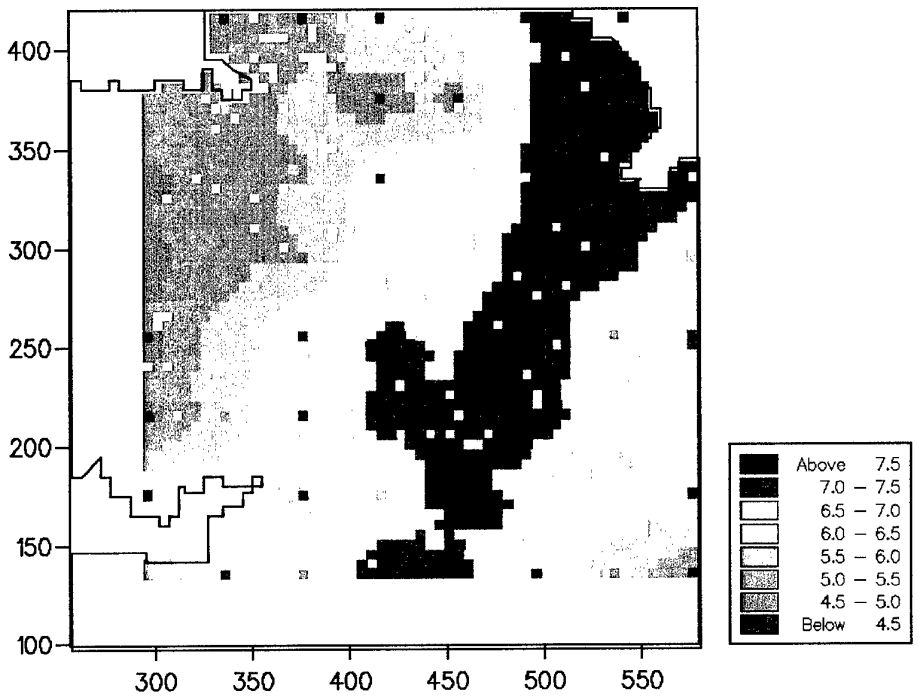

b)

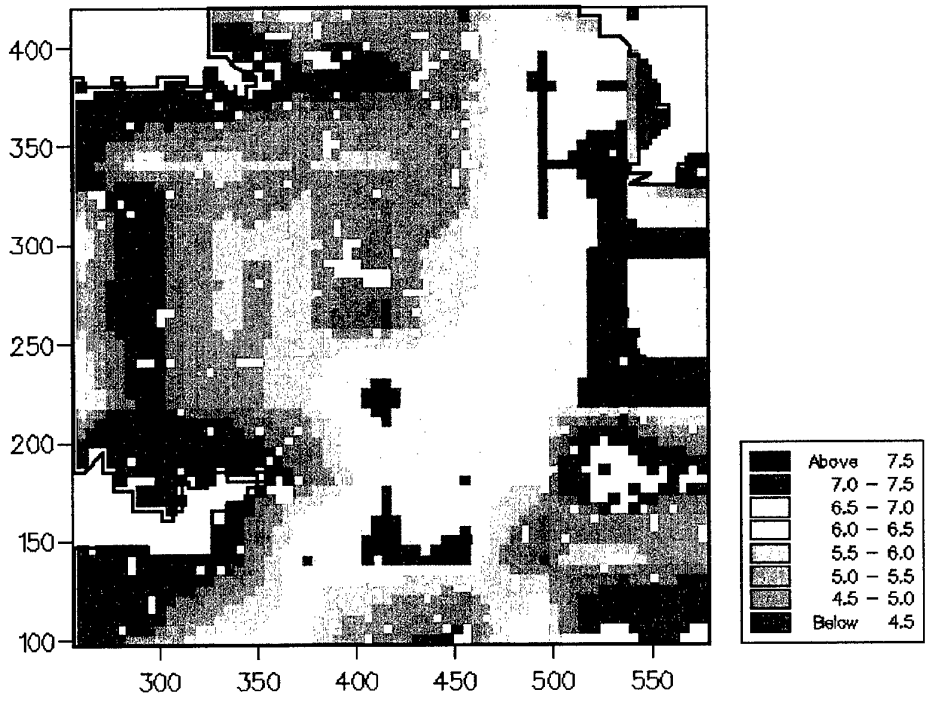

Figure 80. Predictions of pH at a 5-km interval from data on a 40-km grid: a) kriged estimates and b) low frequency wavelet transform.

a)

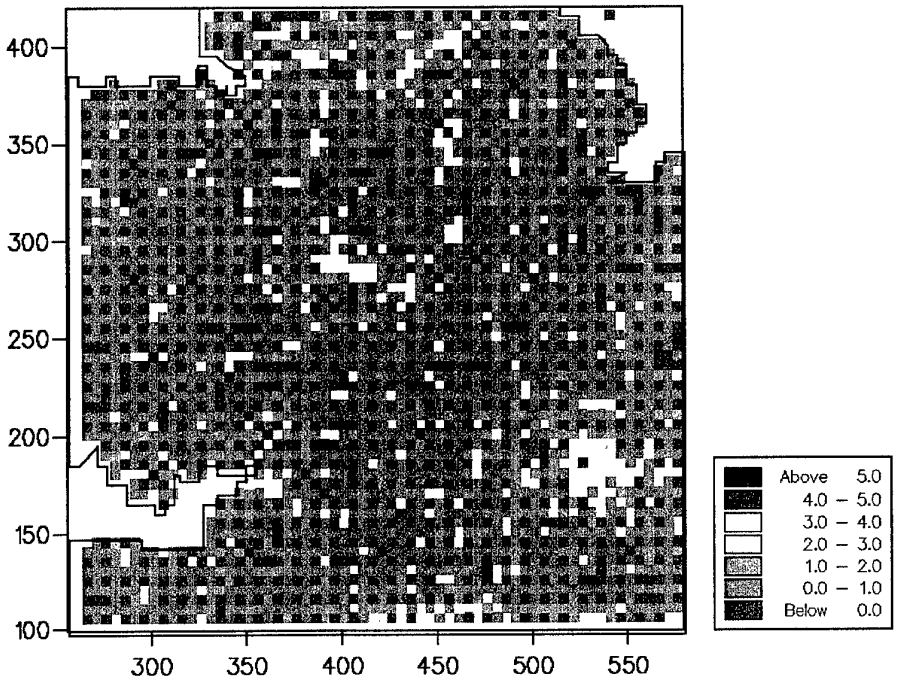

b)

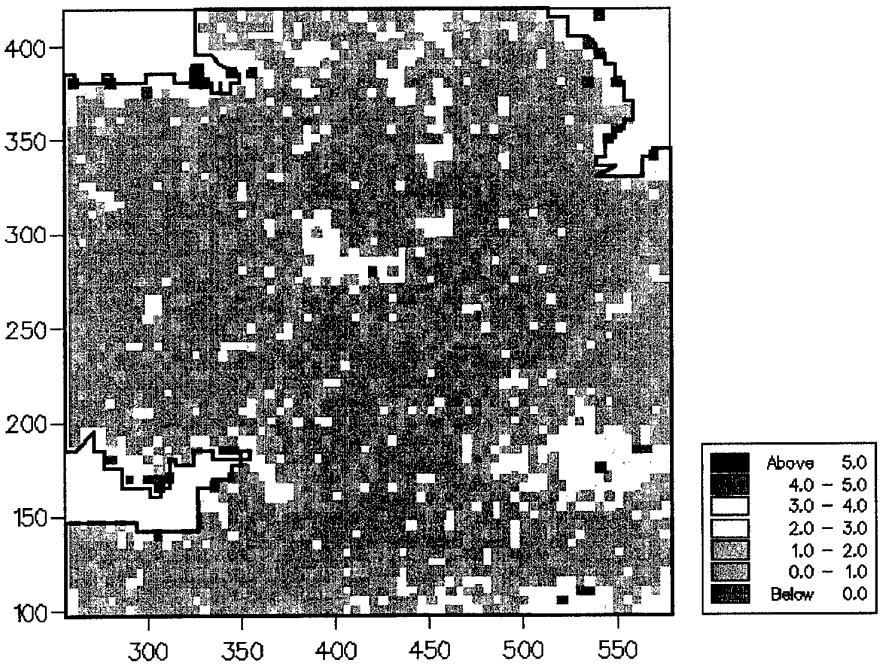

Figure 81. Comparisons between estimates for pH from data on a 10-km grid: a) kriging and b) wavelet analysis.

a)

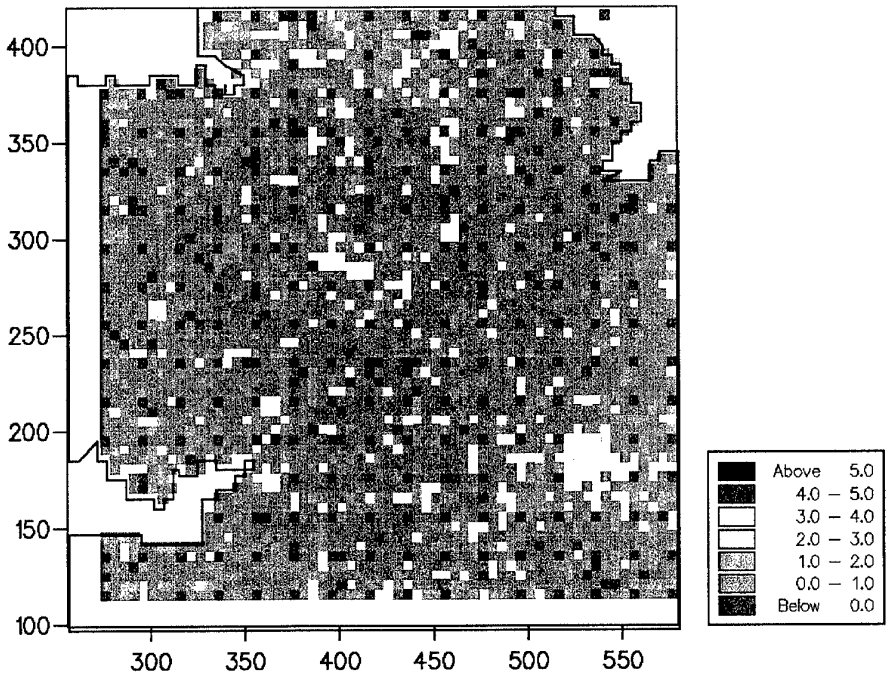

b)

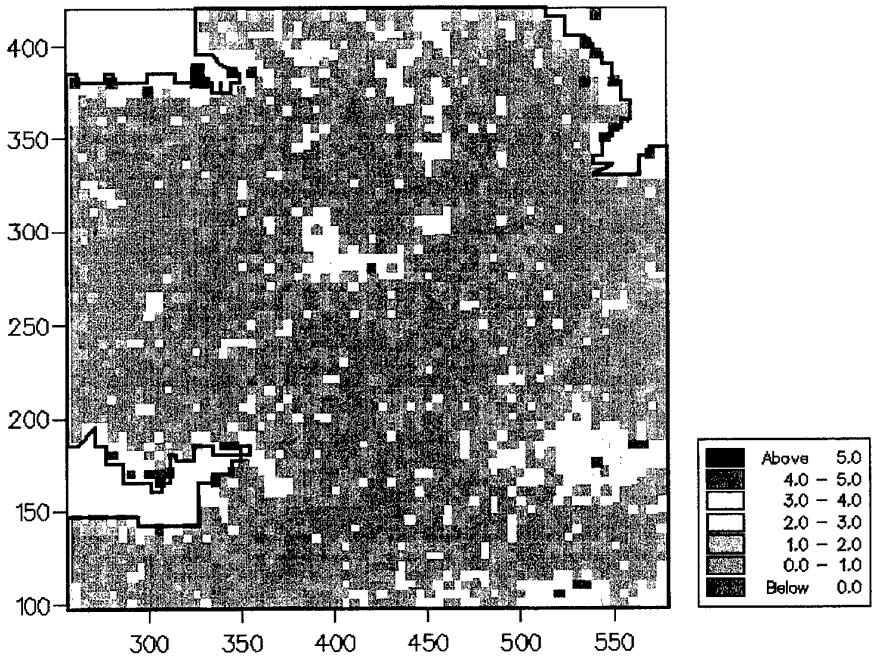

Figure 82. Comparisons between estimates of pH from data on a 20-km grid: a) kriging and b) wavelet analysis.

a)

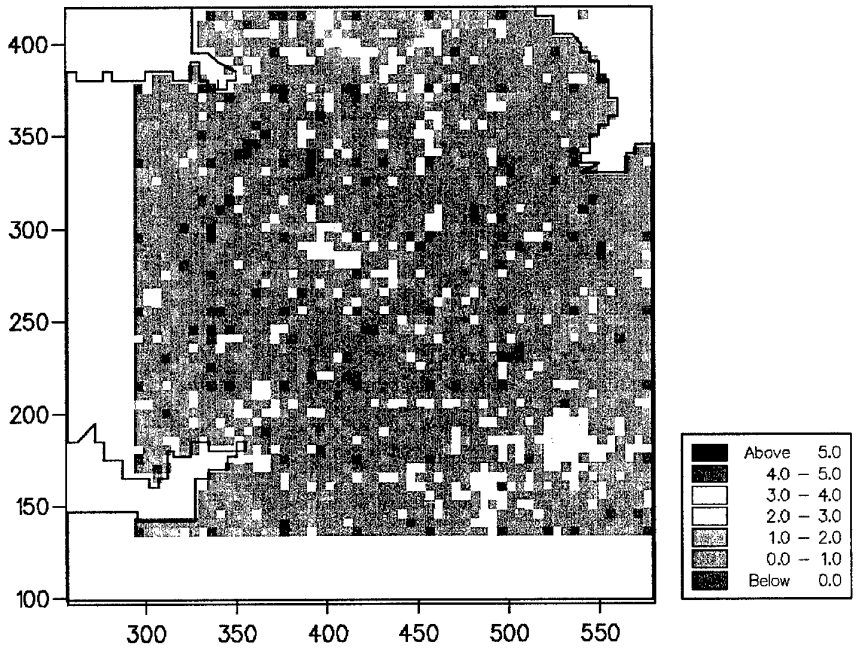

b)

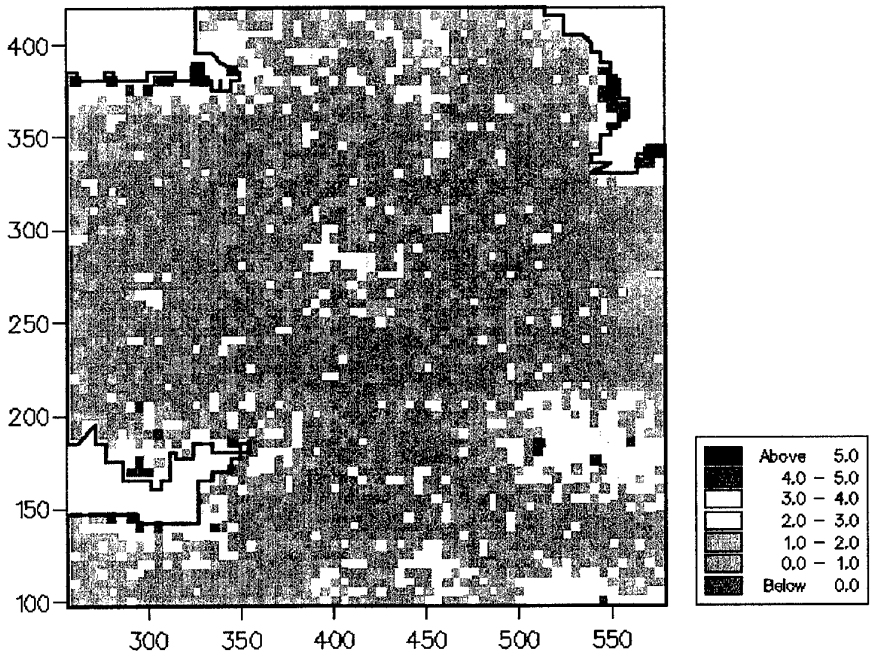

Figure 83. Comparisons between estimates of pH on for data on a 40-km grid: a) kriging and b) wavelet analysis.

a) Kriged pH sampled at 1 in 4

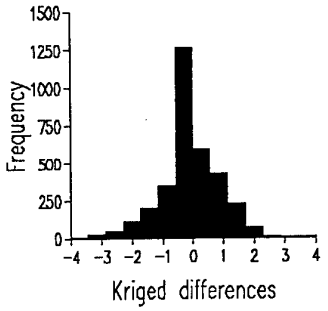

b) Wavelet pH sampled at 1 in 4

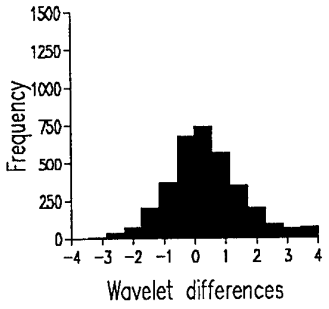

c) Kriged pH sampled at 1 in 16

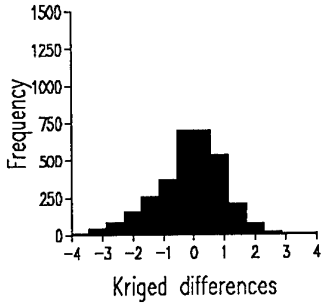

c) Wavelet pH sampled at 1 in 16

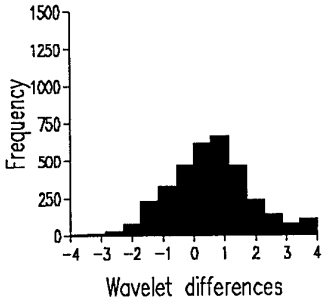

d) Kriged pH sampled at 1 in 64

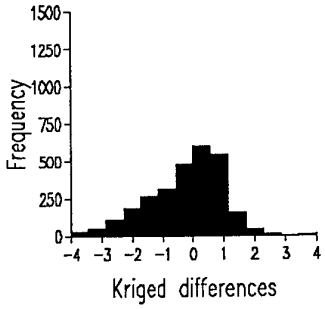

e) Wavelet pH sampled at 1 in 64

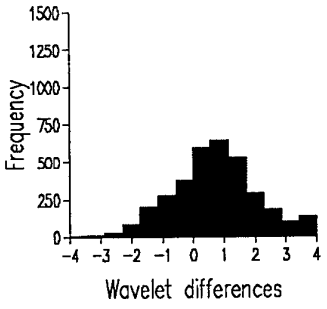

Figure 84. Histograms of the differences for pH from kriging and wavelet analysis.

Results of factorial kriging and wavelet analysis for pH

Factorial kriging was applied to the data on the 5-km grid, but the equivalent analysis for wavelets was done on all of the subsamples.. The reasons for this were given in the previous final report. Figure 85 shows the long-range component from kriging analysis. The results for all of England and Wales are given at the end of the report, Figure 98.

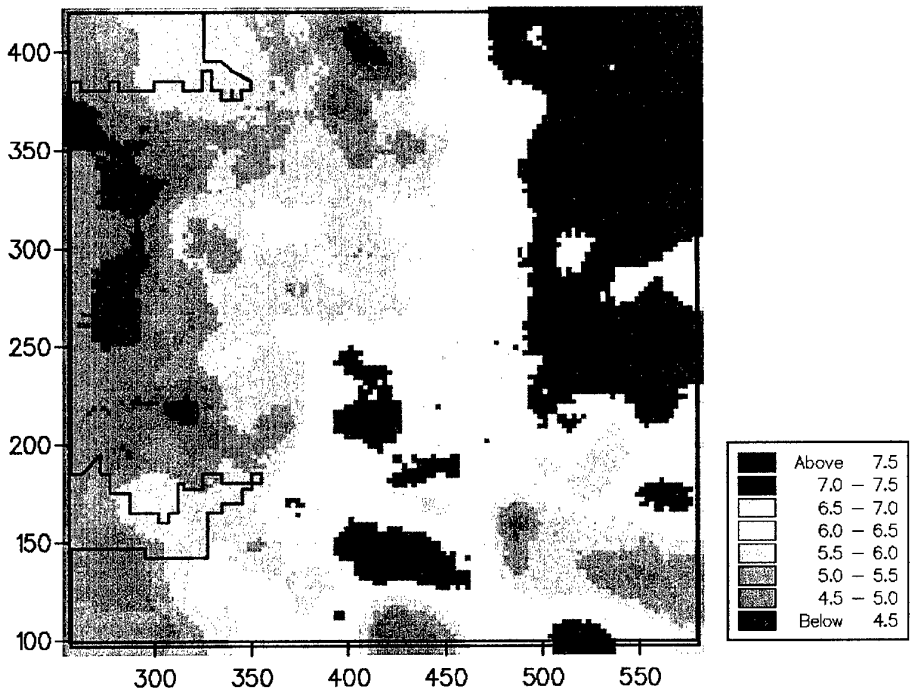

Figure 85. Long-range estimates of pH from kriging analysis.

The map of the long-range estimates for pH is similar to the kriged estimates from the 20-km grid, they are not as similar to any of the low frequency wavelet predictions, Figures 78 to 89. The long-range variation, Figure 85 shows that the larger values are generally associated with the lowland areas and the limestone uplands. However, the western coastal areas have large values of pH which are most probably associated with the deposition of sodium ions by rain in these areas.

Figures 86b and 87 a and b show the high frequency wavelet component for pH from the wavelet analysis. It is evident that the result for the 20-km grid is the closest. This reflects the same resolution for extracting the long-range component also. There are some similarities in the detail of the distributions, but there are also differences. In the future we shall examine the differences between these particular results to assess their relative

performances in more detail. The high frequency component for the 40-km grid has not identified the relevant short-range component.

Again an interesting point emerges that we observed in the previous analysis of the SPOT data. The level of resolution at which the wavelet analysis has identified the long- and short-range components of the variation is related to the short-range parameter of the variogram. We can now suggest more forcibly that for a multiresolution analysis using wavelets the best approach is to compute the variogram first.

a)

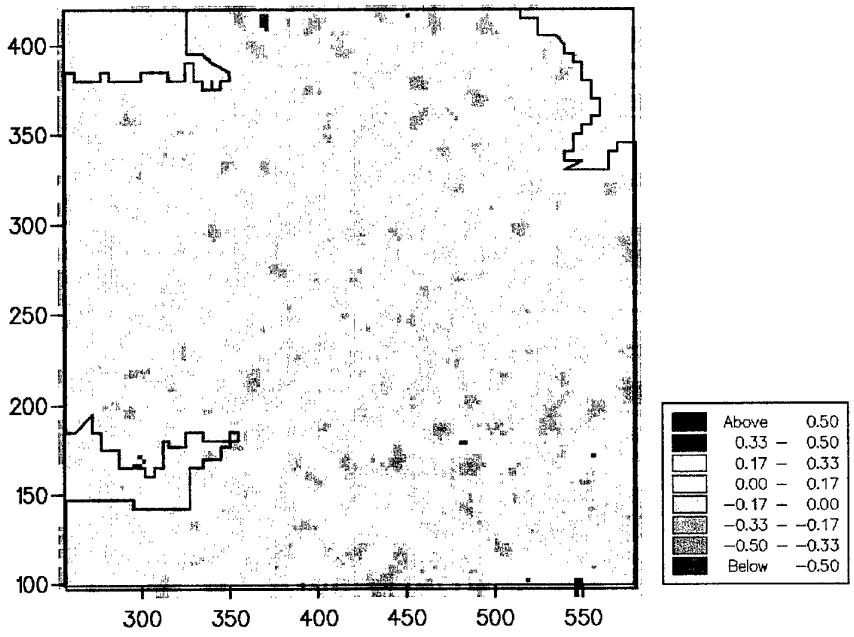

b)

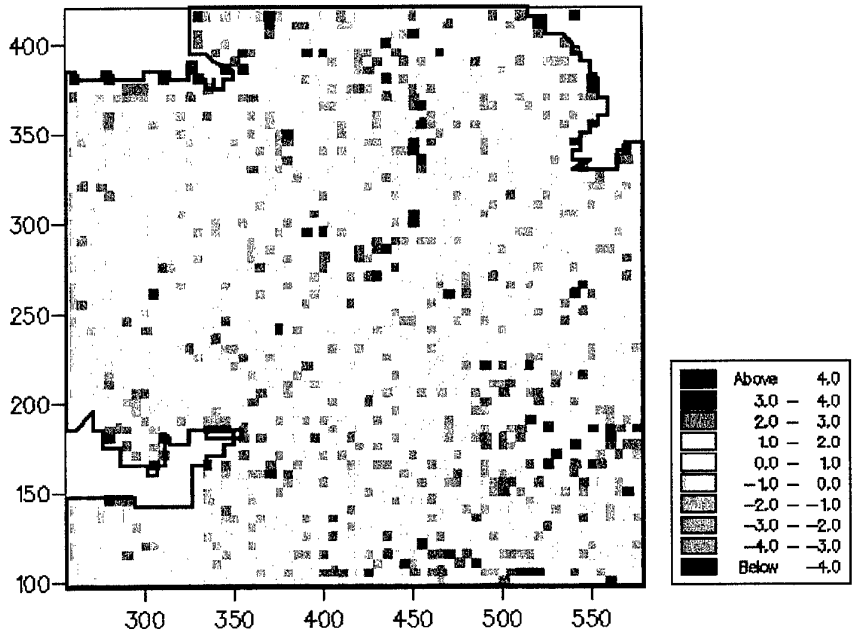

Figure 86. Short-range variation of pH: a) from kriging analysis based on the 5-km grid, and b) the high frequency wavelet coefficient from data on the 10-km grid.

a)

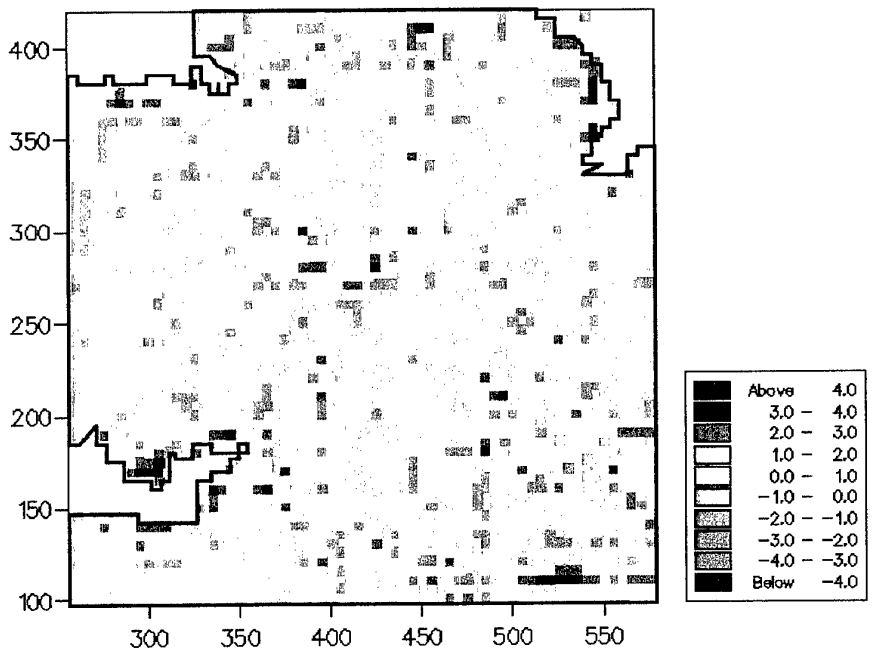

b)

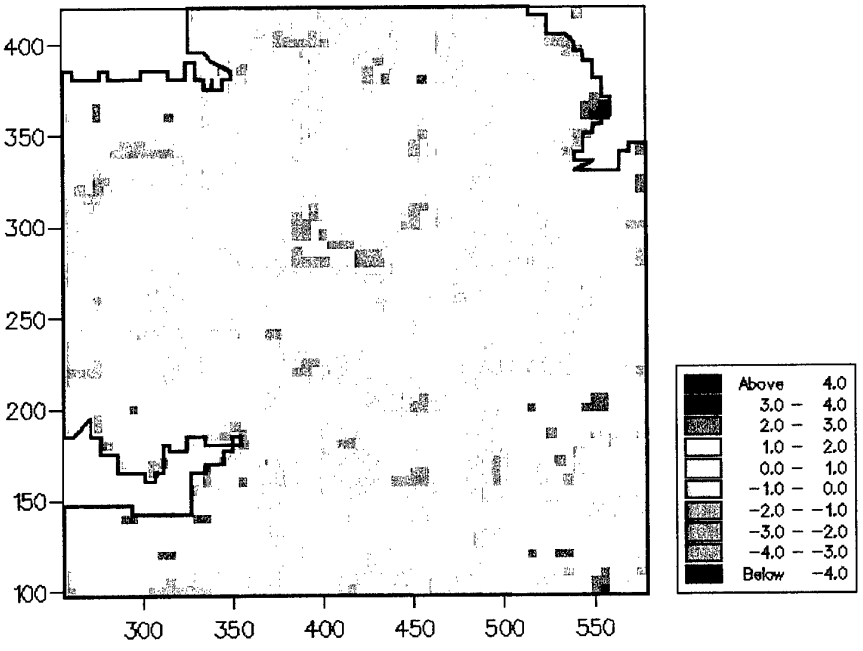

Figure 87. Short-range variation of pH: a) high frequency wavelet coefficient from data on the 20-km grid, and b) high frequency wavelet coefficient from data on the 40-km grid.

RESULTS FOR ZINC

Figure 75a and b show the original values for total $\log_{10}$Zn. There are many areas with large concentrations, and the most extensive of these follows the Jurassic clay band from SW to NE approximately. There are other areas trending N to S from the Midlands of England to the north. These seem to be associated with the Carboniferous shales and sandstones, as do the areas in central Wales. The large values around Avonmouth (SW) are associated with the smelting industry there.

For Zn the common logarithms were analysed and the values back-transformed for mapping as described above. Figure 88a and b shows the maps of the predictions using ordinary punctual kriging and the low frequency wavelet coefficients for data on the 10-km grid. The results are similar. The spotty appearance of the kriged map arises from the fact that kriging restores the data at the sampling points with non error. The overall result shows that kriging smooths more than the wavelet analysis. Nevertheless the maps are similar to those for the original data, Figure 75b.

The pattern of variation in the estimates from the 20-km grid for both analyses is also preserved well, Figure 89a and b. The degradation in detail is clear, but the large-scale pattern is still evident. Again the results for both methods of analysis are similar – more so than for pH.

Figure 90a and b shows the results for the 40-km grid. The results from the wavelet analysis, although showing a loss of detail, still show a similar pattern of variation, Figure 90b, to that of Figure 89b. The kriged results so not show such a good resemblance to the original pattern of variation. Note particularly the loss of accuracy in the north western part of the country.

These results again accord with the findings for pH and for the analysis of the SPOT image. When the number of samples is few and the distance between them large kriging restores the data less well than the wavelet analysis. This effect is supported by the maps of the differences, Figures 91 to 93 and of the histograms, Figure 94.

Figures 91 to 93 show the maps of the absolute differences between the predictions from ordinary punctual kriging and the low frequency wavelet transform, and the original values at the sampling sites of the 5-km grid. Figure 91a and b shows the comparisons, for predictions based on the 10-km sampling grid. Figure 91a for the kriged comparisons is a more spotty map than the one from the wavelet analysis: the sampling points are evident as the blue pixels where there is no error. For the wavelet analysis for this sampling grid there are fewer zero or small errors than for kriging, This is confirmed by the histograms of the differences, Figure 94a and b. The same negative skew in the errors is evident for Zn as for pH. Kriging does not appear to have performed quite as well for Zn for the 20-km grid as the wavelet analysis in terms of the small errors, Figure 94c and d. The maps of the differences, Figure 92a and b do not show this as clearly. Both methods appear to have performed similarly from these two maps. The slight negative skewness in this histogram again suggests that there is some bias in the predictions. The

comparisons for the predictions from the 40-km grid suggest that there is less difference between the wavelet analysis and kriging than the maps of the estimates suggested there would be, Figure 93. The histograms, Figure 94d and e confirm this, although direct comparison is not possible because kriging has not gone to the edges of the area for the reasons given before.

Summary

These results are interesting when compared with the analysis of the SPOT data. The NSI data for zinc again do not appear not contain locally non-stationary data as for pH. This explains the somewhat better performance of kriging for the 10-km grid.

The zinc values were skewed and this means that the variances when computing the variogram are unstable. The values were transformed to common logarithms, $\log_{10}$Zn, and kriging was performed on the logarithms and these values were back-transformed afterwards so that the values could be shown on their original measurement scale as for the wavelet analysis. Again this is clearly involves additional effort over and above the wavelet analysis, which does not require non-normal distributions to be transformed. This has an additional advantage because the transformation causes additional smoothing of the predictions. This does not seem to be particularly evident from the results given here.

a)

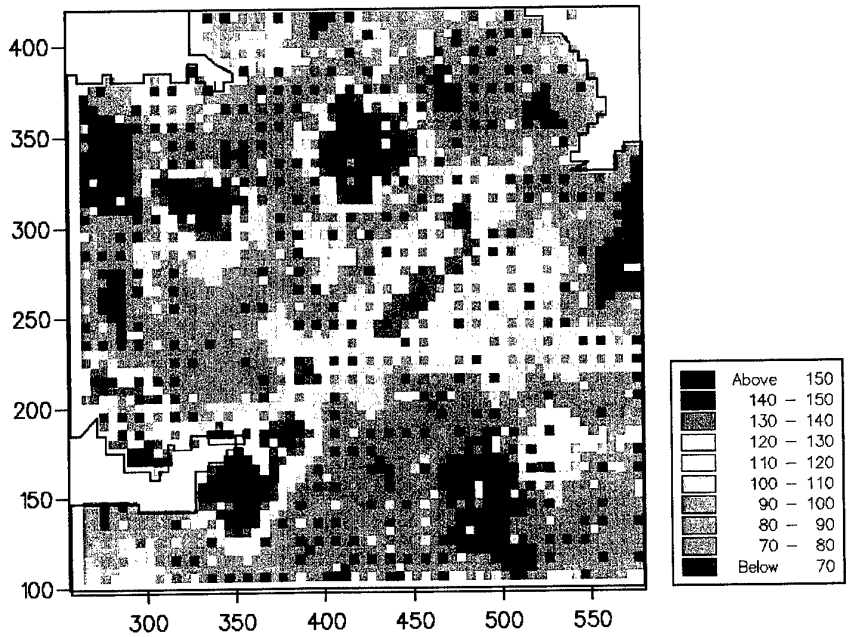

b)

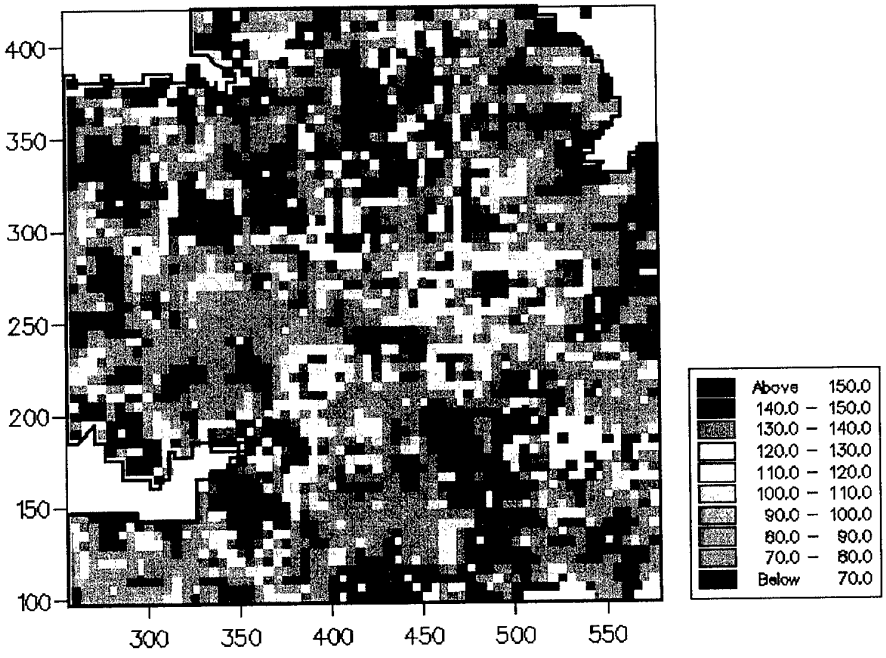

Figure 88. Predictions of Zn at a 5-km interval from data on a 10-km grid: a) kriged estimates, and b) low frequency wavelet coefficients.

a)

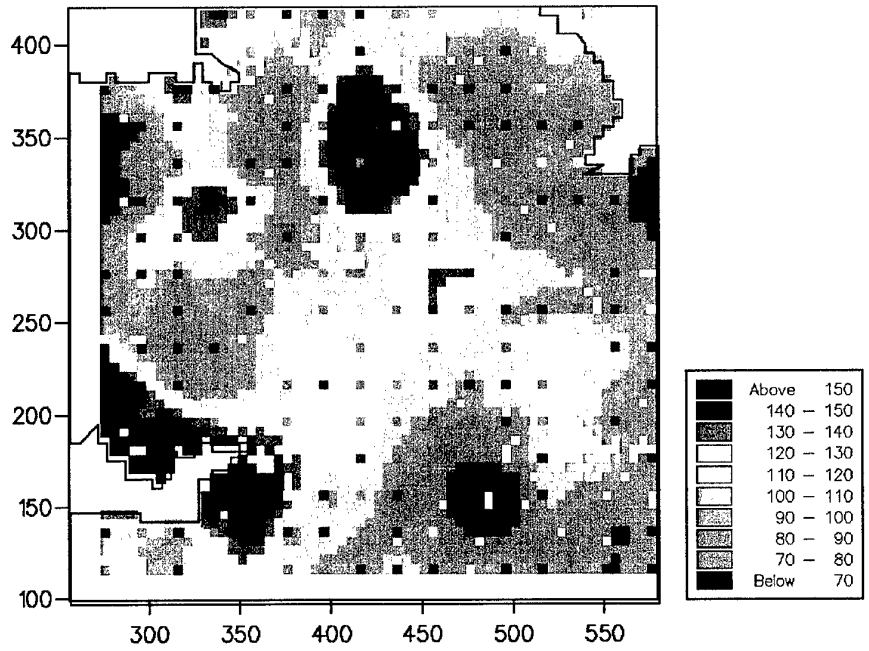

b)

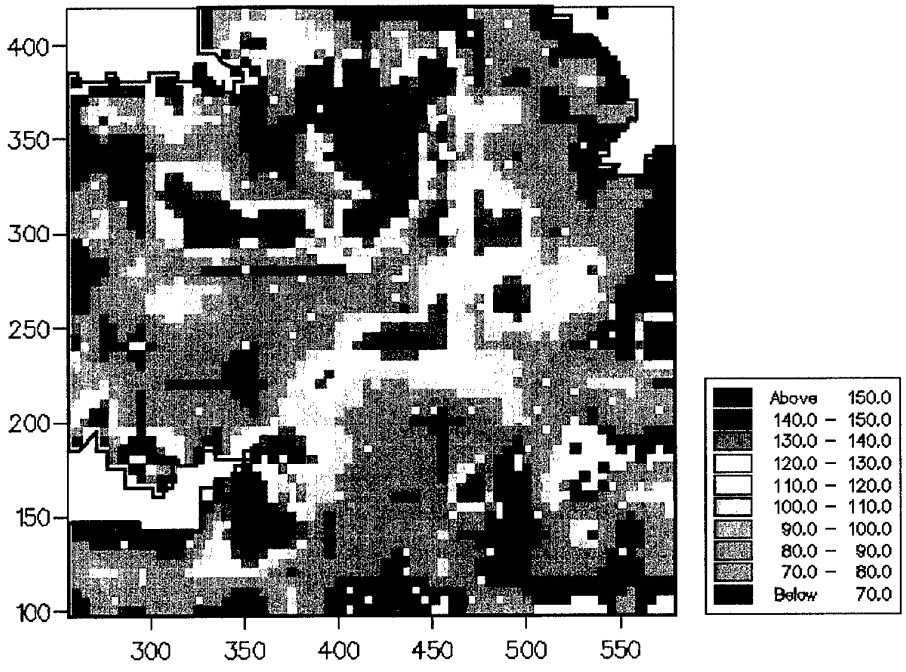

Figure 89. Predictions of Zn at a 5-km interval from data on a 20-km grid: a) kriged estimates, and b) low frequency wavelet coefficients.

a)

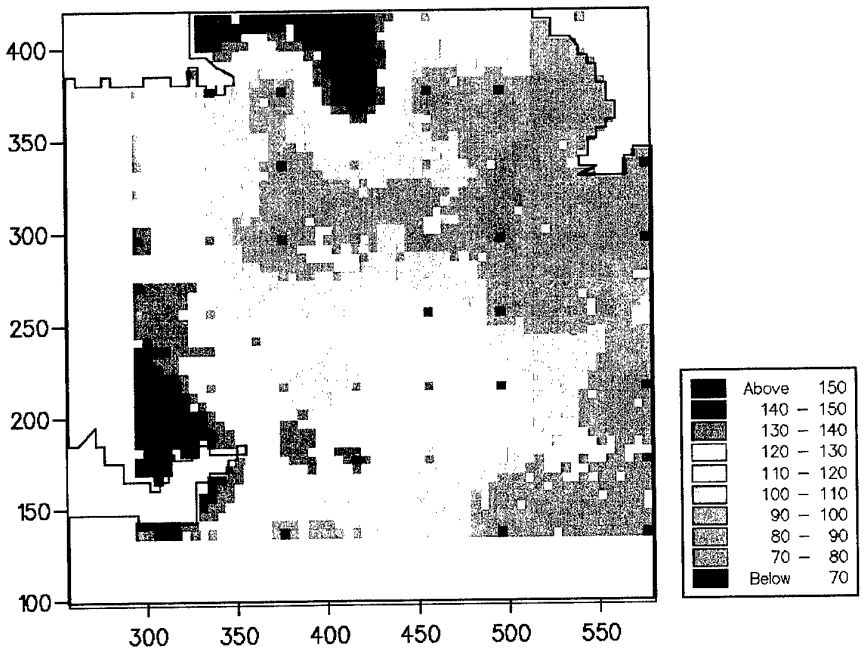

b)

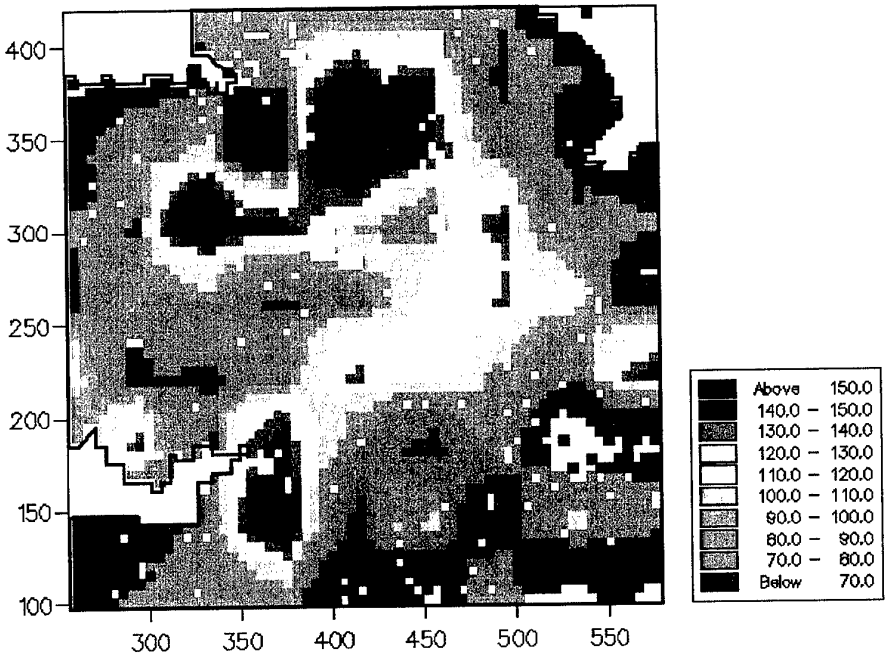

Figure 90. Predictions of Zn at a 5-km interval from data on a 40-km grid: a) kriged estimates, and b) low frequency wavelet coefficients.

a)

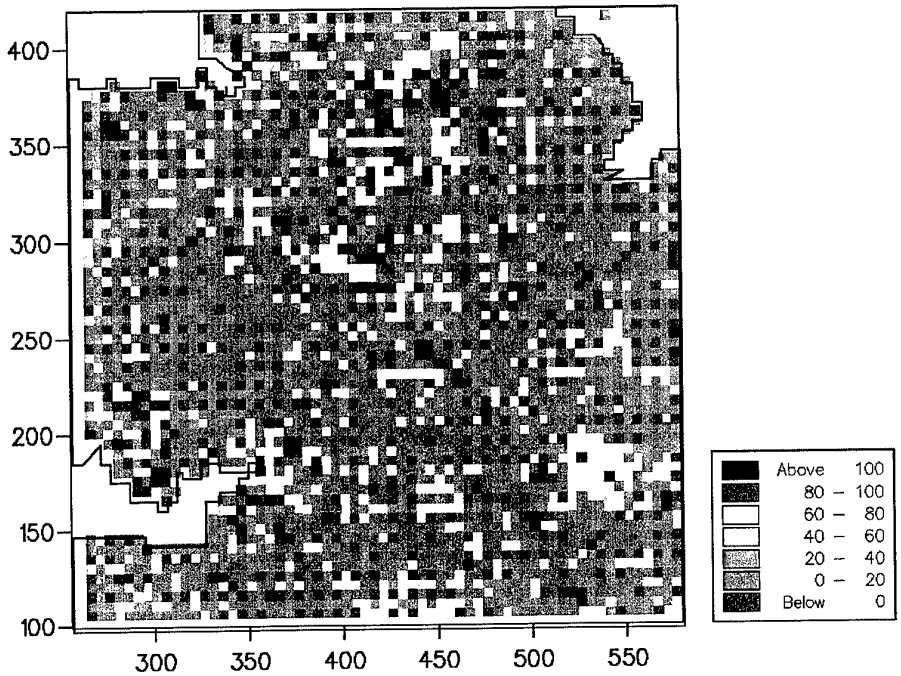

b)

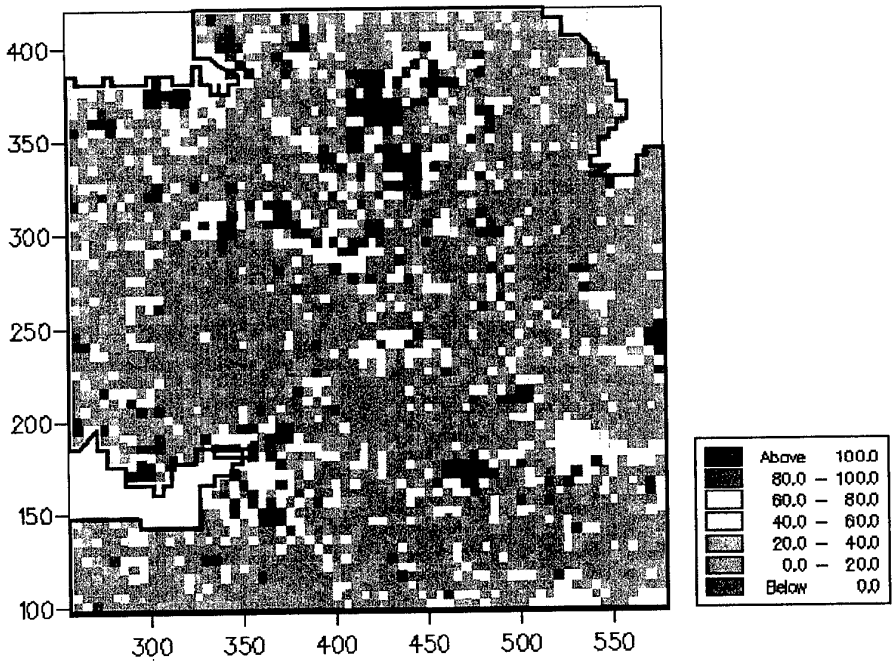

Figure 91. Comparisons between estimates of Zn from data on a 10-km grid : a) for kriging, and b) for wavelet analysis.

a)

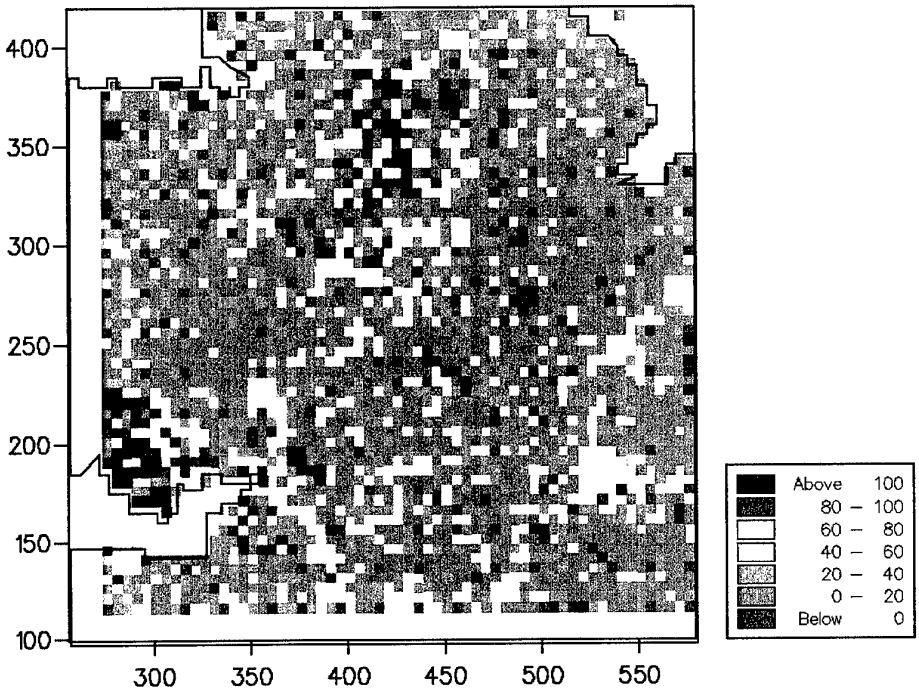

b)

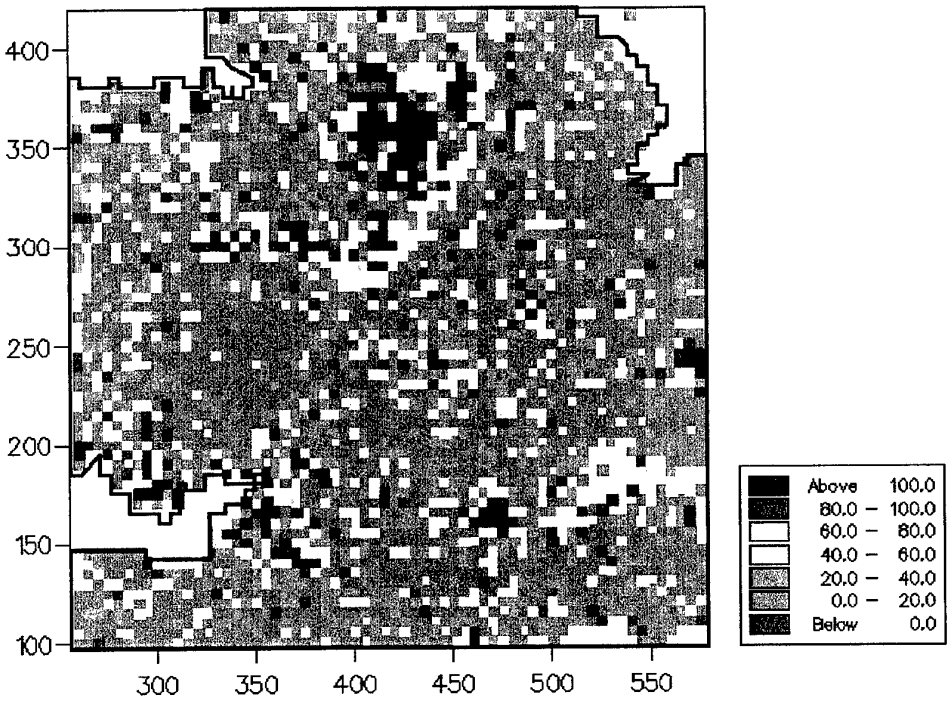

Figure 92. Comparisons between estimates of Zn from data on a 20-km grid: a) for kriging, and b) for wavelet analysis.

a)

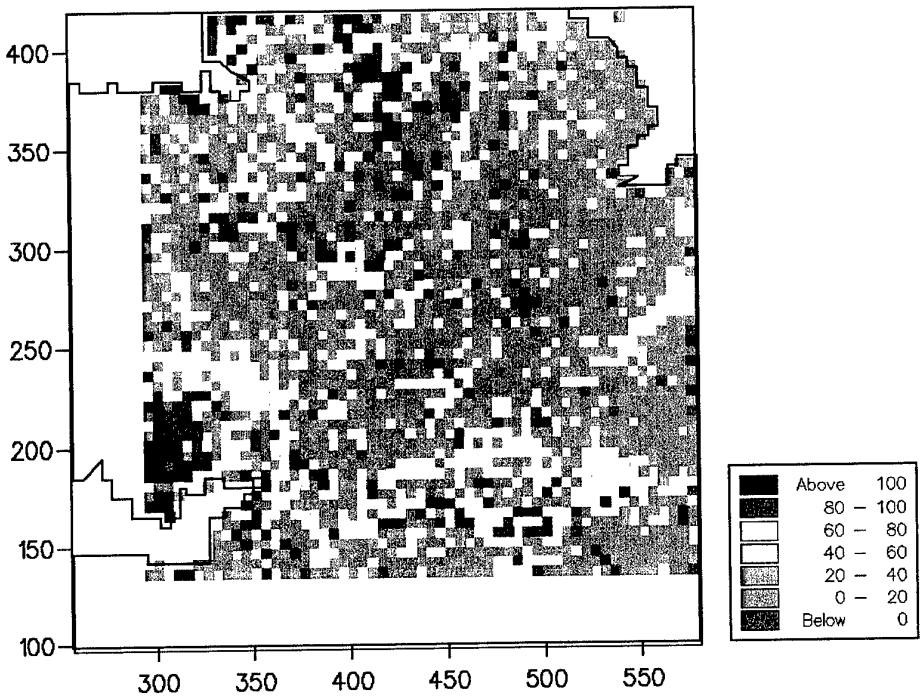

b)

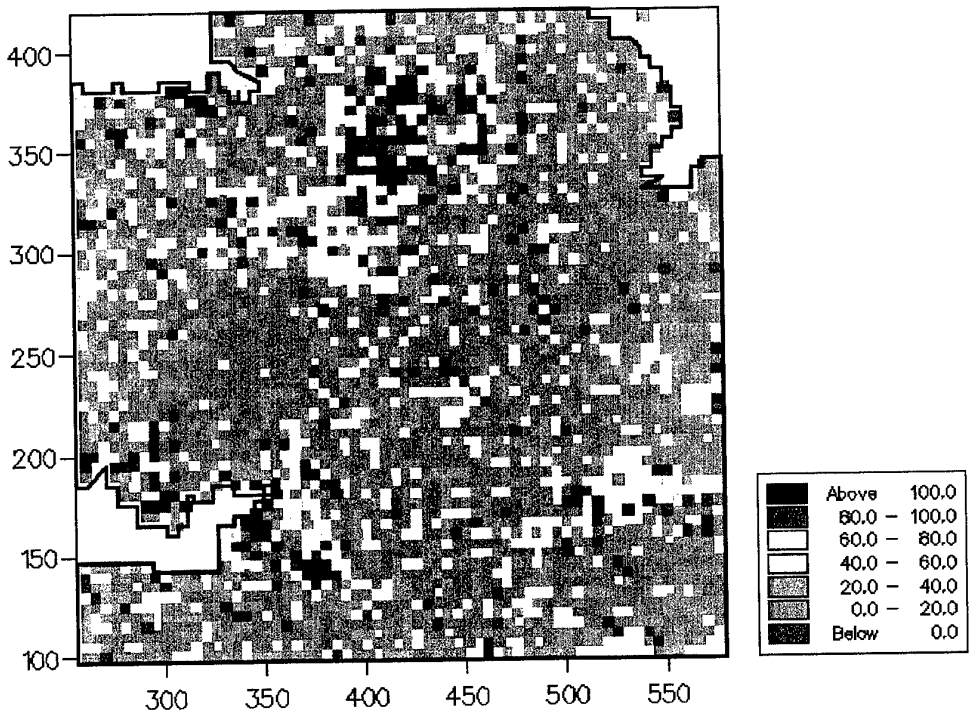

Figure 93. Comparisons between estimates for Zn from data on a 40-km grid: a) for kriging, and b) for wavelet analysis.

a) Kriged Zn sampled at 1 in 4

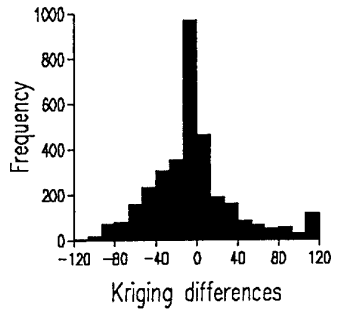

b) Wavelet Zn sampled at 1 in 4

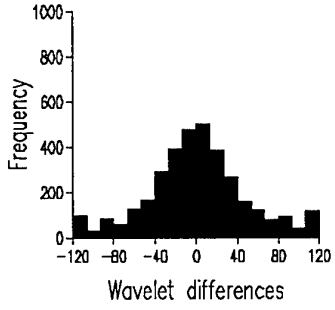

c) Kriged Zn sampled at 1 in 16

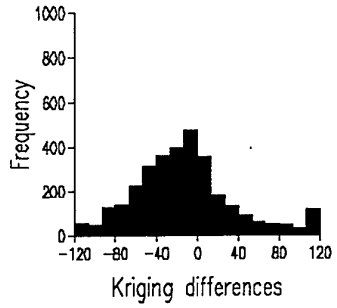

c) Wavelet Zn sampled at 1 in 16

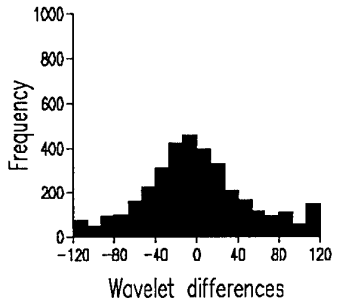

d) Kriged Zn sampled at 1 in 64

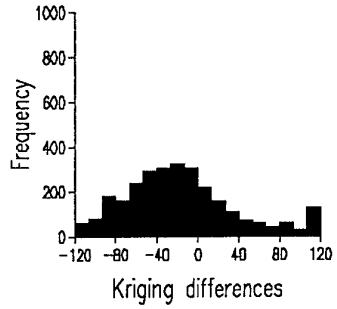

e) Wavelet Zn sampled at 1 in 64

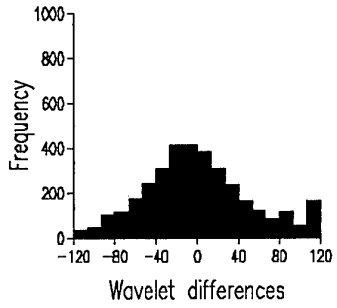

Figure 94. Histograms of the differences for Zinc from kriging and wavelet analysis

Results of factorial kriging and wavelet analysis for Zinc

Factorial kriging was applied to the data on the 5-km grid, but the equivalent analysis for wavelets was done on all of the subsamples.. The reasons for this were given in the previous final report. Figure 95 shows the long-range component from kriging analysis on the logarithmic scale. These results were not back-transformed because of the way in which these estimates are derived. The long-range kriged estimates for $\log_{10}$ Zn show that the largest values occur near to the Avonmouth smelter in the west of England, and another area in Derbyshire. There are large values associated with the Jurassic clays trending from SW to NE, to the Carboniferous limestone in Derbyshire, Carboniferous shales in the NE and Ordovician rocks in Wales. This distribution has some similarities with that for Cr. The values for $\log_{10}$ Zn for all of England Wales are shown in the end. These results show the closest relations with the 20-km grid wavelet analysis, Figure 90b, even though the colour scales appear somewhat different because Figure 95 is for logarithms.

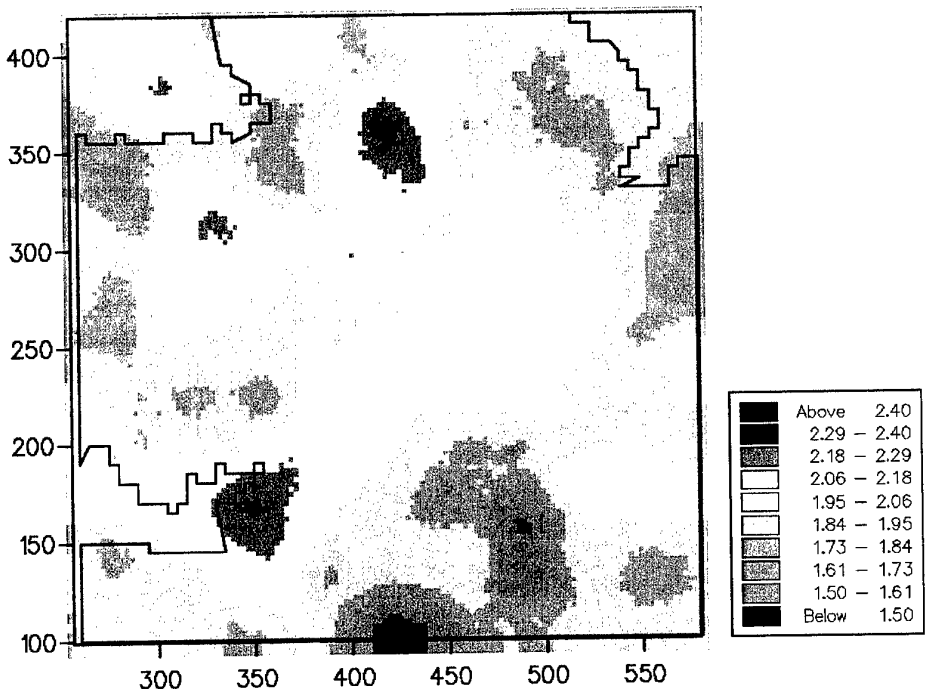

Figure 95. Long-range component from factorial kriging for Zinc.

a)

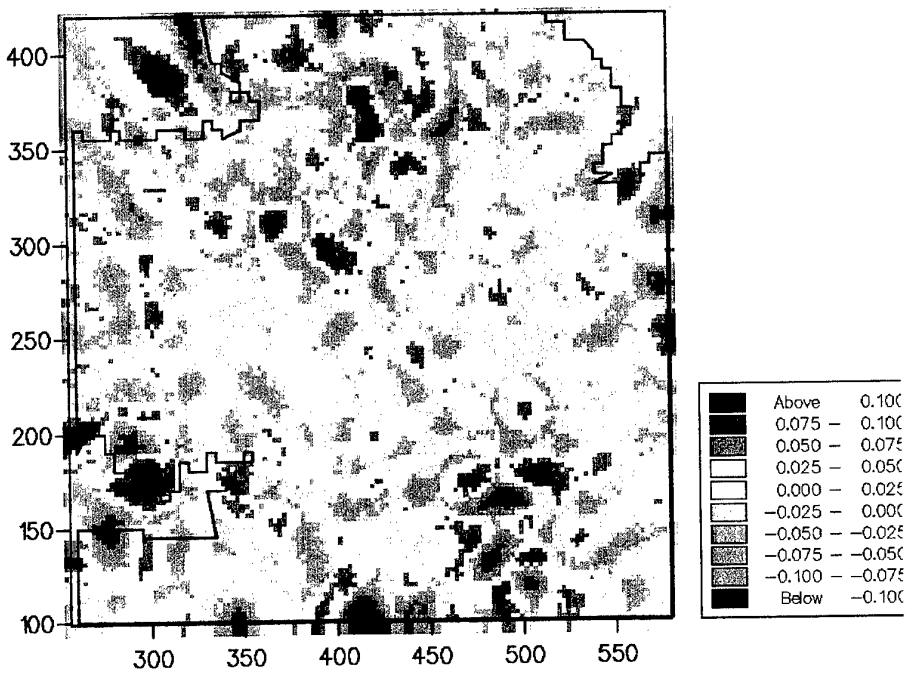

b)

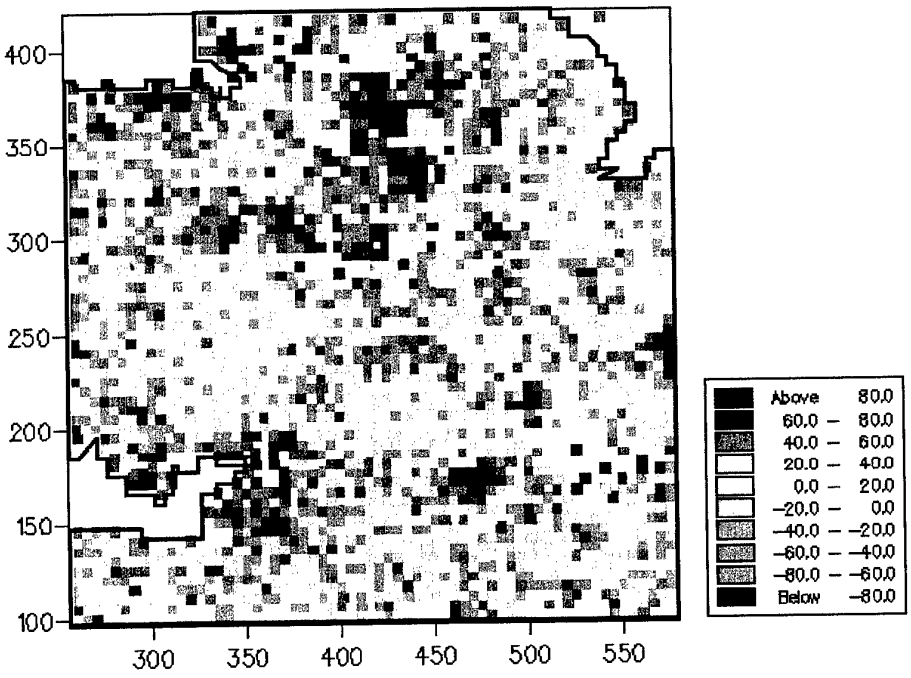

Figure 96. Short-range spatial component of Zinc: a) from factorial kriging on the 5-km grid, and b) high frequency wavelet coefficient for data on the 10-km grid

a)

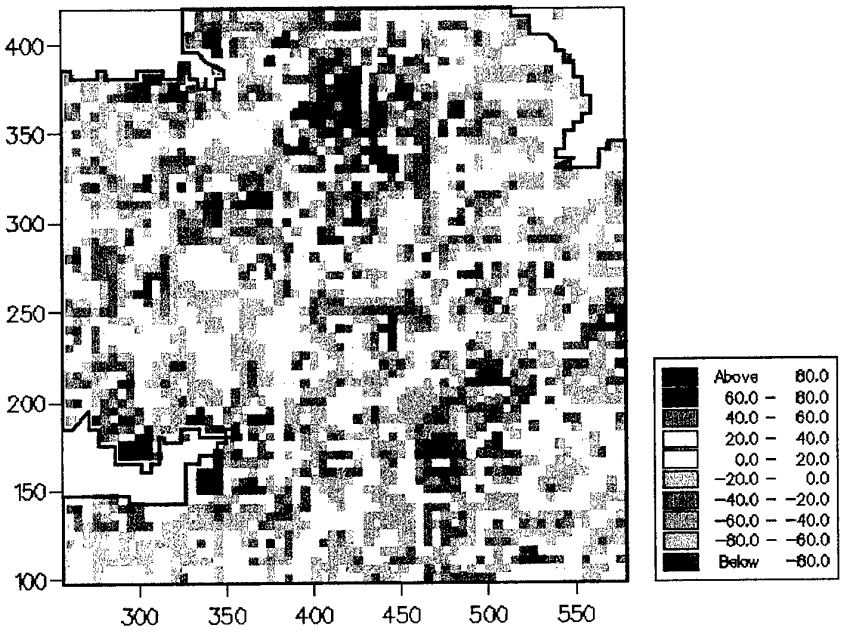

b)

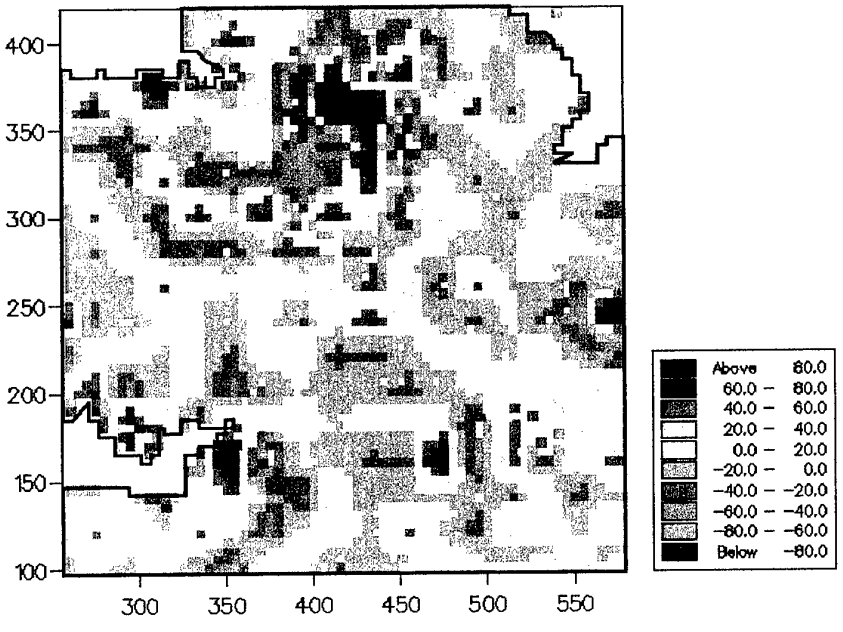

Figure 97. Short-range variation of Zn: a) – high frequency wavelet coefficient for data on the 20-km grid, and b) high frequency wavelet coefficient from data on the 40-km grid.

Figure 96a shows the short-range component of the variation from kriging analysis, and the maps for the whole of England and Wales for this analysis are given at the end of the report, Figure 99. The short-range component was investigated previously, it has a strong similarity with the map of the short-range component for Cr (not shown). These distributions also show a relation with the small scale drainage basins and local changes in rock and soil types.

Figures 96b and 97 a and b show the high frequency wavelet component for Zn from the wavelet analysis. It is evident that the result for the 20-km grid is the closest to that for the short-range component from kriging analysis. This reflects the same resolution for extracting the long-range component also. There are some similarities in the detail of the distributions, but there are also differences. In the future we shall examine the differences between these particular results to assess their relative performances in more detail. The high frequency component for the 40-km grid has also identified some of the relevant short-range component.

Again an interesting point emerges that we observe above is that the level of resolution at which the wavelet analysis has identified the long- and short-range components of the variation is related to the short-range parameter of the variogram.

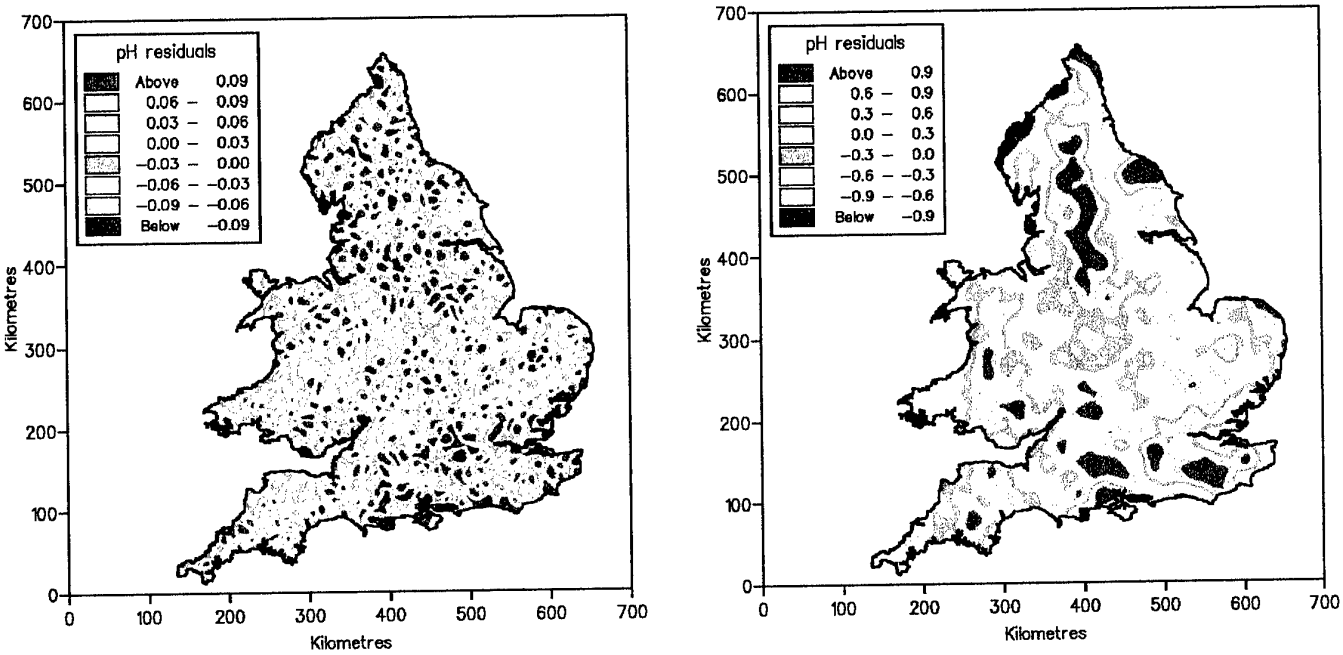

Figure 98. pH – results of factorial kriging: short- and long-range components.

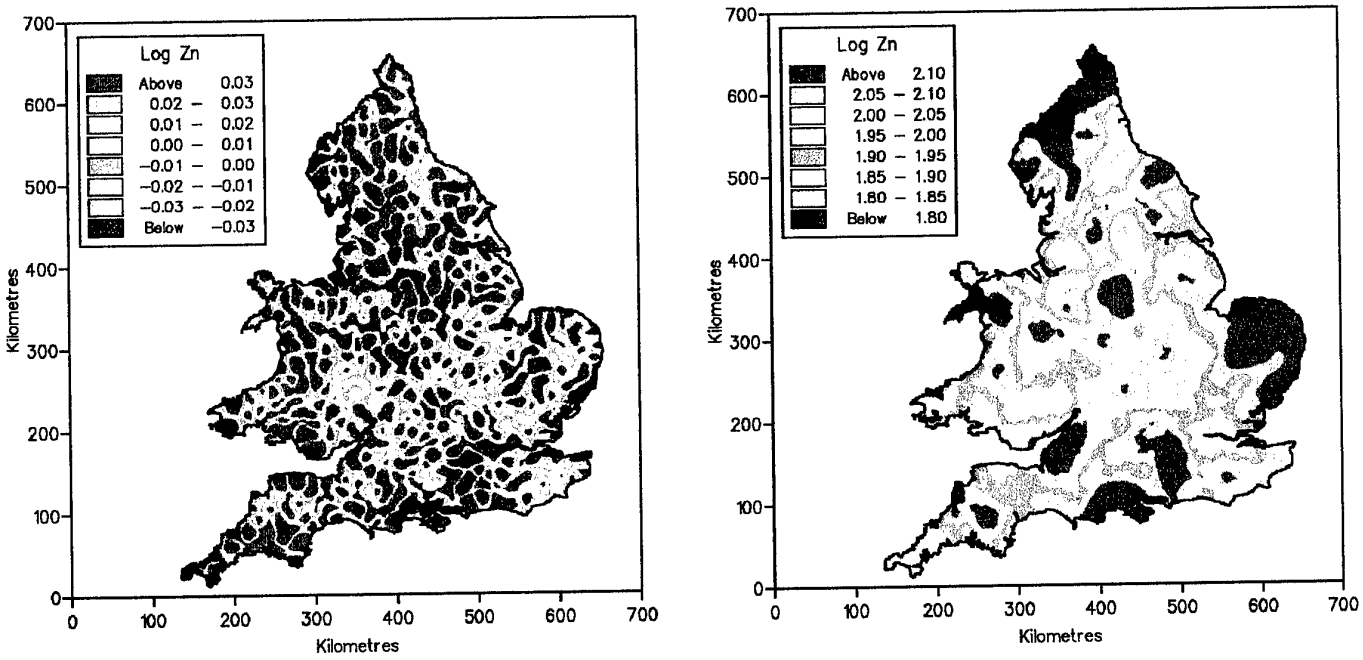

Figure 99. Zinc – results of factorial kriging: short- and long-range components.

PART IV: AIDE MÉMOIRE – SPATIAL SAMPLING

Introduction

The land surface, the materials of which it is composed and the environment more generally are continuous. In general measurements or observations can be made on only small portions of them, i.e. on samples, because of the large areas involved. For example, in a single agricultural field there is an infinite number of potential sampling points. Samples intended to represent the areas from which they are drawn must be planned with care. The information from a sample location should represent a surrounding area, the extent of which we might not know. Since many environmental properties vary locally in a complex and erratic way the values from a single sampling point include a sampling effect. To increase the information from a sampling location so that it is representative a bulked sample can be taken, and provided that the property is additive the measurement made on it will equal the regional mean apart from sampling error.

At the outset consider the use that will be made of the sample information. For instance, will the mean values of the properties observed for the entire area or for strata within the area be used to predict at unsampled places? Or will the information be used to predict locally, either using mathematical interpolators or geostatistical ones. For either of the latter the sample data must be spatially autocorrelated for them to have any merit.

This aide lists the matters that must be considered and resolved in planning sampling of a geographic region, which for present purposes we treat as two-dimensional.

Defining the target

The domain

The domain is the region of interest. Circumscribe it by a boundary on a map so that every point can be assigned to the domain or not with certainty. The domain may comprise a single parcel of land or several. Denote it by D.

Support

The support is the area or volume of material on which you make measurements. It has size and shape, and may have orientation. In remote sensing it is the `footprint' of the pixel; in vegetation surveys it is the quadrat; in soil survey it is the core of soil taken from the ground. Cores of soil may be taken from areas larger than the cross-section of the cores and bulked for analysis in the laboratory. In these cases the supports are the larger areas.

In any one survey define the support and keep it constant throughout.

The population and units

Within D are units that have the dimensions of the supports. In a remote image their number is finite though large. In soil survey they are so many that they may be regarded as infinite. Define them by their spatial coordinates and their spatial extents. Together they comprise the population. The terms 'population' and 'units' may be used to refer to the values of a variable of the supports.

The target

Within D there may be only certain kinds of terrain or land use that are of interest, e.g. only dry land (not water), only farm land (not towns, not parks, not golf-courses, etc.). The units falling in these classes constitute the target population. The others do not belong.

Samples

Whole populations cannot be measured in ground survey; you can measure only subsets of the units that comprise them. Such a subset of units is a sample.

Typically you will want two characteristics in a sample – accuracy and reliability. The first means that a sample represents the population without bias, i.e. any value that we obtain from a sample will be as likely to exceed the true value of the population as it will be to fall short. The second implies that repeated sampling will give sensibly the same result. It is measured by the estimation variance or standard error of the mean, s.e.

These characteristics can be assured by the sampling design in which there is sufficient randomness.

Notation

We adopt the following basic notation.

D denotes the domain.

$|D|$ is the area of D.

z is the variable of interest.

Z is a random variable.

$Z(\mathbf{x})$ is a random process, random field, stochastic process, in which Z may take any one of two or more values at random at each point $\mathbf{x}$ in D.

N is the size of the sample in D, i.e. the number of units in it.

D_k denotes the kth subdivision of D, of which there may be K.

n_k is the number of units in a sample of D_k.

μ denotes the mean of z in D.

$\bar{z}$ is the mean of the N data drawn from D.
σ^2 is the variance of z in D.

$s^2 = \hat{\sigma}^2$ is the estimate of σ^2 from the N data.

$s^2(D)$ is the estimation variance of μ in D.

$s(D)$ is the standard error of μ.

h denotes the lag separating two places, and is a vector in two dimensions; |**h**| is the distance component of the lag.

$\gamma(\mathbf{h})$ signifies the semivariance at lag **h**.

λ_i are the kriging weights.

Sampling designs for design-based estimation

This is essentially the classical statistical approach to sample design and prediction.

Simple random sampling

In simple random sampling N units are chosen with equal probability from the target population. The result is unbiased, and the estimation variance $s^2(D)$ is given by s^2/N.

If there is any spatial correlation at the working scale then this is inefficient in the sense that the same estimation variance could be achieved with a smaller sample by a better design.

Stratified random sampling

Divide the region into strata, D_k, k=1,2, . . , K, and represent each by a few units, ideally two, chosen at random independently. The sizes n_k may be chosen in proportion to the areas of the D_k, $|D_k|$, if they are not equal.

If other sizes are chosen then the mean in D may be calculated as the weighted average of the individual stratum means with weights proportional to the $|D_k|$. The estimation variance of stratified sampling depends on the variance within the strata, or the pooled within stratum variance. In the presence of spatial dependence the latter is less than the total variance in the population, and so stratified sampling is more efficient than simple random sampling.

The estimation variance is given by

$$s^2(D)_{\text{stratified}} = \sum_{k=1}^{K} w_k^2 s^2(D_k),$$

where $s^2(D_k)$ is the estimation variance within stratum D_k, and w_k is the weight assigned to the stratum. The weights should sum to 1 to avoid bias.

There are numerous ways in which this general scheme can be elaborated according to what you know of the region and the variation within it. For example the strata could have unequal spatial extents as in classification. In this case the different areas are taken into account through the weight w_k, such that

$$w_k = \frac{\text{area of stratum } k}{\text{total area}} .$$

Systematic sampling

Sampling is usually most efficient when done on a regular grid. It has two disadvantages:

(1) it provides no ready estimate of the variance;

(2) it may lead to biased estimates of the mean.

The first arises because once the origin and orientation of the grid are decided there is no further randomization possible. It is not easily overcome, but the estimation variance may be approximated by methods such as Yates's balanced differences.

The second, bias, can happen where there is trend or periodicity in z in the region. Periodicity is usually evident, and if it is then you can choose an interval and orientation that will be out of tune with it. Alternatively, choose a non-aligned scheme in which each sampling point on the grid is offset from its node by a random distance along its row and down its column according to a rule.

Sample size

The size of sample N may depend on the budget or the tolerance, i.e. error that can be tolerated in the estimate from the survey. If the budget is fixed then choose a stratified scheme to minimize the error for that budget.

If the error is specified as $s(D)$ then for simple random sampling

$$N = s^2 / s^2(D) ,$$

The formula for stratified sampling is more elaborate.

You usually do not know s^2 in advance, and so choosing N is problematic. Therefore sample in stages, starting with a sparse design that can be intensified as necessary. At each stage calculate the estimation variance to see whether it meets the tolerance. If it does then stop; otherwise intensify the sampling and recompute the estimation variance as the next stage.

Geostatistical (model-based) sampling design and prediction

Geostatistics is used to estimate local values rather than regional ones, i.e. to predict. It is based on the assumption that z in the real world is a realization of the random process $Z(\mathbf{x})$. For this reason there is no need to randomize the sampling, and grid sampling is preferred because of its efficiency.

Geostatistical prediction (kriging) requires a model of the correlation structure, expressed either as a covariance function, or rather more generally as a variogram. Like the variance in design-based estimation, these functions are not known *a priori* and must be estimated from sample data. Sampling must therefore serve two purposes:

(1) estimation and modelling of the variogram, and

(2) local prediction once the variogram has been estimated and modelled.

To satisfy item (1) sampling must be sufficient to estimate the semivariances precisely. It must also be dense enough to estimate the spatial characteristics of the variation, such as correlation range and general form of the variogram.

Sampling for item (2) will depend either on the budget or on the tolerable error of local predictions and the variogram.

Sampling to estimate the variogram

Nested sampling and analysis

Start with nested sampling and a hierarchical analysis of variance of the sample data if you know nothing of variation in the region. Choose five or six sampling intervals in geometric progression from the smallest lag distance of interest to the largest. Choose the angular separations at random. Replicate at the longer distances to give sufficient degrees of freedom in the analysis of variance to estimate the components. Expect to have a total sample, N, of about 100. Figure 1 shows the kind of sampling plan to aim for.

Accumulate the components of variance to estimate $\gamma(|\mathbf{h}|)$ at the distances of the design and draw a crude variogram with the logarithm of $|\mathbf{h}|$ on the abscissa as in Figure 2.

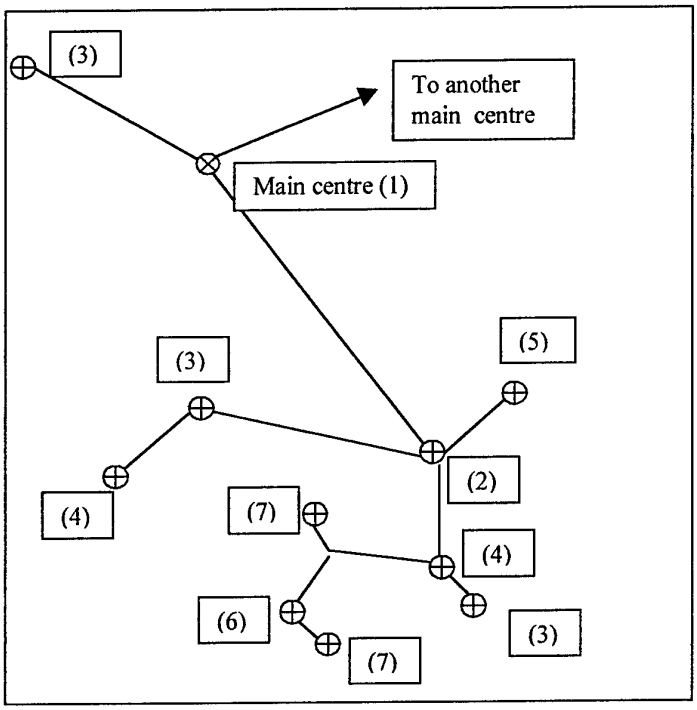

Figure 100. The plan of sampling for one main centre in a nested survey with 7 stages. The stages in the hierarchy are given for each sampling site.

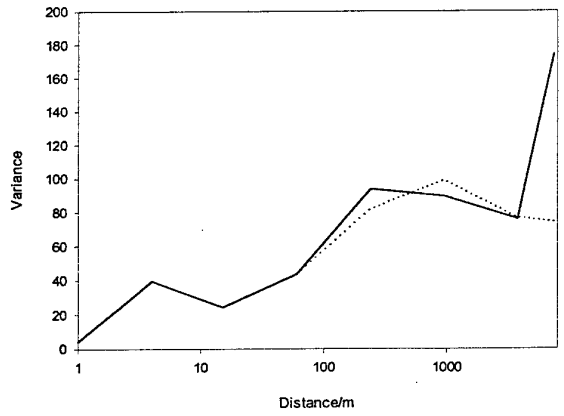

Figure 101. The accumulated components of variance from a hierarchical analysis of variance giving a first approximation to the variogram.

Such a result this can be used to identify the range of distance within which most variance occurs and to plan further sampling to estimate the conventional variogram.

If all the variance appears to occur within the smallest distance of interest then local prediction is not feasible. So stop! Figure 3 shows an example of a pure nugget reconnaissance variogram. All of the variation is occurring within the shortest sampling interval.

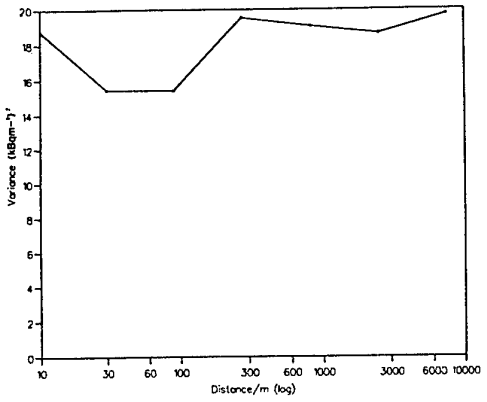

Figure 3. A pure nugget reconnaissance variogram from a nested survey.

Estimating the variogram parameters

Use the result from the hierarchical analysis above or other knowledge of the variation in D to estimate semivariances, $\gamma(\mathbf{h})$, at several lags, $\mathbf{h}$, within the correlation range. Design a scheme with approximately 100 to 150 sampling points if the variation appears isotropic. If a square grid with this number gives you sufficient estimates of $\gamma(\mathbf{h})$ within the correlation range then use it. If not then cluster the sampling in some way. Intensify sampling around a subset of grid nodes, bearing in mind that you are likely to want a grid for kriging later. Alternatively, sample in clusters with a range of sampling distances between locations, and spread the clusters evenly over D so that the

Do not cluster sampling in parts of D that you know or suspect to have unusually large values of z (as you might in mineral surveys or pollution studies) or unusually small ones (as in studies of deficiency diseases). This will result in bias.

Compute the sample variogram and plot the result. If the estimated values fall close to a smooth curve then choose an authorized model to describe it, estimate its parameters, and proceed to kriging.

If there is too much scatter to identify a plausible function then increase the sampling, either by intensifying the grid or by adding clusters, and recompute the variogram. Repeat until a smooth form is identifiable.

If the variation is anisotropic and you wish to model the anisotropy then you must expect to sample at 200 points or more.

Kriging

In kriging Z at an unknown point $\mathbf{x}_0$ minimize the prediction variance

$$\sigma^2(\mathbf{x}_0) = 2\sum_{i=1}^{n} \lambda_i \gamma(\mathbf{x}_0 - \mathbf{x}_i) - \sum_{i=1}^{n}\sum_{j=1}^{n} \lambda_i \lambda_j \gamma(\mathbf{x}_i - \mathbf{x}_j)\,, \qquad (1)$$

where $n << N$ is the number of sampling points near to the target point $\mathbf{x}_0$. The quantities $\gamma(\mathbf{x}_i - \mathbf{x}_j)$ and $\gamma(\mathbf{x}_0 - \mathbf{x}_j)$ depend on the separations $\mathbf{x}_i - \mathbf{x}_j$ and $\mathbf{x}_0 - \mathbf{x}_j$; the larger these are the larger is $\sigma^2(\mathbf{x}_0)$.

The maximum value of $\sigma^2(\mathbf{x}_0)$ is minimized by sampling on a regular grid. A triangular grid is usually the most efficient, but rectangular grids are almost as good (Figure 3a), and as they are easier to lay out and document they are preferred. If variation is isotropic then use a square grid.

If the budget is fixed then sample as intensely as it permits. If a maximum tolerance is specified, say s_{Kmax}, then solve the kriging system for a range of sampling intensities (grid intervals) and plot the kriging variance (or its square root, the kriging error) on the ordinate against the grid interval on the abscissa. Connect the points by a smooth line, Figure 3. From s^2_{Kmax}, or s_{Kmax}, draw a horizontal line until it meets the curve, and from that intersection drop a perpendicular. The value at which the perpendicular cuts the abscissa is the required sampling interval, Figure 3b.

Determine the number of cores in bulked samples similarly. Compute the estimation variances using Equation (1) for equispaced sampling configurations and sample sizes from 4 to about 50 and join the values to form a curve (Figure 4). Draw a horizontal line at the maximum tolerable variance, and drop a perpendicular from the point at where it intercepts the curve to the abscissa. The value on the abscissa is the optimum size of sample.

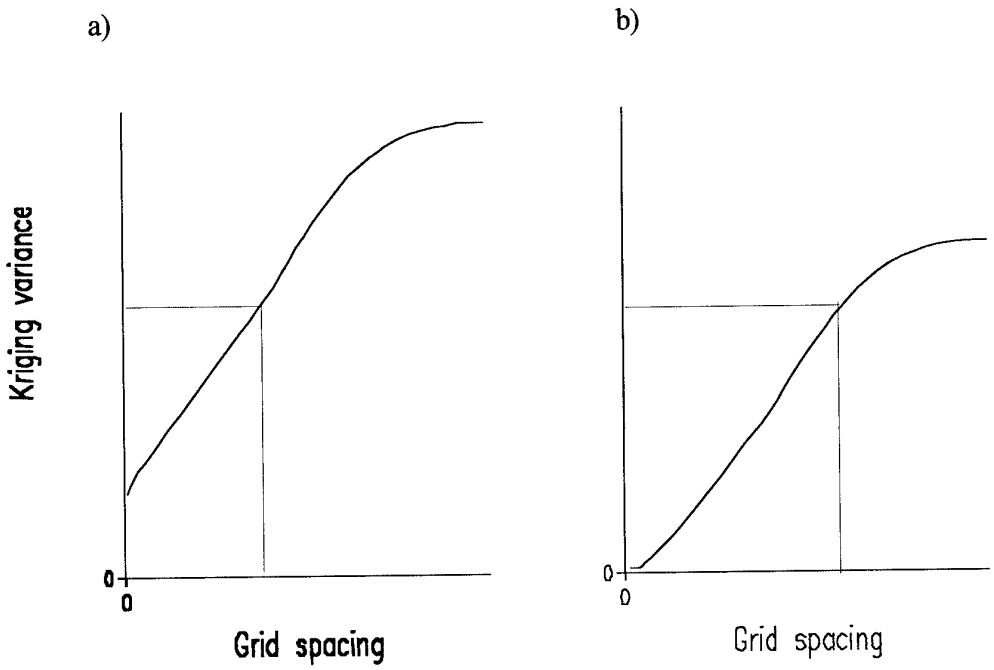

Figure 102. Kriging variances from (a) punctual kriging, and (b) block kriging.

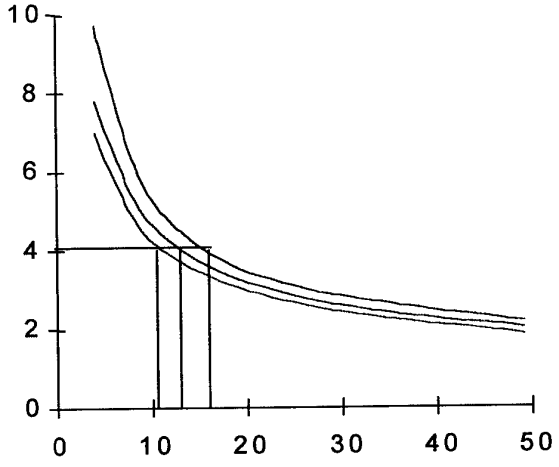

Figure 103. Graphs of standard error plotted against sample size for bulking from 4, 9, 16, 25, 36 and 49 cores, and for three different sample supports.

ACKNOWLEDGEMENTS

The National Soil Iventory of England and Wales was funded by the Ministry of Agriculture, Fisheries and Food of London.

Assistance in analysis and preparation of figures was provided by:

Dr Z. L. Frogbrook in Part I,
Dr S. D. Heming in Part II
Professor R. Webster in Parts I and IV.

REFERENCES

Avery, B.W. 1987. *Soil Survey Methods: a review.* Technical Monograph No. 18. Soil Survey and Land Research Centre, Silsoe.

Chang, C_I. and Du, Q. 1999. Interference and noise-adjusted prinicpal components analysis. *IEEE Transactions on Geosciences and Remote Sensing*, **37**, 2387-2396.

Green, A. A., Berman, M, Switzer, P. and Craig, M. D. 1988. A transformation for ordering multispectral data in terms of image quality with implications for noise removal. *IEEE Transactions on Geosciences and Remote Sensing*, 26, 65-74.

Hodgson, J.M. 1974. *Soil Survey Field Handbook*, 1st edn. Technical Monograph No. 5. Soil Survey of England and Wales, Harpenden.

Loveland, P.J. 1990. *The National Soil Inventory of England and Wales.* In: *Element Concentration Cadasters in Ecosystems* (eds H. Lieth and B. Markert), pp. 73-80. VCH, Weinheim, Germany.

MAFF. 1986. *The Analysis of Agricultural Materials.* Reference Book 427. HMSO, London.

McGrath, S.P. & Cunliffe, C.H. 1985. A simplified method for the extraction of the metals Fe, Zn, Cu, Ni, Cd, Pb, Cr, Co and Mn from soils and sewage sludges. *Journal of the Science of Food and Agriculture* **36**, 794-798.

McGrath, S.P. & Loveland, P.J. 1992. *The Soil Geochemical Atlas of England and Wales.* Blackie Academic and Professional, Glasgow.

Oliver, M. A., Webster, R, and Slocum, K. 2000. Filtering SPOT imagery by kriging analysis. *International Journal of Remote Sensing*, **21**, 735-752.

Waters, D.F. & Sweetman, I.C. 1955. The Rukuhia Soil Grinder. *Soil Science* **79**, 411-413.

APPENDIX I

Correlation matrix for the 126 hyperspectral bands.

	1	2	3	4	5	6	7	8	9
1	1.000								
2	0.930	1.000							
3	0.924	0.996	1.000						
4	0.920	0.994	0.998	1.000					
5	0.916	0.990	0.996	0.998	1.000				
6	0.914	0.982	0.989	0.991	0.995	1.000			
7	0.903	0.951	0.957	0.960	0.966	0.985	1.000		
8	0.887	0.923	0.929	0.932	0.940	0.966	0.995	1.000	
9	0.884	0.921	0.928	0.931	0.940	0.966	0.994	0.999	1.000
10	0.892	0.942	0.950	0.955	0.964	0.982	0.994	0.991	0.993
11	0.891	0.949	0.959	0.964	0.973	0.987	0.987	0.978	0.982
12	0.887	0.948	0.959	0.966	0.974	0.985	0.980	0.969	0.974
13	0.880	0.945	0.957	0.964	0.973	0.981	0.971	0.957	0.963
14	0.876	0.943	0.955	0.962	0.971	0.976	0.961	0.943	0.949
15	0.869	0.942	0.954	0.962	0.970	0.972	0.949	0.928	0.935
16	0.863	0.938	0.951	0.959	0.966	0.965	0.937	0.914	0.921
17	0.858	0.930	0.944	0.952	0.960	0.962	0.939	0.919	0.926
18	0.822	0.848	0.858	0.864	0.876	0.907	0.941	0.950	0.954
19	0.620	0.568	0.569	0.570	0.582	0.640	0.744	0.794	0.792
20	0.365	0.266	0.259	0.255	0.264	0.330	0.464	0.533	0.525
21	0.247	0.130	0.121	0.114	0.120	0.184	0.322	0.395	0.385
22	0.209	0.086	0.076	0.069	0.074	0.136	0.273	0.347	0.338
23	0.192	0.072	0.061	0.054	0.059	0.121	0.258	0.331	0.320
24	0.191	0.068	0.058	0.051	0.056	0.117	0.253	0.327	0.317
25	0.189	0.066	0.055	0.049	0.054	0.115	0.251	0.325	0.315
26	0.186	0.064	0.054	0.048	0.053	0.114	0.250	0.324	0.314
27	0.182	0.059	0.049	0.043	0.048	0.109	0.245	0.318	0.309
28	0.177	0.054	0.044	0.038	0.043	0.103	0.239	0.313	0.304
29	0.175	0.052	0.042	0.036	0.041	0.102	0.237	0.311	0.302
30	0.177	0.054	0.044	0.038	0.043	0.103	0.239	0.312	0.304
31	0.177	0.054	0.044	0.038	0.043	0.103	0.239	0.312	0.304
32	0.182	0.058	0.048	0.042	0.047	0.106	0.241	0.314	0.307
33	0.184	0.065	0.056	0.050	0.056	0.116	0.251	0.324	0.316
34	0.194	0.071	0.063	0.057	0.062	0.121	0.255	0.329	0.322
35	0.208	0.090	0.083	0.078	0.084	0.144	0.277	0.350	0.342
36	0.211	0.096	0.089	0.084	0.091	0.151	0.283	0.355	0.347
37	0.211	0.096	0.089	0.084	0.091	0.151	0.283	0.355	0.348
38	0.208	0.090	0.083	0.078	0.085	0.144	0.277	0.350	0.343
39	0.203	0.083	0.076	0.071	0.077	0.136	0.269	0.342	0.336
40	0.192	0.073	0.065	0.060	0.066	0.126	0.259	0.332	0.325
41	0.186	0.066	0.058	0.053	0.059	0.120	0.253	0.326	0.319
42	0.181	0.061	0.053	0.048	0.054	0.114	0.248	0.321	0.314
43	0.178	0.059	0.051	0.046	0.052	0.112	0.246	0.319	0.311
44	0.182	0.062	0.054	0.049	0.055	0.115	0.248	0.321	0.314
45	0.191	0.071	0.063	0.058	0.064	0.124	0.257	0.329	0.323
46	0.208	0.089	0.082	0.077	0.083	0.142	0.273	0.345	0.340
47	0.232	0.121	0.115	0.112	0.120	0.181	0.311	0.382	0.376
48	0.269	0.164	0.160	0.159	0.167	0.227	0.353	0.422	0.418
49	0.291	0.190	0.187	0.186	0.195	0.254	0.379	0.446	0.442
50	0.300	0.201	0.198	0.197	0.206	0.264	0.388	0.455	0.452
51	0.310	0.210	0.208	0.207	0.216	0.273	0.396	0.463	0.461
52	0.311	0.212	0.210	0.210	0.219	0.276	0.399	0.465	0.463
53	0.304	0.205	0.202	0.201	0.210	0.268	0.391	0.458	0.455
54	0.295	0.194	0.191	0.190	0.199	0.256	0.380	0.447	0.444
55	0.290	0.187	0.184	0.183	0.192	0.249	0.373	0.440	0.438
56	0.287	0.185	0.182	0.181	0.189	0.247	0.371	0.438	0.435
57	0.289	0.188	0.185	0.184	0.193	0.251	0.374	0.441	0.438
58	0.297	0.197	0.195	0.194	0.203	0.260	0.382	0.448	0.446
59	0.313	0.216	0.215	0.214	0.223	0.279	0.399	0.464	0.462
60	0.335	0.243	0.243	0.243	0.252	0.307	0.423	0.486	0.485
61	0.364	0.277	0.278	0.278	0.287	0.340	0.451	0.512	0.513
62	0.372	0.284	0.285	0.286	0.294	0.345	0.452	0.512	0.515
63	0.201	0.149	0.146	0.143	0.142	0.144	0.147	0.147	0.151

64	0.327	0.272	0.274	0.273	0.274	0.279	0.282	0.282	0.289
65	0.580	0.542	0.548	0.553	0.558	0.567	0.572	0.571	0.581
66	0.695	0.691	0.704	0.713	0.722	0.735	0.743	0.744	0.755
67	0.724	0.740	0.755	0.765	0.775	0.789	0.798	0.800	0.810
68	0.723	0.737	0.751	0.761	0.771	0.787	0.800	0.804	0.814
69	0.708	0.724	0.739	0.749	0.759	0.777	0.796	0.803	0.814
70	0.698	0.711	0.725	0.735	0.746	0.766	0.791	0.801	0.811
71	0.687	0.694	0.707	0.717	0.728	0.751	0.782	0.796	0.806
72	0.674	0.675	0.688	0.697	0.709	0.735	0.772	0.789	0.798
73	0.662	0.657	0.669	0.678	0.690	0.718	0.761	0.782	0.790
74	0.650	0.641	0.653	0.661	0.674	0.704	0.752	0.776	0.783
75	0.640	0.626	0.638	0.646	0.659	0.691	0.744	0.769	0.777
76	0.630	0.613	0.624	0.632	0.645	0.679	0.735	0.762	0.770
77	0.622	0.601	0.612	0.620	0.633	0.668	0.727	0.757	0.764
78	0.614	0.590	0.601	0.609	0.622	0.658	0.719	0.750	0.757
79	0.607	0.582	0.592	0.600	0.613	0.651	0.714	0.746	0.752
80	0.602	0.575	0.586	0.594	0.607	0.645	0.710	0.742	0.749
81	0.600	0.572	0.583	0.591	0.604	0.642	0.708	0.741	0.748
82	0.601	0.573	0.584	0.592	0.605	0.644	0.710	0.744	0.750
83	0.603	0.576	0.587	0.595	0.608	0.647	0.714	0.747	0.753
84	0.606	0.579	0.590	0.598	0.611	0.650	0.716	0.749	0.755
85	0.611	0.588	0.599	0.607	0.621	0.659	0.724	0.756	0.762
86	0.619	0.599	0.610	0.618	0.632	0.669	0.732	0.762	0.769
87	0.627	0.608	0.620	0.628	0.641	0.679	0.739	0.769	0.775
88	0.633	0.616	0.628	0.637	0.650	0.686	0.745	0.774	0.780
89	0.636	0.622	0.634	0.643	0.656	0.691	0.748	0.775	0.782
90	0.642	0.631	0.643	0.651	0.664	0.699	0.753	0.779	0.786
91	0.647	0.639	0.651	0.659	0.673	0.706	0.758	0.782	0.789
92	0.650	0.643	0.655	0.664	0.677	0.709	0.759	0.783	0.790
93	0.649	0.644	0.656	0.665	0.678	0.710	0.759	0.782	0.788
94	0.636	0.632	0.644	0.653	0.666	0.697	0.743	0.765	0.771
95	0.589	0.630	0.646	0.654	0.658	0.654	0.622	0.602	0.613
96	0.746	0.822	0.841	0.852	0.859	0.854	0.817	0.792	0.804
97	0.763	0.835	0.852	0.863	0.871	0.866	0.832	0.809	0.818
98	0.765	0.831	0.846	0.858	0.866	0.862	0.833	0.811	0.821
99	0.757	0.822	0.840	0.852	0.860	0.860	0.837	0.819	0.830
100	0.776	0.837	0.853	0.864	0.872	0.873	0.853	0.837	0.846
101	0.783	0.841	0.857	0.867	0.876	0.879	0.863	0.849	0.859
102	0.786	0.841	0.857	0.868	0.877	0.882	0.871	0.859	0.868
103	0.789	0.841	0.856	0.867	0.876	0.883	0.876	0.866	0.875
104	0.786	0.836	0.851	0.862	0.872	0.881	0.877	0.869	0.878
105	0.784	0.831	0.846	0.857	0.867	0.878	0.877	0.871	0.880
106	0.779	0.824	0.839	0.850	0.860	0.873	0.875	0.870	0.878
107	0.772	0.814	0.830	0.841	0.852	0.865	0.870	0.867	0.875
108	0.764	0.803	0.819	0.829	0.840	0.856	0.863	0.862	0.870
109	0.754	0.790	0.806	0.817	0.828	0.844	0.854	0.855	0.863
110	0.751	0.786	0.802	0.812	0.824	0.840	0.852	0.853	0.861
111	0.753	0.788	0.803	0.814	0.825	0.842	0.853	0.854	0.862
112	0.758	0.794	0.810	0.820	0.832	0.848	0.858	0.858	0.867
113	0.769	0.810	0.825	0.836	0.847	0.861	0.867	0.865	0.874
114	0.775	0.818	0.833	0.844	0.855	0.868	0.871	0.867	0.876
115	0.772	0.819	0.835	0.846	0.856	0.869	0.869	0.864	0.873
116	0.770	0.817	0.834	0.844	0.855	0.866	0.865	0.859	0.869
117	0.766	0.815	0.832	0.843	0.853	0.864	0.861	0.854	0.863
118	0.767	0.821	0.838	0.849	0.859	0.868	0.861	0.852	0.862
119	0.776	0.833	0.849	0.860	0.870	0.876	0.865	0.853	0.863
120	0.777	0.838	0.855	0.867	0.876	0.880	0.863	0.849	0.859
121	0.782	0.846	0.862	0.873	0.882	0.884	0.865	0.848	0.858
122	0.773	0.843	0.860	0.872	0.880	0.881	0.856	0.838	0.848
123	0.780	0.851	0.868	0.879	0.887	0.886	0.859	0.839	0.849
124	0.766	0.840	0.857	0.868	0.876	0.873	0.843	0.821	0.831
125	0.753	0.827	0.844	0.855	0.862	0.858	0.826	0.804	0.814
126	0.498	0.556	0.571	0.580	0.583	0.579	0.551	0.533	0.544

	10	**11**	**12**	**13**	**14**	**15**	**16**	**17**	**18**
10	1.000								
11	0.997	1.000							
12	0.992	0.998	1.000						
13	0.985	0.995	0.998	1.000					
14	0.976	0.990	0.995	0.997	1.000				

15	0.966	0.982	0.990	0.995	0.998	1.000			
16	0.955	0.974	0.983	0.990	0.995	0.999	1.000		
17	0.958	0.975	0.984	0.991	0.995	0.998	0.999	1.000	
18	0.953	0.950	0.950	0.945	0.940	0.927	0.916	0.929	1.000
19	0.741	0.706	0.692	0.671	0.651	0.623	0.600	0.625	0.860
20	0.444	0.391	0.367	0.339	0.311	0.278	0.253	0.279	0.586
21	0.297	0.238	0.212	0.182	0.152	0.120	0.095	0.121	0.434
22	0.247	0.188	0.162	0.132	0.102	0.070	0.047	0.071	0.381
23	0.231	0.172	0.146	0.116	0.087	0.055	0.032	0.057	0.370
24	0.228	0.169	0.144	0.114	0.085	0.053	0.031	0.055	0.367
25	0.226	0.168	0.143	0.114	0.085	0.054	0.031	0.056	0.368
26	0.226	0.168	0.144	0.115	0.086	0.055	0.033	0.058	0.371
27	0.221	0.164	0.139	0.110	0.082	0.052	0.030	0.055	0.368
28	0.216	0.159	0.134	0.106	0.078	0.048	0.026	0.051	0.364
29	0.214	0.158	0.133	0.105	0.078	0.047	0.026	0.051	0.366
30	0.216	0.160	0.136	0.108	0.081	0.051	0.029	0.054	0.368
31	0.217	0.160	0.137	0.109	0.081	0.051	0.029	0.055	0.368
32	0.220	0.164	0.141	0.114	0.086	0.057	0.036	0.061	0.370
33	0.230	0.175	0.152	0.125	0.098	0.069	0.048	0.074	0.388
34	0.237	0.181	0.160	0.134	0.106	0.078	0.057	0.082	0.389
35	0.259	0.206	0.184	0.158	0.132	0.104	0.083	0.110	0.419
36	0.265	0.213	0.192	0.166	0.142	0.114	0.093	0.120	0.430
37	0.266	0.214	0.193	0.168	0.143	0.115	0.095	0.122	0.432
38	0.261	0.208	0.187	0.162	0.137	0.109	0.089	0.116	0.424
39	0.252	0.200	0.179	0.154	0.128	0.101	0.081	0.107	0.415
40	0.242	0.189	0.168	0.143	0.118	0.090	0.070	0.096	0.406
41	0.236	0.183	0.162	0.136	0.111	0.083	0.063	0.090	0.402
42	0.230	0.177	0.156	0.131	0.106	0.078	0.058	0.085	0.397
43	0.228	0.175	0.155	0.129	0.105	0.076	0.056	0.083	0.397
44	0.231	0.178	0.158	0.133	0.108	0.080	0.060	0.088	0.399
45	0.240	0.188	0.168	0.144	0.119	0.092	0.072	0.099	0.408
46	0.258	0.206	0.188	0.164	0.139	0.112	0.093	0.120	0.424
47	0.298	0.249	0.231	0.208	0.185	0.159	0.140	0.168	0.473
48	0.344	0.298	0.281	0.259	0.239	0.214	0.196	0.224	0.521
49	0.371	0.327	0.311	0.290	0.271	0.246	0.229	0.258	0.549
50	0.381	0.337	0.322	0.302	0.283	0.259	0.242	0.271	0.558
51	0.391	0.347	0.333	0.314	0.294	0.271	0.254	0.283	0.566
52	0.393	0.350	0.336	0.317	0.297	0.274	0.258	0.286	0.570
53	0.385	0.342	0.328	0.308	0.289	0.266	0.249	0.278	0.563
54	0.374	0.330	0.315	0.296	0.277	0.253	0.237	0.266	0.552
55	0.367	0.323	0.308	0.289	0.269	0.246	0.230	0.259	0.544
56	0.364	0.320	0.306	0.287	0.268	0.245	0.229	0.257	0.543
57	0.368	0.324	0.310	0.291	0.272	0.249	0.233	0.262	0.548
58	0.377	0.334	0.320	0.302	0.283	0.261	0.245	0.274	0.556
59	0.395	0.353	0.341	0.323	0.305	0.283	0.269	0.297	0.574
60	0.421	0.382	0.370	0.354	0.337	0.316	0.302	0.331	0.598
61	0.452	0.415	0.405	0.390	0.373	0.355	0.342	0.369	0.623
62	0.455	0.418	0.409	0.397	0.377	0.361	0.348	0.376	0.616
63	0.149	0.147	0.150	0.154	0.145	0.149	0.150	0.155	0.162
64	0.289	0.289	0.294	0.301	0.293	0.298	0.300	0.307	0.310
65	0.588	0.593	0.603	0.612	0.608	0.615	0.618	0.628	0.629
66	0.766	0.774	0.787	0.797	0.795	0.803	0.808	0.821	0.825
67	0.824	0.833	0.846	0.855	0.858	0.864	0.868	0.881	0.890
68	0.825	0.833	0.844	0.852	0.854	0.860	0.863	0.877	0.895
69	0.820	0.826	0.837	0.845	0.844	0.849	0.852	0.867	0.896
70	0.815	0.819	0.829	0.835	0.835	0.838	0.840	0.856	0.898
71	0.806	0.807	0.816	0.821	0.822	0.823	0.823	0.840	0.898
72	0.795	0.794	0.801	0.805	0.805	0.804	0.804	0.822	0.894
73	0.783	0.780	0.786	0.789	0.788	0.786	0.784	0.803	0.889
74	0.773	0.768	0.773	0.774	0.772	0.769	0.767	0.786	0.884
75	0.764	0.757	0.761	0.761	0.759	0.754	0.751	0.771	0.879
76	0.754	0.745	0.749	0.749	0.745	0.740	0.736	0.757	0.872
77	0.746	0.736	0.739	0.738	0.734	0.728	0.724	0.745	0.867
78	0.737	0.726	0.729	0.728	0.723	0.717	0.712	0.734	0.860
79	0.732	0.719	0.722	0.720	0.715	0.708	0.704	0.726	0.857
80	0.727	0.714	0.716	0.714	0.709	0.702	0.697	0.719	0.854
81	0.725	0.712	0.714	0.712	0.706	0.698	0.693	0.716	0.853
82	0.727	0.713	0.715	0.713	0.707	0.699	0.694	0.716	0.854
83	0.730	0.716	0.718	0.716	0.710	0.702	0.696	0.718	0.856
84	0.732	0.719	0.721	0.718	0.712	0.705	0.699	0.721	0.857

85	0.740	0.727	0.729	0.727	0.722	0.714	0.708	0.730	0.864
86	0.748	0.737	0.739	0.737	0.732	0.724	0.719	0.740	0.868
87	0.756	0.745	0.747	0.746	0.741	0.734	0.728	0.750	0.873
88	0.762	0.752	0.755	0.753	0.749	0.742	0.737	0.758	0.877
89	0.766	0.756	0.759	0.759	0.755	0.748	0.744	0.764	0.880
90	0.771	0.763	0.767	0.766	0.763	0.757	0.753	0.773	0.884
91	0.776	0.769	0.773	0.773	0.771	0.766	0.762	0.782	0.888
92	0.779	0.772	0.777	0.777	0.776	0.771	0.768	0.787	0.888
93	0.778	0.772	0.777	0.777	0.776	0.771	0.769	0.788	0.888
94	0.762	0.758	0.762	0.762	0.762	0.758	0.755	0.774	0.869
95	0.639	0.657	0.673	0.689	0.682	0.699	0.708	0.714	0.629
96	0.841	0.866	0.884	0.900	0.903	0.920	0.930	0.934	0.836
97	0.857	0.883	0.899	0.913	0.924	0.937	0.947	0.950	0.860
98	0.858	0.883	0.899	0.911	0.924	0.935	0.944	0.947	0.868
99	0.861	0.882	0.898	0.912	0.916	0.929	0.937	0.944	0.875
100	0.877	0.897	0.912	0.923	0.932	0.941	0.948	0.953	0.895
101	0.886	0.904	0.918	0.928	0.934	0.943	0.949	0.955	0.905
102	0.893	0.908	0.921	0.930	0.935	0.942	0.947	0.954	0.913
103	0.897	0.912	0.923	0.931	0.936	0.942	0.946	0.953	0.921
104	0.898	0.911	0.922	0.929	0.933	0.938	0.941	0.949	0.925
105	0.898	0.910	0.920	0.927	0.930	0.935	0.937	0.946	0.928
106	0.896	0.906	0.916	0.923	0.926	0.930	0.932	0.941	0.929
107	0.891	0.901	0.911	0.917	0.920	0.924	0.925	0.935	0.929
108	0.884	0.893	0.903	0.910	0.913	0.916	0.917	0.928	0.929
109	0.876	0.884	0.894	0.901	0.903	0.906	0.908	0.919	0.925
110	0.873	0.882	0.891	0.898	0.900	0.903	0.905	0.916	0.926
111	0.875	0.883	0.893	0.899	0.902	0.904	0.906	0.918	0.927
112	0.880	0.889	0.898	0.905	0.907	0.910	0.911	0.923	0.929
113	0.889	0.899	0.909	0.915	0.917	0.920	0.922	0.932	0.930
114	0.893	0.904	0.914	0.921	0.923	0.927	0.929	0.938	0.929
115	0.892	0.903	0.914	0.922	0.924	0.929	0.932	0.941	0.924
116	0.888	0.901	0.912	0.921	0.924	0.929	0.932	0.941	0.921
117	0.885	0.899	0.910	0.919	0.923	0.929	0.933	0.941	0.918
118	0.885	0.900	0.913	0.922	0.925	0.933	0.938	0.946	0.912
119	0.889	0.905	0.918	0.927	0.932	0.940	0.945	0.952	0.910
120	0.887	0.905	0.918	0.929	0.933	0.942	0.948	0.954	0.901
121	0.888	0.907	0.921	0.931	0.938	0.946	0.952	0.957	0.898
122	0.879	0.899	0.914	0.926	0.929	0.941	0.947	0.952	0.880
123	0.882	0.903	0.917	0.928	0.935	0.945	0.952	0.955	0.879
124	0.865	0.887	0.901	0.914	0.918	0.930	0.938	0.940	0.855
125	0.848	0.869	0.883	0.895	0.899	0.911	0.918	0.920	0.831
126	0.566	0.581	0.593	0.605	0.598	0.613	0.619	0.623	0.544

	19	**20**	**21**	**22**	**23**	**24**	**25**	**26**	**27**
19	1.000								
20	0.912	1.000							
21	0.821	0.982	1.000						
22	0.783	0.965	0.997	1.000					
23	0.775	0.963	0.996	0.998	1.000				
24	0.773	0.962	0.996	0.999	0.999	1.000			
25	0.773	0.961	0.995	0.999	0.999	1.000	1.000		
26	0.775	0.962	0.995	0.998	0.999	1.000	1.000	1.000	
27	0.773	0.961	0.994	0.997	0.998	0.999	1.000	1.000	1.000
28	0.770	0.959	0.993	0.996	0.998	0.999	0.999	1.000	1.000
29	0.771	0.959	0.992	0.995	0.998	0.998	0.999	0.999	1.000
30	0.773	0.959	0.992	0.995	0.997	0.998	0.999	0.999	1.000
31	0.773	0.959	0.992	0.996	0.996	0.998	0.999	0.999	0.999
32	0.772	0.954	0.988	0.994	0.991	0.994	0.996	0.996	0.996
33	0.785	0.963	0.991	0.991	0.995	0.995	0.996	0.997	0.998
34	0.783	0.956	0.985	0.991	0.987	0.991	0.993	0.993	0.994
35	0.803	0.966	0.988	0.988	0.989	0.991	0.992	0.993	0.994
36	0.809	0.967	0.985	0.983	0.986	0.987	0.988	0.990	0.991
37	0.810	0.966	0.984	0.983	0.986	0.986	0.988	0.990	0.991
38	0.805	0.963	0.984	0.985	0.985	0.987	0.989	0.990	0.991
39	0.799	0.960	0.982	0.985	0.983	0.986	0.988	0.990	0.991
40	0.794	0.959	0.983	0.985	0.985	0.988	0.989	0.991	0.992
41	0.792	0.960	0.984	0.985	0.986	0.988	0.990	0.991	0.992
42	0.789	0.958	0.983	0.985	0.985	0.988	0.989	0.991	0.992
43	0.789	0.958	0.982	0.983	0.985	0.987	0.988	0.990	0.991
44	0.790	0.957	0.981	0.983	0.983	0.985	0.987	0.989	0.990

45	0.794	0.956	0.978	0.981	0.979	0.982	0.984	0.986	0.987
46	0.802	0.954	0.974	0.977	0.973	0.978	0.980	0.981	0.983
47	0.831	0.964	0.972	0.967	0.969	0.970	0.972	0.975	0.976
48	0.854	0.961	0.957	0.950	0.951	0.953	0.955	0.959	0.960
49	0.866	0.957	0.946	0.936	0.937	0.939	0.941	0.945	0.946
50	0.869	0.954	0.942	0.932	0.932	0.934	0.936	0.940	0.941
51	0.871	0.950	0.935	0.927	0.924	0.927	0.930	0.934	0.935
52	0.873	0.950	0.934	0.925	0.922	0.925	0.928	0.932	0.933
53	0.869	0.950	0.936	0.927	0.925	0.928	0.931	0.934	0.936
54	0.864	0.949	0.938	0.930	0.927	0.930	0.934	0.937	0.939
55	0.859	0.947	0.937	0.931	0.927	0.931	0.934	0.937	0.939
56	0.858	0.947	0.937	0.930	0.927	0.930	0.933	0.937	0.939
57	0.860	0.947	0.935	0.927	0.925	0.928	0.931	0.935	0.936
58	0.862	0.942	0.929	0.920	0.917	0.921	0.924	0.928	0.929
59	0.867	0.936	0.918	0.909	0.905	0.909	0.912	0.916	0.918
60	0.874	0.926	0.902	0.892	0.887	0.891	0.895	0.899	0.900
61	0.877	0.909	0.879	0.868	0.860	0.866	0.870	0.874	0.875
62	0.861	0.887	0.858	0.851	0.838	0.845	0.850	0.853	0.854
63	0.149	0.107	0.087	0.083	0.076	0.079	0.079	0.079	0.080
64	0.261	0.170	0.129	0.118	0.108	0.112	0.113	0.113	0.114
65	0.508	0.315	0.222	0.196	0.183	0.186	0.189	0.191	0.192
66	0.664	0.411	0.286	0.250	0.234	0.238	0.241	0.245	0.245
67	0.715	0.443	0.307	0.266	0.252	0.255	0.258	0.263	0.263
68	0.733	0.467	0.331	0.290	0.277	0.279	0.283	0.288	0.288
69	0.753	0.496	0.363	0.324	0.309	0.312	0.316	0.321	0.321
70	0.772	0.524	0.394	0.355	0.341	0.344	0.348	0.353	0.353
71	0.792	0.557	0.429	0.391	0.377	0.380	0.385	0.390	0.390
72	0.809	0.587	0.463	0.425	0.412	0.415	0.420	0.425	0.425
73	0.824	0.614	0.494	0.457	0.444	0.447	0.452	0.457	0.457
74	0.836	0.637	0.520	0.485	0.472	0.475	0.479	0.485	0.485
75	0.846	0.657	0.543	0.507	0.495	0.498	0.503	0.508	0.508
76	0.853	0.673	0.561	0.527	0.514	0.518	0.522	0.527	0.528
77	0.859	0.685	0.577	0.543	0.530	0.534	0.538	0.543	0.544
78	0.861	0.694	0.587	0.554	0.541	0.545	0.549	0.555	0.555
79	0.865	0.703	0.598	0.565	0.552	0.556	0.560	0.565	0.566
80	0.867	0.709	0.605	0.572	0.560	0.564	0.568	0.573	0.574
81	0.869	0.713	0.609	0.576	0.564	0.568	0.572	0.577	0.578
82	0.870	0.714	0.610	0.577	0.565	0.568	0.572	0.578	0.578
83	0.871	0.714	0.609	0.576	0.564	0.567	0.572	0.577	0.577
84	0.871	0.712	0.607	0.574	0.561	0.565	0.569	0.574	0.574
85	0.870	0.707	0.600	0.566	0.554	0.557	0.561	0.566	0.567
86	0.865	0.695	0.587	0.552	0.539	0.543	0.547	0.552	0.552
87	0.864	0.689	0.578	0.543	0.530	0.533	0.537	0.543	0.543
88	0.861	0.681	0.569	0.533	0.520	0.523	0.528	0.533	0.533
89	0.856	0.672	0.559	0.523	0.510	0.513	0.518	0.523	0.523
90	0.852	0.662	0.547	0.510	0.498	0.501	0.505	0.510	0.510
91	0.847	0.653	0.535	0.498	0.487	0.489	0.493	0.498	0.498
92	0.841	0.643	0.525	0.487	0.476	0.478	0.482	0.488	0.488
93	0.838	0.639	0.520	0.481	0.471	0.473	0.477	0.483	0.483
94	0.815	0.619	0.502	0.463	0.454	0.456	0.459	0.465	0.465
95	0.390	0.133	0.021	-0.011	-0.024	-0.023	-0.021	-0.019	-0.020
96	0.525	0.188	0.038	-0.006	-0.020	-0.020	-0.018	-0.014	-0.015
97	0.549	0.208	0.055	0.009	-0.004	-0.004	-0.002	0.003	0.002
98	0.567	0.230	0.077	0.032	0.019	0.019	0.021	0.026	0.025
99	0.595	0.268	0.118	0.073	0.059	0.060	0.062	0.066	0.065
100	0.620	0.294	0.142	0.096	0.083	0.083	0.086	0.090	0.089
101	0.642	0.321	0.170	0.125	0.111	0.112	0.114	0.119	0.118
102	0.664	0.349	0.200	0.155	0.140	0.141	0.144	0.148	0.146
103	0.681	0.371	0.222	0.177	0.163	0.163	0.166	0.170	0.168
104	0.695	0.388	0.240	0.195	0.181	0.182	0.184	0.188	0.187
105	0.705	0.402	0.254	0.209	0.195	0.195	0.198	0.202	0.201
106	0.713	0.414	0.266	0.221	0.207	0.208	0.210	0.215	0.213
107	0.721	0.426	0.279	0.233	0.219	0.220	0.223	0.227	0.226
108	0.729	0.438	0.292	0.247	0.233	0.234	0.237	0.241	0.240
109	0.736	0.450	0.305	0.261	0.246	0.248	0.251	0.256	0.254
110	0.740	0.456	0.312	0.268	0.253	0.255	0.258	0.263	0.262
111	0.741	0.457	0.313	0.268	0.254	0.255	0.258	0.263	0.262
112	0.737	0.450	0.305	0.261	0.246	0.248	0.251	0.255	0.254
113	0.727	0.434	0.288	0.243	0.229	0.230	0.233	0.238	0.236
114	0.717	0.419	0.271	0.226	0.212	0.213	0.216	0.220	0.219

115	0.704	0.402	0.254	0.209	0.195	0.196	0.198	0.203	0.201
116	0.696	0.392	0.244	0.199	0.185	0.186	0.188	0.193	0.191
117	0.687	0.381	0.232	0.186	0.173	0.174	0.176	0.181	0.180
118	0.670	0.358	0.209	0.164	0.150	0.150	0.153	0.158	0.156
119	0.657	0.340	0.189	0.143	0.130	0.130	0.133	0.137	0.136
120	0.635	0.313	0.162	0.117	0.103	0.104	0.106	0.110	0.109
121	0.622	0.296	0.145	0.098	0.086	0.086	0.088	0.092	0.091
122	0.596	0.267	0.116	0.071	0.057	0.057	0.060	0.064	0.062
123	0.586	0.254	0.103	0.057	0.044	0.044	0.046	0.050	0.048
124	0.558	0.228	0.079	0.036	0.021	0.022	0.024	0.027	0.026
125	0.535	0.212	0.068	0.026	0.012	0.012	0.014	0.017	0.015
126	0.339	0.117	0.023	-0.003	-0.016	-0.014	-0.012	-0.011	-0.012

	28	**29**	**30**	**31**	**32**	**33**	**34**	**35**	**36**
28	1.000								
29	1.000	1.000							
30	1.000	1.000	1.000						
31	1.000	1.000	1.000	1.000					
32	0.997	0.996	0.997	0.998	1.000				
33	0.998	0.999	0.998	0.998	0.994	1.000			
34	0.994	0.993	0.995	0.996	0.999	0.993	1.000		
35	0.994	0.995	0.996	0.996	0.994	0.998	0.995	1.000	
36	0.991	0.993	0.993	0.993	0.989	0.997	0.990	0.998	1.000
37	0.991	0.992	0.993	0.993	0.990	0.997	0.991	0.999	1.000
38	0.992	0.992	0.994	0.994	0.994	0.996	0.996	0.999	0.998
39	0.991	0.991	0.993	0.994	0.996	0.994	0.998	0.998	0.995
40	0.993	0.993	0.995	0.995	0.995	0.996	0.997	0.998	0.996
41	0.993	0.994	0.995	0.995	0.994	0.997	0.996	0.998	0.997
42	0.993	0.993	0.995	0.995	0.995	0.996	0.996	0.998	0.996
43	0.992	0.993	0.994	0.994	0.993	0.996	0.994	0.997	0.996
44	0.991	0.991	0.993	0.993	0.994	0.994	0.995	0.997	0.995
45	0.988	0.988	0.991	0.991	0.993	0.992	0.996	0.995	0.992
46	0.983	0.983	0.986	0.987	0.991	0.987	0.995	0.993	0.989
47	0.977	0.979	0.980	0.980	0.979	0.986	0.984	0.993	0.995
48	0.960	0.962	0.964	0.964	0.963	0.973	0.970	0.983	0.986
49	0.947	0.949	0.951	0.951	0.950	0.961	0.958	0.974	0.978
50	0.942	0.944	0.946	0.947	0.948	0.956	0.957	0.970	0.974
51	0.936	0.937	0.940	0.941	0.945	0.949	0.955	0.965	0.967
52	0.934	0.936	0.939	0.939	0.942	0.948	0.953	0.964	0.967
53	0.936	0.938	0.941	0.941	0.944	0.951	0.954	0.966	0.969
54	0.939	0.941	0.944	0.944	0.948	0.953	0.958	0.968	0.970
55	0.940	0.941	0.945	0.945	0.950	0.953	0.959	0.968	0.969
56	0.939	0.941	0.944	0.945	0.949	0.953	0.959	0.968	0.969
57	0.937	0.939	0.942	0.942	0.945	0.951	0.955	0.966	0.968
58	0.930	0.932	0.935	0.936	0.940	0.944	0.951	0.961	0.963
59	0.919	0.920	0.924	0.925	0.930	0.934	0.941	0.952	0.954
60	0.901	0.902	0.907	0.907	0.913	0.917	0.927	0.938	0.940
61	0.876	0.877	0.882	0.883	0.892	0.892	0.908	0.917	0.918
62	0.855	0.855	0.862	0.863	0.878	0.869	0.894	0.896	0.894
63	0.080	0.079	0.082	0.082	0.088	0.079	0.091	0.089	0.085
64	0.114	0.113	0.117	0.118	0.126	0.117	0.134	0.135	0.133
65	0.191	0.191	0.197	0.198	0.209	0.206	0.227	0.241	0.243
66	0.244	0.245	0.252	0.253	0.266	0.269	0.290	0.313	0.320
67	0.262	0.264	0.270	0.271	0.282	0.292	0.309	0.337	0.347
68	0.286	0.288	0.295	0.295	0.306	0.316	0.334	0.361	0.372
69	0.320	0.321	0.328	0.329	0.342	0.350	0.370	0.396	0.405
70	0.352	0.354	0.361	0.361	0.374	0.382	0.402	0.428	0.438
71	0.389	0.391	0.397	0.398	0.410	0.420	0.437	0.465	0.475
72	0.424	0.426	0.433	0.433	0.445	0.455	0.472	0.499	0.509
73	0.456	0.458	0.465	0.465	0.477	0.487	0.504	0.530	0.540
74	0.484	0.486	0.492	0.493	0.504	0.514	0.531	0.557	0.567
75	0.507	0.509	0.516	0.516	0.527	0.538	0.553	0.580	0.589
76	0.526	0.529	0.535	0.536	0.547	0.556	0.573	0.598	0.607
77	0.542	0.544	0.551	0.552	0.562	0.572	0.588	0.613	0.622
78	0.554	0.556	0.562	0.563	0.575	0.583	0.600	0.624	0.632
79	0.565	0.567	0.573	0.574	0.585	0.594	0.610	0.635	0.643
80	0.572	0.575	0.581	0.581	0.592	0.601	0.618	0.642	0.650
81	0.577	0.579	0.585	0.586	0.596	0.605	0.621	0.646	0.654
82	0.577	0.579	0.585	0.586	0.596	0.606	0.621	0.646	0.654
83	0.576	0.578	0.584	0.585	0.595	0.605	0.620	0.645	0.653

84	0.573	0.575	0.581	0.582	0.593	0.602	0.618	0.642	0.650
85	0.565	0.567	0.573	0.574	0.584	0.594	0.609	0.635	0.643
86	0.551	0.553	0.559	0.560	0.570	0.580	0.596	0.621	0.629
87	0.541	0.543	0.549	0.550	0.560	0.571	0.586	0.611	0.620
88	0.531	0.533	0.539	0.540	0.550	0.561	0.576	0.602	0.611
89	0.521	0.523	0.530	0.530	0.540	0.551	0.566	0.593	0.602
90	0.509	0.511	0.517	0.518	0.527	0.539	0.554	0.581	0.591
91	0.497	0.499	0.505	0.506	0.515	0.528	0.541	0.570	0.580
92	0.486	0.489	0.495	0.495	0.504	0.518	0.530	0.559	0.570
93	0.481	0.484	0.489	0.490	0.498	0.513	0.524	0.554	0.566
94	0.463	0.466	0.471	0.472	0.479	0.495	0.505	0.535	0.547
95	-0.021	-0.021	-0.017	-0.016	-0.007	-0.005	0.011	0.028	0.033
96	-0.017	-0.016	-0.011	-0.010	0.000	0.009	0.025	0.051	0.062
97	-0.001	0.001	0.006	0.007	0.015	0.028	0.041	0.071	0.083
98	0.023	0.025	0.030	0.030	0.039	0.052	0.065	0.095	0.108
99	0.063	0.064	0.070	0.071	0.082	0.092	0.108	0.136	0.147
100	0.087	0.089	0.094	0.094	0.103	0.117	0.130	0.160	0.172
101	0.115	0.117	0.122	0.122	0.132	0.144	0.158	0.188	0.200
102	0.144	0.145	0.151	0.151	0.161	0.173	0.188	0.216	0.228
103	0.166	0.167	0.172	0.173	0.182	0.195	0.209	0.238	0.250
104	0.184	0.185	0.191	0.191	0.201	0.213	0.228	0.256	0.268
105	0.198	0.199	0.205	0.205	0.214	0.227	0.241	0.270	0.282
106	0.210	0.212	0.217	0.218	0.227	0.240	0.254	0.283	0.294
107	0.223	0.225	0.230	0.231	0.240	0.253	0.267	0.297	0.308
108	0.238	0.239	0.245	0.245	0.255	0.268	0.282	0.311	0.323
109	0.252	0.254	0.259	0.260	0.270	0.282	0.298	0.326	0.337
110	0.259	0.261	0.267	0.267	0.277	0.290	0.305	0.334	0.345
111	0.260	0.262	0.267	0.268	0.277	0.290	0.305	0.334	0.345
112	0.252	0.253	0.259	0.260	0.269	0.282	0.296	0.326	0.337
113	0.234	0.235	0.241	0.241	0.251	0.263	0.278	0.307	0.318
114	0.216	0.218	0.223	0.224	0.233	0.246	0.259	0.289	0.300
115	0.199	0.200	0.206	0.206	0.216	0.228	0.243	0.271	0.282
116	0.189	0.190	0.196	0.196	0.206	0.219	0.233	0.262	0.273
117	0.177	0.179	0.184	0.185	0.194	0.207	0.221	0.251	0.262
118	0.154	0.155	0.161	0.161	0.171	0.183	0.198	0.227	0.238
119	0.133	0.135	0.140	0.141	0.150	0.163	0.176	0.206	0.218
120	0.106	0.108	0.113	0.113	0.123	0.135	0.149	0.178	0.189
121	0.088	0.090	0.094	0.095	0.103	0.117	0.129	0.159	0.172
122	0.059	0.060	0.065	0.066	0.075	0.087	0.101	0.129	0.140
123	0.045	0.046	0.051	0.052	0.061	0.073	0.086	0.114	0.126
124	0.023	0.024	0.029	0.029	0.039	0.049	0.064	0.090	0.100
125	0.012	0.013	0.018	0.018	0.028	0.037	0.052	0.077	0.087
126	-0.014	-0.014	-0.010	-0.009	0.001	0.001	0.018	0.029	0.031

	37	**38**	**39**	**40**	**41**	**42**	**43**	**44**	**45**
37	1.000								
38	0.999	1.000							
39	0.996	0.999	1.000						
40	0.997	0.999	0.999	1.000					
41	0.998	0.999	0.999	1.000	1.000				
42	0.997	0.999	0.999	1.000	1.000	1.000			
43	0.997	0.998	0.998	0.999	1.000	1.000	1.000		
44	0.996	0.998	0.999	0.999	1.000	1.000	1.000	1.000	
45	0.994	0.998	0.999	0.999	0.998	0.999	0.998	0.999	1.000
46	0.991	0.996	0.998	0.997	0.996	0.996	0.995	0.997	0.999
47	0.996	0.995	0.993	0.993	0.993	0.993	0.993	0.993	0.993
48	0.988	0.986	0.983	0.982	0.982	0.981	0.981	0.981	0.982
49	0.980	0.977	0.973	0.972	0.972	0.970	0.971	0.971	0.972
50	0.976	0.975	0.972	0.970	0.969	0.967	0.967	0.969	0.971
51	0.970	0.971	0.969	0.966	0.964	0.963	0.962	0.965	0.969
52	0.970	0.970	0.967	0.964	0.963	0.962	0.961	0.964	0.967
53	0.971	0.971	0.969	0.966	0.965	0.964	0.964	0.966	0.969
54	0.973	0.974	0.972	0.969	0.968	0.967	0.967	0.969	0.973
55	0.972	0.974	0.973	0.970	0.968	0.968	0.967	0.970	0.974
56	0.972	0.974	0.973	0.970	0.968	0.968	0.968	0.970	0.974
57	0.971	0.972	0.970	0.968	0.967	0.966	0.966	0.968	0.972
58	0.966	0.967	0.966	0.963	0.961	0.961	0.961	0.963	0.968
59	0.957	0.959	0.958	0.954	0.952	0.951	0.951	0.954	0.959
60	0.944	0.946	0.944	0.940	0.937	0.936	0.936	0.940	0.946
61	0.922	0.926	0.925	0.919	0.915	0.914	0.913	0.918	0.926

62	0.899	0.907	0.909	0.901	0.895	0.895	0.892	0.900	0.910
63	0.085	0.088	0.090	0.085	0.082	0.082	0.080	0.084	0.089
64	0.134	0.137	0.138	0.132	0.127	0.126	0.124	0.129	0.136
65	0.246	0.247	0.245	0.235	0.228	0.226	0.223	0.230	0.243
66	0.324	0.324	0.319	0.307	0.299	0.296	0.294	0.302	0.317
67	0.351	0.349	0.343	0.330	0.324	0.320	0.318	0.326	0.341
68	0.376	0.373	0.367	0.355	0.348	0.344	0.343	0.350	0.365
69	0.409	0.409	0.403	0.390	0.383	0.380	0.378	0.386	0.401
70	0.442	0.441	0.436	0.423	0.416	0.412	0.411	0.419	0.434
71	0.479	0.478	0.472	0.460	0.453	0.449	0.448	0.455	0.470
72	0.514	0.512	0.506	0.494	0.488	0.484	0.483	0.490	0.504
73	0.545	0.543	0.537	0.526	0.519	0.516	0.514	0.522	0.536
74	0.571	0.570	0.564	0.553	0.547	0.543	0.542	0.549	0.562
75	0.594	0.592	0.586	0.575	0.569	0.566	0.565	0.571	0.584
76	0.612	0.611	0.605	0.594	0.588	0.585	0.583	0.590	0.603
77	0.627	0.626	0.620	0.609	0.603	0.600	0.599	0.606	0.619
78	0.637	0.637	0.632	0.620	0.615	0.611	0.610	0.617	0.630
79	0.648	0.647	0.642	0.631	0.625	0.622	0.621	0.628	0.640
80	0.655	0.654	0.649	0.638	0.633	0.630	0.628	0.635	0.648
81	0.659	0.658	0.653	0.642	0.637	0.633	0.632	0.639	0.652
82	0.659	0.658	0.653	0.642	0.637	0.633	0.632	0.639	0.651
83	0.658	0.656	0.651	0.641	0.635	0.632	0.631	0.637	0.650
84	0.655	0.654	0.649	0.638	0.632	0.629	0.628	0.635	0.647
85	0.648	0.646	0.641	0.630	0.625	0.621	0.620	0.627	0.639
86	0.633	0.632	0.627	0.616	0.610	0.607	0.606	0.612	0.625
87	0.625	0.623	0.618	0.607	0.601	0.597	0.596	0.603	0.615
88	0.615	0.613	0.608	0.597	0.591	0.588	0.586	0.593	0.606
89	0.606	0.604	0.599	0.587	0.582	0.578	0.577	0.583	0.596
90	0.595	0.593	0.586	0.575	0.570	0.566	0.565	0.571	0.584
91	0.584	0.581	0.574	0.564	0.558	0.554	0.554	0.560	0.572
92	0.574	0.571	0.564	0.553	0.548	0.544	0.543	0.549	0.562
93	0.570	0.566	0.558	0.548	0.543	0.539	0.538	0.544	0.556
94	0.550	0.546	0.538	0.528	0.523	0.519	0.519	0.524	0.536
95	0.034	0.034	0.031	0.021	0.014	0.011	0.009	0.015	0.028
96	0.065	0.062	0.056	0.044	0.037	0.033	0.032	0.039	0.053
97	0.086	0.081	0.074	0.063	0.057	0.053	0.052	0.058	0.073
98	0.111	0.106	0.098	0.088	0.081	0.077	0.077	0.083	0.097
99	0.150	0.147	0.141	0.129	0.122	0.118	0.116	0.123	0.139
100	0.176	0.171	0.163	0.152	0.145	0.141	0.140	0.146	0.160
101	0.203	0.198	0.191	0.179	0.172	0.168	0.167	0.173	0.187
102	0.231	0.227	0.220	0.207	0.200	0.196	0.195	0.201	0.215
103	0.253	0.248	0.241	0.229	0.222	0.217	0.216	0.222	0.236
104	0.271	0.267	0.259	0.247	0.240	0.236	0.234	0.240	0.255
105	0.285	0.281	0.273	0.261	0.254	0.250	0.248	0.254	0.268
106	0.298	0.294	0.286	0.274	0.267	0.263	0.261	0.268	0.281
107	0.311	0.307	0.300	0.288	0.281	0.277	0.275	0.282	0.295
108	0.326	0.322	0.315	0.303	0.296	0.292	0.291	0.297	0.311
109	0.341	0.338	0.331	0.319	0.312	0.308	0.306	0.313	0.327
110	0.349	0.345	0.338	0.326	0.319	0.315	0.314	0.320	0.335
111	0.349	0.345	0.338	0.326	0.320	0.315	0.314	0.321	0.335
112	0.340	0.337	0.329	0.317	0.311	0.306	0.305	0.311	0.326
113	0.321	0.317	0.310	0.298	0.291	0.286	0.285	0.291	0.305
114	0.304	0.299	0.292	0.280	0.273	0.269	0.267	0.273	0.287
115	0.286	0.282	0.275	0.262	0.255	0.251	0.250	0.256	0.270
116	0.277	0.273	0.265	0.253	0.246	0.242	0.241	0.247	0.261
117	0.266	0.262	0.254	0.242	0.235	0.231	0.230	0.236	0.250
118	0.242	0.238	0.230	0.218	0.211	0.207	0.206	0.212	0.227
119	0.221	0.216	0.209	0.197	0.190	0.186	0.185	0.191	0.205
120	0.193	0.188	0.181	0.169	0.162	0.158	0.157	0.163	0.177
121	0.175	0.169	0.161	0.150	0.143	0.139	0.138	0.144	0.158
122	0.143	0.139	0.132	0.120	0.113	0.109	0.108	0.114	0.128
123	0.129	0.124	0.117	0.105	0.098	0.094	0.093	0.099	0.113
124	0.103	0.100	0.093	0.081	0.074	0.070	0.068	0.074	0.088
125	0.090	0.086	0.080	0.068	0.061	0.056	0.055	0.061	0.074
126	0.034	0.036	0.034	0.024	0.018	0.016	0.013	0.019	0.031

	46	**47**	**48**	**49**	**50**	**51**	**52**	**53**	**54**
46	1.000								
47	0.992	1.000							
48	0.983	0.997	1.000						

49	0.974	0.992	0.999	1.000					
50	0.974	0.990	0.998	0.999	1.000				
51	0.974	0.986	0.995	0.996	0.999	1.000			
52	0.972	0.986	0.995	0.997	0.999	1.000	1.000		
53	0.974	0.987	0.996	0.997	0.999	1.000	1.000	1.000	
54	0.977	0.989	0.996	0.997	0.999	0.999	0.999	1.000	1.000
55	0.979	0.988	0.995	0.995	0.998	0.999	0.999	0.999	1.000
56	0.979	0.988	0.995	0.995	0.998	0.998	0.998	0.999	1.000
57	0.976	0.988	0.995	0.996	0.998	0.998	0.998	0.999	1.000
58	0.973	0.984	0.993	0.994	0.997	0.998	0.998	0.999	0.999
59	0.965	0.978	0.989	0.992	0.995	0.997	0.998	0.998	0.998
60	0.953	0.967	0.982	0.987	0.991	0.995	0.995	0.995	0.994
61	0.937	0.949	0.967	0.973	0.980	0.987	0.986	0.985	0.985
62	0.924	0.927	0.945	0.950	0.960	0.971	0.969	0.968	0.968
63	0.097	0.096	0.103	0.109	0.114	0.122	0.121	0.118	0.118
64	0.148	0.155	0.172	0.182	0.191	0.202	0.201	0.197	0.195
65	0.262	0.289	0.329	0.353	0.365	0.381	0.381	0.375	0.369
66	0.340	0.382	0.436	0.467	0.483	0.500	0.502	0.495	0.487
67	0.364	0.413	0.472	0.507	0.521	0.537	0.540	0.533	0.524
68	0.388	0.437	0.496	0.530	0.545	0.561	0.564	0.557	0.547
69	0.425	0.471	0.529	0.562	0.578	0.595	0.597	0.591	0.581
70	0.457	0.504	0.561	0.594	0.609	0.625	0.628	0.621	0.612
71	0.493	0.540	0.597	0.629	0.643	0.658	0.661	0.655	0.646
72	0.527	0.573	0.629	0.660	0.674	0.689	0.692	0.685	0.677
73	0.557	0.603	0.657	0.688	0.702	0.716	0.718	0.712	0.704
74	0.584	0.629	0.682	0.711	0.725	0.738	0.741	0.735	0.727
75	0.605	0.650	0.702	0.731	0.744	0.757	0.760	0.754	0.746
76	0.624	0.667	0.718	0.746	0.759	0.773	0.775	0.769	0.761
77	0.639	0.682	0.732	0.759	0.772	0.785	0.787	0.782	0.774
78	0.651	0.692	0.741	0.768	0.780	0.794	0.796	0.791	0.783
79	0.660	0.702	0.750	0.777	0.789	0.802	0.804	0.799	0.792
80	0.667	0.709	0.757	0.783	0.795	0.808	0.810	0.805	0.798
81	0.671	0.712	0.760	0.786	0.798	0.811	0.813	0.808	0.800
82	0.671	0.712	0.759	0.786	0.798	0.810	0.813	0.808	0.800
83	0.669	0.711	0.758	0.785	0.797	0.809	0.812	0.806	0.799
84	0.667	0.708	0.756	0.782	0.794	0.807	0.809	0.804	0.796
85	0.659	0.701	0.750	0.776	0.789	0.801	0.803	0.798	0.790
86	0.645	0.688	0.736	0.764	0.776	0.790	0.792	0.786	0.778
87	0.635	0.679	0.728	0.756	0.769	0.782	0.784	0.779	0.770
88	0.626	0.670	0.720	0.748	0.761	0.774	0.776	0.771	0.762
89	0.617	0.661	0.712	0.741	0.754	0.767	0.769	0.763	0.755
90	0.604	0.651	0.702	0.732	0.744	0.757	0.760	0.754	0.745
91	0.592	0.640	0.693	0.723	0.735	0.747	0.750	0.744	0.735
92	0.582	0.631	0.684	0.714	0.726	0.739	0.742	0.736	0.727
93	0.575	0.626	0.680	0.711	0.722	0.733	0.737	0.731	0.722
94	0.555	0.606	0.658	0.688	0.699	0.710	0.714	0.708	0.699
95	0.048	0.078	0.122	0.147	0.161	0.177	0.179	0.172	0.164
96	0.077	0.124	0.184	0.220	0.235	0.252	0.255	0.248	0.237
97	0.095	0.148	0.210	0.247	0.261	0.276	0.280	0.273	0.262
98	0.119	0.173	0.235	0.272	0.287	0.301	0.305	0.298	0.287
99	0.163	0.212	0.273	0.309	0.325	0.342	0.345	0.338	0.327
100	0.183	0.236	0.299	0.336	0.350	0.364	0.368	0.361	0.350
101	0.210	0.262	0.324	0.360	0.375	0.390	0.394	0.386	0.375
102	0.238	0.289	0.351	0.386	0.401	0.416	0.420	0.412	0.401
103	0.259	0.311	0.372	0.408	0.422	0.437	0.440	0.433	0.421
104	0.278	0.329	0.390	0.425	0.440	0.454	0.458	0.450	0.439
105	0.291	0.343	0.404	0.439	0.453	0.468	0.472	0.464	0.452
106	0.304	0.356	0.417	0.452	0.466	0.481	0.485	0.477	0.465
107	0.318	0.370	0.431	0.466	0.480	0.495	0.499	0.491	0.479
108	0.334	0.386	0.446	0.481	0.496	0.510	0.514	0.506	0.495
109	0.350	0.401	0.461	0.496	0.511	0.526	0.530	0.522	0.511
110	0.358	0.409	0.469	0.504	0.518	0.533	0.537	0.529	0.518
111	0.357	0.409	0.469	0.504	0.518	0.533	0.537	0.529	0.518
112	0.348	0.400	0.460	0.495	0.509	0.524	0.527	0.520	0.509
113	0.328	0.379	0.440	0.475	0.489	0.504	0.507	0.499	0.488
114	0.310	0.362	0.422	0.458	0.472	0.486	0.490	0.482	0.471
115	0.293	0.344	0.405	0.440	0.455	0.470	0.474	0.466	0.454
116	0.284	0.336	0.396	0.432	0.447	0.462	0.465	0.457	0.446
117	0.273	0.326	0.387	0.423	0.437	0.452	0.456	0.448	0.436
118	0.250	0.301	0.362	0.398	0.413	0.428	0.432	0.424	0.413

119	0.227	0.280	0.342	0.378	0.392	0.407	0.411	0.403	0.391
120	0.200	0.251	0.313	0.349	0.364	0.379	0.382	0.374	0.363
121	0.180	0.233	0.295	0.331	0.345	0.359	0.363	0.355	0.344
122	0.151	0.201	0.261	0.297	0.312	0.327	0.330	0.323	0.311
123	0.135	0.186	0.246	0.282	0.297	0.311	0.315	0.307	0.296
124	0.111	0.159	0.218	0.253	0.267	0.282	0.286	0.278	0.267
125	0.097	0.142	0.200	0.233	0.248	0.263	0.266	0.258	0.247
126	0.049	0.069	0.106	0.127	0.140	0.155	0.155	0.150	0.143

	55	**56**	**57**	**58**	**59**	**60**	**61**	**62**	**63**
55	1.000								
56	1.000	1.000							
57	0.999	1.000	1.000						
58	0.999	0.999	1.000	1.000					
59	0.998	0.998	0.998	0.999	1.000				
60	0.994	0.994	0.994	0.997	0.999	1.000			
61	0.985	0.985	0.984	0.988	0.993	0.997	1.000		
62	0.970	0.969	0.967	0.972	0.978	0.984	0.992	1.000	
63	0.120	0.117	0.116	0.120	0.124	0.131	0.144	0.155	1.000
64	0.197	0.194	0.193	0.199	0.208	0.220	0.240	0.256	0.616
65	0.369	0.366	0.368	0.379	0.396	0.420	0.452	0.467	0.547
66	0.484	0.482	0.486	0.500	0.522	0.555	0.594	0.607	0.388
67	0.520	0.518	0.523	0.537	0.562	0.596	0.634	0.640	0.282
68	0.543	0.542	0.547	0.561	0.584	0.618	0.656	0.662	0.276
69	0.578	0.577	0.581	0.595	0.619	0.652	0.691	0.700	0.242
70	0.609	0.607	0.612	0.626	0.649	0.681	0.718	0.725	0.218
71	0.642	0.641	0.645	0.659	0.681	0.712	0.746	0.750	0.206
72	0.673	0.672	0.676	0.689	0.710	0.740	0.773	0.775	0.202
73	0.700	0.699	0.703	0.715	0.736	0.765	0.796	0.797	0.203
74	0.723	0.722	0.726	0.738	0.758	0.786	0.815	0.815	0.200
75	0.742	0.741	0.745	0.756	0.776	0.802	0.830	0.828	0.196
76	0.758	0.757	0.760	0.772	0.790	0.816	0.843	0.843	0.198
77	0.770	0.769	0.773	0.784	0.802	0.827	0.853	0.852	0.197
78	0.780	0.779	0.782	0.793	0.811	0.836	0.862	0.861	0.199
79	0.788	0.787	0.791	0.801	0.819	0.843	0.868	0.866	0.196
80	0.794	0.793	0.797	0.807	0.824	0.848	0.872	0.870	0.194
81	0.797	0.796	0.800	0.810	0.827	0.850	0.874	0.872	0.195
82	0.797	0.796	0.799	0.809	0.826	0.849	0.874	0.871	0.194
83	0.795	0.794	0.798	0.808	0.825	0.848	0.872	0.869	0.192
84	0.793	0.792	0.795	0.805	0.823	0.846	0.871	0.869	0.194
85	0.786	0.785	0.789	0.799	0.816	0.840	0.864	0.861	0.187
86	0.775	0.773	0.777	0.787	0.805	0.829	0.855	0.854	0.191
87	0.766	0.765	0.769	0.779	0.797	0.822	0.848	0.846	0.190
88	0.758	0.757	0.760	0.771	0.789	0.815	0.841	0.840	0.189
89	0.751	0.750	0.753	0.764	0.783	0.809	0.836	0.834	0.190
90	0.741	0.740	0.744	0.755	0.774	0.800	0.827	0.824	0.189
91	0.731	0.730	0.735	0.745	0.765	0.791	0.818	0.814	0.184
92	0.722	0.721	0.726	0.737	0.757	0.784	0.811	0.807	0.183
93	0.717	0.716	0.721	0.732	0.751	0.778	0.805	0.798	0.184
94	0.694	0.693	0.698	0.709	0.728	0.754	0.780	0.774	0.183
95	0.163	0.160	0.162	0.175	0.195	0.225	0.266	0.288	0.359
96	0.233	0.232	0.237	0.253	0.279	0.317	0.364	0.379	0.210
97	0.257	0.256	0.263	0.278	0.304	0.342	0.385	0.393	0.176
98	0.282	0.281	0.288	0.303	0.329	0.366	0.407	0.414	0.183
99	0.323	0.322	0.327	0.342	0.369	0.407	0.451	0.464	0.199
100	0.344	0.344	0.350	0.364	0.390	0.427	0.468	0.474	0.177
101	0.369	0.369	0.374	0.388	0.414	0.450	0.492	0.498	0.185
102	0.396	0.394	0.399	0.414	0.439	0.475	0.516	0.524	0.188
103	0.416	0.414	0.420	0.433	0.458	0.494	0.534	0.539	0.183
104	0.433	0.432	0.437	0.451	0.475	0.510	0.550	0.556	0.185
105	0.447	0.445	0.450	0.464	0.488	0.523	0.562	0.567	0.185
106	0.460	0.458	0.463	0.477	0.501	0.536	0.574	0.579	0.185
107	0.474	0.473	0.478	0.491	0.515	0.550	0.588	0.592	0.186
108	0.490	0.488	0.494	0.507	0.531	0.565	0.603	0.606	0.187
109	0.506	0.505	0.510	0.523	0.547	0.581	0.619	0.624	0.192
110	0.513	0.512	0.517	0.531	0.554	0.588	0.626	0.629	0.191
111	0.513	0.511	0.517	0.530	0.554	0.587	0.624	0.628	0.190
112	0.503	0.502	0.507	0.520	0.544	0.578	0.615	0.619	0.191
113	0.483	0.481	0.486	0.499	0.523	0.557	0.596	0.600	0.193
114	0.465	0.463	0.468	0.482	0.506	0.540	0.578	0.582	0.190

115	0.449	0.447	0.452	0.466	0.490	0.525	0.564	0.570	0.192
116	0.440	0.439	0.444	0.458	0.482	0.517	0.557	0.562	0.192
117	0.431	0.429	0.435	0.449	0.473	0.508	0.548	0.552	0.183
118	0.407	0.406	0.411	0.425	0.450	0.486	0.527	0.534	0.186
119	0.386	0.384	0.390	0.404	0.429	0.465	0.505	0.510	0.180
120	0.358	0.356	0.362	0.376	0.401	0.438	0.480	0.487	0.178
121	0.338	0.337	0.343	0.357	0.382	0.418	0.459	0.464	0.170
122	0.306	0.305	0.310	0.325	0.350	0.387	0.430	0.440	0.181
123	0.291	0.289	0.295	0.309	0.335	0.371	0.414	0.422	0.170
124	0.262	0.260	0.265	0.280	0.305	0.342	0.385	0.395	0.177
125	0.242	0.241	0.245	0.259	0.284	0.320	0.363	0.375	0.178
126	0.142	0.139	0.140	0.152	0.170	0.196	0.232	0.252	0.162

	64	**65**	**66**	**67**	**68**	**69**	**70**	**71**	**72**
64	1.000								
65	0.678	1.000							
66	0.550	0.843	1.000						
67	0.447	0.780	0.955	1.000					
68	0.438	0.775	0.954	0.993	1.000				
69	0.405	0.744	0.943	0.988	0.992	1.000			
70	0.380	0.722	0.930	0.983	0.989	0.997	1.000		
71	0.365	0.708	0.918	0.976	0.983	0.993	0.998	1.000	
72	0.360	0.700	0.910	0.968	0.976	0.988	0.995	0.999	1.000
73	0.359	0.695	0.902	0.960	0.969	0.982	0.990	0.996	0.999
74	0.354	0.686	0.892	0.950	0.960	0.974	0.985	0.992	0.997
75	0.348	0.677	0.882	0.941	0.952	0.967	0.978	0.988	0.994
76	0.349	0.674	0.877	0.933	0.945	0.961	0.973	0.984	0.991
77	0.346	0.669	0.870	0.926	0.938	0.955	0.968	0.979	0.987
78	0.348	0.667	0.866	0.920	0.933	0.951	0.964	0.976	0.984
79	0.343	0.661	0.859	0.914	0.927	0.946	0.960	0.972	0.982
80	0.341	0.656	0.855	0.910	0.923	0.942	0.956	0.969	0.979
81	0.341	0.656	0.853	0.907	0.921	0.939	0.954	0.967	0.977
82	0.340	0.655	0.851	0.906	0.919	0.938	0.953	0.966	0.977
83	0.338	0.652	0.850	0.905	0.919	0.938	0.953	0.966	0.976
84	0.341	0.655	0.853	0.907	0.921	0.940	0.954	0.967	0.977
85	0.334	0.651	0.852	0.909	0.923	0.941	0.956	0.969	0.979
86	0.340	0.658	0.859	0.915	0.928	0.947	0.960	0.972	0.981
87	0.340	0.660	0.862	0.919	0.932	0.950	0.963	0.974	0.983
88	0.339	0.662	0.866	0.923	0.936	0.954	0.966	0.977	0.985
89	0.341	0.665	0.870	0.928	0.941	0.958	0.970	0.980	0.987
90	0.340	0.668	0.874	0.934	0.946	0.961	0.973	0.983	0.990
91	0.335	0.667	0.875	0.938	0.949	0.964	0.976	0.985	0.991
92	0.337	0.669	0.879	0.942	0.953	0.966	0.978	0.987	0.992
93	0.334	0.670	0.876	0.940	0.951	0.963	0.975	0.984	0.990
94	0.323	0.650	0.856	0.918	0.929	0.941	0.952	0.961	0.966
95	0.485	0.690	0.765	0.738	0.731	0.715	0.688	0.661	0.641
96	0.371	0.690	0.879	0.920	0.914	0.906	0.888	0.865	0.843
97	0.334	0.671	0.873	0.933	0.926	0.916	0.905	0.887	0.866
98	0.340	0.679	0.879	0.940	0.934	0.923	0.913	0.898	0.879
99	0.362	0.698	0.903	0.954	0.950	0.947	0.935	0.917	0.899
100	0.337	0.683	0.892	0.956	0.953	0.946	0.939	0.926	0.910
101	0.346	0.692	0.900	0.961	0.959	0.954	0.947	0.935	0.920
102	0.349	0.694	0.904	0.964	0.963	0.961	0.954	0.943	0.929
103	0.345	0.691	0.902	0.965	0.965	0.963	0.958	0.948	0.935
104	0.347	0.693	0.905	0.966	0.967	0.966	0.962	0.953	0.942
105	0.346	0.692	0.904	0.967	0.968	0.968	0.964	0.957	0.946
106	0.347	0.693	0.906	0.968	0.970	0.970	0.968	0.961	0.951
107	0.348	0.695	0.908	0.970	0.972	0.973	0.972	0.965	0.956
108	0.349	0.696	0.910	0.972	0.975	0.977	0.976	0.970	0.962
109	0.355	0.701	0.914	0.975	0.979	0.982	0.981	0.976	0.968
110	0.354	0.701	0.914	0.976	0.979	0.983	0.982	0.978	0.971
111	0.352	0.700	0.913	0.975	0.978	0.981	0.981	0.977	0.970
112	0.354	0.700	0.913	0.974	0.977	0.979	0.978	0.973	0.966
113	0.355	0.700	0.910	0.970	0.973	0.974	0.972	0.966	0.957
114	0.352	0.696	0.907	0.968	0.969	0.970	0.967	0.960	0.950
115	0.355	0.698	0.908	0.967	0.968	0.968	0.964	0.956	0.945
116	0.354	0.698	0.908	0.967	0.968	0.967	0.963	0.954	0.943
117	0.344	0.689	0.902	0.965	0.965	0.964	0.961	0.952	0.940
118	0.347	0.691	0.903	0.962	0.962	0.961	0.955	0.944	0.931
119	0.339	0.684	0.895	0.957	0.956	0.952	0.947	0.935	0.921

120	0.340	0.681	0.892	0.951	0.949	0.945	0.937	0.924	0.908
121	0.327	0.670	0.879	0.943	0.940	0.934	0.927	0.914	0.898
122	0.339	0.673	0.877	0.932	0.929	0.924	0.913	0.896	0.877
123	0.327	0.663	0.865	0.926	0.921	0.914	0.904	0.888	0.869
124	0.327	0.652	0.849	0.903	0.898	0.891	0.879	0.860	0.841
125	0.327	0.636	0.825	0.877	0.871	0.864	0.851	0.832	0.812
126	0.257	0.464	0.585	0.599	0.595	0.596	0.579	0.557	0.540

	73	**74**	**75**	**76**	**77**	**78**	**79**	**80**	**81**
73	1.000								
74	0.999	1.000							
75	0.997	0.999	1.000						
76	0.995	0.998	0.999	1.000					
77	0.993	0.997	0.999	1.000	1.000				
78	0.991	0.995	0.997	0.999	1.000	1.000			
79	0.989	0.993	0.996	0.998	0.999	1.000	1.000		
80	0.987	0.992	0.995	0.997	0.999	0.999	1.000	1.000	
81	0.985	0.991	0.994	0.997	0.998	0.999	1.000	1.000	1.000
82	0.984	0.990	0.994	0.996	0.998	0.999	0.999	1.000	1.000
83	0.984	0.990	0.994	0.996	0.998	0.998	0.999	0.999	1.000
84	0.985	0.990	0.994	0.996	0.998	0.999	0.999	0.999	1.000
85	0.986	0.991	0.995	0.997	0.998	0.998	0.999	0.999	0.999
86	0.988	0.992	0.995	0.997	0.998	0.998	0.998	0.998	0.998
87	0.989	0.993	0.996	0.997	0.998	0.998	0.998	0.997	0.997
88	0.990	0.994	0.996	0.997	0.998	0.997	0.997	0.997	0.997
89	0.992	0.996	0.997	0.998	0.998	0.997	0.997	0.996	0.996
90	0.994	0.997	0.998	0.998	0.997	0.996	0.996	0.995	0.994
91	0.995	0.997	0.998	0.997	0.996	0.994	0.994	0.993	0.992
92	0.995	0.997	0.997	0.996	0.995	0.993	0.992	0.991	0.990
93	0.992	0.994	0.994	0.993	0.991	0.989	0.988	0.987	0.986
94	0.969	0.970	0.970	0.968	0.967	0.964	0.964	0.963	0.962
95	0.623	0.606	0.589	0.580	0.570	0.565	0.554	0.548	0.545
96	0.821	0.801	0.782	0.768	0.755	0.745	0.735	0.727	0.723
97	0.846	0.827	0.810	0.794	0.781	0.770	0.761	0.754	0.749
98	0.860	0.842	0.826	0.811	0.799	0.787	0.779	0.772	0.768
99	0.881	0.864	0.848	0.836	0.824	0.815	0.806	0.799	0.795
100	0.893	0.877	0.863	0.850	0.839	0.828	0.820	0.814	0.810
101	0.904	0.889	0.876	0.863	0.853	0.843	0.835	0.829	0.826
102	0.914	0.901	0.888	0.876	0.866	0.857	0.850	0.844	0.841
103	0.922	0.909	0.898	0.887	0.877	0.868	0.862	0.856	0.853
104	0.929	0.917	0.906	0.896	0.887	0.879	0.872	0.867	0.864
105	0.934	0.923	0.913	0.903	0.895	0.887	0.881	0.875	0.873
106	0.940	0.930	0.920	0.910	0.902	0.895	0.889	0.884	0.882
107	0.946	0.936	0.927	0.918	0.910	0.903	0.897	0.893	0.891
108	0.953	0.944	0.935	0.927	0.919	0.912	0.907	0.902	0.900
109	0.960	0.951	0.943	0.935	0.928	0.922	0.916	0.912	0.910
110	0.962	0.954	0.946	0.938	0.931	0.925	0.920	0.916	0.913
111	0.961	0.953	0.945	0.937	0.930	0.924	0.918	0.914	0.912
112	0.957	0.948	0.940	0.931	0.924	0.918	0.912	0.908	0.906
113	0.947	0.938	0.929	0.920	0.912	0.905	0.899	0.895	0.892
114	0.940	0.930	0.920	0.911	0.903	0.895	0.889	0.884	0.882
115	0.934	0.923	0.912	0.903	0.894	0.887	0.880	0.875	0.873
116	0.931	0.920	0.909	0.899	0.890	0.882	0.876	0.871	0.868
117	0.928	0.916	0.905	0.894	0.885	0.877	0.870	0.865	0.862
118	0.917	0.904	0.892	0.881	0.872	0.863	0.856	0.850	0.847
119	0.907	0.893	0.881	0.869	0.859	0.849	0.842	0.836	0.833
120	0.892	0.877	0.864	0.851	0.841	0.831	0.823	0.817	0.814
121	0.881	0.865	0.852	0.838	0.827	0.817	0.809	0.803	0.799
122	0.860	0.843	0.827	0.814	0.802	0.793	0.784	0.777	0.773
123	0.850	0.833	0.818	0.804	0.792	0.781	0.772	0.765	0.762
124	0.822	0.804	0.787	0.773	0.761	0.751	0.741	0.734	0.730
125	0.792	0.774	0.758	0.744	0.732	0.722	0.712	0.705	0.701
126	0.525	0.510	0.495	0.488	0.479	0.474	0.465	0.459	0.456

	82	**83**	**84**	**85**	**86**	**87**	**88**	**89**	**90**
82	1.000								
83	1.000	1.000							
84	1.000	1.000	1.000						
85	0.999	1.000	1.000	1.000					
86	0.999	0.999	0.999	0.999	1.000				

87	0.998	0.998	0.998	0.999	1.000	1.000			
88	0.997	0.997	0.998	0.998	0.999	1.000	1.000		
89	0.996	0.997	0.997	0.998	0.999	0.999	0.999	1.000	
90	0.995	0.995	0.995	0.997	0.997	0.998	0.999	0.999	1.000
91	0.992	0.993	0.993	0.995	0.995	0.997	0.997	0.998	0.999
92	0.990	0.991	0.991	0.992	0.993	0.995	0.996	0.997	0.998
93	0.986	0.986	0.986	0.989	0.989	0.991	0.992	0.993	0.995
94	0.962	0.962	0.962	0.965	0.965	0.967	0.968	0.970	0.972
95	0.544	0.543	0.548	0.548	0.561	0.565	0.573	0.579	0.584
96	0.722	0.722	0.726	0.731	0.743	0.751	0.760	0.768	0.778
97	0.748	0.749	0.751	0.758	0.768	0.776	0.785	0.794	0.805
98	0.767	0.767	0.769	0.776	0.785	0.794	0.802	0.810	0.821
99	0.794	0.794	0.797	0.803	0.813	0.820	0.828	0.836	0.844
100	0.809	0.810	0.812	0.819	0.827	0.835	0.843	0.850	0.860
101	0.825	0.826	0.828	0.834	0.843	0.850	0.858	0.865	0.873
102	0.840	0.841	0.844	0.850	0.858	0.865	0.872	0.879	0.887
103	0.853	0.854	0.856	0.862	0.870	0.877	0.884	0.890	0.898
104	0.864	0.865	0.868	0.874	0.882	0.888	0.895	0.900	0.907
105	0.873	0.875	0.877	0.883	0.890	0.897	0.903	0.908	0.915
106	0.882	0.883	0.885	0.891	0.899	0.905	0.911	0.916	0.922
107	0.891	0.892	0.894	0.900	0.907	0.913	0.919	0.923	0.929
108	0.901	0.902	0.904	0.909	0.916	0.922	0.927	0.932	0.937
109	0.910	0.911	0.913	0.918	0.925	0.930	0.935	0.939	0.945
110	0.914	0.915	0.916	0.921	0.928	0.933	0.938	0.942	0.947
111	0.912	0.913	0.915	0.920	0.926	0.932	0.937	0.941	0.946
112	0.906	0.907	0.909	0.914	0.921	0.926	0.931	0.936	0.941
113	0.893	0.894	0.896	0.902	0.909	0.915	0.920	0.925	0.931
114	0.882	0.884	0.886	0.892	0.899	0.906	0.911	0.916	0.922
115	0.873	0.875	0.877	0.883	0.891	0.897	0.903	0.908	0.914
116	0.868	0.869	0.872	0.877	0.886	0.892	0.898	0.903	0.910
117	0.862	0.864	0.866	0.872	0.880	0.886	0.893	0.898	0.905
118	0.847	0.849	0.851	0.857	0.866	0.872	0.879	0.885	0.892
119	0.833	0.834	0.836	0.843	0.852	0.859	0.866	0.872	0.880
120	0.813	0.815	0.817	0.824	0.833	0.841	0.848	0.855	0.863
121	0.799	0.800	0.802	0.810	0.819	0.827	0.834	0.842	0.851
122	0.773	0.774	0.777	0.784	0.794	0.802	0.810	0.818	0.826
123	0.761	0.762	0.765	0.772	0.782	0.791	0.799	0.807	0.816
124	0.729	0.731	0.734	0.741	0.752	0.760	0.768	0.776	0.786
125	0.700	0.701	0.705	0.712	0.723	0.731	0.739	0.747	0.756
126	0.455	0.456	0.460	0.463	0.473	0.477	0.485	0.489	0.494

	91	**92**	**93**	**94**	**95**	**96**	**97**	**98**	**99**
91	1.000								
92	0.999	1.000							
93	0.996	0.996	1.000						
94	0.973	0.973	0.973	1.000					
95	0.586	0.592	0.587	0.574	1.000				
96	0.785	0.793	0.792	0.776	0.803	1.000			
97	0.815	0.823	0.824	0.808	0.754	0.984	1.000		
98	0.831	0.839	0.840	0.824	0.741	0.973	0.996	1.000	
99	0.851	0.858	0.857	0.839	0.778	0.989	0.991	0.986	1.000
100	0.869	0.875	0.876	0.858	0.738	0.972	0.993	0.994	0.992
101	0.881	0.887	0.887	0.869	0.743	0.971	0.988	0.990	0.992
102	0.893	0.899	0.898	0.880	0.743	0.967	0.982	0.983	0.990
103	0.904	0.909	0.908	0.890	0.730	0.958	0.976	0.979	0.985
104	0.913	0.918	0.917	0.898	0.729	0.953	0.970	0.974	0.982
105	0.921	0.925	0.924	0.905	0.721	0.946	0.965	0.970	0.978
106	0.927	0.931	0.930	0.911	0.717	0.941	0.961	0.966	0.974
107	0.935	0.938	0.937	0.917	0.713	0.937	0.957	0.962	0.972
108	0.942	0.946	0.944	0.924	0.708	0.931	0.953	0.959	0.968
109	0.949	0.952	0.951	0.930	0.709	0.928	0.947	0.954	0.966
110	0.952	0.955	0.953	0.933	0.705	0.925	0.946	0.952	0.964
111	0.951	0.954	0.953	0.932	0.704	0.924	0.946	0.953	0.964
112	0.946	0.949	0.947	0.927	0.710	0.928	0.948	0.954	0.966
113	0.935	0.939	0.937	0.917	0.718	0.935	0.953	0.958	0.970
114	0.928	0.931	0.930	0.911	0.718	0.938	0.957	0.962	0.972
115	0.919	0.923	0.922	0.903	0.730	0.946	0.961	0.965	0.977
116	0.916	0.920	0.919	0.900	0.731	0.949	0.965	0.968	0.978
117	0.912	0.916	0.916	0.897	0.725	0.949	0.968	0.971	0.979
118	0.898	0.903	0.902	0.884	0.741	0.961	0.973	0.974	0.985

119	0.888	0.893	0.893	0.875	0.734	0.961	0.979	0.981	0.985
120	0.870	0.876	0.876	0.858	0.749	0.971	0.982	0.981	0.989
121	0.859	0.866	0.866	0.849	0.732	0.965	0.985	0.985	0.984
122	0.834	0.841	0.840	0.824	0.762	0.976	0.981	0.976	0.986
123	0.825	0.832	0.832	0.816	0.746	0.971	0.984	0.980	0.982
124	0.794	0.802	0.801	0.786	0.749	0.961	0.967	0.961	0.967
125	0.764	0.771	0.771	0.758	0.736	0.940	0.943	0.935	0.943
126	0.496	0.501	0.496	0.489	0.592	0.678	0.643	0.627	0.663

	100	**101**	**102**	**103**	**104**	**105**	**106**	**107**	**108**
100	1.000								
101	0.998	1.000							
102	0.996	0.999	1.000						
103	0.993	0.997	0.999	1.000					
104	0.990	0.995	0.998	0.999	1.000				
105	0.987	0.992	0.996	0.998	0.999	1.000			
106	0.984	0.990	0.994	0.997	0.999	1.000	1.000		
107	0.982	0.988	0.992	0.995	0.998	0.999	1.000	1.000	
108	0.979	0.985	0.990	0.993	0.996	0.998	0.999	0.999	1.000
109	0.975	0.981	0.987	0.990	0.993	0.995	0.997	0.998	0.999
110	0.974	0.980	0.986	0.990	0.993	0.995	0.996	0.998	0.999
111	0.974	0.981	0.986	0.990	0.993	0.995	0.996	0.998	0.999
112	0.975	0.982	0.987	0.991	0.994	0.996	0.997	0.998	0.998
113	0.978	0.985	0.991	0.994	0.996	0.997	0.998	0.998	0.998
114	0.982	0.988	0.992	0.995	0.997	0.998	0.998	0.998	0.997
115	0.983	0.989	0.993	0.995	0.997	0.997	0.997	0.996	0.995
116	0.985	0.990	0.994	0.995	0.996	0.996	0.996	0.995	0.994
117	0.987	0.991	0.993	0.995	0.995	0.995	0.994	0.993	0.992
118	0.989	0.992	0.995	0.994	0.994	0.993	0.992	0.991	0.989
119	0.992	0.995	0.995	0.995	0.994	0.992	0.991	0.989	0.986
120	0.992	0.994	0.994	0.992	0.991	0.988	0.986	0.983	0.980
121	0.993	0.993	0.992	0.990	0.987	0.985	0.982	0.979	0.975
122	0.984	0.985	0.984	0.980	0.977	0.973	0.970	0.966	0.961
123	0.985	0.985	0.983	0.979	0.975	0.971	0.967	0.963	0.958
124	0.965	0.965	0.963	0.958	0.954	0.949	0.944	0.939	0.934
125	0.940	0.940	0.938	0.933	0.929	0.923	0.918	0.913	0.907
126	0.632	0.637	0.639	0.630	0.629	0.622	0.617	0.613	0.607

	109	**110**	**111**	**112**	**113**	**114**	**115**	**116**	**117**
109	1.000								
110	1.000	1.000							
111	0.999	0.999	1.000						
112	0.999	0.999	0.999	1.000					
113	0.997	0.997	0.998	0.999	1.000				
114	0.996	0.996	0.996	0.998	0.999	1.000			
115	0.994	0.993	0.994	0.996	0.998	0.999	1.000		
116	0.992	0.992	0.993	0.995	0.997	0.998	0.998	1.000	
117	0.991	0.990	0.992	0.994	0.995	0.997	0.997	0.998	1.000
118	0.987	0.986	0.987	0.990	0.993	0.994	0.996	0.997	0.997
119	0.983	0.983	0.984	0.986	0.990	0.992	0.993	0.995	0.995
120	0.976	0.975	0.976	0.979	0.984	0.986	0.989	0.990	0.991
121	0.970	0.969	0.971	0.973	0.978	0.982	0.984	0.986	0.987
122	0.957	0.955	0.956	0.960	0.966	0.970	0.974	0.976	0.976
123	0.953	0.951	0.952	0.956	0.962	0.967	0.970	0.973	0.974
124	0.929	0.926	0.927	0.932	0.940	0.944	0.949	0.951	0.952
125	0.901	0.899	0.900	0.905	0.914	0.918	0.924	0.926	0.927
126	0.606	0.603	0.603	0.610	0.618	0.620	0.631	0.631	0.628

	118	**119**	**120**	**121**	**122**	**123**	**124**	**125**	**126**
118	1.000								
119	0.996	1.000							
120	0.993	0.994	1.000						
121	0.989	0.993	0.992	1.000					
122	0.982	0.984	0.987	0.985	1.000				
123	0.979	0.983	0.986	0.986	0.983	1.000			
124	0.959	0.962	0.967	0.967	0.968	0.968	1.000		
125	0.935	0.938	0.944	0.943	0.947	0.947	0.935	1.000	
126	0.643	0.638	0.650	0.638	0.664	0.650	0.657	0.650	1.000